EHT PERDO

สถาบันวิจัยจุฬาภรณ์ | สถาบันบัณฑิตศึกษาจุฬาภรณ์ | มหาวิทยาลัยมหิดล | มหาวิทยาลัยบูรพา | มหาวิทยาลัยธรรมศาสตร์

Center of Excellence on Environmental Health and Toxicology (EHT)

Proceedings of the Conference

on The Role and Challenges of Environmental Health in National Development

October 8th, 2022

at the Convention Center, Chulabhorn Research Institute, Bangkok, Thailand

Proceedings of the Conference on The Role and Challenges of Environmental Health in National Development October 8th, 2022

Center of Excellence on Environmental Health and Toxicology (EHT)
The Role and Challenges of Environmental Health in National Development (2022)

Organizing Committee

Chairperson

Prof. Dr. *Khunying* Mathuros Ruchirawat	Director, EHT

Committee Members

1. Prof. Dr. Suchart Upatham	Advisor, EHT
2. Prof. Dr. Pornchai Matangkasombut	Advisor, EHT
3. Prof. Dr. Skorn Mongkolsuk	Advisor, EHT
4. Assoc. Prof. Dr. Jutamaad Satayavivad	Deputy Director, EHT
5. Assoc. Prof. Nardtida Tumrasvin	Assistant Management Director, EHT
6. Asst. Prof. Sosapin Bhumiratana	Assistant Director in Research and Academic, EHT
7. Assoc. Prof. Dr. Prayad Pokethitiyook	Representative, Faculty of Science, Mahidol University
8. Prof. Dr. Somsak Ruchirawat	Representative, Chulabhorn Graduate Institute
9. Assoc. Prof. Dr. Panida Navasumrit	Representative, Chulabhorn Research Institute
10. Assoc. Prof. Dr. Prayoon Fongsatitkul	Representative, Faculty of Public Health, Mahidol University
11. Asst. Prof. Dr. Bhumiphat Pachana	Representative, Faculty of Science, Burapha University

Scientific Committee

1. Assoc. Prof. Dr. Panida Navasumrit	Chulabhorn Research Institute/ Chulabhorn Graduate Institute
2. Assoc. Prof. Dr. Piyajit Watcharasit	Chulabhorn Research Institute/ Chulabhorn Graduate Institute
3. Dr. Poonsakdi Ploypradith	Chulabhorn Research Institute/ Chulabhorn Graduate Institute
4. Assoc. Prof. Dr. Prasat Kittakoop	Chulabhorn Research Institute/ Chulabhorn Graduate Institute
5. Assoc. Prof. Dr. Paiboon Vattanaviboon	Chulabhorn Research Institute/ Chulabhorn Graduate Institute
6. Assoc. Prof. Dr. Dr. Mayuree Fuangthong	Chulabhorn Research Institute/ Chulabhorn Graduate Institute
7. Assoc. Prof. Dr. Prayad Pokethitiyook	Faculty of Science, Mahidol University
8. Assoc. Prof. Dr. Choowong Auesukaree	Faculty of Science, Mahidol University
9. Assoc. Prof. Dr. Dakrong Pissuwan	Faculty of Science, Mahidol University
10. Assoc. Prof. Dr. Arthit Chairoungdua	Faculty of Science, Mahidol University
11. Assoc. Prof. Dr. Suphaphat Kwonpongsagoon	Faculty of Public Health, Mahidol University
12. Assoc. Prof. Dr. Ubolluk Rattanasak	Faculty of Science, Burapha University
13. Dr. Jakkaphun Nanuam	Faculty of Science, Burapha University
14. Asst. Prof. Dr. Chantima Piyapong	Faculty of Science, Burapha University

Logistics Committee

1. Mrs. Sujin Gitpot	Head of Finance and Procurement Unit, EHT
2. Mr. Preecha Sowanthip	Manager of Central Facility, Mahidol University, EHT
3. Mrs. Sasiwimol Hoontrakul	Academic Officer, EHT
5. Ms. Photjaman Nilbai	Financial Officer, EHT
6. Ms. Thitipat La-Ongnual	Coordinating Officer, Faculty of Science, Mahidol University
7. Ms. Preeyapatra Boonma	Coordinating Officer, Faculty of Public Health, Mahidol University
8. Ms. Phunyisa Boonkunth	Coordinating Officer, Faculty of Science, Burapha University

Abbreviations

BUU	=	Environmental Science, Faculty of Science, Burapha University
CGI	=	Chulabhorn Graduate Institute
CRI	=	Chulabhorn Research Institute
PH	=	Faculty of Public Health, Mahidol University
SCBI	=	Environmental Biology / Biology, Faculty of Science, Mahidol University
SCTX	=	Toxicology, Faculty of Science, Mahidol University
EHT	=	Center of Excellence on Environmental Health and Toxicology
PERDO	=	S&T Postgraduate Education and Research Development Office

CONTENTS

IMPACTS OF CHEMICALS AND CLIMATE CHANGE ON HUMAN HEALTH AND DISEASE DEVELOPMENT AND FACTORS MODULATING SUCH IMPACTS (*Continued*) **Pages**

DEVELOPMENT OF BIOLOGICALLY ACTIVE COMPOUNDS FOR CONTROL, PREVENTION AND TREATMENT OF ENVIRONMENTAL HEALTH PROBLEMS/DISEASES

INNOVATIVE TECHNOLOGY FOR PRODUCTION, DETECTION, TREATMENT, DETOXIFICATION, REMEDIATION, REDUCTION, REUSE AND RECYCLING OF CHEMICALS **Pages**

SAFETY AND TOXICITY OF FOOD, DRUGS AND OTHER CHEMICALS INCLUDING BIOFUELS

ENVIRONMENT / HEALTH IMPACT ASSESSMENT AND MANAGEMENT **Pages**

Impacts of chemicals and climate change on human health and disease development and factors modulating such impacts

7-CYANO-7DEAZAGUANINE REDUCTASE IN *Pseudomonas aeruginosa* PAO1 CONFERS SUSCEPTIBILITY TO OXIDATIVE STRESS

Chonthicha Khotchakasorn[1], Sopapan Atichartpongkul[2], Skorn Mongkolsuk[1,2,3] and Mayuree Fuangthong[1,2,3]

[1]Applied Biological Sciences Program, Chulabhorn Graduate Institute, Bangkok, Thailand
[2]Laboratory of Biotechnology, Chulabhorn Research Institute, Bangkok, Thailand
[3]Center of Excellence on Environmental Health and Toxicology (EHT), OPS, MHESI, Thailand

Abstract:

Pseudomonas aeruginosa is one of pathogens that infects patients with dominantly cystic fibrosis and immunodeficiency. In this work, we identified a nicotinamide adenine dinucleotide phosphate (NADPH)-dependent nitrile reductase gene or QueF in *P. aeruginosa* PAO1, which is a tRNA modifying gene. A *queF* mutant strain was constructed by clean deletion method using a suicide vector pKNOCK-Ap and was verified by colony PCR and Southern blot analysis. The *queF* complemented strain was constructed by transforming the plasmid containing a full-length *queF* gene, called pBBR-*queF*-FL to the *queF* mutant strain. The *queF* complemented strain was verified by PCR and sequencing. The results show that the *queF* mutant strain was sensitive to hydrogen peroxide (H_2O_2) and tert-butyl hydroperoxide. The mRNA level of *queF* was also increased when cells were exposed to H_2O_2. Further studies are needed to understand the mechanism of *queF* under oxidative conditions.

Keywords: PA2806, *Pseudomonas*, oxidative stress, tRNA modification

Introduction:

Pseudomonas aeruginosa, which is gram-negative bacterium, is one of opportunistic pathogens that causes infections in humans particularly affecting immunocompromised individuals with chronic obstructive pulmonary disease (COPD) and cystic fibrosis (1). During *P. aeruginosa* infection, host defense systems such as the innate immune system play an important role in fighting with *P. aeruginosa* by phagocytosis and inflammatory responses to remove the pathogens including the generation of reactive oxygen species leading to oxidative stress. Unfortunately, *P. aeruginosa* secretes a wide range of virulence factors, which contribute to its adaptability and survival under oxidative stress conditions (2). Therefore, it is needed to understand the mechanism how *P. aeruginosa* survive in poor environments because it might be a gateway to target *P. aeruginosa*.

tRNA modification, especially in the anticodon region, plays an important role in the efficiency and fidelity of translation process. From our preliminary study, *queF* gene was considered potentially being one of candidate tRNA modifying genes that plays a major role in oxidative stress response (3). QueF from *Bacillus subtilis* is the nicotinamide adenine dinucleotide phosphate (NADPH)-dependent nitrile reductase, which functions in the biosynthetic pathway of the tRNA-modified nucleoside queuosine. Moreover, excessive expression of the *queF* genes causes perchlorate resistance and confers resistance to other stress condition such as H_2O_2 in the *B. subtilis* PY79 (4). However, the role of *queF* in *P. aeruginosa* is still unclear. In this project, we would like to study the role of *queF* in response to oxidative stress in *P. aeruginosa*.

Methodology:

Bacterial strains and growth conditions

The strains used in this study were *P. aeruginosa* strain PAO1 and *Escherichia coli* strains namely BW20767 and DH5α. They were grown on lysogeny broth (LB) agar plate at 37 °C and in LB medium at 37 °C with shaking. Antibiotics were added in some conditions at the following concentrations: for *P. aeruginosa*, at 200 µg/mL of carbenicillin (Cb), at 75 µg/mL of gentamicin (Gm), and at 200 µg/mL of tetracycline (Tc); for *E. coli*, at 15 µg/mL of gentamicin (Gm), at 100 µg/mL of ampicillin (Ap), and at 15 µg/mL of tetracycline (Tc).

Construction of a *queF* mutant strain

The *queF* gene is one of tRNA modifying genes shown to be hydrogen peroxide sensitive in library screening from previous study (3). The *queF* mutant strain was constructed by clean deletion technique. Fragments of approximately 700 bp from the upstream and downstream regions of the *queF* gene were amplified by PCR using *Taq* DNA polymerase. The amplified fragments of each region were cloned into pKNOCK-Ap plasmid that is digested with *Sma*I giving the recombinant plasmid, called pKN-*queF*. This plasmid was used in a double-cross-over recombination in *P. aeruginosa* strain PAO1 with *E. coli* BW20767 as a donor strain through conjugation. The *queF* gene was replaced by the Gm resistance cassette that was also eventually deleted by Cre expressed from pCM157 plasmid, producing the *queF* mutant strain called Δ*queF* (5). At the end of the experiment, the *queF* mutant was verified by colony PCR with primers BT8347 and BT8348 and sequencing.

Construction of *queF* complemented strain

The full-length fragment of *queF* was amplified with primers BT8347 and BT8348 and *Pfu* polymerase by PCR followed by cloning into the broad-host-range cloning vector pBBR1MCS-4 at the *Xho*I and *Xba*I sites (6). Then, the pBBR-*queF*-FL plasmid was obtained and was transformed into the *queF* mutant strain by electroporation, producing *queF* complemented strain. This strain was selected by plating on LB agar plate containing 200 µg/mL of Cb and 75 µg/mL of Gm. The pBBR1MCS-4 plasmid was also electroporated into the wild type (WT) and *queF* mutant strain to normalize the effect of pBBR1MCS-4 plasmid in further experiments.

Oxidants susceptibility analysis

The overnight cultures of wild type PAO1 and mutant strain were sub-cultured in LB medium, and grown at 37 °C with shaking to the exponential phase. The semi-solid medium without antibiotics was mixed to the exponential phase cultures to final OD_{600} of 0.1. The mixtures were poured over solid layer of LB agar plate. Ten microliters of oxidants namely 8.8 M of H_2O_2 or 7.3 M of tert-butyl hydroperoxide was added on paper disc. Oxidant-added paper disc was placed on the surface of semi-solid culture. After overnight incubation at 37 °C, the clear zones were measured, and compared between mutant and wild type strain.

Semiquantitative real-time PCR

Overnight cultures were sub-cultured to a final OD_{600} of 0.05 in 5 mL of LB containing appropriate antibiotics and grown to the exponential phase (OD_{600} of 0.4-0.6). Then, cells were treated with various concentrations of H_2O_2 at 37 °C with shaking for 10 min. Total RNA was extracted by hot acid phenol method. After that, the samples were treated with DNase to eliminate residual DNA. For cDNA synthesis, the reverse transcription reaction was preformed using random hexa-primers and a RevertAid™ M-MuLV Reverse Transcriptase kit. Semiquantitative real-time PCR was performed according to the manufacturer's instructions using KAPA SYBR FAST reagent, and a StepOnePlus™ real-time PCR system.

Results:

Construction of *queF* mutant strain

The *queF* mutant strain was constructed by double-cross-over recombination method by using a suicide vector pKNOCK-Ap plasmid. The *queF* gene was replaced by *lox*Gm and, then *lox*Gm was deleted by Cre expressed from pCM157 plasmid, giving the *queF* mutant strain. The scheme of construction of mutant strain was shown in Figure 1A. The mutant strain was verified by colony PCR with primer pairs of BT8347/BT8348. The size of PCR products of mutant colonies was shown approximately 349 bp as expected in Figure 1B.

(A) (B)

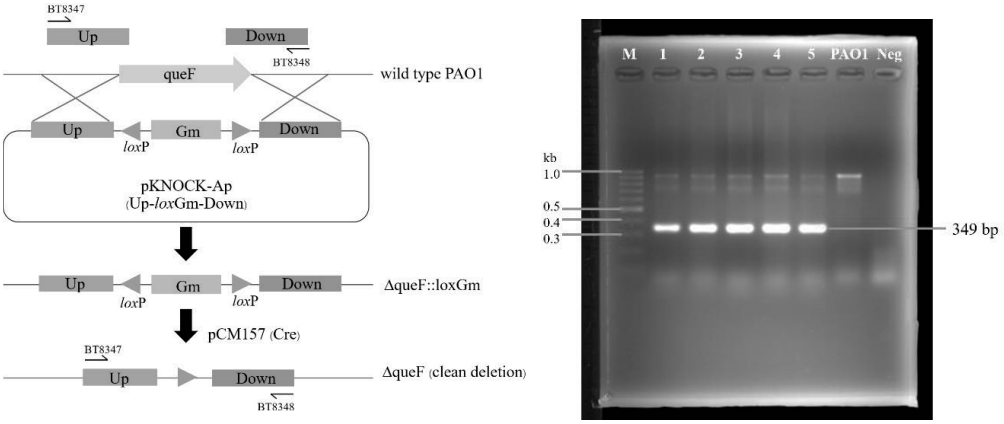

Figure 1 Construction of *queF* mutant strain. (A) The scheme of double crossover recombination method using a suicide vector pKNOCK-Ap to construct *queF* mutant strain (Δ*queF*). (B) The PCR product of colonies PCR with primers BT8347 and BT8348. The band 349 bp band was observed for samples from *queF* mutant strain as seen in colonies number 1-4.

Construction of *queF* complemented strain

The *queF* complemented strain was constructed by transformation of pBBR-*queF*-FL into *queF* mutant strain. The *queF* complemented strain was verified by PCR with primers M13F and M13R, and DNA sequencing. Colonies PCR of *queF* complemented strain showed expected size of fragments 1,100 bp in Figure 2.

(A) (B)

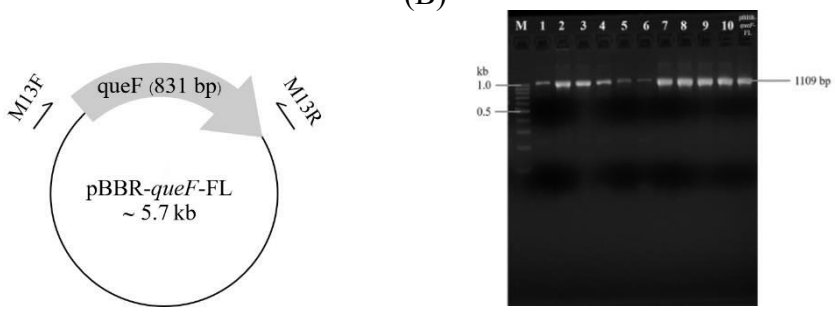

Figure 2 Construction of *queF* complemented strain. (A) The scheme of how complemented strain verified by PCR with primers M13F and M13R. (B) The PCR product of colonies of complemented strain. Colonies number 1-10 were *queF* complemented strain.

Oxidant susceptibility analysis

Clear zone of *P. aeruginosa* PAO1 and *queF* mutant that exposed to 8.8 M of H_2O_2 or 7.3 M of tert-butyl hydroperoxide disc were compared. The results revealed that the *queF* mutant strain showed significantly larger clear zone than the wild type strain indicating that *queF* plays an important role in cellular response to oxidants shown in figure 4.

(A) (B)

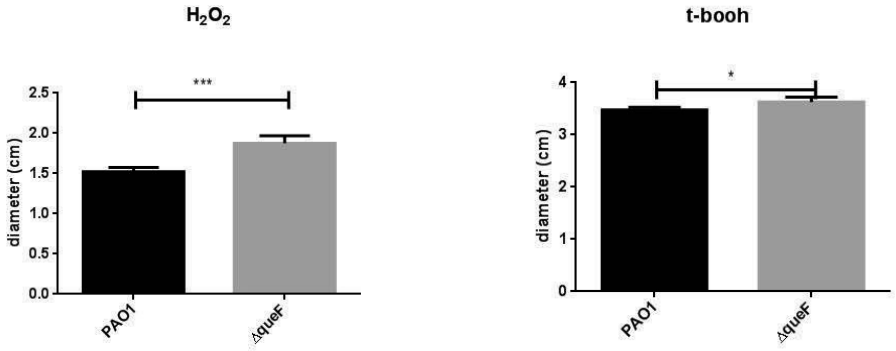

Figure 4 Sensitivity of mutant strain to oxidants compared to the wild type PAO1 strain, when oxidants are (A) H_2O_2 and (B) *tert*-butyl hydroperoxide. Asterisks denote a significant difference by *t*-test (p-value ≤ 0.05).

Quantitative real time-PCR assay (qRT-PCR)

After wild-type PAO1 was induced with H_2O_2, the relative expression level of mRNA was observed in Figure 5. In the 1, 5, and 10 mM of H_2O_2 induced conditions, the *queF* mRNA level was higher than the uninduced condition of wild-type. The increased expression of genes after exposure to H_2O_2 indicating the gene may contribute to the response against H_2O_2.

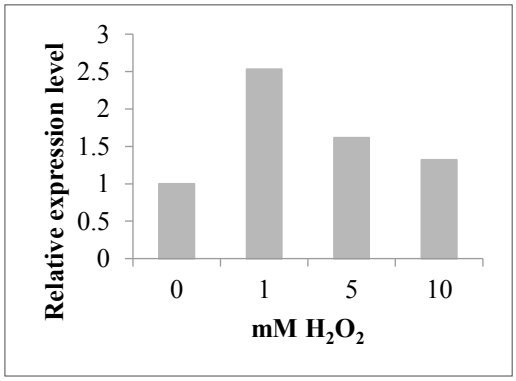

Figure 5 The relative expression level of wild-type PAO1 mRNA treated in 1, 5, and 10 mM H_2O_2 with uninduced samples being as a control.

Conclusions:

In this work, the *P. aeruginosa* PAO1 *queF* mutant strain (Δ*queF*) and *queF* complemented strain was constructed. Considering the susceptibility toward oxidants, the mutant strain was susceptible to oxidants namely H_2O_2 and tert-butyl hydroperoxide than the wild type and its expression was induced by H_2O_2, suggesting that *queF* gene may plays an important role in the oxidative stress response. Therefore, our further studies are needed to understand more clearly and investigate the mechanism of *queF* under oxidative conditions.

References:

1. Moradali MF, Ghods S, Rehm BHA. *Pseudomonas aeruginosa* Lifestyle: A Paradigm for adaptation, survival, and persistence. Frontiers in Cellular and Infection Microbiology. 2017;7.
2. Qin S, Xiao W, Zhou C, Pu Q, Deng X, Lan L, et al. *Pseudomonas aeruginosa*: pathogenesis, virulence factors, antibiotic resistance, interaction with host, technology advances and emerging therapeutics. Signal Transduction and Targeted Therapy. 2022;7(1):199.
3. Narumon T. Role of m^7G46 tRNA modification in oxidative stress response in *Pseudomonas aeruginosa*: Chulabhorn Graduate Institute 2018.
4. Díaz-Rullo J, Rodríguez-Valdecantos G, Torres-Rojas F, Cid L, Vargas IT, González B, et al. Mining for perchlorate resistance genes in microorganisms from sediments of a hypersaline pond in Atacama desert, Chile. Frontiers in Microbiology. 2021;12.
5. Marx CJ, Lidstrom ME. Broad-host-range *cre-lox* system for antibiotic marker recycling in gram-negative bacteria. BioTechniques. 2002;33(5):1062-7.
6. Kovach ME, Elzer PH, Hill DS, Robertson GT, Farris MA, Roop RM, 2^{nd}, et al. Four new derivatives of the broad-host-range cloning vector pBBR1MCS, carrying different antibiotic-resistance cassettes. Gene. 1995;166(1):175-6.

CYTOTOXICITY STUDY OF A POTENT SELECTIVE CANNABINOID RECEPTOR SUBTYPE 2 AGONIST, HU308 BY USING AN *IN VITRO* CHOLANGIOCARCINOMA CELLS AS A TEST MODEL: INTERACTION WITH CHOLINERGIC RECEPTORS

Ammarind Anantjitsupha[1] Jantamas Kanitwithayanun[1,2,3], Nedsai Uddin Babar[2], Noppawan Rittapai[2], Tawit Suriyo[2,3], and Jutamaad Satayavivad[1,2,3]

[1]Environmental Toxicology program, Chulabhorn Graduate Institute, Bangkok 10210, Thailand
[2]Laboratory of Pharmacology, Chulabhorn Research Institute, Bangkok 10210, Thailand
[3]Center of Excellence on Environmental Health and Toxicology (EHT), OPS, MHESI, Thailand

Abstract:

HU308, a potent selective cannabinoids receptor subtype 2 (CB2) agonist, is a novel nonpsychotropic cannabinoid-derivative compound that has been reported as new therapies for neuropathic pain, hypertension, and inflammation. However, cellular toxicity of this nonpsychotropic cannabinoid in cancer cells is limited. Previous study demonstrated that cannabinoid- modulated cholinergic activity is a mechanism underlying the cannabinoid induced memory impairments. However, little is known about the role of CBs on growth inhibiting effect in cancer cells and their interactions with cholinergic signaling. Cholangiocarcinoma (CCA) is a poor prognostic bile duct cancer. Since, it has been well documented that both cannabinoids receptors (CBs) and cholinergic acetylcholine receptors (AChRs) express and play some certain roles in CCA cells. In the present study, *in vitro* cytotoxicity of HU308 has been explored by using CCA cells as a test model. The molecular cytotoxicity mechanisms and its crosstalk with AChRs including muscarinic acetylcholine receptor subtype 3 (M3-mAChR), and nicotinic acetylcholine receptor subtype alpha 7 (α7-nAChR) were also investigated.

The results from Western immunoblotting assay showed a variation of basal CBs expression in various CCA cell lines. Almost CCA cell lines expressed much lower levels of CB1 when compared to the normal immortalized cholangiocyte MMNK-1. KKU213 cell line expressed the highest level of CB2 while it expressed very low level of CB1. KKU213 cell line was selected for further investigation by treating with HU308. The effects on cell viability, expression of cholinergic receptors, and apoptotic level were determined by MTT viability, Western immunoblotting, and flow cytometry assays, respectively. After 24 hr of the treatment, HU308 (25-400 μM) exhibited a reduction of cell viability in a concentration dependent manner. This effect was mitigated by pre- and co-treatment with a selective CB2 antagonist (AM630, 10 and 25 nM), confirming the involvement of CB2 receptor in HU308 induced KKU213 cell death. Apoptotic cell death was significantly increased after HU308 treatment compared to the control group. Moreover, an intrinsic pro-apoptosis Bax protein had a trend to increase while an anti- apoptotic Bcl2 protein had decreased by HU308 treatment. Down- regulation of α7-nAChR, but not M3-mAChR was also evidenced. In conclusion, a synthetic selective CB2 agonist, HU308, produced a cytotoxic effect to a CB2 positive CCA KKU213 cell via an induction of intrinsic apoptotic pathway and down-regulating α7-nAChR, which may alter inflammation-associated responses of CCA cells.

Keywords: Cannabinoid receptor, cytotoxicity, cholinergic receptor, selective CB2 agonist, cholangiocarcinoma, apoptosis.

Introduction:

Cannabinoids are a group of chemical compounds found in the marijuana plant *Cannabis sativa* L., which represented a source of several different natural active compounds. So far, based on their origins, cannabinoid compounds can be separated into three groups including (1) Phytocannabinoids, produced by plant such as delta 9 tetrahydrocannabinol (Δ9-THC) (Niaz et al., 2017) (2) Endocannabinoids, synthesized within the body, and (3) Synthetic cannabinoids, manmade compounds which are produced to mimic the activity of phytocannabinoids and endocannabinoids. Various biological effects of cannabinoid compounds are exerted through binding with cannabinoid receptors (CBs) in human body (Andre et al., 2016). There are two main types of CBs, including cannabinoid receptor type 1 (CB1) and cannabinoid receptors type 2 (CB2) (Thomas et al., 2007). CB1 is mainly distributed in the central nervous system (CNS) but it is also found in the peripheral body while CB2 is mostly distributed in the immune cells. These two receptors exhibited a wide range of biological processes including cell fate. In the last decades, the use of CBs to mediate anti-tumor effects has been suggested since activation of these receptors can regulate mechanisms of cell death in various manners. For example, they can induce cell cycle arrest, promote apoptosis, and inhibit proliferation and angiogenesis in tumor cells (Khan et al., 2016; Pertwee, 1999). However, their molecular mechanisms underlying the antitumor activity are largely dependent on the type of cancers, ligand selectivity, and potency of ligand required for induction of the effects. A previous study reported that activation of CBs by THC exhibited anticancer effect in glioblastoma by down regulating MMP-2 (matrix metalloproteinase 2), which is involved in cancer invasion of glioma and also reduced glioma tumor size both in mouse model and experimental studies (Blázquez et al., 2008). Furthermore, a study by Carracedo et al., (2006) reported that THC could induce synthesis of ceramide (sphingolipid on the cell membrane) through CB2, then up-regulate the subsequent downstream compounds such as AFT-4, and TRB3 in pro-apoptotic signaling leading to induction of apoptosis in pancreatic tumor cells (Carracedo et al., 2006). The endogenous cannabinoids as well as phytocarnabinoid THC activate both CB1 and CB2 cannabinoid receptors, and exerts various pharmacological activities. However, these compounds could produce the psychoactive side effects via CB1 activation. Regarding nonpsychotropic CB2, its expression possesses a variety of therapeutic functions, including anti-inflammation, anti-fibrosis, and regulation of bone metabolism. CB2 is mainly expressed in peripheral tissues; however, CB2 has also been detected in the brain but in a rather lower extent in comparison to the immune system or CB1 level (An et al., 2020). Moreover, the up-regulation of CB2 was also demonstrated when there is active inflammation or injury in the peripheral nervous system or the CNS (Kibret et al., 2022) to down-regulating cytokines and chemokines production suggesting that CB2 plays an important role in neurological activities such as neuroinflammation and neurodegenerative conditions (Bie et al., 2018). HU-308 was one of the first fully characterized, highly selective, and highly efficacious synthetic CB2 agonist (Hanuš et al., 1999). Previous evidence suggested physiological and therapeutic roles for HU308 as it reduced hypertension, and elicited anti-inflammation, anti-osteoporotic, and peripheral analgesic activity (Y Sun, 2007). Moreover, it could inhibit forskolin-stimulated cyclic AMP (cAMP) production in CB2-transfected cells (Hanuš et al., 1999). The inhibition of cAMP was revealed in death pathways that responsible for induction of cytotoxic effects to inhibit cell growth in various cancer cells (Calvaruso et al., 2012). Therefore, based on this information, it is likely to provide new insights to the use of synthetic selective CB2 agonist, which devoid of undesired psychotropic effects or addiction liability, as a possible effective target for cancer therapy. However, the underlying mechanisms of selective CB2 agonist-mediated cytotoxicity in cancer cells are remained to be further clarified. Furthermore, It has been demonstrated that

cannabinoid and cholinergic systems interact during performance of a short-term memory task (Goonawardena et al., 2010). Mishima and coworkers (2002) reported that a block of cholinesterase with physostigmine and tetrahydroaminoacridine protects against working memory impairments induced by Δ9−THC. These findings further support a potential role of the cholinergic system in cannabinoid-induced memory impairments (Mishima et al., 2002).

Cholangiocarcinoma (CCA) is a malignant tumor that originates from the epithelial cells of bile duct. In Thailand, the highest incidence rate of CCA has been reported especially in the northeastern region. CCA has a poor prognosis and usually asymptomatic in the early stage, which leading to decrease the effectiveness of therapeutic treatment (Jesus et al., 2020; Shaib and El-Serag, 2004). Nowadays, a number of studies have shown an elevation of CB1 and CB2 expression in different human malignancies such as in hepatocellular carcinoma (Xu et al., 2006), prostate cancer (Sarfaraz et al., 2006), and breast cancer (Kisková et al., 2019). Moreover, they also addressed the association of CBs expression with a prognosis of diseases. However, not much is known about the information of CBs expression in various types of CCA cells. The molecular mechanisms of cannabinoids on anti-cancer effects in CCA cells also remain unclear. A previous report by Leelawat et. al, (2010) demonstrated the anti-proliferation and anti-migration effects of THC in human CCA cell lines (HUCCA-1 and RMCCA-1) by activating the Akt and ERK1/2 signaling pathways (Leelawat et al., 2010). Another study by DeMorrow et al (2008) reported the opposite effect of two endocannabinoids on CCA cells derived from human intrahepatic bile duct. They found that anandamide (AEA) exerted anti-proliferation while 2-arachidonylglycerol (2-AG) stimulated cell growth (DeMorrow et al., 2007). The cholinergic neuron is a specific nerve cell that produce ACh. It has been reported that cholinergic receptors such as M3-mAChR and α7-AChR were found highly expressed in CCAs (Chen et al., 2019; Feng et al., 2018). Moreover, the over expression of M3-mAChR was found associated with perineural invasion and lymph node metastasis in CCA patients leading to a poor prognosis (Feng et al., 2018). α7nAChR expression plays a crucial role in cancer-related properties including proliferative, anti-apoptotic, and pro-metastatic activities (Singh et al., 2011). It is also an essential regulator of inflammation (Wang et al., 2003). It has been shown that modulation of CBs was extensively studied for the anti-tumorigenic activity (Miller and Devi, 2011). However, there is limited information related to the role of CBs on growth inhibiting effect in cancer cells and their interactions with cholinergic components. Therefore, the present study aimed to determine the *in vitro* cytotoxicity of HU308, a potent selective cannabinoids receptor subtype 2 (CB2) agonist in CCA cells. The effects of cannabinoid agonist on CCA cell growth and the modulation of cholinergic components (M3-mAChR and α7-nAChR) as well as the possible mechanisms underlying their effects were also determined.

Methodology:

Cell culture

CCA cell lines isolates from Thai CCA patients including HUCCA-1, RMCCA-1, KKU055, KKU100, and KKU213 were cultured in Ham's F-12 Nutrient Mixture (Ham's F-12). CCLP-1, a CCA cell line isolates from American patient and the normal immortalized cholangiocyte MMNK-1 cell line were cultured in DMEM. All the culture plates were supplemented with 5% fetal bovine serum (FBS), 1% L-Glutamine, 1% antibiotics (100U/mL of penicillin and 100 μg/mL of streptomycin). The plates were maintained at 37˚C in a humidified incubator with 5% CO_2.

Cell lysate preparation

CCA cells were harvested in ice- cold lysis buffer containing 50 mM Tris- HCL, 150 mM NaCl, 1 mM EDTA, 0.1% sodium deoxycholate, 1% NP-40, 1 mM sodium orthovanadate (Na_3VO_4), 1 mM phenylmethylsulphonyl fluoride (PMSF), okadaic acid (OA), 20 mM sodium fluoride (NaF), and protease cocktail inhibitor. The lysates were then sonicated, incubated on ice for 30 min, and cleared by centrifugation at 14,000 rpm for 20 min at 4 ˚C. The supernatant was collected and stored at - 80 ˚C until analysis until use. Protein concentration in each cell lysate was measured by using Bradford assay.

Immunoblotting

For CB1 determination, 50 μg of total protein in cell lysate was subjected to a 7.5% SDS-polyacrylamide gels before transferring to a nitrocellulose membrane, then blotting with 1:500 dilution of CB1 antibody and 1:5,000 dilution of anti-rabbit antibody. For CB2, M3-mAChR, α7-nAChR, and PARP1 determination, 30 μg of total protein in cell lysate were subjected to 7.5% SDS-polyacrylamide gels before transferring to nitrocellulose membrane then blotting with 1:500 dilution of CB2 antibody or 1:1,000 dilution of M3-mAChR antibody, 1:500 dilution of α7-nAChR antibody, 1:1,500 dilution of PARP1 antibody, and 1:5,000 dilution of anti-rabbit or anti-mouse antibody. For Bax and Bcl2 determination, 40 μg of total protein in cell lysate was subjected to 12.5% SDS-polyacrylamide gels before transferring to nitrocellulose membrane then blotting with 1:1,500 dilution of Bax antibody or 1:1,000 dilution of Bcl2 antibody, and 1:5,000 dilution of anti-rabbit or anti-mouse antibody. The protein of interest on the membrane was quantified using the ChemiDoc Imaging Machine with the ChemiDoc system, Bio-rad. The signal of each immunoblot sample was normalized with β-actin. CCA cell that has high expression level of CB2 but low expression level of CB1 was selected for further investigation on the anti-cancer effects of HU308, a selective CB2 agonist.

Cell viability assay

The effect of HU308 (selective CB2 receptor agonist) on viability of KKU213 cells, was determined by using MTT assay. Cells were seeded on 96-well plates before treating with different concentrations of HU308 (0.001, 0.01, 0.025, 0.05, 0.1, 0.2, 0.4, 1, 10, 25, 50, 100, 200, and 400 μM) for 24 hr at 37˚C. For antagonist treatment, KKU213 cells were pre-treated with AM630, a CB2 selective antagonist, at 10 or 25 nM for 30 min before being co- treated with HU308 (25- 100 uM) for 24 hr. Afterward, the supernatant was removed and KKU213 cells were then incubated with 3-(4,5-dimethylthiazol-2-yl)-2,5-diphenyl tetrazolium bromide (MTT) solution for 4 hr. Cell viability was measured by dissolving formazan salt with DMSO. The optical density was read at 570 nm by using a microplate reader.

Apoptosis detection

To determine the apoptotic effect of HU308 on KKU213 cells, cells were cultured in 60 mm. tissue culture dish with a density of 8×10^5 cells/mL. Cells were then treated with various concentrations of HU308 (10, 25, 50, and 100 μM) for 24 hr at 37˚C. After treatment, treated cells were harvested and stained with Annexin V conjugated with fluorescein isothiocyanate (FITC) and propidium iodide (PI) for 15 min. Levels of apoptotic cells were analyzed by using flow cytometry.

Statistical analysis

All data were obtained from independent experiments and presented as mean ± standard error of mean (SEM. The statistically significant differences between samples were determined using the Student's t-test. Differences of $p < 0.05$ were considered a statistically significant difference.

Results and discussion:

Basal expression of CB1, CB2, and M3-mAChR receptors in various CCA cell lines

Almost all of the tested CCA cell lines as well as the MMNK-1 normal immortalized cholangiocyte cell line expressed CB1 and CB2 proteins in different levels as demonstrated in (Figure 1). High expression of CB1 was observed in CCLP-1 followed by KKU100 and HUCCA-1, whereas RMCCA-1, KKU055, and KKU213 showed very low CB1 expression. The expression of CB2 was found in all cell lines. KKU213, KKU100, RMCCA-1, HUCCA-1, and CCLP-1 cells expressed CB2 higher than that of normal cholangiocyte MMNK-1. Meanwhile, KKU055 and CCLP-1 cell lines expressed CB2 at lower level. Furthermore, the expression of M3-mAChR receptor was observed in all cells lines with the highest expression was found in KKU100. KKU213 cell line which contained high basal expression of CB2 while CB1 was expressed at very low level, was selected for further investigation. The effect of the selective CB2 agonist compound (HU308) on cell viability, protein expression of cholinergic components (α7-nAChR and M3-mAChR), and mechanism of HU308- mediated CCA cell death were determined.

HU308, the specific CB2 agonist, induced a concentration-dependent reduction of KKU213 cell viability

The results from the MTT assay showed that treatment of HU308 at various concentrations (25-400 nM) for 24 hr suppressed the viability of KKU213 cells in a concentration-dependent manner (Figure 2). The reduction of KKU213 cell viability after being treated with HU308 (25, 50, and 100 μM) was reversed by pre- and co-treatment with AM630 (specific CB2 antagonist) at either concentration of 25 or 10 nM (Figure 3). The 50% inhibitory concentration (IC50) of HU308 treatment alone was 49 μM. Meanwhile, IC50 values of CB2 antagonist pre-treatment at 10 μM or 25 μM prior to HU308 treatment were increased to 98.9 and 9.46 μM, respectively. These results suggested that the growth inhibitory effect of HU308 on KKU213 cells was involved with CB2 receptor activation.

Cannabinoid receptor agonist induced apoptotic cell death and a noticeable alteration of apoptotic-related protein in KKU213 cells

We next investigated whether the reduction of cell viability was associated with cell apoptosis by using flow cytometry assay. As shown in (Figure 4), the result showed a concentration-response increase of total apoptosis (early and late stage) following treatment with HU308 at 10, 25, 50, and 100 μM for 24 hr. The percentage of early apoptotic cells was significantly increased by 1.77, 2.76, 2.48, and 2.41-fold respectively, compared to those of control. Similarly, the percentage of late apoptotic cell was significantly increased by 1.03, 1.51, 1.86, and 4.17-fold respectively, compared to control. Therefore, this result suggested that the mechanism by which HU308 inhibits KKU213 cell growth involved with an induction of cell apoptosis.

To further explore the apoptotic mechanism, the effect of HU308 on apoptosis-associated proteins was evaluated. The result showed a noticeable up-regulation of 89 kDa cleaved PARP1 which is a protein that mediated DNA fragmentation in the apoptotic process

(Figure 5) and Bax (Figure 6) which is an intrinsic pro-apoptotic protein. In contrast, it significantly down regulated the expression of cell survival marker protein, Bcl2 (Figure 6), which is an anti-apoptotic protein. Moreover, an increase in Bax/Bcl2 ratio (Figure 7) was noticeably observed in a concentration-related manner following HU308 treatment. These results suggested that HU308 induced KKU213 cell death may associated with intrinsic apoptotic signaling pathway that is influenced by Bax and Bcl2 regulatory proteins. However, the molecular pathways underlying the apoptotic activity are needed for further elucidation.

Cannabinoid receptor agonist promoted down-regulation of the cholinergic components.

A previous report (Chen et al., 2019; Feng et al., 2012) showed that the cholinergic receptors are able to regulate cholangiocarcinoma cell growth and metastasis. In this study, the expression levels of nicotinic receptor 7 (α7-nAChR), which plays roles in inducing inflammation and block apoptosis, and muscarinic receptor type 3 (M3-mAChR), which could induce proliferation and metastasis, were investigated following exposure to HU308 by Western immunoblot analysis. The results demonstrated that the expression of α7-nAChR (Figure 8) showed significantly decreased with HU308 at 10 μM for 24 hr. Meanwhile, no significant difference was observed for the M3-mAChR expression in KKU213 cell (Figure 9). According to the results, we suggested that HU308 exhibited growth inhibitory effect in KKU213 cells were associated with reduction of α7-nAChR.

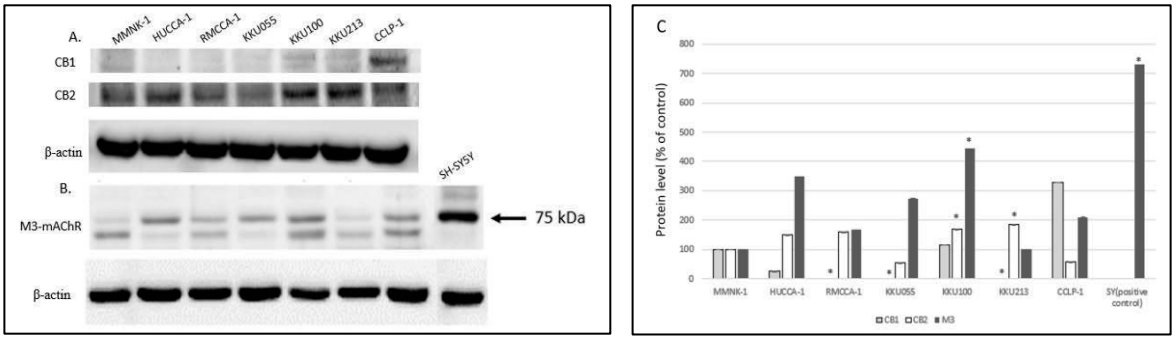

Figure 1 The basal expression profiles of CB1, CB2, and M3-mAChR in various CCA cell lines. (**A.)** Representative immunoblot bands of CB1 and CB2. **(B.)** Representative immunoblot bands of M3-mAChR. **(C.)** Quantification of CB1, CB2, and M3-mAChR normalized to β-actin in MMNK-1 cholangiocyte and various CCA cell lines. SH-SY5Y was served as M3-AChR positive control. Data are expressed as mean ± SEM of four independent experiments. * $p < 0.05$ compared with the immortalized cholangiocyte (MMNK-1) cell line

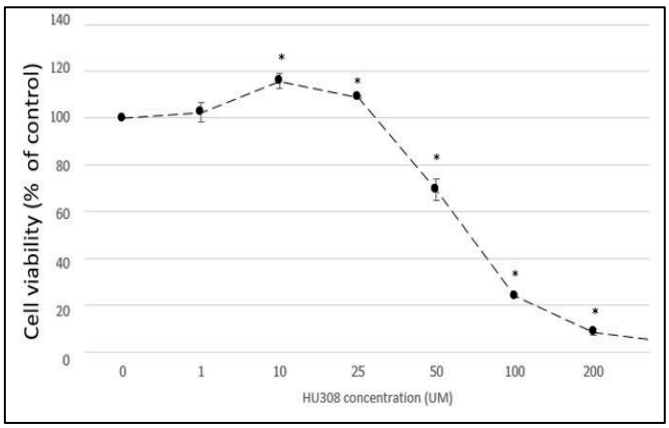

Figure 2 Effect of HU308 (a selective CB2 agonist) on KKU213 cell viability after 24 hr. treatment. * $p < 0.05$ compared with the control (untreated group).

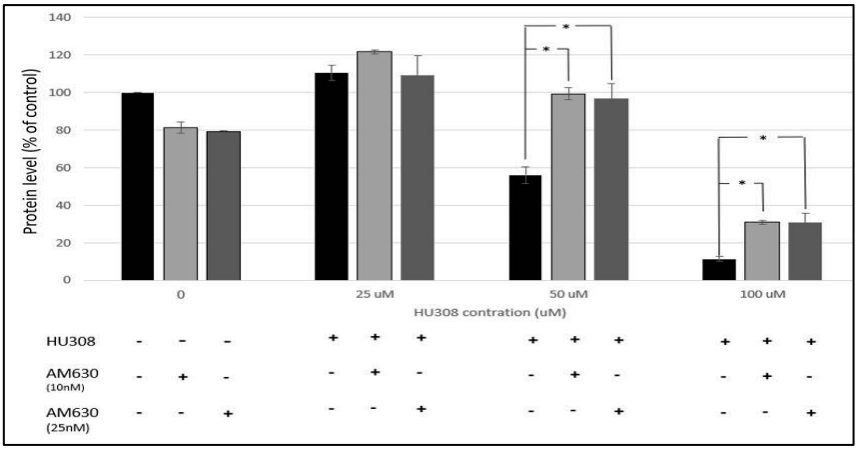

Figure 3 Effect of HU308 on cell viability in the presence or absence of pre- and co-treated with AM630 (a selective CB2 antagonist) in KK213 cells. Data are expressed as mean ± SEM of four independent experiments. * $p < 0.05$ compared with HU308 alone in the same treatment group.

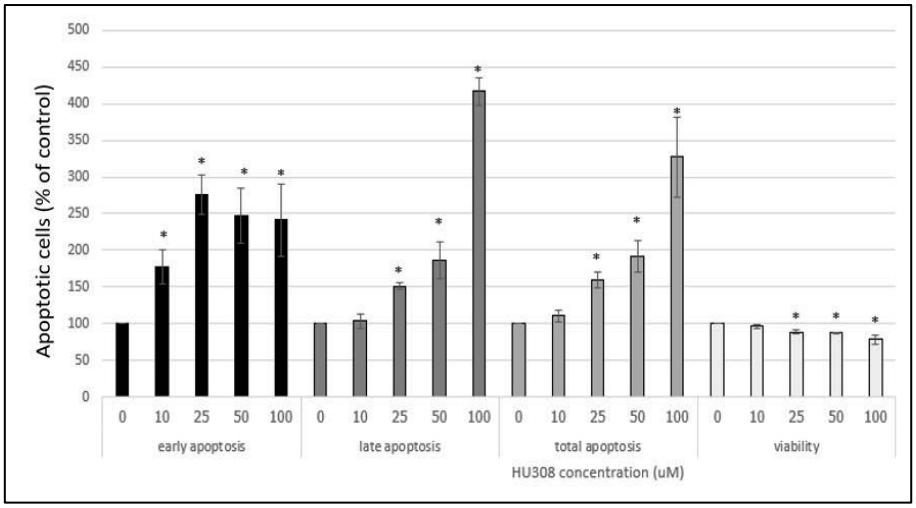

Figure 4 Apoptosis detection in KKU213 after treated with HU308 for 24 hr. Data are expressed as mean ± SEM of four independent experiments. * $p < 0.05$ compared with the control (untreated group).

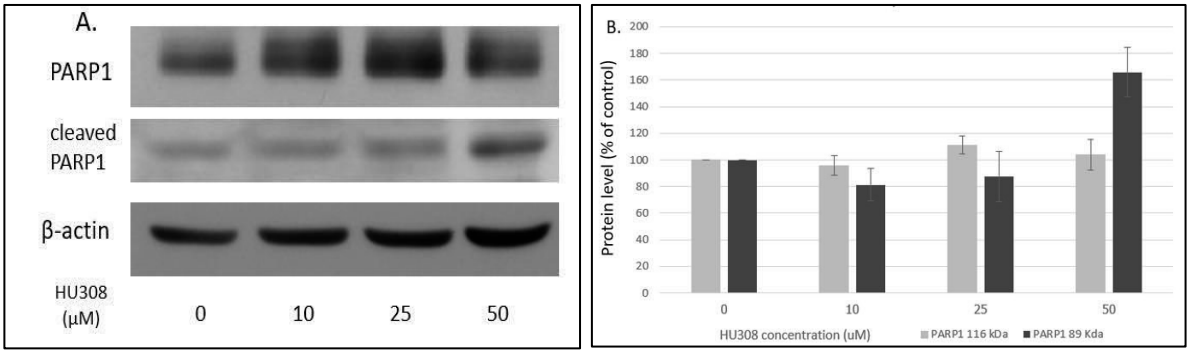

Figure 5 The effect of HU308 on the expression of PARP1 (116 kDa) and cleaved PARP1 (89 kDa) in KKU213 cells. **(A.)** Representative immunoblot bands of PARP1 and cleaved PARP1. **(B.)** Quantification of PARP1 and cleaved PARP1 normalized to β-actin. Data are expressed as mean ± SEM of four independent experiments.

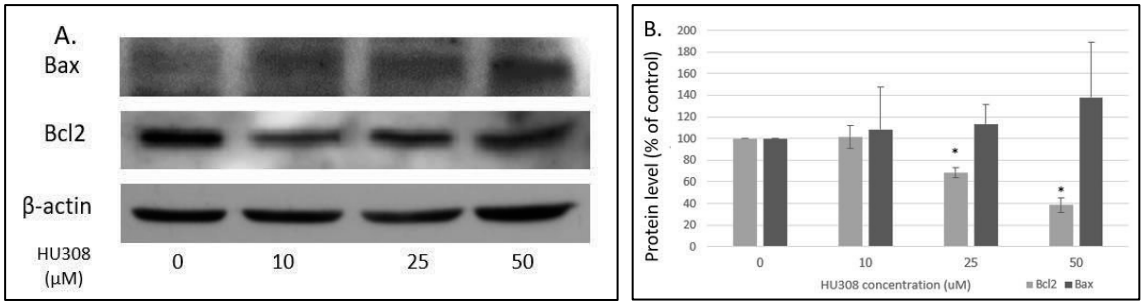

Figure 6 The effect of HU308 on the expression of Bcl2 and Bax in KKU213 cells. **(A.)** Representative immunoblot bands of Bcl2 and Bax. **(B.)** Quantification of Bcl2 and Bax normalized to β-actin and expressed as mean ± SEM of four independent experiments. * $p < 0.05$ compared with the control group (untreated group).

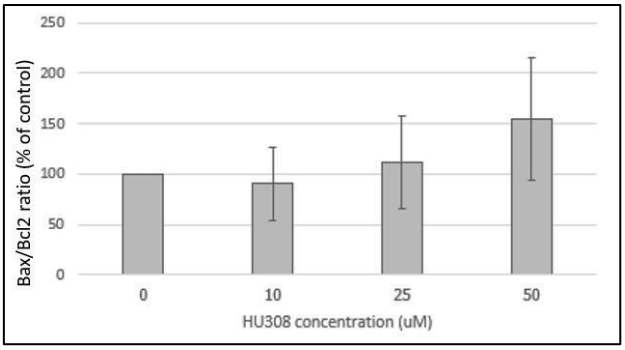

Figure 7 The ratio of Bax/Bcl2 protein in HU308 treated KKU213 cells. Data are expressed as mean ± SEM of four independent experiments.

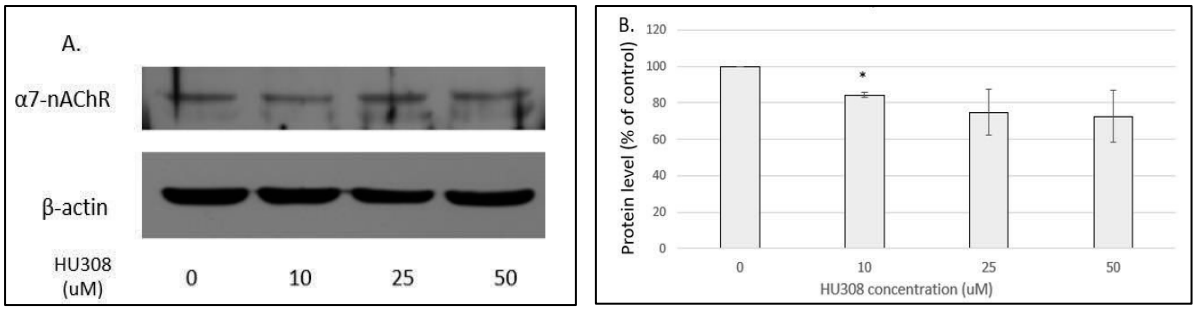

Figure 8 The effect of HU308 on the expression of α7-nAChR in treated KKU213 cells. **(A.)** Representative immunoblots band of α7-nAChR. **(B.)** Quantification of α7-nAChR normalized to β-actin and expressed as mean ± SEM of four independent experiments. * $p < 0.05$ compared with the control group (untreated group).

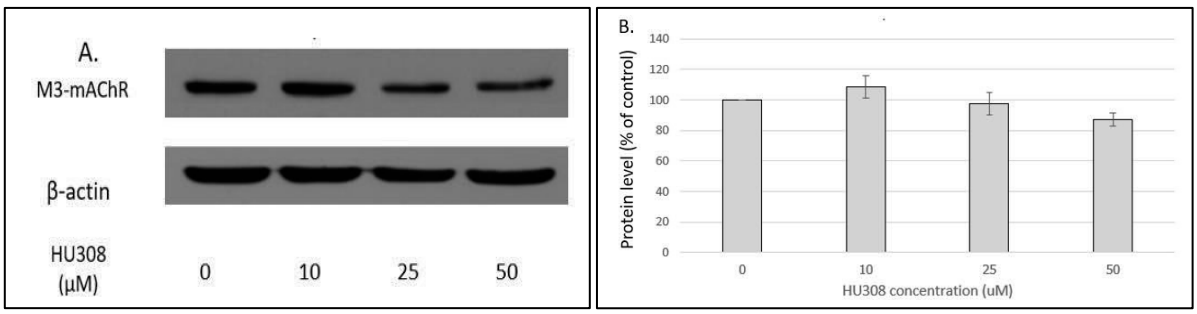

Figure 9 The effect of HU308 on the expression of M3-mAChR in KKU213 cells. **(A.)** Representative immunoblots band of M3-mAChR. **(B.)** Quantification of M3-mAChR normalized to β-actin. Data are expressed as mean ± SEM of four independent experiments.

Conclusion:

The present study shows that all CCA cell lines were positive for CB2 and M3-mAChR receptors. Moreover, the expression levels of CBs and M3-mAChR were depended on types of CCA cells. Activation of CB2 receptor by HU308, a selective CB2 agonist exhibited growth inhibitory effect in KKU213 which is a CB2 positive cell line. The possible mechanism underlying this cytotoxic effect is at least in part through induction of intrinsic apoptotic pathway. In addition, the expression of α7-nAChR, which plays a role in cancer development, was found significantly decreased after HU308 treatment. Altogether, these results suggest that activation of the CB2 receptor by a selective synthetic CB2 agonist, HU308, produced cytotoxic effect to CB2 positive CCA cell and also modulated cholinergic receptor α7-nAChR expression which may alter inflammation-associated responses of CCA cells.

References:

1. An, D., Peigneur, S., Hendrickx, L. A., and Tytgat, J. (2020). Targeting cannabinoid receptors: current status and prospects of natural products. *International Journal of Molecular Sciences,* 21(14), 5064. doi:10.3390/ijms21145064
2. Andre, C. M., Hausman, J.-F., and Guerriero, G. (2016). *Cannabis sativa*: the plant of the thousand and one molecules. *Frontiers in Plant Science,* 7, 19. doi:10.3389/fpls.2016.00019
3. Bie, B., Wu, J., Foss, J. F., and Naguib, M. (2018). An overview of the cannabinoid type 2 (CB2) receptor system and its therapeutic potential. *Current Opinion in Anaesthesiology,* 31(4), 407. doi:10.1097/ACO.0000000000000616
4. Blázquez, C., Salazar, M., Carracedo, A., Lorente, M., Egia, A., González-Feria, L., Haro, A., Velasco, G., and Guzmán, M. (2008). Cannabinoids inhibit glioma cell invasion by down-regulating matrix metalloproteinase-2 expression. *Cancer Research,* 68(6), 1945-1952. doi:10.1158/0008-5472.CAN-07-5176
5. Calvaruso, G., Pellerito, O., Notaro, A., and Giuliano, M. (2012). Cannabinoid-associated cell death mechanisms in tumor models. *International Journal of Oncology,* 41(2), 407-413. doi:10.3892/ijo.2012.1476
6. Carracedo, A., Lorente, M., Egia, A., Blázquez, C., García, S., Giroux, V., Malicet, C., Villuendas, R., Gironella, M., González-Feria, L., Piris, M. Á., Iovanna, J. L., Guzmán, M., and Velasco, G. (2006). The stress-regulated protein p8 mediates cannabinoid-induced apoptosis of tumor cells. *Cancer Cell,* 9(4), 301-312. doi:10.1016/j.ccr.2006.03.005
7. Chen, S., Kang, X., Liu, G., Zhang, B., Hu, X., and Feng, Y. (2019). α7-Nicotinic acetylcholine receptor promotes cholangiocarcinoma progression and epithelial–mesenchymal transition process. *Digestive Diseases and Sciences,* 64(10), 2843-2853. doi:10.1007/s10620-019-05609-3
8. DeMorrow, S., Glaser, S., Francis, H., Venter, J., Vaculin, B., Vaculin, S., and Alpini, G. (2007). Opposing actions of endocannabinoids on cholangiocarcinoma growth: recruitment of Fas and Fas ligand to lipid rafts. *Journal of Biological Chemistry,* 282(17), 13098-13113. doi:10.1074/jbc.M608238200
9. Feng, Y., Hu, X., Liu, G., Lu, L., Zhao, W., Shen, F., Ma, K., Sun, C., Zhu, C., and Zhang, B. (2018). M3 muscarinic acetylcholine receptors regulate epithelial–mesenchymal transition, perineural invasion, and migration/metastasis in cholangiocarcinoma through the AKT pathway. *Cancer Cell International,* 18(1), 1-12. doi:10.1186/s12935-018-0667-z

10. Feng, Y., Zhang, B., Yao, R., and Lu, Y. (2012). Muscarinic acetylcholine receptor M3 in proliferation and perineural invasion of cholangiocarcinoma cells. *Hepatobiliary & Pancreatic Diseases International,* 11(4), 418-423. doi:10.1016/S1499-3872(12)60201-X

11. Goonawardena, A. V., Robinson, L., Hampson, R. E., and Riedel, G. (2010). Cannabinoid and cholinergic systems interact during performance of a short-term memory task in the rat. *Learning & Memory,* 17(10), 502-511. doi:10.1101/lm.1893710

12. Hanuš, L., Breuer, A., Tchilibon, S., Shiloah, S., Goldenberg, D., Horowitz, M., Pertwee, R., Ross, R., Mechoulam, R., and Fride, E. (1999). HU-308: a specific agonist for CB2, a peripheral cannabinoid receptor. *Proceedings of the National Academy of Sciences,* 96(25), 14228-14233. doi:10.1073/pnas.96.25.14228

13. Jesus, B., Jose, M., Angela, L., Pedro, R., Shahid, K., Lewis, R., Vincenzo, C., Guido, C., Jesper, A., Chiara, B., Diego, C., Maria, P., Luce, F., Luke, B., Rocio, M., Eugenio, G., Domenico, A., Sergio, G., Mario, S., Marco, M., Cédric, C., Laura, F., Chiara, R., Pietro, I., Joachim, M., Anja, M., Sumera, R., Julie, H., Groot, K. B., Jordi, B., Alejandro, F., John, B., Juan, V., and Gregory, G. (2020). Cholangiocarcinoma 2020: the next horizon in mechanisms and management. *Nature Reviews Gastroenterology & Hepatology,* 17(9), 557-588. doi:10.1038/s41575-020-0310-z

14. Khan, M. I., Sobociska, A. A., Czarnecka, A. M., Król, M., Botta, B., and Szczylik, C. (2016). The therapeutic aspects of the endocannabinoid system (ECS) for cancer and their development: From nature to laboratory. *Current Pharmaceutical Design,* 22(12), 1756-1766.

15. Kibret, B. G., Ishiguro, H., Horiuchi, Y., and Onaivi, E. S. (2022). New insights and potential therapeutic targeting of CB2 cannabinoid receptors in CNS disorders. *International Journal of Molecular Sciences,* 23(2), 975. doi:10.3390/ijms23020975

16. Kisková, T., Mungenast, F., Suváková, M., Jäger, W., and Thalhammer, T. (2019). Future aspects for cannabinoids in breast cancer therapy. *International Journal of Molecular Sciences,* 20(7), 1673. doi:10.3390/ijms20071673

17. Leelawat, S., Leelawat, K., Narong, S., and Matangkasombut, O. (2010). The dual effects of Δ9-tetrahydrocannabinol on cholangiocarcinoma cells: Anti-invasion activity at low concentration and apoptosis induction at high concentration. *Cancer Investigation,* 28(4), 357-363. doi:10.1080/07357900903405934

18. Miller, L. K., and Devi, L. A. (2011). The highs and lows of cannabinoid receptor expression in disease: Mechanisms and their therapeutic implications. *Pharmacological Reviews,* 63(3), 461. doi:10.1124/pr.110.003491

19. Mishima, K., Egashira, N., Matsumoto, Y., Iwasaki, K., and Fujiwara, M. (2002). Involvement of reduced acetylcholine release in Δ9-tetrahydrocannabinol-induced impairment of spatial memory in the 8-arm radial maze. *Life Sciences,* 72(4-5), 397-407. doi:10.1016/S0024-3205(02)02274-9

20. Niaz, K., Khan, F., Maqbool, F., Momtaz, S., Ismail Hassan, F., Nobakht-Haghighi, N., Rahimifard, M., and Abdollahi, M. (2017). Endo-cannabinoids system and the toxicity of cannabinoids with a biotechnological approach. *Excli j,* 16, 688-711. doi:10.17179/excli2017-257

21. Pertwee, R. G. (1999). Pharmacology of cannabinoid receptor ligands. *Current Medicinal Chemistry,* 6, 635-664.

22. Sarfaraz, S., Afaq, F., Adhami, V. M., Malik, A., and Mukhtar, H. (2006). Cannabinoid receptor agonist-induced apoptosis of human prostate cancer cells LNCaP proceeds through sustained activation of ERK1/2 leading to G1 cell cycle arrest. *Journal of Biological Chemistry,* 281(51), 39480-39491. doi:10.1074/jbc.M603495200

23. Shaib, Y., and El-Serag, H. B. (2004). *The epidemiology of cholangiocarcinoma.* Paper presented at the Seminars in Liver Disease.

24. Singh, S., Pillai, S., and Chellappan, S. (2011). Nicotinic acetylcholine receptor signaling in tumor growth and metastasis. *Journal of Oncology,* 2011.

25. Thomas, A., Baillie, G., Phillips, A., Razdan, R., Ross, R. A., and Pertwee, R. G. (2007). Cannabidiol displays unexpectedly high potency as an antagonist of CB1 and CB2 receptor agonists in vitro. *British Journal of Pharmacology,* 150(5), 613-623. doi:10.1038/sj.bjp.0707133

26. Wang, H., Yu, M., Ochani, M., Amella, C. A., Tanovic, M., Susarla, S., Li, J. H., Wang, H., Yang, H., and Ulloa, L. (2003). Nicotinic acetylcholine receptor α7 subunit is an essential regulator of inflammation. *Nature,* 421(6921), 384-388.

27. Xu, X., Liu, Y., Huang, S., Liu, G., Xie, C., Zhou, J., Fan, W., Li, Q., Wang, Q., and Zhong, D. (2006). Overexpression of cannabinoid receptors CB1 and CB2 correlates with improved prognosis of patients with hepatocellular carcinoma. *Cancer Genetics and Cytogenetics,* 171(1), 31-38. doi:10.1016/j.cancergencyto.2006.06.014

28. Y Sun, S. A., MJ Garle, CL Gibson, K Hewitt, SP Murphy, DA Kendall, AJ Bennett. (2007). HU308. *British Journal of Pharmacology and Chemotherapy,* 152(5), 734. doi:10.1016/B978-008055232-3.61891-4

EFFECTS OF EXPOSURE TO GLYPHOSATE ON DNA DAMAGE AND CELL TRANSFORMATION IN CHOLANGIOCYTES (MMNK-1)

Phyo Bo Bo Aung[1], Panida Navasumrit[1,2,3], Ankamene Buranarom[2], Chalida Chompoobut[2] and Mathuros Ruchirawat[1,2,3]

[1]Graduate Program of Environmental Toxicology, Chulabhorn Graduate Institute, Bangkok 10210, Thailand
[2]Laboratory of Environmental Toxicology, Chulabhorn Research Institute, Bangkok 10210, Thailand
[3]Center of Excellence on Environmental Health and Toxicology (EHT), OPS, MHESI, Thailand

Abstract:

Cholangiocarcinoma (CCA) is a bile duct cancer with poor survival prognosis and the incidences are relatively high in Southeast Asian regions. Several risk factors for CCA have been identified which exposure to environmental carcinogens is increasingly recognized as risk factor for CCA. Nowadays, the use of pesticides and herbicides is increasing worldwide. Glyphosate is the most used herbicide and has been classified as probably carcinogenic to human (Group 2A; IARC, 2015). Preliminary finding revealed the contamination of glyphosate in the environment and local foods in high CCA incidence area. This study aimed to investigate the effects glyphosate on cytotoxicity, mutagenic DNA damage and cell transformation in cholangiocytes, MMNK-1.

In vitro study of cytotoxicity of glyphosate treatment in MMNK-1 cells (0.10 -10 ppm for 7 days) indicated that the cell viability was significant reduced to below 80% at 10 ppm, compared to untreated cells. At the non-cytotoxic concentrations of glyphosate treatment (0.10-1 ppm, 7 days), immunocytochemistry detection of mutagenic DNA damage in treated cells showed significant increases ($p<0.05$) by 1.66-, 1.79-, 1.52-fold for 8-hydroxydeoxyguanosine (8-OHdG) and 1.61-, 2.01-, 1.82-fold for 8-nitroguanine at 0.1, 0.5 and 1 ppm, respectively. Expression of various genes including inflammatory responses (*IL-6* and *IL-8*), DNA repair (*OGG1* and *XRCC1*) and antioxidative response (*Nrf2*) were increased in MMNK-1 cells treated at 0.5 ppm. In addition, glyphosate induced MMNK-1 cells transformation at 1 ppm after 7 days treatment of glyphosate. The formation of 8-OHdG and 8-nitroguanine were also increased in transformed MMNK-1 cells.

Taken together, this study suggested that glyphosate induces cytotoxicity, mutagenic DNA damage and cell transformation in cholangiocytes. Therefore, chronic exposure to glyphosate contamination in environment and food may be a risk factor for CCA development.

Keywords: Cholangiocarcinoma, glyphosate, mutagenic DNA damage,

Introduction:

Cholangiocarcinoma (CCA) is the formation of a tumor in the epithelial cells of the biliary tree (1) and the second most prevalence primary hepatic malignancy around the world (2). The incidences of CCA are relatively high in Southeast Asia such as Thailand, Myanmar, Laos and Cambodia, because of daily consumption of pickled, raw or fermented fish in the population of these regions (2-4). Liver fluke endemic also has been found widely, and its infestation is the well-established risk factor in these areas. The consumption of parasite-infected fish in the population could be potential for the development of CCA (5). However, there are several risk factors that could link to CCA development. Some other common risk factors are high consumption of alcohol, hepatitis B and C virus infections, obesity (7, 9) as well as exposure to environmental and occupational chemical carcinogens (6).

Currently, the use of pesticide and herbicide is increasing worldwide to fulfill the food demands in the population (10). Overuse and misuse of pesticides and herbicide especially in developing countries could contaminate into the environment (11). As a consequence, pesticide residues have been detected in foods (10, 12). Many studies have shown that the exposure to pesticide intentionally and accidentally could be related to endocrine disruption and carcinogenesis (13). Glyphosate, a non-selective herbicide, was the highest selling worldwide and extensively used in more than 130 countries for over 100 crops due to its specific mode of action and less toxic effect to humans. In 2015, the International Agency for Research on Cancer (IARC) clarified the glyphosate as (Group 2A) probably carcinogenic to humans (14-16). Hence, the detection of glyphosate and its metabolite residues in soil, water and food products are becoming frequent.

Therefore, the present study conducted the preliminary assessment of the concentrations of glyphosate and its metabolite, aminomethylphosphonic acid (AMPA) in food including fish pastes and shrimp pastes and to investigate the potential development of cholangiocarcinoma caused by both acute and chronic exposure to glyphosate.

Objectives:

This study aimed to investigate the possible mechanisms of glyphosate-induced DNA damage and cell transformation in cholangiocytes (MMNK-1).

Methodology and Experimental protocol:

Preliminary assessment of the contamination of glyphosate in local food samples

In this study, three different types of local food samples such as fish paste, shrimp paste, and mixed shrimp-fish paste were purchased from local markets of Myanmar. Gas chromatography-tandem mass spectrometry (GC-MS/MS) was used to analyze the glyphosate and its major metabolite aminomethylphosphonic acid (AMPA) in food samples.

Investigation of the biological effects of glyphosate on cytotoxicity, DNA damage and cell transformation in MMNK-1

The immortalized cholangiocyte cell line, MMNK-1 cells were cultured and treated with various concentrations of glyphosate for 24 h and 7 days at 37ºC before harvesting. Then, determination of cell cytotoxicity, DNA damage and cell transformation were performed.

Determination of cytotoxicity: MMNK-1 cells (2 x 10^4 cells) were cultured and treated with various concentrations of glyphosate for 7 days. Cell viability was determined by using MTT assay in order to determine the non-cytotoxic concentrations of glyphosate to use for further experimental study.

Determination of DNA damage: MMNK- 1 cells were treated with non-cytotoxic concentrations of glyphosate (0.1, 0.5 and 1 ppm) for 7 days. After treatment, cells were collected and determined the formation of mutagenic DNA damage of 8- OHdG and 8-nitroguanine by using immunocytochemistry (ICC).

Determination of gene expression: MMNK- 1 cells treated with non-cytotoxic concentrations of glyphosate (0.1, 0.5 and 1 ppm) for 7 days. Subsequently, RNA extraction was performed following the manufacturer's protocol. Then, the extracted RNA was converted into cDNA, and the synthesized cDNA was used to detect the level of gene expression using real-time RT-PCR. The expression of various genes involved in DNA damage including *IL-6*, *IL-8*, *OGG1, XRCC1* and *Nrf2* were determined. *GADPH* was used as a reference gene.

Determination of cell transformation: MMNK-1 cells (6×10^4 cells) were cultured and treated with non-cytotoxic concentrations of glyphosate (0.1, 0.5 and 1 ppm) for 7 days. The treated cells were harvested and re-cultured (5×10^3 cells) in CytoSelected^{TM} 96-well for 7 days. The colony formation of transformed cells was measured by using MTT Assay.

Determination of DNA damage in transformed MMNK-1 cells: After transformation assay, the transformed cells (2×10^4 cells) were harvested and re-cultured in a 4-chambers slide, and incubated for 24 days at 37°C with 5% CO_2. The determination of DNA damage in transformed cells was performed by using ICC.

Statistical analysis: The results were expressed as the mean ± standard error of the mean (SEM). One-way analysis of variance (ANOVA) was used to analyze the results of *in vitro* cytotoxicity test and cell transformation, and student t-test was used to determine the statistically significant differences for the *in vitro* studies of DNA adduct, gene expression. Each experiment was performed in triplicates. A p-value of < 0.05 was considered as statistically significant.

Results and discussion:

Preliminary assessment of the contamination of glyphosate in local food samples

Concentrations of glyphosate and AMPA were determined in three different local food samples. The highest concentration of glyphosate was 61.60 ng/g which found in the shrimp paste, whereas the glyphosate concentrations in fish paste and mixed shrimp-fish paste were 35.7 ng/g and 25.36 ng/g respectively. In line with glyphosate contamination, the concentration of AMPA was 26.1, 24.6 and 22.2 ng/g, for shrimp paste, fish paste, and mixed shrimp-fish paste, respectively.

Investigation of the biological effects of glyphosate on cytotoxicity, DNA damage and cell transformation in MMNK-

Cell cytotoxicity

After treatment of glyphosate (0-10 ppm, 7 days), the viability of MMNK-1 cells was decreased 17%, 19% and 28% ($p < 0.01$) at the concentration of 0.1, 1 and 10 ppm, respectively when compared to untreated cells. Hence, the concentrations of glyphosate at 0.1, 0.5 and 1 ppm were chosen as non-cytotoxic concentrations for subsequent experiments. Moreover, these concentrations are comparable to environmentally relevant concentrations of glyphosate observed in food samples.

Determination of glyphosate treatment on DNA damage in MMNK-1 cells

To investigate the effect of glyphosate on oxidative DNA damage in cholangiocytes, MMNK-1 cells were treated with glyphosate at concentrations 0.1 ppm, 0.5 ppm and 1 ppm for 7 days. Mutagenic DNA damage formation, both 8-OHdG and 8-nitroguanine, was detected by using ICC assay. The results showed that fluorescence intensity of 8-OHdG was significantly increased ($p < 0.05$) in all treatment groups by 1.66-fold for 0.1 ppm, 1.79-fold for 0.5 ppm, and 1.52-fold for 1 ppm compared to those of control. In line with 8-OHdG formation, the fluorescence intensity of 8-nitroguanine was also significantly increased compared to control; by 1.61-, 2.01-, and 1.82-fold for 0.1, 0.5 and 1 ppm, respectively.

Determination of gene expression level in glyphosate treated MMNK-1 cells

Cells were treated with 0.1, 0.5 and 1ppm of glyphosate concentrations for 7 days. After treatment, transcript expressions of various genes were determined using qRT-PCR.

The result showed that mRNA level of *IL-6* was significant significantly increased at 0.5 ppm (1.58-fold, $p < 0.05$), then it slightly decreased (0.83-fold) at 1 ppm, compared to control. For *IL-8*, the expression level was significant increased (1.73-fold, $p < 0.01$) at 0.5 ppm, then, decreased at 1 ppm (0.54-fold, $p < 0.01$).

For DNA repair genes, the mRNA expression of *OGG1* was significantly increased at 0.5 ppm towards 1 ppm (1.33-fold, $p < 0.05$), compared to control. In the case of *XRCC1*, mRNA expression, all glyphosate treatment groups showed lower expression levels

On the other hand, mRNA level of *Nrf2* slightly decreased at 0.1 and 1 ppm, but significantly increased at 0.5 ppm (1.32-fold, $p < 0.01$).

Determination of the effect of glyphosate on malignant transformation in MMNK-1 cells

To study whether glyphosate induces malignant transformation, MMNK-1 cells were treated with glyphosate (0.1-1ppm, for 7 days). The ability of treated cell on malignant transformed was assessed by using soft agar transformation assay. The result showed that glyphosate-induced MMNK-1 cells transformation was observed signigicantly at the highest concentration (1 ppm) by 1.3-fold ($p < 0.05$), compared to that of untreated cells.

Analysis of glyphosate induced DNA damage in transformed MMNK-1 cells

To further investigate the formation of DNA damage in transformed MMNK-1 cells, the immunocytochemistry detection of 8-OHdG and 8-nitroguanine was carried out. The formation of 8-OHdG in all glyphosate treatment groups showed higher intensity staining of 8-OHdG in treated MMNK-1 cells than the control group. In contrast, level of 8-nitroguanine detected in transformed cell was significantly increased at 0.1 ppm (1.28-fold, $p < 0.01$), 0.5 ppm (1.32-fold, $p < 0.05$) and 1 ppm (1.19-fold, $p < 0.5$) when compared to control group.

Conclusion:

This study found that glyphosate and its metabolite (AMPA) residues can be detected in local food samples. *In vitro* study showed that glyphosate treatment can cause cytotoxicity, increase the formation of mutagenic DNA damage (8-OHdG and 8-nitroguanine) and induce cell transformation in cholangiocytes (MMNK-1 cells). Therefore, chronic exposure to glyphosate via food consumption could be one of the risk factors associated with CCA development.

References:

1. Malhi H, Gores G. The modern diagnosis and therapy of cholangiocarcinoma. Alimentary pharmacology & therapeutics. 2006;23(9):1287-96.
2. Blechacz B. Cholangiocarcinoma: Current Knowledge and New Developments. Gut Liver. 2017;11(1):13-26.
3. Alsaleh M, Leftley Z, Barbera TA, Sithithaworn P, Khuntikeo N, Loilome W, et al. Cholangiocarcinoma: a guide for the nonspecialist. International journal of general medicine. 2019;12:13.

4. Khuntikeo N, Titapun A, Loilome W, Yongvanit P, Thinkamrop B, Chamadol N, et al. Current Perspectives on Opisthorchiasis Control and Cholangiocarcinoma Detection in Southeast Asia. Frontiers in Medicine. 2018;5:117.
5. Myint E, Sereemaspun A, Rocklöv J, Nithikathkul C. Discovery of Carcinogenic Liver Fluke Metacercariae in Second Intermediate Hosts and Surveillance on Fish-Borne Trematode Metacercariae Infections in Mekong Region of Myanmar. International Journal of Environmental Research and Public Health. 2020;17:4108.
6. Squadroni M, Tondulli L, Gatta G, Mosconi S, Beretta G, Labianca R. Cholangiocarcinoma. Critical Reviews in Oncology/Hematology. 2017;116:11-31.
7. Ustundag Y, Bayraktar Y. Cholangiocarcinoma: a compact review of the literature. World J Gastroenterol. 2008;14(42):6458-66.
8. Sripa B, Pairojkul C. Cholangiocarcinoma: lessons from Thailand. Current opinion in gastroenterology. 2008;24(3):349-56.
9. Banales JM, Marin JJG, Lamarca A, Rodrigues PM, Khan SA, Roberts LR, et al. Cholangiocarcinoma 2020: the next horizon in mechanisms and management. Nature Reviews Gastroenterology & Hepatology. 2020;17(9):557-88.
10. Jin F, Wang J, Shao H, Jin M. Pesticide use and residue control in China. Journal of Pesticide Science. 2010:1004280123-.
11. González-Rodríguez R, Rial-Otero R, Cancho-Grande B, Gonzalez-Barreiro C, Simal-Gándara J. A review on the fate of pesticides during the processes within the food-production chain. Critical reviews in food science and nutrition. 2011;51(2):99-114.
12. Virgínia C. Fernandes VFD, Nuno Mateus, and Cristina Delerue-Matos. Determination of Pesticides in Fruit and Fruit Juices by Chromatographic Methods. An Overview. Journal of Chromatographic Science. 2011;49.
13. Soto AM, Sonnenschein C. Environmental causes of cancer: endocrine disruptors as carcinogens. Nat Rev Endocrinol. 2010;6(7):363-70.
14. (IARC) IAfRoC. Some organophosphate insecticides and herbicides. IARC Monographs on the Evaluation of Carcinogenic Risks to Humans. Geneva: World Health Organization Press. Available on the World Wide Web: https://monographs.iarc.fr/ENG/Monographs/vol112/mono112.pdf. (2017).
15. Brookes G. Glyphosate use in Asia and implications of possible restrictions on its use. AgBioForum. 2019;22:1.
16. (IARC) IAfRoC. Some organophosphate insecticides and herbicides. IARC Monographs on the Evaluation of Carcinogenic Risks to Humans. Geneva: World Health Organization Press. Available on the World Wide Web: https://monographs.iarc.fr/ENG/Monographs/vol112/mono112.pdf

EFFECTS OF GLYPHOSATE TREATMENT ON DNA DAMAGE IN UMBILICAL CORD-DERIVED MESENCHYMAL STEM CELLS AND DIFFERENTIATED HEPATOCYTES

Ratsameedara Krongsinlatham[1], Panida Navasumrit[1,2,3], Preeyanut Ratanayut[2] Somchamai Waraprasit[2], Varabhorn Parnlob[2], Mathuros Ruchirawat[1,2,3]

[1]Graduate Program of Environmental Toxicology, Chulabhorn Graduate Institute, Lak Si, Bangkok 10210, Thailand,
[2] Laboratory of Environmental Toxicology, Chulabhorn Research Institute, Lak Si, Bangkok 10210, Thailand,
[3]Center of Excellence on Environmental Health and Toxicology (EHT), OPS, MHESI, Thailand

Abstract:

Glyphosate is the most common herbicide use worldwide and has been classified as probably carcinogenic to human (Group 2A; IARC, 2015). In the recent years, there are concerns on its potential health effects on human with the raising evidence of its potential carcinogenicity. Most importantly, pregnant women are vulnerable groups and glyphosate can be passed through the placenta. Prenatal exposure to glyphosate-based herbicides can alter the fetal-placental circulation and affect embryonic development. Exposure to chemicals during pregnancy alters the number of stem cells during embryonic or fetal development and this may affect stem cell-based developmental processes that increase the risk of disease later in life. This study aimed to investigate the effects of glyphosate on the formation of DNA damage in umbilical cord mesenchymal stem cells (UC-MSCs) and in differentiated hepatocytes derived from UC-MSCs.

In vitro study of cytotoxicity of glyphosate treatment in human UC-MSCs cell line (0-100 ppm for 24 hours) using MTT assay showed that the cell viability was significant reduced to below 80% at 100 ppm, compared to the untreated cells. At the non-cytotoxic concentrations of glyphosate treatment (0-10 ppm, for 24 hours), immunocytochemistry detection of DNA damage showed significant increases in mutagenic DNA damage determined as 8-hydroxydeoxyguanosine (8-OHdG) and 8-nitroguanine in treated cells, compared to those of untreated cells. The maximum increased 8-OHdG and 8-nitroguanine in glyphosate-treated UC-MSCs was observed at 1 ppm. Upon UC-MSCs derived hepatocytes differentiation for 21 days, the expression of hepatic-specific gene markers including *ALB* (Albumin), a protein coding gene, was increased, and *SOX9*, a stemness marker, was decreased when compared to those of undifferentiated UC-MSCs. In addition, glyphosate treatment at 1 ppm caused significantly higher formation of 8-OHdG and 8-nitroguanine in differentiated hepatocytes than those of undifferentiated UC-MSCs. The increase in these mutagenic DNA damage was in agreement with increased inflammatory-related genes (*IL-6* and *IL-8*) and decreased DNA repair gene (*OGG1*).

In conclusion, this study suggested the potential risk of glyphosate on mutagenic DNA damage in fetal mesenchymal stem cells and differentiated hepatocytes which may increase risk of liver disease and cancer development later in life.

Keywords: Glyphosate, DNA damage, Umbilical cord mesenchymal stem cells (UC-MSCs), UC-MSCs-derived hepatocytes like cells

Introduction:

Glyphosate (N-phosphonomethyl-glycine), is the main active ingredient in glyphosate-based herbicide (GBH) called 'Roundup". It is a non-selective herbicide that is the most widely used in the world both in agricultural and non-agricultural areas. Glyphosate inhibit the shikimate pathway of the plant by acting on the enzyme 5-enolpyruvylshikimate-3-phosphate synthase (EPSPS) involved in the aromatic amino acid production. This pathway is found only in plants and microorganism but absent in animals (1). Due to the increase of glyphosate resistant crops the use of glyphosate has increased and leads to glyphosate residues in crops such as corn and soybean. In 2015, World Health Organization (WHO) International Agency for Research on Cancer (IARC) classified the herbicide glyphosate as "probably carcinogenic to humans"(2). For the past year glyphosate was considered safe for human as its mechanism of action does not target human. However, there are increasing evidence that glyphosate has DNA damaging properties, induce oxidative stress and endocrine disruptor (3-5). Increasing evidence suggests that glyphosate may cause adverse health effects on human beings such as liver disease.

Environment and dietary are the routes that human may be exposed to glyphosate. The contamination of glyphosate raises public concern as traces of glyphosate and its metabolite aminomethylphosphonic acid (AMPA) are found in vegetables, fruits and cereals (6, 7). This implies that human are indirectly exposed to glyphosate residues contaminated in food (8). Exposure during pregnancy also show an evidence of correlation of glyphosate exposure and shortened pregnancy length (9). Furthermore, prenatal exposure to glyphosate-based herbicides can alter the fetal-placental circulation and affect embryonic development (10-11). There are growing evidence that shows prenatal exposure increase the risk of autism spectrum disorder with comorbid intellectual disability in infants (12). It has been proposed that exposure to chemicals during pregnancy alters the number of stem cells during embryonic or fetal development and this may affect stem cell-based developmental processes that increase the risk of disease later in life. Umbilical cord mesenchymal stem cells (UC-MSCs) possess characteristics of stemness properties, highly self-renewal and multi-direction differentiation potential into multiple lineages including bone, cartilage, adipose tissue, neuronal cells and other tissues such as hepatocytes. Therefore, this study aimed to investigate the effects of glyphosate on the formation of 8-hydroxydoeoxyguanosine (8-OHdG) and 8-nitroguanoine which are mutagenic DNA damage in UC-MSCs cell line and UC-MSCs derived hepatocytes

Objectives:

The overall objective of this study is to investigate the effects of glyphosate exposure on DNA damage and transcript expression of genes related to DNA damage in cell line derived from umbilical cord mesenchymal stem cells (UC-MSCs) and in differentiated hepatocytes derived from UC-MSCs.

Methodology:

Cell viability by MTT assay

A human UC-MSCs cell line obtained from ATCC was cultured and treated with various concentrations of glyphosate (0-100 ppm) for 24 hours. After treatment, cell viability was determined by using MTT assay in order to determine the non-cytotoxic concentrations of glyphosate to use for further experimental investigations.

Determination of DNA damage by fluorescence immunocytochemistry

UC-MSCs cells were treated with non-cytotoxic concentrations of glyphosate (0-10 ppm) for 24 hours. After treatment, cells were collected and determined the formation of mutagenic DNA damage of 8-OHdG and 8-nitroguanine by using immunocytochemistry (ICC).

Analysis of transcript expression of DNA damage related genes by reverse transcriptase-polymerase chain reaction (RT-PCR)

UC-MSCs cells were treated with non-cytotoxic concentrations of glyphosate (0-10 ppm) for 24 hours. Subsequently, RNA extraction was performed following the manufacturer's protocol. Then, the extracted RNA was converted into cDNA, and the synthesized cDNA was used to detect the level of gene expression using real-time RT-PCR. The expression of various genes involved in DNA damage including DNA repair gene (*OGG1*) and inflammatory genes (*IL-6*, *IL-8*), were determined. GADPH was used as a reference gene.

Differentiation of hepatocyte-like cells

Hepatogenic differentiation of UC-MSCs was induced using a modified two-step hepatic standard protocol (13). The differentiated hepatocytes were characterized based on gene expression and functions tests; (albumin; ALB and stemmness marker; SOX9) were performed

During differentiation, cells were treated with glyphosate (0-10 ppm) for 21 days. Formation of DNA damage (8-OHdG and 8-nitroguanine) and expression of study genes (*OGG1*, *IL-6* and *IL-8*) in treated cells was determined.

Statistical analysis

The results were expressed as the mean ± standard error of the mean (SEM). Each experiment was performed in triplicates. Student t-test was used to determine the statistically significant differences between control and treatment group. A p-value of < 0.05 was considered as statistically significant.

Results and Discussion:

Cytotoxicity of glyphosate on UC-MSCs cell viability

After treatment of glyphosate (0-100 ppm, 24 hours), the viability of UC-MSCs was significantly decreased ($p < 0.05$) at the concentrations above 10 ppm, when compared to untreated cells. Hence, the concentrations of glyphosate at 0.10-10 ppm were chosen as non-cytotoxic concentrations for subsequent experiments.

Effects of glyphosate on DNA damage in UC-MSCs

In order to investigate whether glyphosate can induce DNA damage in fetal stem cells, UC-MSCs, which used as surrogate of fetal stem cells, were treated with glyphosate at non-cytotoxic concentrations (0.0-10 ppm), for 24 hours. Mutagenic DNA damage formation, both 8-OHdG and 8-nitroguanine, was detected by using ICC assay. The results showed that fluorescence intensity of 8-OHdG was significantly increased at all treated concentrations. The profile of the dose-response effects of glyphosate induced 8-OHdG showed a sharp increase at 0.1 ppm (1.44-fold, $p < 0.05$), reach a maximum increased at 1 ppm (1.70-fold, $p<0.01$), then slightly decreased (1.50-fold, $p<0.05$), when compared to those of control. In line with 8-OHdG formation, the fluorescence intensity of 8-nitroguanine was also significantly increased in treated UC-MSCs by 1.50-, 1.80 and 1.40-fold, at 0.1, 1 and 10 ppm, respectively.

Effects of glyphosate treatment on expression of genes related to DNA damage in UC-MSCs

In order to gain insight into possible mechanisms that contribute to glyphosate-induced 8-OHdG and 8-nitroguanine formation in UC-MSCs, the transcript levels of genes associated with DNA damage were determined including DNA repair (OGG1) AND inflammation (*CXCL6* and *CXCL8*).

UC-MSCs were treated with 0.10-10 ppm of glyphosate for 24 hours. After treatment, transcript expressions of various genes were determined using qRT-PCR. The result showed that the increase in these mutagenic DNA damage was in agreement with increased inflammatory-related genes (*IL-6* and *IL-8*) and decreased DNA repair gene (*OGG1*).

Effects of glyphosate treatment on DNA damage in differentiated hepatocyte derived from UC-MSCs

Characterization of hepatocyte-like cells derived from UC-MSCs

Initially, the potential for UC-MSC differentiation into hepatocyte-like cells was explored by determining of the presence of hepatocyte markers including morphology, mRNA expression of ALB (Albumin) and SOX9 (SRY-Related HMG-Box 9)

The morphological changes during UC-MSC differentiation showed the contraction of the cytoplasm progressed and most differentiated cells became dense and formed an ovoid shape with a polygonal structure. The expression of hepatic-specific gene markers was observed as an increased expression of *ALB* (Albumin), a protein coding gene, and decreased expression of *SOX9*, a stemness marker, when compared to those of undifferentiated UC-MSCs.

Glyphosate-induced DNA damage in differentiated hepatocyte

As reported earlier, glyphosate treatment increased 8-OHdG and 8-nitroguanine formation in UC-MSCs. In order to determine if this mutagenic DNA damage in UC-MSCs can persist upon differentiation into hepatocytes, 8-OHdG and 8-nitroguanine levels were examined in UC-MSCs treated with glyphosate during differentiation into hepatocytes after 21 days.

The results clearly showed that glyphosate treatment at 1 ppm significantly increased the formation of 8-OHdG and 8-nitrogiuanine in differentiated hepatocytes by 1.5-fold ($p < 0.05$), compared to those of undifferentiated cells.

Conclusion:

The *in vitro* study showed that glyphosate treatment can cause cytotoxicity and increase in 8-OHdG and 8-nitroguanine in UC-MSCs and differentiated hepatocytes. The obtained results suggested the potential risk of glyphosate on the formation of mutagenic DNA damage in fetal stem cells and in differentiated hepatocytes which may increase risk of liver disease and cancer development later in life.

References:

1. Xu J, Smith S, Smith G, Wang W, Li Y. Glyphosate contamination in grains and foods: An overview. Food Control. 2019;106:106710.
2. Gillezeau C, van Gerwen M, Shaffer RM, Rana I, Zhang L, Sheppard L, et al. The evidence of human exposure to glyphosate: a review. Environmental Health. 2019;18(1):2.
3. Koller VJ, Fürhacker M, Nersesyan A, Mišík M, Eisenbauer M, Knasmueller S. Cytotoxic and DNA-damaging properties of glyphosate and Roundup in human-derived buccal epithelial cells. Arch Toxicol. 2012;86(5):805-13.
4. Kašuba V, Milić M, Rozgaj R, Kopjar N, Mladinić M, Žunec S, et al. Effects of low doses of glyphosate on DNA damage, cell proliferation and oxidative stress in the HepG2 cell line. Environmental Science and Pollution Research. 2017;24(23):19267-81.
5. Gasnier C, Dumont C, Benachour N, Clair E, Chagnon MC, Séralini GE. Glyphosate-based herbicides are toxic and endocrine disruptors in human cell lines. Toxicology. 2009;262(3):184-91.
6. Zoller O, Rhyn P, Rupp H, Zarn JA, Geiser C. Glyphosate residues in Swiss market foods: monitoring and risk evaluation. Food Addit Contam Part B Surveill. 2018;11(2):83-91.
7. Kronberg M, Rossen A, Munarriz E. Glyphosate-based herbicides and oxidative stress. 2021. p. 79-90.
8. Agostini LP, Dettogni RS, dos Reis RS, Stur E, dos Santos EVW, Ventorim DP, et al. Effects of glyphosate exposure on human health: Insights from epidemiological and in vitro studies. Science of The Total Environment. 2020;705:135808.
9. Parvez S, Gerona R, Proctor C, Friesen M, Ashby J, Reiter J, et al. Glyphosate exposure in pregnancy and shortened gestational length: a prospective Indiana birth cohort study. Environmental Health. 2018;17.
10. Simasotchi C, Chissey A, Jungers G, Fournier T, Seralini GE, Gil S. A Glyphosate-Based Formulation but Not Glyphosate Alone Alters Human Placental Integrity. Toxics. 2021 9(9):220.
11. Serra L, Estienne A, Vasseur C, Froment P, Dupont J. Review: Mechanisms of Glyphosate and Glyphosate-Based Herbicides Action in Female and Male Fertility in Humans and Animal Models. Cells. 2021;10(11):3079.
12. von Ehrenstein OS, Ling C, Cui X, Cockburn M, Park AS, Yu F, et al. Prenatal and infant exposure to ambient pesticides and autism spectrum disorder in children: population based case-control study. BMJ. 2019;364:l962.
13. Panta, W., Imsoonthornruksa, S., Yoisungnern, T., Suksaweang, S., Ketudat-Cairns, M., & Parnpai, R. (2019). Enhanced Hepatogenic Differentiation of Human Wharton's Jelly-Derived Mesenchymal Stem Cells by Using Three-Step Protocol. International Journal of Molecular Sciences, 20(12), 3016. doi:10.3390/ijms20123016
14. Truzzi F, Mandrioli D, Gnudi F, Scheepers PTJ, Silbergeld EK, Belpoggi F, et al. Comparative Evaluation of the Cytotoxicity of Glyphosate-Based Herbicides and Glycine in L929 and Caco2 Cells. Front Public Health. 2021;9:643898.
15. Kašuba V, Milić M, Rozgaj R, Kopjar N, Mladinić M, Žunec S, et al. Effects of low doses of glyphosate on DNA damage, cell proliferation and oxidative stress in the HepG2 cell line. Environ Sci Pollut Res Int. 2017;24(23):19267-81.

EFFECTS OF POLYSTYRENE MICROPLASTIC PARTICLES ON DNA DAMAGE IN HUMAN BRONCHIAL EPITHELIAL CELLS

Thita Sangthongsuk[1], Panida Navasumrit[1,2,3], Potchanee Hunsonthi[2], Ankamene Buranarom[2], Thitirat Ngaotepprutaram[2], Mathuros Ruchirawat[1,2,3]

[1]Graduate Program of Environmental Toxicology, Chulabhorn Graduate Institute, Lak Si, Bangkok 10210, Thailand,
[2] Laboratory of Environmental Toxicology, Chulabhorn Research Institute, Lak Si, Bangkok 10210, Thailand,
[3]Center of Excellence on Environmental Health and Toxicology (EHT), OPS, MHESI, Thailand

Abstract:

Microplastics and nanoplastics are an emerging threat to environment and human health. Recent studies have demonstrated the existence of atmospheric pollution of micro-nanoplastics. Polystyrene micro-nanoplastics are one of the plastics most commonly used, which is also found contaminated in ambient air. Airborne micro-nanoplastics can be directly and continuously inhaled into human body, however health risks due to their inhalation remain unclear. This study aimed to investigate the effects of polystyrene nanoparticles on DNA damage in human bronchial epithelial (BEAS-2B) cells.

Human bronchial epithelial cells (BEAS-2B cells) were treated with polystyrene nanoparticles (100 nm) at various concentrations (0-1000 μg/ml) for 24 hours to determine cytotoxicity and to identify the non-cytotoxic concentrations of polystyrene to study the effects of polystyrene on DNA damage. The MTT assay showed that polystyrene significantly induced cytotoxic effects at the concentrations 500-1000 μg/ml. At the non-cytotoxic concentrations of treatment (0-100 μg/ml, 24 hour), a dose-dependent increase in the intracellular uptake of polystyrene nanoparticles was observed using flow cytometry analysis. Immunocytochemistry detection clearly revealed that levels of oxidative-stress mediated DNA damage measured as 8-hydroxydeoxyguanosine (8-OHdG) and 8-nitroguanine in BEAS-2B cells were significantly increased with increasing concentrations of polystyrene treatment. Furthermore, polystyrene nanoparticles reduced the transcript expression of DNA repair genes, *OGG1* and *XRCC1*, in BEAS-2B cells, compared to that of untreated cells.

Taken together, polystyrene nanoparticles can induce mutagenic DNA damage indicated as increased formation of 8-OHdG and 8-nitroguanine as well as reduced expression of DNA repair genes. These results suggest the potential health risk of exposure to airborne nanoplastics which may contribute to the pathogenesis of respiratory diseases.

Keywords: Micro-nanoplastics, oxidative DNA damage**,** DNA repair gene

Introduction:

Polystyrene plastics are one of the most commonly used types of plastics, and also found to have a low reuse rate. They are known to make into a foam material, and used as food containers, packaging, and utensils (1). The majority of plastic wastes get discarded improperly and as a result contributes to global warming, as well as more plastic wastes, in the form of microplastics (MPs) and nanoplastics (NPs).

Defining MPs in general, are less than 5mm in diameter, and NPs are within the size range from 1 to 1000 nm diameter (2). Plastic wastes, MPs and NPs contamination are known to already exist in oceans, and bodies of water for around 250,000 tons (3). Microplastics can

be passed up to humans up the food chain, from seafood consumption, table salt, sugar, bottled water and through fruits and vegetables from soil contamination (4, 5). Although many studies have shown the toxicity of MPs and NPs towards the environment and organisms, focusing on aquatic organisms, there are limited studies on human exposure and the toxicity of MPs and NPs towards human health.

Polystyrene micro-nanoplastics are one of the plastics most commonly used, which is also found contaminated in ambient air. Airborne micro-nanoplastics can be directly and continuously inhaled into human body. However, the effects of exposure to ambient air MPs and NPs on the human respiratory system remain unclear. Initially, existing studies suggest that MPs and NPs that enter the respiratory system can block the airway and may cause inflammatory reactions. This may lead to chronic diseases like chronic destructive pulmonary disease (6). However, the smaller particles can potentially penetrate into cells and enter the circulatory system to cause toxicity to other organs in the body. In addition, polystyrene nanoparticles were found to induce genotoxicity, affecting the inflammatory gene expression in human gastric adenocarcinoma epithelial cells (7). Therefore, the effects of polystyrene nanoparticles on DNA damage formation in respiratory cells and the possible mechanisms related to DNA damage are of particular interests for investigation.

Objective:

This study aimed to investigate the effects of polystyrene nanoparticles on mutagenic DNA damage and DNA damage-related genes on human lung bronchial epithelial cells (BEAS-2B). Evaluation of polystyrene-induced DNA damage was focused on the formation of 8-hydroxydeoxyguanosine (8-OHdG) and 8-nitroguanine. In addition, the transcript expression of DNA repair genes (*OGG1* and *XRCC1*) was investigated.

Methodology:

Cell culture

Human bronchial epithelial cells (BEAS-2B) were used to evaluate the toxicity of nanoparticles. The cells were cultured with DMEM with 10% FBS, 1% L-glutamine, and 1% pen-strep solution. Cells will be cultured in 37°C and 5% CO2 incubator.

Cell viability analysis

BEAS-2B cells were cultured and treated with polystyrene nanoparticles (100 nm in diameter, Sigma Aldrich, Product 43302) at various concentrations (0-1000 µg/ml) for 24 hours. After treatment, cell viability of treated BEAS-2 cells was ananlysed by MTT assay. The non-cytotoxic concentrations were determined and subjected to use in subsequent experiments.

Intracellular uptake

BEAS-2B cells were treated with polystyrene nanospheres Fluorophorex™ (Cat no 2211) with various concentrations (0-100 µg/ml, 24 hours). After cell treatment, the treated cells were collected and subjected to analysis in flow cytometer at the excitation 530 nm and emission 582 nm. The cellular uptake of nanoparticle was determined as the size and granularity of uptaken polystyrene nanaoparticles

Detection and determination of DNA damage

To determine the formation of DNA damage, the immunocytochemistry method will be used. The biomarkers of DNA damage used to measure DNA damage is 8-hydroxyguanine, a biomarker of free radical oxidation by reactive oxygen species, and 8-nitroguanine, a product of nitrative DNA damage caused by reactive nitrogen species which is a common occurrence in inflammation and carcinogenesis (8).

BEAS-2B cells (2 x 10^4 cells) were seeded and treated with the non-cytotoxic concentrations of polystyrene nanoparticles (0-100 µg/ml, 24 hours). After treatment, cells were washed and fixed onto the slides. Then, DNA was denatured and subjected to dual immunocytochemical detection of 8-OHdG and 8-nitroguanine (8-NO_2G). The fluorescence intensity staining was analyzed using fluorescence microscopy equipped with TissueFAXS (TissueGnostics).

Determination of *OGG1*, *IL-6* and *IL-8* expression using RT-PCR

BEAS-2B cells (2 x 10^4 cells) were treated with the non-cytotoxic concentrations of polystyrene nanoparticles (100 µg/ml, 24 hours). After treatment, cells were harvested, and the total RNA was isolated using the RNeasy mini kit (QIAGEN). Prior to quantification of gene expression, RNA was converted to cDNA, and the synthesized cDNA was used to detect the level of gene expression using real-time RT-PCR. The expression of DNA repair genes involved in repairing DNA damage including *OGG1* and *XRCC1* was determined. GADPH was used as a reference gene

Statistical analysis

The results were expressed as the mean ± standard error of the mean (SEM). The student t-test was used to determine the statistically significant differences between control and treatment gropus. Each experiment was performed in triplicates. A p-value of < 0.05 was considered as statistically significant

Results and Discussion:

Cytotoxic effects of polystyrene nanoparticles in BEAS-2B cells

This study was designed to determine the dose-response relationship between polystyrene nanoparticles treatment and cell viability in BEAS-2B cells. Furthermore, the non-cytotxic concentrations of UFPs was identified.

The cytotoxicity of polystyrene nanoparticles treatment in BEAS-2B cells was determined at various concentrations up to 100 µg/ml for 24 hours. The results showed that cell viability of treated cells was significantly decreased at 50 µg/ml towards 100 µg/ml ($P<0.05$). The concentrations of polystyrene nanoparticles up to 25 µg/ml gave rise to the cell viability above 90%. Therefore, the concentrations of polystyrene nanoparticles up to 25 µg/ml were selected as non-cytotoxic concentrations for subsequent experiments**.**

Intracellular uptake of polystyrene nanoparticles in BEAS-2B cells

The amount of intracellular polystyrene nanoparticles in BEAS-2B cells was increased with increasing concentrations of polystyrene nanoparticles. As shown in Figure 1, the percentage of the green area (B-gated) is the percentage of cells that have uptake polystyrene nanoparticles by 3%, 11% and 99% at the concentrations 25 µg/ml, 50 µg/ml and 100 µg/ml, respectively.

Based on the proposed mechanisms of NPs toxicity, this is either by endocytosis or simply permeabilizing through the membrane. With these initial reports, it corresponds with existing studies that polystyrene nanopartcles can be taken up by cells and be cytotoxic (10). In addition, the results are dose-dependent, where almost all cells uptake NPs at 100 µg/ml treatment.

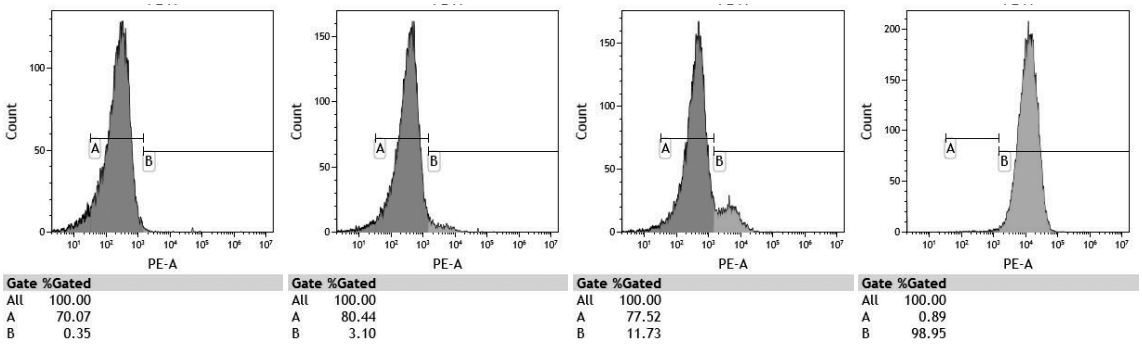

Figure 1 Flow cytometry analysis of intracellular uptake of polystyrene nanoparticles in BEAS-2B cells

Determination of polystyrene nanoparticles treatment on DNA damage in BEAS-2B cells

To investigate the effect of polystyrene nanoparticles on DNA damage in BEAS-2B cells, cells were treated with polystyrene nanoparticles at concentrations 0-100 µg/ml for 24 hours. Mutagenic DNA damage formation, both 8-OHdG and 8-nitroguanine, was detected by using immunocytochemical analysis. The results showed that fluorescence intensity of 8- OHdG was significantly increased ($p < 0.05$) in all treatment groups, compared to those of control. In line with 8-OHdG formation, the fluorescence intensity of 8-nitroguanine was also significantly increased compared to control

Both types of damage measured as 8-OHdG and 8-nitroguanine increases in a dose-dependent manner, indicating the mechanism of toxicity of MPs and NPs that induce reactive oxygen and nitrogen species. As mentioned in other studies, chronic toxicity for example cytotoxicity can lead to inflammation, and can also lead to DNA damage (11).

Determination of expression of DNA repair genes, *OGG1* and *XRCC1,* in treated BEAS-2B cells

Cells were treated with polystyrene nanoparticles (0-100 µg/ml for 24 hours). After treatment, transcript expressions of DNA reapir genes were determined using qRT-PCR.

The result showed that mRNA expression of *OGG1* and *XRCC1* was decreased in treated cells, compared to that of control.

Conclusion:

Polystyrene nanoplastic particles can induce mutagenic DNA damage indicated as increased formation of 8-OHdG and 8-nitroguanine as well as reduced expression of DNA repair genes. These results suggest the potential health risk of exposure to airborne nanoplastics which may contribute to the pathogenesis of respiratory diseases.

References:

1. Guimarães ATB, Estrela FN, Pereira PS, de Andrade Vieira JE, de Lima Rodrigues AS, Silva FG, et al. Toxicity of polystyrene nanoplastics in Ctenopharyngodon idella juveniles: A genotoxic, mutagenic and cytotoxic perspective. Science of the Total Environment. 2021;752:141937.
2. Campanale C, Massarelli C, Savino I, Locaputo V, Uricchio VF. A Detailed Review Study on Potential Effects of Microplastics and Additives of Concern on Human Health. International Journal of Environmental Research and Public Health. 2020;17(4).
3. Zhang R, Silic MR, Schaber A, Wasel O, Freeman JL, Sepúlveda MS. Exposure route affects the distribution and toxicity of polystyrene nanoplastics in zebrafish. Science of the Total Environment. 2020;724:138065.
4. Dong C-D, Chen C-W, Chen Y-C, Chen H-H, Lee J-S, Lin C-H. Polystyrene microplastic particles: In vitro pulmonary toxicity assessment. Journal of Hazardous Materials. 2020;385:121575.
5. Prata JC, da Costa JP, Lopes I, Duarte AC, Rocha-Santos T. Environmental exposure to microplastics: An overview on possible human health effects. The Science of the total environment. 2020;702:134455.
6. Hogg JC. Pathophysiology of airflow limitation in chronic obstructive pulmonary disease. Lancet. 2004;364(9435):709-21.
7. Forte M, Iachetta G, Tussellino M, Carotenuto R, Prisco M, De Falco M, et al. Polystyrene nanoparticles internalization in human gastric adenocarcinoma cells. Toxicology In Vitro. 2016;31:126-36.
8. Ohshima H, Sawa T, Akaike T. 8-nitroguanine, a product of nitrative DNA damage caused by reactive nitrogen species: formation, occurrence, and implications in inflammation and carcinogenesis. Antioxidants and Redox Signaling. 2006;8(5-6):1033-45.
9. Palaniappan S, Sadacharan CM, Rostama B. Polystyrene and Polyethylene Microplastics Decrease Cell Viability and Dysregulate Inflammatory and Oxidative Stress Markers of MDCK and L929 Cells In Vitro. Expo Health. 2022;14(1):75-85.
10. Yong CQY, Valiyaveettil S, Tang BL. Toxicity of Microplastics and Nanoplastics in Mammalian Systems. International Journal of Environmental Research and Public Health. 2020;17(5).
11. Prata JC. Airborne microplastics: Consequences to human health? Environmental Pollution. 2018;234:115-26.

EFFECTS OF ULTRAFINE PARTICLES ON DNA METHYLATION AND DNA ADDUCT IN UMBILICAL CORD-DERIVED MESENCHYMAL STEM CELLS

Noor Ul Ain[1], Panida Navasumrit [2,3,4], Ponpat Intarasunanont[3], Somchamai Waraprasit[3], Varabhorn Panlop[3] and Mathuros Ruchirawat[2,3,4]

[1]Applied Biological Sciences: Environmental Health Program, Chulabhorn Graduate Institute, Bangkok, Thailand
[2]Environmental Toxicology Program, Chulabhorn Graduate Institute, Lak Si, Bangkok10210, Thailand
[3]Laboratory of Environmental Toxicology, Chulabhorn Research Institute, Bangkok, Thailand
[4]Center of Excellence on Environmental Health and Toxicology (EHT), OPS, MHESI, Thailand

Abstract:

Exposure to particulate matter (PM) during pregnancy is associated with adverse birth outcomes and diseases development in later life. The ultrafine particles (UFPs, size ≤100 nm) are more potent than large particles due to their smaller size, large surface area to mass ratio, and ability to translocate to various organs resulting in inflammation and oxidative DNA damage. In addition, exposure to UFPs can cause epigenetic modifications, especially DNA methylation which regulate gene expression. *In utero* exposure to UFPs may impact the fetal and child health development through oxidative stress-mediated DNA methylation alterations and DNA damage resulting in disruption of stem cell differentiation. Thus, this study aimed to investigate the effects of exposure to UFPs in umbilical cord mesenchymal stem cells (UC-MSCs) on DNA methylation, both global and promoter methylation of inflammatory genes, inflammatory gene expression and inflammatory-related DNA adduct (*1,N^6*-etheno-2'deoxyadenosine DNA adduct, εdA).

The umbilical cord mesenchymal stem cells (UC-MSCs) were treated with various concentrations of UFPs up to 1 mg/ml for 24 h. According to cytoxicity test, UFPs treatment showed a dose-dependent decrease in viability of MSCs with a significant decrease at 1 mg/ml. UFPs at non-cytotoxic concentrations (0.05-0.5 mg/ml) were used for subsequent study. Pyrosequencing analysis of DNA methylation showed a significant change of global *LINE-1* methylation at 0.05, 0.1 and 0.25 mg/ml ($P<0.05$), while DNA methylation at the promoter region of *IL-6* and *IL-8* was significantly decreased at 0.05 and 0.1 mg/ml ($P<0.05$). In contrast, real time RT-PCR analysis showed a significant increase in expression of *IL-6* and *IL-8* in MSC treated with UFPs at at 0.05 and 0.1 mg/ml ($P<0.05$). Interestingly, the profile of promoter hypomethylation *IL-6* and *IL-8* was significantly negatively correlated with their transcript levels ($P<0.05$). By immunocytochemistry detection of DNA adduct, UFPs treatment showed a significant increase in εdA in UC-MSC and the highest formation was observed at 0.01 mg/ml by 1.7-fold ($p<0.01$), compared to that of untreated cell.

In conclusion, UFPs treatment in UC-MSC results in promoter DNA hypomethylation of inflammatory genes (*IL-6* and *IL-8*), which is correlated with increased transcription expression as well as enhanced formation of εdA, which is inflammatory-related mutagenic DNA adducts. Therefore, *in utero* exposure to UFPs on mutagenic DNA damage in MSCs should be further investigated, particularly the consequences on umbilical cord MSC differentiation and functions in order to prevent health risk of disease development later in life.

Keywords: Ultrafine particles, cord blood mesenchymal stem cells, DNA methylation, *1,N^6*-etheno-2'-deoxyadenosine, *LINE-1*, *IL-6*, *IL-8*

Introduction:

Exposure to particulate matter (PM) is one of the major risk factors for mortality and long-term health effects globally. The organic chemicals and toxic heavy metals present on traffic PM are associated with carcinogenesis and the development of respiratory and cardiovascular diseases and cancer (1, 2). The ultrafine particles (UFPs) having an aerodynamic diameter of ≤ 0.1nm are considered more potent as they can penetrate lungs and reach systemic circulation, thereby exerting toxicity to distant organs (3). Pregnant women are considered among the most vulnerable groups because maternal exposure to traffic can alter molecular events in the placenta and cause long-term chronic diseases in post-natal life (4). For instance, *in utero* exposure to traffic UFPs was associated with childhood cancer (2). Oxidative stress is one of the important mechanisms of particles induced toxicity that cause oxidation of DNA bases, proteins, and lipids and also initiates the activation of inflammatory responses. Including the transcriptional activation of inflammatory cytokines *IL-6* and *IL-8* resulting in inflammatory diseases (5). Many studies suggest an association of PM exposure with oxidative stress-induced DNA methylation changes that can cause altered gene expression and genomic instability resulting in malignancies. The methylation sites are highly located in repetitive elements such as Long interspersed element 1 (*LINE-1*) and *Alu* (6). In this study, the cytotoxicity of UFPs was determined at various concentrations. And the non-cytotoxic concentrations were used to determine the effect of UFPs on global *LINE-1* methylation and promotor methylation and gene expression of *IL-6* and *IL-8* in umbilical cord derived mesenchymal stem cells (UC-MSCs).

Materials and Methods:

Cell culture and cell treatment

The commercially mesenchymal stem cells (MSCs) derived from human umbilical cord were cultured in Minimum Essential Medium Alpha Medium (MEMα gibco™), 20% fetal bovine serum (FBS), 2% penicillin-streptomycin (pen-strep), and 2% L-glutamine.

Analysis of cell viability

The MSC were seeded in 96-well-plate at the density of 10,000 cells in 100 µl medium per well for 24 h. Subsequently, the medium was removed and cells were treated with UFPs suspension (0-1 mg/ml) in serum-free medium and incubated at 37°C. After 24 h of treatment, 10 µl of WST-1 reagent was added to each well and incubated for 2 h at 37°C. The absorbance was measured in each well at 450 nm using the microplate reader (SpectraMax® i3x). The non-cytotoxic concentrations were determined and subjected to use in subsequent experiments.

Determination of DNA methylation of *LINE-1*, *IL-6,* and *IL-8* using bisulfite pyrosequencing

The MSCs were treated with the non-cytotoxic concentrations of UFPs suspension (0-0.5 mg/ml) in the serum-free medium. After 24 h, the cells were harvested, and the DNA was extracted using QIAamp® DNA mini kit (QIAGEN). The DNA was bisulfite converted using EpiTech® Plus DNA Bisulfite kit (QIAGEN) and thermal cycler (Eppendorf). The bisulfite converted DNA was amplified using PyroMark PCR Master Mix, CoralLoad Concentrate, and PCR primers for *LINE-1*, *IL-6,* and *IL-8*. The PCR products were analyzed using gel electrophoresis. The pyrosequencing was performed using Streptavidin Sepharose HP beads, PyroMark and Binding Buffer. The PCR product was immobilized using beads in 96-well plate. The immobilized PCR product was captured using filter probes, washed sequentially with wash buffers, and released into PyroMark Q96 HS plate containing sequencing primer. The methylation level was analyzed using PyroMark CpG Software.

Determination of *IL-6* and *IL-8* expression using RT-PCR

The MSCs were treated with the non-cytotoxic concentrations of UFPs suspension (0-0.5 mg/ml) in the serum-free medium, for 24 h. After treatment, cells were harvested, and the total RNA was isolated using the RNeasy mini kit (QIAGEN). Prior to quantification of gene expression, RNA was converted to cDNA using qScript cDNA SuperMix (Quantabio) and thermal cycler (Eppendorf). The cDNA templates were analyzed for relative expression of *IL-6* and *IL-8* by CFX96^{TM} Real-Time system (BIO RAD), QuantiFast SYBRGreen RT-PCR kit (QIAGEN) with forward and reverse primers of each gene including *GAPDH*, used as reference gene in the reaction. The gene expression level was normalized with *GAPDH* using the ΔΔCT method.

Determination of *1,N^6*-etheno-2'-deoxyadenosine DNA adduct (εdA) using immunocytochemical detection

To determine εdA level using immunocytochemistry, 2.5 x 10^4 cells on chamber slides were treated with UFPs suspension at various concentrations (0-0.5 mg/ml) for 24 h. Subsequently, cells were washed, fixed using 95% ethanol and 0.05 N HCl and then permeabilization using RNAse A in 150 mM NaCl and 15 mM sodium citrate. The DNA was denatured with 0.15 N NaOH in 70% EtOH. After sequential washing with ethanol and PBS, the cells in chamber slides were incubated with 5 µg/ml proteinase K in 20 mM Tris, 1 mM EDTA, pH7.5 (T.E). Cells were washed with PBS and incubated with εdA primary antibody (1:250 dilution) at 37 °C for 1 h, followed by incubation of εdA secondary antibody Alexa Flour^{TM} 594 at 37 °C for 1 h. Before mounting cells were stained using DAPI for labelling nuclei. The fluorescence was measured using fluorescence microscopy and TissueFAXS (TissueGnostics).

Results and Discussion:

Cytotoxicity of UFPs treatment in UC-MSCs

This study was designed to determine the dose-response relationship between UFPs treatment and cell viability in MSCs. Furthermore, the non-cytotxic concentrations of UFPs was identified.

The cytotoxicity of UFPs treatment in UC-MSCs was determined at various concentrations up to 1 mg/ml, for 24 h using WST-1 assay. The results showed that cell viability of treated MSCs slightly decreased towards the concentration 0.5 mg/ml, however, the viability was significantly decreased at 1 mg/ml by approximately 80% ($P<0.05$). The concentrations of UFPs ≤ 0.5 mg/ml gave rise to the cell viability above 80%. Therefore, the concentrations of UFPS (0-0.5 mg/ml) were selected as non-cytotoxic concentrations for subsequent experiments**.**

Effect of UFPs treatment on global *LINE-1* methylation

Exposure to PM changes global DNA methylation. This study was conducted to investigate the effect of UFPs exposure on global *LINE-1* methylation.

After treatment with UFPs (0-0.5 mg/ml) for 24 h, the total methylation level calculated from 4 CpGs of *LINE-1* was significantly decreased at 0.05, 0.1 and 0.25 mg/ml and a non-significant decreased was seen at 0.5 mg/ml.

Effect of UFPs treatment on promoter DNA methylation of *IL-6* and *IL-8*

IL-6 and IL-8 are inflammatory mediators, and their dysregulation leads to chronic inflammation, autoimmunity, and other inflammation-related diseases such as cancer (7). Increased expression of *IL-6* and *IL-8* has been reported to be associated with PM exposure in experimental and epidemiological studies (8). Exposure to PM causes a change in methylation in specific genes and induces inflammation. This study was conducted to investigate whether UFPs exposure can alter specific gene methylation, such as promoter methylation of *IL-6* and IL-8.

The total methylation level at the promoter region was calculated from 4 and 3 CpG loci of *IL-6* and *IL-8* promoter regions, respectively. When compared to control, the promoter methylation level of *IL-6* showed a significant hypomethylation ($P<0.05$) at 0.05 mg/ml, then gradually increased. In contrast, promoter methylation of *IL-8* was significantly hypomethylated at 0.05 mg/ml ($P<0.05$), followed by hypermethylation towards 0.5 mg/ml.

Effect of UFPs treatment on gene expression of *IL-6 and IL-8*

According to DNA methylation regulates gene expression, this study was conducted to determine the gene expression of *IL-6* and *IL-8* in relation to their promoter methylation level.

The gene expression of *IL-6* significantly increased ($P<0.05$) at 0.05 mg/ml, and no significant effect was seen at increasing concentrations. In line with *IL-6* expression, the gene expression of *IL-8* was increased at 0.1 mg/ml ($P<0.05$), then gradually decreased towards 0.5 mg/ml.

A significant inverse correlation between gene expression and promoter DNA methylation was observed for *IL-6* ($r = -0.88$, $P=0.04$) and *IL-8* ($r= -0.98$, $P=0.002$). The results suggested that DNA methylation at the promoter region plays a significant role in control transcription expression.

Effect of UFPs treatment on the formation of εdA

The exposure to particulate air pollution induces oxidative stress and lipid peroxidation (9). This study aimed to determine the level of εdA adducts in UC-MSCs treated with various UFPs concentrations (0-0.5 mg/ml) for 24 h.

The formation of εdA adducts in treated MSCs significantly increased at 0.05, 0.1 and 0.25 mg/ml ($P<0.05$). A significant positive correlation of εdA with *IL-6* ($r =0.9$, $P=0.03$) and non-significant positive correlation with *IL-8* ($r=0.63$, $P=0.24$) was observed. The results suggest that the transcriptional activation of *IL-6* and *IL-8* may induce εdA adducts, the mechanism of which could be oxidative stress-mediated inflammatory responses.

Conclusion:

UFPs treatment in UC-MSC results in promoter DNA hypomethylation of inflammatory genes (*IL-6* and *IL-8*), which is correlated with increased transcription expression as well as enhanced formation of εdA adducts, which is inflammatory-related mutagenic DNA adducts.

Therefore, *in utero* exposure to UFPs on mutagenic DNA damage in MSCs should be further investigated, particularly the consequences on umbilical cord MSC differentiation and functions in order to prevent health risk of disease development later in life.

References:

1. Jakubiak-Lasocka J, Lasocki J, Siekmeier R, Chlopek Z. Impact of traffic-related air pollution on health. Environment Exposure to Pollutants: Springer; 2014. p. 21-9.
2. Lavigne E, Lima I, Hatzopoulou M, Van Ryswyk K, van Donkelaar A, Martin RV, et al. Ambient ultrafine particle concentrations and incidence of childhood cancers. Environment International. 2020;145:106135.
3. Kelly FJ, Fussell JC. Size, source and chemical composition as determinants of toxicity attributable to ambient particulate matter. Atmospheric environment. 2012;60:504-26.
4. Shang L, Huang L, Yang L, Leng L, Qi C, Xie G, et al. Impact of air pollution exposure during various periods of pregnancy on term birth weight: a large-sample, retrospective population-based cohort study. Environmental Science and Pollution Research. 2021;28(3):3296-306.
5. Ovrevik J, Refsnes M, Lag M, Holme JA, Schwarze PE. Activation of Proinflammatory Responses in Cells of the Airway Mucosa by Particulate Matter: Oxidant- and Non-Oxidant-Mediated Triggering Mechanisms. Biomolecules. 2015;5(3):1399-440.
6. Ding R, Jin Y, Liu X, Zhu Z, Zhang Y, Wang T, et al. Characteristics of DNA methylation changes induced by traffic-related air pollution. Mutation Research/Genetic Toxicology and Environmental Mutagenesis. 2016;796:46-53.
7. Tanaka T, Narazaki M, Kishimoto T. IL-6 in inflammation, immunity, and disease. Cold Spring Harb Perspect Biol. 2014;6(10):a016295-a.
8. He R-W, Gerlofs-Nijland ME, Boere J, Fokkens P, Leseman D, Janssen NAH, et al. Comparative toxicity of ultrafine particles around a major airport in human bronchial epithelial (Calu-3) cell model at the air–liquid interface. Toxicology in Vitro. 2020;68:104950.
9. Ambroz A, Vlkova V, Rossner P, Rossnerova A, Svecova V, Milcova A, et al. Impact of air pollution on oxidative DNA damage and lipid peroxidation in mothers and their newborns. International Journal of Hygiene and Environmental Health. 2016;219(6):545-56.

EFFECTS OF ULTRAFINE PARTICLES TREATMENT ON LIPID PEROXIDATION, DNA DAMAGE AND GENE EXPRESSION (*OGG1, PARP1* AND *Nrf2)* IN UMBILICAL CORD-DERIVED MESENCHYMAL STEM CELLS

Afreeda Mohideen[1], Panida Navasumrit[1,2,3], Preeyanut Ratanayut[2], Chanya Archapraditkul[2], Potchanee Hunsonti[2] and Mathuros Ruchirawat[1,2,3]

[1]Applied Biological Sciences: Environmental Health Program, Chulabhorn Graduate Institute, Lak Si, Bangkok 10210, Thailand,
[2]Laboratory of Environmental Toxicology, Chulabhorn Research Institute, Lak Si, Bangkok 10210, Thailand,
[3]Center of Excellence on Environmental Health and Toxicology (EHT), OPS, MHESI, Thailand

Abstract:

Particulate matter (PM) becomes a major environmental health concern, worldwide. The toxicity of PM depends on its chemical compositions and particle size. Ultrafine particles (UFP), a small particle size (≤ 0.1 μm), can translocate to the systemic circulation causing inflammation and oxidative stress-mediated to DNA damage. Emerging evidence indicates that prenatal exposure to UFPs can disrupt the *in utero* environment, influencing fetal developmental process which may affect health in later life. During early life, mesenchymal stem cells (MSCs) originate in the human embryo and have multipotent differentiation capability. Damage to the MSC system would serious affect the maintenance of steady-state conditions. Therefore, this study aimed to investigate the effects of exposure to UFPs on oxidative stress-mediated lipid peroxidation, mutagenic DNA damage and expression of genes associated with DNA damage in umbilical cord-derived mesenchymal stem cells (UC-MSCs).

The results showed that UC-MSCs treated with UFPs (0-1 mg/ml for 24 hours) caused a significant cytotoxic effect at 1 mg/ml. At the non-cytotoxic concentrations treatment (0- 0.5 mg/ml, 24 hours), lipid peroxidation measured as malondialdehyde (MDA) was significantly increased with increasing concentrations of UFPs in UC-MSCs. This was in line with the significant increases in MDA-DNA adducts (M_1dG) in treated cells. In addition, immunocytochemical detection of 8-hydroxydeoxyguanosine (8-OHdG) and 8-nitroguanine showed significantly increases in UC-MSCs at all concentrations. In addition, the expression of genes related to DNA damage (*OGG1*, *PARP1* and *Nrf*2) was altered. When compared to control cell, the transcript expression of *OGG1* and *Nrf2* was increased, while *PARP1* was decreased in treated cells.

In conclusion, the *in vitro* study clearly showed that UFPs increases lipid peroxidation and mutagenic DNA damage including MDA-DNA adducts, 8-OHdG and 8-nitroguanine in UC-MSCs. The obtained results suggested that exposure to UFPs could have detrimental health impacts, particularly at prenatal exposure. Therefore, it is necessary to increase the public awareness and establish guidelines of environmental exposure to UFPs in order to prevent human health risks.

Keywords: Ultrafine particle, lipid peroxidation, DNA damage, DNA repair genes

Introduction:

Air pollution is one of the greatest environmental concern worldwide, not just because of its effect on climate change, but also because of its impact on public and individual health due to increased morbidity and mortality (1, 2) . Recently, World Health Organization (WHO) estimated that almost 4.2 million deaths occur every year from exposure to air pollution. Moreover, the WHO describes six major air pollutants, explicitly ambient particle pollution, ground-level ozone, carbon monoxide, sulfur oxides, nitrogen oxides, and lead. Predominantly ground-level ozone and particulate matter (PM) are the most common air contaminants. Outdoor air pollution has been categorized as Group 1 carcinogen (carcinogen to humans) by IARC (3). PM is varied by particle sizes: coarse particles diameter 2.5 to 10 μm (PM_{10}), fine particles diameter less than 2.5 μm ($PM_{2.5}$), and ultrafine particles (UFPs) diameter less than 0.1 μm ($PM_{0.1}$) (2, 4). Combustion sources, in particular, motor vehicles emissions are a significant source of UFPs (5).The international agency for research on cancer (IARC) has classified outdoor air pollution and PM as group 1 (Carcinogenic to humans) (6). Exposure to air pollutants has linked to a wide a range of health effects including impaired lung function, asthma, myocardial infarction, lung cancer and mortality (1). Furthermore, according to WHO, in 2016 it was reported that exposure to ambient particulate matters such as fine particles like PM (2.5) and UFPs like ($PM_{0.1}$) are known to cause premature mortality in more than 3 million people worldwide (7).

Mesenchymal Stem cells (MSC) are described as undifferentiated cells and are also known as multipotent stem cells that originate in the human embryo. They have the potential to self-renew and differentiate into a variety of cell types, including chondrocytes, adipocytes, osteocytes, myocytes and neuron-like cells (8). MSC can be extracted from a variety of sources including bone, marrow, adipose tissue, placenta and umbilical cord blood. The period of fetal development is a critical period of vulnerability, during which exposure can result in negative health outcomes at birth and later in life. The placenta acts as a barrier between the mother and the fetus (9). Due to the technological challenges and ethical concerns, data regarding the barrier capacity of placenta and UFPs or nanoparticle is limited (10). However, epidemiologic studies showed that pregnant women and developing embryos and fetuses encompass a particularly vulnerable population as ultrafine nanoparticles that infiltrate the bloodstream that may reach the placenta and possibly the fetus (9, 10). There is also a growing epidemiologic evidence of associations between maternal exposure to ambient air pollution and adverse birth outcomes such as preterm birth, low birth weight and some common pregnancy complications such as preeclampsia and gestational diabetes mellitus.

Therefore, it is of interest to study the effects of UFPs exposure on oxidative stress-mediated mutagenic DNA damage in umbilical cord-derived MSCs.

Objective:

This study aimed to assess the genotoxic effects associated with UFPs exposure focusing on lipid peroxidation, mutagenic DNA damage and expression of genes related to DNA repair and anti-oxidative response in UC-MSC.

Method and experimental protocol:

Cell culture: Human umbilical cord mesenchymal stem cell (UC-MSC) obtained from ATCC was used to study the effects of UFPs treatment. The UC-MSC cells were cultured in complete medium that consisted of basal medium supplement with 10% FBS, 1%L-Glutamine and 1%Penicillin/Streptomycin.

Cytotoxicity testing: UC-MSC ($1x10^4$ cells) were cultured and treated with various concentrations of UFPS (0-1 mg/ml) in serum free medium for 1hr. After treatment, cell viability was determined by WST-1 method.

Determination of Lipid Peroxidation: Cells were cultured and treated with various concentrations of UFPs (0- 0.50 mg/ml) for 24 h. Subsequently, lipid peroxidation in control or treated cells was determined by measurement of malondialdehyde (MDA) by immunocytochemistry using primary antibody (MDA) and secondary antibody (594, Alexa Fluor combined with phalloedein. The fluorescence intensity of cytoplasmic staining of MDA was measured using fluorescence microscopy and TissueFAXS (TissueGnostics) analysis.

Determination of mutagenic DNA damage: UC-MSC were cultured in DMEM medium at 37 °C with 5% CO_2 and seeded in T75 flask. Cells were treated with various concentrations of UFPs (0- 0.50 mg/ml) for 24 h. Various types of mutagenic DNA damage including lipid peroxidation-derived malondialdehyde DNA adduct (M_1dG), 8-hydroxydeoxyguanosine (8-OHdG) and 8-nitroguanine were determined by immunocytochemistry. The fluorescence intensity in nuclei staining was measured using fluorescence microscopy and TissueFAXS (TissueGnostics) analysis.

Determination of gene expression of OGG-1 PARP-1 and Nrf2: UC-MSC were cultured and treated with UFPs 0- 0.50 mg/ml) for 24 h. The mRNA expression of *OGG-1*, *PARP-1* and *Nrf-2* was analyzed by quantitative real-time-polymerase chain reaction (RT-PCR). The expression of these genes was expressed in relation to the reference gene.

Statistical analysis: The statistical program prism software was used to analyze the statistical value. The statistical significance of the difference between each group was tested by student-t test Welch's correction. An independent sample t-test was used to evaluate the statistical significance of the difference between treatment and control group. A probability value (p-value) less than 0.05 was considered as a statistical significance.

Results and Discussions:

Cytotoxic effects of UFP treatment in UC-MSCs

UC-MSC treated with UFP (0-1 mg/ml) was significant decreased in cell viability (below 80%) at the concentration of 1 mg/ml ($p<0.05$). Therefore, UFPs at non- cytotoxic concentrations ranging from 0.01-0.50 mg/ml were used for all subsequent studies.

Effect of UFP treatment on lipid peroxidation measured as MDA

Polyunsaturated fatty acids are subject to oxidation giving rise to lipid hydro peroxides as the initial step in ROS generation. The effect of UFP on lipid peroxidation measured as MDA was determined in this study.

The image analysis of UC-MSC treated with UFP (0-0.5 mg/ml, 24 h) revealed that the intensity of cytoplasmic staining of MDA in UC-MSCs was increased with increasing concentration of UFPs in a dose dependent manner. When compared to the control, the level of MDA in UFP-treated cells increased at all concentrations of UFP treatment which was 1.34-fold ($p<0.05$),1.6-fold ($p<0.1$),1.75- fold ($p<0.25$) and 2-fold ($p<0.5$) respectively.

UFP treatment induces mutagenic DNA damage in UC-MSC

(1) Lipid peroxidation derived-MDA DNA adduct, M_1dG

MDA is a degradation product of lipid peroxidation that can react with DNA to form exocyclic adducts such as M_1dG. After UFPs treatment (0-0.50 mg/ml), the intensity of nuclei staining of M_1dG in treated UC-MSCs was increased with increasing concentrations of UFPs in a dose dependent manner. When compared to the control, the level of M1dG in UFPs treated cells increased at all concentrations of UFPs treatment which was ($p<0.05$), 1.6-fold ($p<0.1$), 1.77-fold ($p<0.25$) and 1.75-fold ($p<0.5$) respectively.

(2) Oxidative DNA damage measured as 8-OHdG

Due to UFP can induce generation of ROS, this study was conducted to determined oxidative DNA damage in UC-MSC. It is clearly showed that the UFP treatment (0- 0.5 mg/ml for 24) induces 8-OHdG indicated as increased fluorescence intensity staining of 8-OHdG in treated UC-MSCs. The level of 8-OHdG in UFP- treated cells increased at all concentrations of UFP treatment which was 1.22-fold ($p<0.05$), 1.25-fold ($p<0.1$), 2-fold ($p<0.25$) and 2.6-fold ($p<0.5$) respectively.

(3) Nitrative DNA damage, 8-nitroguanine

To determine whether the UFP can induce nitrative stress mediated to DNA damage, UC-MSCs were treated with UFP (0- 0.5 mg/ml) for 24 h. The results showed that the level of immunofluorescence intensity staining of 8-nitroguanine in UC-MSC was increased with increasing concentration. The level of 8-nitroguanine in UFPs treated cells increased at all concentrations of UFP treatment which was 1.3-fold ($p<0.05$), 1.71-fold ($p<0.1$), 2.1-fold ($p<0.25$) and 2-fold ($p<0.5$) respectively.

Effect of UFPs treatment on mRNA expression of *OGG1*, *PARP-1 and Nrf-2*,

In order to investigate whether UFP-induced DNA damage in UC-MSCs can be affected by the expression of genes related to DNA damage, the mRNA expression of DNA repair gene (*OGG1* and *PARP1*) and anti-oxidative response gene (Nrf2) were determined. The results showed that the transcript expressions of *OGG1* and *Nrf2* were significantly decreased, while the expression of *PARP-1* was significantly increased in UC-MSCs treated with UFPs.

Conclusion:

This *in vitro* study clearly demonstrated that UFPs treatment increases lipid peroxidation and mutagenic DNA damage including MDA-DNA adducts, 8-OHdG and 8-nitroguanine in UC-MSCs. The obtained results suggested that exposure to UFPs could have detrimental health impacts to MSC, particularly at prenatal exposure.

References:

1. Jiang X-Q, Mei X-D, Feng D. Air pollution and chronic airway diseases: what should people know and do? Journal of thoracic disease. 2016;8(1):E31.
2. Manisalidis I, Stavropoulou E, Stavropoulos A, Bezirtzoglou E. Environmental and health impacts of air pollution: a review. Frontiers in public health. 2020;8.
3. Loomis D, Grosse Y, Lauby-Secretan B, El Ghissassi F, Bouvard V, Benbrahim-Tallaa L, et al. The carcinogenicity of outdoor air pollution. Lancet Oncology. 2013;14(13):1262-3.

4. Kulas JA, Hettwer JV, Sohrabi M, Melvin JE, Manocha GD, Puig KL, et al. In utero exposure to fine particulate matter results in an altered neuroimmune phenotype in adult mice. Environmental Pollution. 2018;241:279-88.
5. De Kok TM, Driece HA, Hogervorst JG, Briedé JJ. Toxicological assessment of ambient and traffic-related particulate matter: a review of recent studies. Mutation Research/Reviews in Mutation Research. 2006;613(2-3):103-22.
6. Loomis D, Grosse Y, Lauby-Secretan B, El Ghissassi F, Bouvard V, Benbrahim-Tallaa L, et al. The carcinogenicity of outdoor air pollution. Lancet Oncology. 2013;14(13):1262.
7. Brook RD, Rajagopalan S, Pope III CA, Brook JR, Bhatnagar A, Diez-Roux AV, et al. Particulate matter air pollution and cardiovascular disease: an update to the scientific statement from the American Heart Association. Circulation. 2010;121(21):2331-78.
8. Kim J-Y, Jeon HB, Yang YS, Oh W, Chang JW. Application of human umbilical cord blood-derived mesenchymal stem cells in disease models. World journal of stem cells. 2010;2(2):34.
9. Bové H, Bongaerts E, Slenders E, Bijnens EM, Saenen ND, Gyselaers W, et al. Ambient black carbon particles reach the fetal side of human placenta. Nature communications. 2019;10(1):1-7.
10. Bongaerts E, Nawrot TS, Van Pee T, Ameloot M, Bové H. Translocation of (ultra) fine particles and nanoparticles across the placenta; a systematic review on the evidence of in vitro, ex vivo, and in vivo studies. Particle and fibre toxicology. 2020;17(1):1-26.

FORECASTING PM $_{2.5}$ CONCENTRATION IN BANGKOK, THAILAND BY TIME SERIES ANALYSIS

Siriwimol Wetjakwen[1,2], Suwimon Kanchanasuta[*1,2], Chatchawal Singhakant[1,2], Thongchai Kanabkaew[3] and Sirapong Sooktawee[4]

[1]Department of Environmental Health Sciences, Faculty of Public Health, Mahidol University, Thailand

[2]Center of Excellence on Environmental Health and Toxicology (EHT), OPS, MHESI, Thailand

[3]Faculty of Public Health, Thammasat University, Thailand.

[4]Environmental Research and Training Center, Department of Environmental Quality Promotion, Ministry of Natural Resources and Environment, Thailand.

**Corresponding author: Suwimon.kan@mahidol.ac.th*

Abstract:

One of the key challenges to completing the Sustainable Development Goals (SDG) is through successfully mitigating the microparticle issue. To track this, a time series analysis was implemented for this study. The Prophet Forecasting Model can predict the tendency of particles with a diameter 2.5 micrometers and smaller ($PM_{2.5}$). This research was divided into three phases for preparation and prediction for $PM_{2.5}$ as follows: 1. Selecting the appropriate duration 2. Forecasting $PM_{2.5}$ concentration by the Prophet Forecasting Model 3. Evaluation of the result from Prophet Forecasting Model. Results in the first part are considered by MSE (Mean Square Error), RMSE (Root-Mean Square Error), MAE (Mean Absolute Error), and coverage leading to the selection the nine-month period. When considering a coverage value of roughly 0.80, nine months was determined to be the best appropriate duration. Then the data collected from air monitoring stations of the Pollution Control Department's (PCD) six stations was selected. These had less missing data compared with the other stations were predicted by The Prophet Forecasting Model. This generated data was used for forecasting $PM_{2.5}$ concentration over a period of nine months for the next 10 days. For analysis, the performance of the model was evaluated by using a 2 x 2 contingency table to project the data that was separated into seven distinct days of the week and continued for over 10 days. The four values of MSE, RMSE, MAE, and COVERAGE demonstrated that the value were not greater than one, with maximum and minimum values of 1.04 and 0.06, respectively. When comparing with the WHO Guideline and Thailand Standards, the results showed that the observed values and forecasted values could not compare because the model displays the trend of the expected value from secondary data. All these results have shown that the Prophet Forecasting Model has a strong power to predict. However, this model did not use meteorology data. As shown with the study data, this model needed to be created in a format that can accurately predict pollution based on time.

Keywords: Air pollution, $PM_{2.5}$, Prophet forecasting model, time series analysis

Rationales and background:

Recently, many studies have shown concern about urban environments, and $PM_{2.5}$ levels. Some research has investigated the ability to predict the future concentration of $PM_{2.5}$ in urban air. Other cases described how $PM_{2.5}$ has an impact on human health. One study of identifying critical supply chain paths and key sectors for mitigating primary carbonaceous $PM_{2.5}$ mortality in Asia described how $PM_{2.5}$ is the leading cause of fatalities in Asia estimated at 2.3 million deaths per year (1) . In 2016 outdoor air pollution caused

4.2 million deaths around the world sourcing from the emissions of on-road vehicles, which is the primary source of air pollution in urban areas. (2)

In 2012 the Cabinet of Thailand had a meeting regarding how particulate pollution concentrations were higher than the standard levels in Thailand. Spikes in pollution occur regularly and is a problem in many provinces including Bangkok and surrounding areas that directly affect the environment economy and public health. The very nature of air pollution allows it to spread and expand to other neighboring provinces in the region as well. Major particulate sources include burning in the open air, transportation, traffic, and industry. Solving such problems requires careful action locally and politically. Current data of $PM_{2.5}$ in AQI form cannot predict $PM_{2.5}$ in real-time over smaller time frames such as a t few hours. The current implementation of AQI requires calculation by an equation before being shown to the public and presented in the five levels of AQI report for the six main air pollutants: $PM_{2.5}$, PM_{10}, O_3, CO, NO_2 and SO_2 .

This study uses The Prophet Forecasting Model which predicts the concentration of air pollutants and forecast accurately when not considering the meteorological conditions by using secondary data from the Air Quality and Noise Management Division Bangkok. The data for the model was collected from a total of 50 stations. After data processing it was discovered that only 24 stations have observations for $PM_{2.5}$ concentration data and to be implemented for prediction from Pollution Control Department six stations.

Methodology:

This study took the following steps to implement The Prophet Forecasting Model to predict $PM_{2.5}$ concentrations in Bangkok, Thailand. At first, the model will need to select an appropriate duration. After the duration is determined, it is then required to validate the Prophet Forecasting Model.

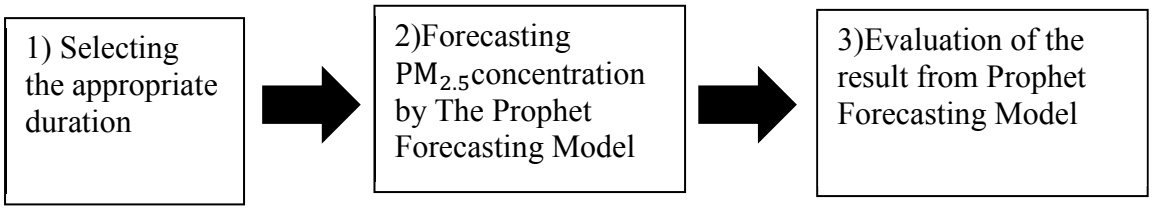

Selecting the appropriate duration

Nine months was chosen as the appropriate time period because it was the maximum indicator. The nine-month data that MAE, MSE, RMSE, and COVERAGE measures took into consideration was the appropriate period. Number of stations with value where MAE, MSE, and RMSE results should be close to 0 (3) based on each statistic's explanation. Coverage should have been at least 0.8 and almost 1(4).

Forecasting $PM_{2.5}$ concentration by The Prophet Forecasting Model

The results were used to adjust the step's time duration. This approach used secondary data from the Pollution Control Department (PCD), selected from 12 stations by less missing data acquired from six stations, to forecast the $PM_{2.5}$ concentration over a period of nine months. The performance of the model was assessed by using a 2 x 2 contingency table. The expected value for six stations was obtained first. The second step was to determine how many times the standard had been exceeded. The Thailand requirement is 50 $\mu g/m^3$, but the WHO guidelines are 25 and 15 $\mu g/m^3$.

Evaluation of the result from Prophet Forecasting Model

Evaluation was done after receiving all the results and then will be inputted into R program. The focus is searching for a consecutive period that is over multiple standards. Results showed in figure 1:

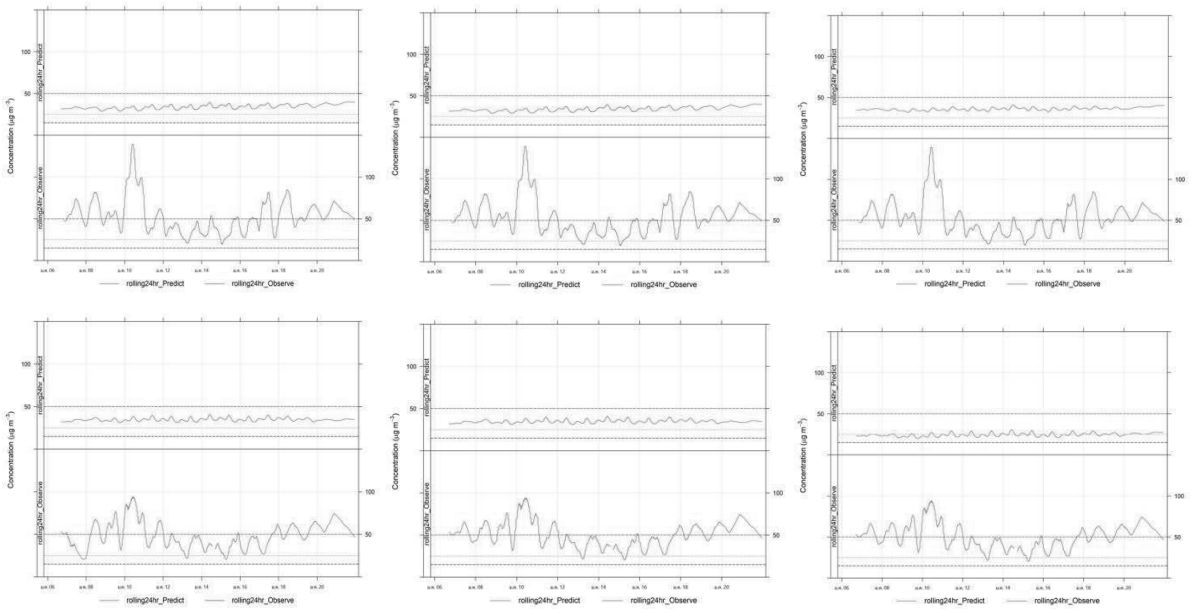

Figure 1 Graph shows all forecasting data and observe data compared between all standards.

The result showed that there are the period over the standard 25 shown in table1.

Table1 The consecutive period of six stations compared with all standards.

	MODEL						Obs				
STATION	TH 50	WHO 25	WHO 15	W25/ TH	w15/ TH	**STATION**	TH 50	WHO 25	WHO 15	W25/ TH	W15/ TH
05t	0	1680	1680	0	0	**05t**	23	810	1680	35.2	73
11t	0	1680	1680	0	0	**11t**	23	810	1680	35.2	73
50t	0	1680	1680	0	0	**50t**	31	161	1680	5.1	54.2
52t	0	1680	1680	0	0	**52t**	32	150	1415	4.6	44.2
53t	0	1680	1680	0	0	**53t**	31	161	1680	5.03	54.1
54t	0	38	1680	0	0	**54t**	32	161	1680	5.03	52.5

Summary of research results:

All these results from Figure 1 and Table from The Prophet Forecasting Model showed that the model has a good performance to predict $PM_{2.5}$. This model did not use meteorology data but it required in order to created that can accurately predict pollution based on time. (2) The lack of meteorological data affects why the model may not predict events that might happen at unexpected times.

Recommendation:

In the future, The Prophet Forecasting Model should be more used in regions without tools for model meteorology. Also, the future researchers should input more local and geographical sensitive situational events into the Prophet Forecasting Model. This would ultimately result in prediction of events with greater accuracy.

Reference:

1. Nagashima F, Kagawa S, Suh S, Nansai K, Moran D. Identifying critical supply chain paths and key sectors for mitigating primary carbonaceous PM $_{2.5}$ mortality in Asia. Econ Syst Res. 2017 Jan 2;29(1):105–23.
2. World Health Organization (WHO). Ambient (outdoor) air pollution [Internet]. 2018. Available from: https://www.who.int/news-room/fact-sheets/detail/ambient-(outdoor)-air-quality-and-health
3. Shen J, Valagolam D, McCalla S. Prophet forecasting model: a machine learning approach to predict the concentration of air pollutants ($PM_{2.5}$, PM_{10}, O_3, NO_2, SO_2, CO) in Seoul, South Korea. PeerJ. 2020 Sep 15;8:e9961.
4. Sean Taylor, Ben Letham. Automatic Forecasting Procedure. 2021 Mar 8; Available from: https://cran.r-project.org/web/packages/prophet/prophet.pdf

MODULATION OF ARSENIC-INDUCED DNA DAMAGE BY INSULIN IN NEUROBLASTOMA SH-SY5Y CELLS

Cheryl Lynn Tan[1,2], Piyajit Watcharasit[1,2,3] and Jutamaad Satayavivad[1,2,3]

[1]Laboratory of Pharmacology, Chulabhorn Research Institute, Thailand
[2]Environmental Toxicology, Chulabhorn Graduate Institute, Thailand
[3]Center of Excellence on Environmental Health and Toxicology (EHT), OPS, MHESI, Thailand

Abstract:

Arsenic (As) is known to induce reactive oxygen species (ROS) production leading to oxidative stress and subsequently, to DNA damage. ROS and DNA double strand break (DSB) triggering an optimal ATM-mediated DNA damage response (DDR) have been shown to require insulin-like growth factor-1 receptor (IGF-1R) signaling. Because of similarities between IGR-1R and insulin receptor (IR) signaling hence, the present study aimed to investigate whether IR signaling also played a role in DDR induced by As. SH-SY5Y cells were treated with $NaAsO_2$ with or without insulin. Immunoblotting was used to detect γH2AX, a marker of DSB, and DDR proteins including pChk2, p53 and p21 while immunofluorescent staining was performed to detect 8-oxo-dG, a marker of oxidative DNA damage. The results showed that insulin did not significantly alter As-induced γH2AX, pChk2, p53 and p21 levels suggesting that insulin signaling could not modulate $NaAsO_2$-induced DSB and DDR. However, disruption of insulin signaling by HNMPA-$(AM)_3$ which inhibits IR kinase activity reduced $NaAsO_2$-induced γH2AX and almost completely abolished DDR proteins (pChk2, p53 and p21) suggesting an inhibitory effect of insulin signaling disruption on As-induced DDR. 8-OHdG immunofluorescent staining revealed that $NaAsO_2$ significantly increased 8-oxo-dG while $NaAsO_2$ and insulin co-treatment has slightly lower 8-oxo-dG compared to the $NaAsO_2$ alone indicating that insulin signaling attenuated As-induced base oxidation. Taken together, the present study demonstrates that insulin signaling is essential for optimal activation of DDR, and insulin signaling mildly modulates As-induced 8-oxo-dG but has little mild effect in As-induced DSB.

Keywords: Arsenic, DNA Double-strand break, 8-oxo-dG, DNA damage response, Insulin

Introduction:

Arsenic (As) is a highly toxic metalloid known for its carcinogenicity. Inorganic As has been classified as a human carcinogen by the International Agency for Research on Cancer (IARC, 1987) based on epidemiological data showing that As exposure increases the risk for certain types of cancer[1, 2]. One of the mechanisms by which As causes cancer is by induction of reactive oxygen species (ROS) production which leads to oxidative stress and subsequently, to oxidative DNA damage such as double strand break (DSB) and base oxidation[2]. ROS and DSB are known to activate an ATM-mediated DNA damage response (DDR)[3, 4] which has been reported to require an intact insulin-like growth factor-1 receptor (IGF-1R) signaling, the disruption of which causes a suboptimal response to DNA damage[5, 6]. Because IGF-1R and insulin receptor (IR) signaling, and their intracellular signaling are highly homologous[7], these signaling pathways are believed to crosstalk leading to the plausibility that IR signaling may also potentially play a role in DNA damage response. Therefore, the present study aimed to investigate whether IR signaling played a role in DDR thereby possibly modulating DSB and base oxidation using As to induce ROS and DNA damage in human neuroblastoma SH-SY5Y cells which are known to be susceptible to As-induced ROS production as well as insulin stimulation.

Materials and Methods:

Cell Culture: Human neuroblastoma SH-SY5Y cells were purchased from the American Type Culture Collection and were maintained in complete medium consisting of equal amounts of Ham's F-12 and minimum essential medium (MEM) supplemented with 10% fetal bovine serum, 100 U/mL penicillin, 100 U/mL streptomycin and 2 mM L-glutamine. Cells were incubated in a humidified atmosphere at 37ºC with 5% CO_2.

Treatment: For DSB and DDR experiments, SH-SY5Y cells were grown in 60-mm plates until they reach 80% to 90% confluency. Before treatment, cells were incubated in serum-free (SF) medium for an hour. Afterwards, SH-SY5Y cells were treated for 6 hours with 10 or 20 μM $NaAsO_2$ with or without 100 ng/mL insulin. Where indicated, cells were pre-treated with 50 μM HNMPA-$(AM)_3$, an IR tyrosine kinase inhibitor, for 30 minutes followed by treatment with 20 μM $NaAsO_2$ in the presence or absence of 100 ng/mL insulin for 6 hours in the experiment investigating the effect of inhibiting IR signaling on DSB and DDR. For base oxidation determination, cells were grown on cover slips until 60 to 70% confluency was reached. Thereafter, the cells were incubated in SF medium for an hour before treatment with 50 μM $NaAsO_2$ with or without 100 ng/mL insulin for 1 and 3 hours.

Immunoblotting: After treatment, SH-SY5Y cells were lysed with NP-40 lysis buffer [10 mM Tris pH 7.4, 150 mM sodium choloride, 1 mM EDTA, 1 mM acid EGTA, 0.5% NP-40, 0.2 mM sodium orthovanadate, 10 mM sodium fluoride, 0.1 mM phenylmethylsulfonyl fluoride, 100 nM okadaic acid and protease inhibitor mixture]. Cell lysates were then sonicated (3 bursts), centrifuged at 14,000 rpm for 15 minutes at 4ºC to remove insoluble material, and the resulting supernatants were collected and kept at -80ºC until further use. Concentration of proteins in the samples were determined using Bradford protein assay. Cell lysates were mixed with Laemmli buffer (1:1) and then boiled for 5 minutes. Protein samples (20 to 30 μg) were resolved on SDS-PAGE then transferred to nitrocellulose membranes. The membranes were blocked with 5% skim milk in Tris-buffered saline containing 0.1% Tween 20, and then probed with primary antibodies against γH2AX (1:1000), pChk2 (1:2000), p53 (1:2000) and p21 (1:2000) followed by incubation with the appropriate secondary antibody conjugated with horseradish peroxidase. Proteins bands were then visualized through enhanced chemiluminescence (ECL), and band intensities were quantified using Chemidoc™ Touch Image System with Lab™ Touch Software. Protein levels were normalized against β-actin derived from the same blot.

Immunofluorescent Staining: After treatment, SH-SY5Y cells were fixed in cold methanol for 10 minutes at -20ºC. Afterwards, cells were incubated in 100 μg/mL ribonuclease for 30 minutes at 37ºC to remove RNA, and then in 4% paraformaldehyde for 10 minutes to re-fix the cells. Cells were incubated in 2N HCl for 10 minutes to denature the DNA and in 50 mM Tris-base solution for 10 minutes to neutralize the acidity. Thereafter, cells were incubated in blocking buffer consisting of 2% BSA and 0.1% Tween 20 in PBS and then probed with mouse anti 8-oxo-dG (1:100) overnight ina humidified chamber at 4ºC. After overnight probe, cells were incubated with Rhodamine Red™-conjugated secondary antibody for 40 minutes and then counterstained with 1 μg/mL Hoechst dye. The cover slips were mounted on clean microscope slides and stored at 4ºC until the time of observation. The slides were observed and photographs were taken using confocal laser scanning microscope (Olympus).

Statistical analysis: Collective data of experiments conducted in triplicates were presented as mean ± standard error of the mean (SEM). One-way ANOVA with Bonferroni multiple comparison post-hoc analysis was used to test for significant difference between control and NaAsO2 treated groups, and $NaAsO_2$ treatment without insulin and with insulin using GraphPad Prism 8 with p-value <0.05 indicating a significant difference.

Results and Discussion:

IR signaling could not modulate As-induced DSB and DDR

To determine the effect of IR signaling on DSB and DDR, SH-SY5Y cells incubated in SF medium for an hour were treated with 10 or 20 μM $NaAsO_2$ with or without 100 ng/mL insulin for 6 hours. SH-SY5Y cells treated with H_2O served as control. Immunoblotting was performed to detect γH2AX, the marker of DSB, and proteins involved in DDR including pChk2, p53 and p21. The results showed that $NaAsO_2$ treatment alone at both concentrations caused a slight increase in γH2AX compared with the control without insulin (Figure 1a) indicating that $NaAsO_2$ at the treatment conditions used weakly induced DSB. Insulin treatment given in conjunction with either concentration of $NaAsO_2$ did not cause a significant change in γH2AX compared with their corresponding counterpart without insulin (Figure 1a). This suggested that IR signaling caused very little effect on As-induced DSB. The results relating to DDR showed that $NaAsO_2$ treatment alone at both concentrations induced a small but not significant increase in pChk2 compared with the control without insulin (Figure 1b). However, p53 which is downstream of pChk2, was significantly increased by treatment with 10 μM and 20 μM $NaAsO_2$ (Figure 1c). Though treatment with $NaAsO_2$ alone induced an increase in p21, only 20 μM $NaAsO_2$ was able to cause a significant increase in the protein level compared with the control without insulin (Figure 1d). These data indicated that $NaAsO_2$ at the treatment conditions used successfully activated DDR. Insulin treatment given in conjunction with either concentration of $NaAsO_2$ did not produce a significant effect in pChk2 (Figure 1b), p53 (Figure 1c) and p21 (Figure 1d) compared with their corresponding counterparts without insulin suggesting that IR signaling could not modulate DSB and DDR by As.

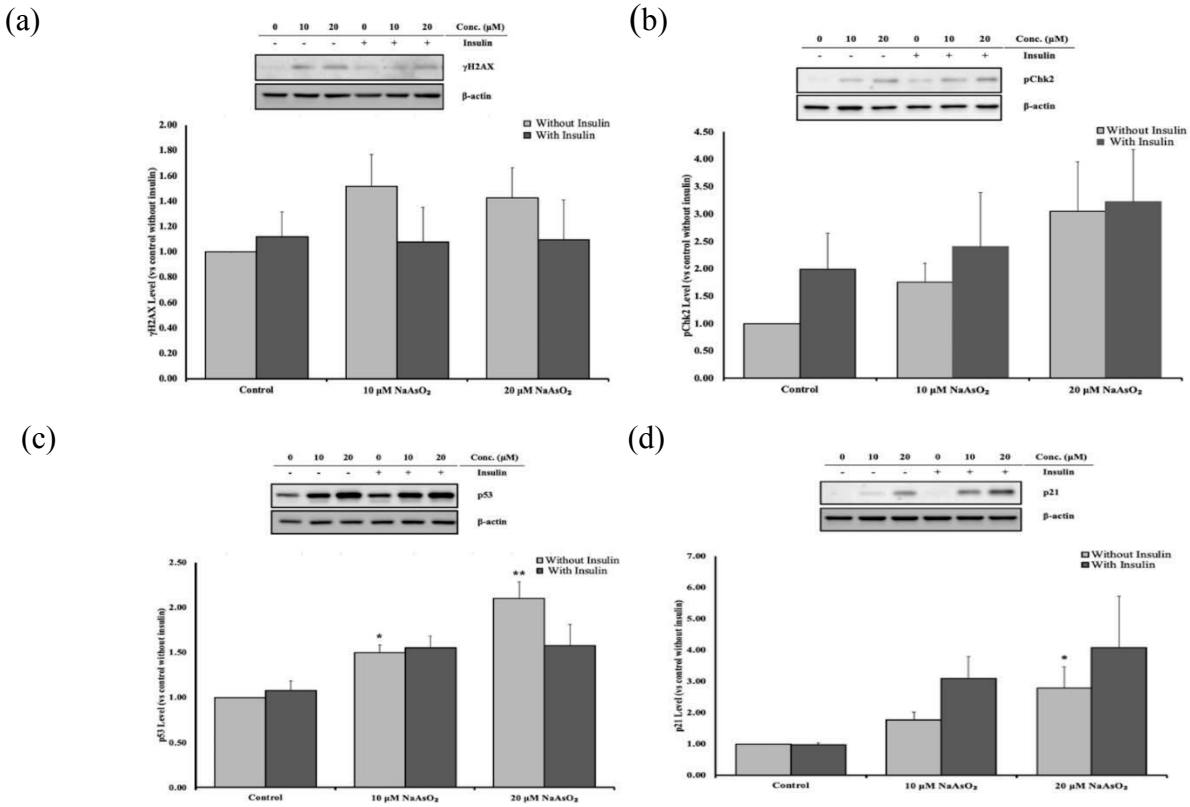

Figure 1 Effects of $NaAsO_2$ and/or insulin treatment on DSB and DDR in human neuroblastoma SH-SY5Y cells. SH-SY5Y cells incubated in SF medium for an hour were treated with either 10 or 20 μM $NaAsO_2$ with or without 100 ng/mL insulin for 6 hours. Immunoblotting was performed to detect and quantify γH2AX, the biomarker of DSB, and pChk2, p53 and p21 which were used to represent activated DDR. Representative blots and quantitative protein levels presented as fold of the control without insulin treatment (n=3) for (a) γH2AX, (b) pChk2, (c) p53 and (d) p21. * and ** represent $p < 0.05$ and $p < 0.01$.

Disruption of insulin signaling negatively modulates As-induced DDR

To determine the effect of inhibiting IR signaling on DSB and DDR, SH-SY5Y cells incubated in SF medium for an hour were pre-treated with 50 μM HNMPA-$(AM)_3$, the IR tyrosine kinase inhibitor, for 30 minutes. This was followed by treatment with 20 μM $NaAsO_2$ alone or with 100 ng/mL insulin for 6 hours. SH-SY5Y cells treated with H_2O served as control. The results showed that SH-SY5Y cells co-treated with $NaAsO_2$ and insulin with HNMPA-$(AM)_3$ pre-treatment had lower γH2AX when compared to $NaAsO_2$ alone (Figure 2a). The levels of DDR proteins, pChk2, p53 and p21, which were increased at comparable level when compared between $NaAsO_2$ alone and with insulin, were prominently reduced when insulin signaling was disrupted by HNMPA-$(AM)_3$ (Figure 2b). These results suggest that disruption of insulin signaling negatively modulates As-induced DDR. Together with the finding that insulin activation did not alter As-induced DDR, we conclude that active insulin signaling is essential for optimal activation of DDR.

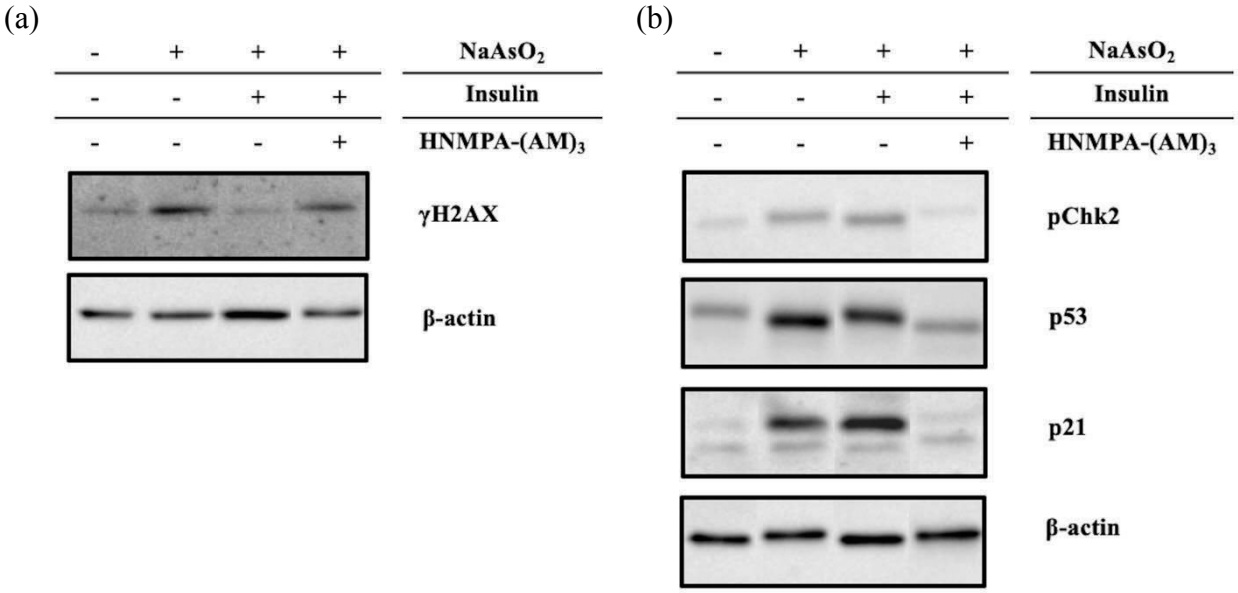

Figure 2 Effects of disrupting IR signaling on DSB and DDR in human neuroblastoma SH-SY5Y cells treated with $NaAsO_2$ and/or insulin. SH-SY5Y cells incubated in SF medium for an hour were pre-treated with 50 μM HNMPA-$(AM)_3$ for 30 minutes followed by treatment with 20 μM $NaAsO_2$ alone or with 100 ng/mL insulin for 6 hours. Immunoblotting was performed to detect and quantify γH2AX which was used as a biomarker of DSB, and pChk2, p53 and p21 which were used to represent activated DDR. Representative blots of (a) γH2AX and (b) pChk2, p53 and p21.

IR signaling caused a mild modulation of As-induced 8-oxo-dG

To determine the effect of IR signaling in base oxidation, SH-SY5Y cells incubated in SF medium for an hour were treated with 50 μM $NaAsO_2$ with or without 100 ng/mL insulin for 1 and 3 hours. Immunofluorescent staining was performed to detect 8-oxo-dG, the marker of base oxidation. The results showed that treatment with 50 μM $NaAsO_2$ alone for 1 and 3 hours caused an increase in levels of 8-oxo-dG compared with the control without insulin treatment (Figure 3). Interestingly, the levels of 8-oxo-dG in insulin treatment given in conjunction with $NaAsO_2$ were lower compared with the $NaAsO_2$ treated group (Figure 3) suggesting IR signaling produced a mild modulation of base oxidation.

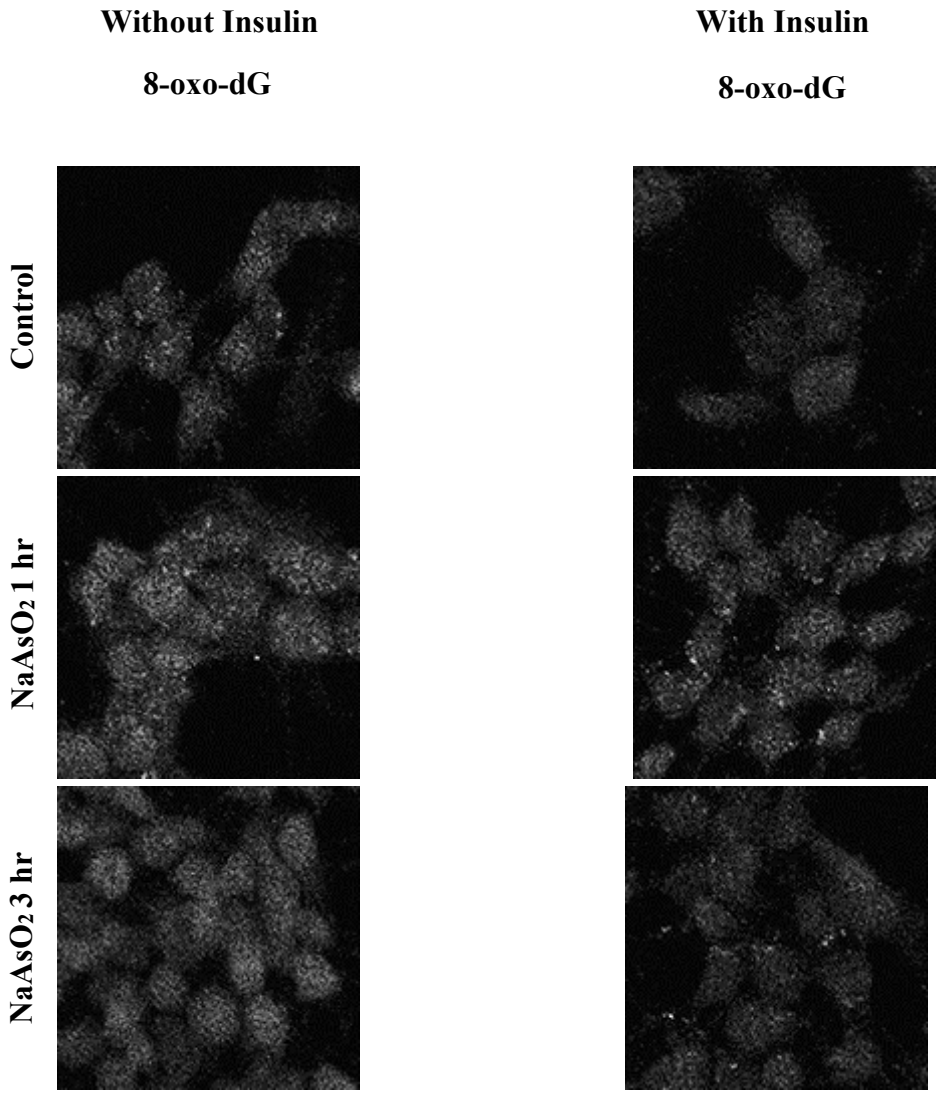

Figure 3 Effects of $NaAsO_2$ and/or insulin treatment in base oxidation in human neuroblastoma SH-SY5Y cells. SH-SY5Y cells incubated in SF medium for an hour were treated with 50 μM $NaAsO_2$ with or without 100 ng/mL insulin for 1 and 3 hours. Immunofluorescent staining was performed to detect 8-oxo-dG which was used as a biomarker of base oxidation, and images were captured using confocal laser scanning microscope.

Conclusion:

The present study provides evidence to support that IR signaling is essential for optimal activation of DDR, and insulin signaling mildly modulates As-induced 8-oxo-dG but has mild effect in As-induced DSB.

Conflict of Interest: The authors declare no conflict of interest that might have affected the results of this research.

Acknowledgements:

We are grateful to Dr. Benjaporn Homkajorn Songvasin for assistance with confocal microscope. This work is supported by grants from the Center of Excellence on Environmental Health and Toxicology (EHT), Ministry of Higher Education, Science, Research and Innovation, Thailand.

References:

1. International Agency for Research on Cancer. Overall evaluations of carcinogenicity: an updating of IARC monographs volumes 1 to 42. Lyon: International Agency for Research on Cancer; 1987. (IARC monographs on the evaluation of the carcinogenic risks to humans, supplement 7).
   Available from: https://www.ncbi.nlm.nih.gov/books/NBK533643/
2. Tam LM, Price NE, Wang Y. Molecular mechanisms of arsenic-induced disruption of DNA repair. *Chem Res Toxicol* 2020; 33: 709-26.
3. Yih LH, Lee TC. Arsenite induces p53 accumulation through an ATM-dependent pathway in human fibroblasts. *Cancer Res* 2000; 60: 6346-52.
4. Guo Z, Kozlov S, Lavin MF, *et al*. ATM activation by oxidative stress. *Science* 2010; 330: 517-21.
5. Liu X, Chen H, Xu X, *et al*. Insulin-like growth factor-1 receptor knockdown enhances radiosensitivity via the HIF-1α pathway and attenuates ATM/H2AX/53BP1 DNA repair activation in human lung squamous carcinoma cells. *Oncol Lett* 2018; 16: 1332-40.
6. Macaulay VM, Salisbury AJ, Bohula EA, *et al*. Downregulation of the type 1 insulin-like growth factor receptor in mouse melanoma cells is associated with enhanced radiosensitivity and impaired activation of ATM kinase. *Oncogene* 2001; 20: 4029-40.
7. Malaguarnera R, Belfiore A. The insulin receptor: a new target for cancer therapy. *Front Endocrinol* 2011; 2: 93.

PrtN IS A TRANSCRIPTION REGULATOR OF PYOCIN S4 GENE IN *Pseudomonas aeruginosa*

Supavich Yodpanaprai[1], Sopapan Rattanaprapanporn[2], Skorn Mongkolsuk[2,3] and Mayuree Fuangthong[1,2,3,*]

[1]Chulabhorn Graduate Institute, Bangkok, Thailand
[2]Laboratory of Biotechnology, Chulabhorn Research Institute, Bangkok, Thailand
[3]Center of Excellence on Environmental Health and Toxicology (EHT), OPS, MHESI, Thailand.

Abstract:

Bacteriocin is antimicrobial peptide that bacteria use against other bacteria. *Pseudomonas aeruginosa* also produces bacteriocin called pyocin. The pyocin expression can be induced by DNA damaging agents such as ciprofloxacin or mitomycin C via SOS response. PrtN is one of the regulatory proteins in SOS response. The presence of R-type pyocin genes is associated with the susceptibility of ciprofloxacin. Pyocin S4 is one of pyocins that *P. aeruginosa* produced. We hypothesized that the transcriptional activator PrtN is required for the expression of pyocin S4 due to the upregulation of the pyocin S4 by hydrogen peroxide. We constructed the *prtN* mutant and *prtN* complement strains and the semi-quantitative real time polymerase chain reaction assay was then performed to observe the effect of *prtN* toward pyocin S4 expression. The results demonstrated that the presence of *prtN* was required for the expression of pyocin S4 in induction condition with 5 mM hydrogen peroxide. While, the pyocin S4 expression in *prtN* mutant strain was not upregulated in induction condition compared to the wild type strain and the expression was restored in complement strain. These results strongly indicate that the PrtN is a transcriptional activator of pyocin S4 in *P. aeruginosa*.

Keywords: Bacteriocin, Pyocin S4, *Pseudomonas aeruginosa*, transcriptional regulator

Introduction:

Pseudomonas aeruginosa is an opportunistic pathogen and a cause of nosocomial infection especially in immunocompromised patients through wound, burn, medical implanted device, or improperly aseptic surgery. In 2019, Centers for Diseases Control and Prevention (CDC) has listed multidrug resistance *P. aeruginosa* as serious threat (1). In addition, carbapenem resistant *P. aeruginosa* is prioritized as critical for the development of new antibiotics by World Health Organization (2). Bacteriocin is an antimicrobial peptide produced by certain strain against others. For example, the integration of nisin with PVDF flat sheet MF membranes to filter *Alicyclobacillus acidoterrestris* out of apple juice for non-thermal sterilization for food industry (3). *P. aeruginosa* also produced bacteriocin called pyocin. There are three types of pyocin, i.e., S-type, F-type, and R-type (4). The expression of these proteins is induced by mutagenic agents and regulated by three regulators, i.e., RecA, PrtR, and PrtN. After bacteria are exposed to mutagenic agents such as hydrogen peroxide or mitomycin C, this exposure will activate the activity of RecA to induce the proteolytic cleavage of PrtR, resulting in the expression of PrtN. The PrtN will then activate the transcription of pyocin genes, resulting in the production of numerous pyocins (5). Pyocin S4 is a putative tRNase pyocin produced by *Pseudomonas aeruginosa* and was upregulated by hydrogen peroxide in microarray analysis (6). We hypothesize that this pyocin will be upregulated in induction condition. The semi-quantitative real time PCR will be performed to compare the expression of pyocin S4 among wild type, *prtN* mutant and *prtN* complement strains exposed to 5 mM hydrogen peroxide.

Methodology:

Construction of *prtN* mutant strain

The fragment of upstream region, downstream region of *prtN* and The *loxGm*^{R} antibiotic cassette were amplified and ligated into pKNOCK-Ap creating pKNOCKΔ*prtN::Gm* that was transformed into *Escherichia coli* BW20767 for conjugation of the recombinant plasmid into *P. aeruginosa* PAO1 wild type. After conjugation, the *loxGm*^{R} antibiotic cassette replaced the *prtN* gene of PAO1 generating the Δ*prtN::Gm*^{R} strain. Then, the transconjugant was electroporated with plasmid pCM157 for Gm^R cassette gene excision generating Δ*prtN* strain.

Constructions of *prtN* complement strain

The full length of *prtN* was amplified with promoter binding site and cloned into pUC18T-mini-Tn7 generating pUC/prtN. The *P. aeruginosa* Δ*prtN* was electroporated with pUC/prtN with helper plasmid pTNS2 giving Δ*prtN/prtN* complement strain

Semi-quantitative real-time PCR (qRT-PCR) assay

Semi-quantitative real-time PCR (qRT-PCR) assay is an *in vivo* experiment to measure mRNA level to confirm that the *prtN* is required for pyocin S4 expression. Three strains, which are wild type, *prtN* mutant and *prtN* complement were used to compare mRNA level of pyocin S4 and immunity genes upon 5 mM hydrogen peroxide according to Chang et al. (7). Total RNA was isolated by hot acid phenol extraction method (8); and 2.5 µg of total RNA was treated with DNase to remove any residual DNAs. The 500 ng RNA was reverse transcribed to cDNA by using random hexamer primer. Synthesized cDNA was mixed with SYBR green master mix and specific primers for pyocin S4 and 16S rRNA genes. The qRT-PCR is performed using Applied Biosystems StepOnePlus. Relative expression was calculated using StepOne software v2.1 by compare RQ. RQ is defined as relative quantification.

Results:

Constructions of *prtN* mutant strain

The *prtN* mutant was confirmed by PCR and Southern blot. The PCR result from *prtN* mutant construction showed that PCR band from wild type was 400 bp compared to mutant, which was 300 bp (Figure 1A). The DNA band from Southern blot for Δ*prtN* was smaller than band from wild type as expected, 1,700 bp for wild type and 900 bp for Δ*prtN* (Figure 1B).

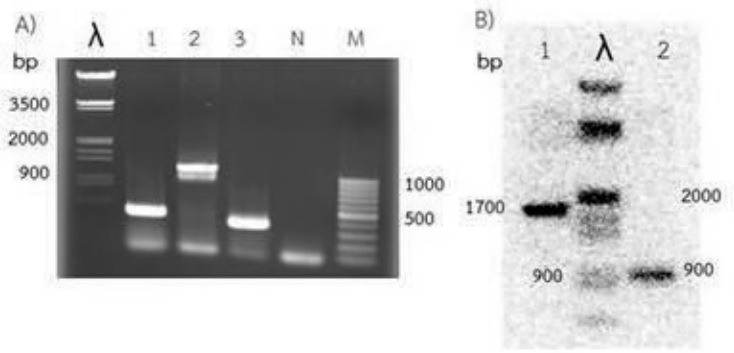

Figure 1 Conformation of the prtN mutant. A) Visualization of PCR product using gel electrophoresis in 1.0% agarose gel confirming Δ*prtN* strain using primer BT8339 and BT8340. Lane 1 is PAO1 wild type with 400 bps PCR product. Lane 2 is *prtN::Gm* strain with 1,300 bps PCR product. Lane 3 is Δ*prtN* strain with 300 bps PCR product. The λ is lambda DNA/*Eco*RI+*Hin*dIII markers. The 100 bps is Generuler 100 bp DNA marker. B) Visualization of Southern blots confirming Δ*prtN* strain using PCR product from BT8363 and BT8364 as probe. Lane 1 PAO1 wild type with 1700 bp, Lane 2 Δ*prtN* with 900 bp, Lane λ lambda DNA/*Eco*RI+*Hin*dIII markers.

Constructions of *prtN* complement strain

The PCR result showed that 280 bp band was observed when DNA from *prtN* complement strain and primers BT2268-3305 were used. Another primer pair BT7589 and 8085 was used in the PCR reaction. The 600 bp DNA band was observed (Figure 2). These results confirm that the *prtN* complement strain was successfully generated.

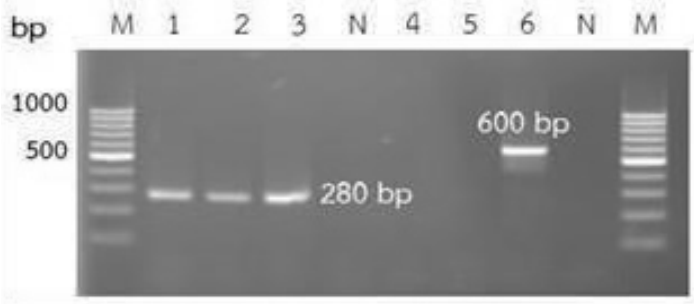

Figure 2 The PCR result of *prtN* complement strain. Lane 1 to 3 were PCR product from BT2268-3305. Lane 4 to 6 were PCR product from BT7589-8085. Lane 1; PAO1/Tn with 280 bp PCR product, Lane 2; Δ*prtN/Tn* with 280 bp PCR product, Lane 3; Δ*prtN/prtN* with 280 bp PCR product, N; negative, Lane 4; PAO1/Tn, Lane 5 Δ*prtN*/Tn, Lane 6; Δ*prtN/prtN* with PCR product 600 bp and M; DNA 100 bp marker.

Semi-quantitative real-time PCR (qRT-PCR) assay

PrtN is a putative transcriptional activator of pyocin gene. In the 5 mM hydrogen peroxide induction, the pyocin S4 mRNA level was higher than normal condition of wild type and complement strains. However, the pyocin S4 mRNA level in *prtN* mutant strain was not increased in hydrogen peroxide induction condition indicating that PrtN is important for the transcription of pyocin S4 as we hypothesized. The mRNA level was restored in complement Δ*prtN/prtN* (Figure 3).

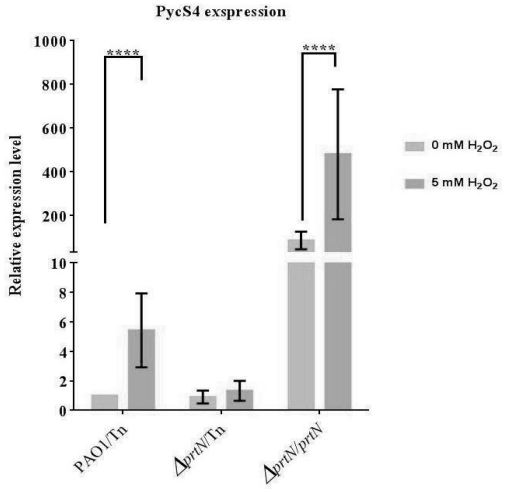

Figure 3 The RQ of pyocin S4 mRNA during 5 mM H_2O_2 induction between wild type, Δ*prtN* and Δ*prtN/prtN*. The fold induction of pyocin S4 mRNA was 5 times in both wild type and complement strains. Mean ± standard deviation is depicted. Statistically significance differences were determined by Mann-Whitney Wilcoxon rank test using GraphPad.

Discussion:

In this study, it was shown that PrtN positively regulates the expression of pyosin S4 gene under H_2O_2 exposure in the similar pathway that had been reported. In addition, the expression of pyocins is also controlled by two additional transcription regulators, RecA and PrtR in *P. aeruginosa* (5). RecA is activated upon exposure to the DNA damaging agent such as ciprofloxacin, UV or mitomycin C (5, 9). The activated RecA induces the autoproteolytic activity of PrtR that represses the expression of PrtN (10, 11). PrtN binds the conserved promoter sequence of pyocin genes called P-box to increase the expression of pyocin genes (5). After bacteria exposed to the H_2O_2, RecA is activated and induces the autoproteolytic activity of PrtR. The degradation of PrtR allows the transcription and translation of PrtN that is the transcriptional activator of pyocin S4.

Conclusion:

This study strongly suggests that PrtN is a transcriptional activator of pyocin S4 gene as the presence of PrtN is necessary for the expression of pyocin S4 during hydrogen peroxide induction.

References:

1. Antibiotic resistance threats in the United States, 2019. 2019.
2. Tacconelli E, Carrara E, Savoldi A, Harbarth S, Mendelson M, Monnet DL, et al. Discovery, research, and development of new antibiotics: the WHO priority list of antibiotic-resistant bacteria and tuberculosis. The Lancet Infectious Diseases. 2018;18(3):318-27.
3. Zhang J, Li S, Wang W, Pei J, Zhang J, Yue T, et al. Bacteriocin assisted food functional membrane for simultaneous exclusion and inactivation of *Alicyclobacillus acidoterrestris* in apple juice. Journal of Membrane Science. 2021;618:118741.
4. Michel-Briand Y, Baysse C. The pyocins of *Pseudomonas aeruginosa*. Biochimie. 2002;84(5-6):499-510.
5. Matsui H, Sano Y, Ishihara H, Shinomiya T. Regulation of pyocin genes in *Pseudomonas aeruginosa* by positive (*prtN*) and negative (*prtR*) regulatory genes. Journal of Bacteriology. 1993;175(5):1257-63.
6. Parret A, De Mot R. Novel bacteriocins with predicted tRNase and pore-forming activities in *Pseudomonas aeruginosa* PAO1. Molecular Microbiology. 2000;35(2):472-3.
7. Chang W, Small DA, Toghrol F, Bentley WE. Microarray analysis of *Pseudomonas aeruginosa* reveals induction of pyocin genes in response to hydrogen peroxide. BMC Genomics. 2005;6:115.
8. Chomczynski P, Sacchi N. Single-step method of RNA isolation by acid guanidinium thiocyanate-phenol-chloroform extraction. Analytical Biochemistry. 1987;162(1):156-9.
9. Brazas MD, Hancock RE. Ciprofloxacin induction of a susceptibility determinant in *Pseudomonas aeruginosa*. Antimicrobial Agents and Chemotherapy. 2005;49(8):3222-7.
10. Penterman J, Singh PK, Walker GC. Biological cost of pyocin production during the SOS response in *Pseudomonas aeruginosa*. Journal of Bacteriology. 2014;196(18):3351-9.
11. Sun Z, Shi J, Liu C, Jin Y, Li K, Chen R, et al. PrtR homeostasis contributes to *Pseudomonas aeruginosa* pathogenesis and resistance against ciprofloxacin. Infection and Immunity. 2014;82(4):1638-47.

THE EFFECT OF HERBICIDES ON ANTIBIOTIC SUSCEPTIBILITY OF HUMAN PATHOGEN, *Stenotrophomonas maltophilia*

Pitthawat Grittanarnan[1], Nisanart Charoenlap[2,3], Veerakit Vanitshavit[2], Skorn Mongkolsuk[1,2,3] and Paiboon Vattanaviboon[1,2,3*]

[1]Applied Biological Sciences: Environmental Health Program, Chulabhorn Graduate Institute, Chulabhorn Royal Academy, Bangkok 10210, Thailand
[2]Research Laboratory of Biotechnology, Chulabhorn Research Institute, Bangkok 10210, Thailand
[3]Center of Excellence on Environmental Health and Toxicology (EHT), OPS, MHESI, Thailand
**E-mail: paiboon@cri.or.th*

Abstract:

Herbicides are widely used in agriculture to eliminate unwanted weeds, in order to increase crop yields. The herbicide residues can contaminate the ground and expose to environmental microorganisms. An increase of herbicide usages in agricultural area has been associated with antibiotic resistance in bacteria. Antimicrobial resistance (AMR) is a major threat to human health as it caused 4.95 million deaths in 2019, and potentially increased in the future. *Stenotrophomonas maltophilia* is an opportunistic and multidrug resistance pathogen that causes hospital-acquired infections, especially in immunocompromised patients. Currently, the study of herbicide exposure involved in antibiotic resistance in *S. maltophilia* is unknown, thus glyphosate (Roundup), which is a widely used herbicide, was used for investigating its effect on antibiotic susceptibility, in this study. *S. maltophilia* were exposed to sub-lethal concentration of glyphosate prior to testing antibiotic susceptibility. The result showed that the susceptibility of *S. maltophilia* to quinolone and aminoglycoside groups was decreased, whereas herbicide induced-cells revealed an increase in tetracycline susceptibility. Additionally, the expression of quinolone resistance-associated genes, *qra1*, *qra2* and *qra3*, induced by glyphosate were increased, compared to uninduced cells, suggesting that these genes are possibly involved in herbicides-antibiotic resistance mechanisms. However, the precise mechanisms of these potential genes related to antibiotic resistances need further studies.

Keywords: *Stenotrophomonas maltophilia*, herbicides, antibiotic resistance (AMR)

Introduction:

Antimicrobial resistance (AMR) has been becoming one of the most global health crises in humans and leading to increasingly ineffective antibiotics to treat bacterial infections. Although, the AMR occurs naturally, but the misuse of antibiotics is accelerating the process. *Stenotrophomonas maltophilia* is the hospital-acquired pathogen that can cause pneumonia, bloodstream infections, and endocarditis in intensive-care unit patients (1). Once *S. maltophilia* develops antibiotic resistance, it could become multidrug-resistant, which is difficult to treat and causes a serious human health problem. Besides, antibiotic residues in the environment, agrochemicals possibly promote antibiotic resistance as well. However, the link between herbicide and antibiotic resistance is not well studied. Thus, the effect of herbicide on antibiotic resistance has been elucidated in this study.

Methodology:

Minimum Inhibitory Concentration (MIC) assay

Overnight cultures were adjusted to 0.5 McFarland standards and diluted 1:20 with 0.9 % sterile normal saline. Glyphosate was two-fold serial diluted in 96-well plate and then 10 µl of cell suspension was added into each well. The MIC value was determined after incubating the cells at 35°C for overnight (2).

Disk diffusion assay

Disk diffusion assay was performed using Kirby-Bauer method (3). Overnight cultures were sub-cultured into 20 ml of Luria-Bertani broth and incubated at 35°C with continuously shaking at 180 rpm until reaching exponential phase. The sub-lethal concentration of glyphosate was added into exponential-phase cell for 30 minutes. Then, 50 µl of the glyphosate-exposed cells were mixed with 15 ml of molten agar before overlaid on Mueller-Hinton plate. The antibiotic disks were then placed on the solidified plate and the clear zone was measured after incubating at 35°C for overnight.

Reverse transcriptase quantitative real-time PCR (RT-qPCR)

The level of *qra1*, *qra2*, and *qra3* expression was measured by RT-qPCR using primers BT8155 and BT8156 for *qra1*, BT8435 and BT8436 for *qra2*, and BT6866 and BT6867 for *qra3*. BT2781 and BT2782 primers were used to amplify 16s rRNA for normalization. The reactions were run on Applied BiosystemStepOne Plus under the following conditions; denaturation at 95 °C for 30 sec, annealing at 60 °C for 30 sec and extension at 72 °C for 30 sec, totally 40 cycles. The relative expression of genes was analyzed by using StepOne software v2.1.

Result and Discussion:

The antibiotic susceptibility of *S. maltophilia* induced by glyphosate (Roundup)

To determine the sub-lethal concentration of glyphosate (Roundup) in *S. maltophilia*, the MIC assay was performed. The result showed that MIC value of glyphosate (Roundup) in *S. maltophilia* was 24 mM. In order to investigate the role of glyphosate on antibiotic resistance in *S. maltophilia*, the cells were exposed to sub-lethal concentration of glyphosate prior to testing the antibiotic susceptibility. Disk diffusion assay of *S. maltophilia* that induced by glyphosate at 6 and 12 mM showed decreased susceptibility to all antibiotics in quinolone and aminoglycoside groups whereas tetracycline sensitivity was increased. Kurenbach et al., reported that exposure to glyphosate (Roundup) and 2,4-dichlorophenoxyacetic acid (2,4-D) in *Escherichia coli* and *Salmonella enterica* serovar Typhimurium showed an increased resistance to ciprofloxacin, kanamycin, ampicillin, and chloramphenicol. Therefore, the phenotypic alteration of *S. maltophilia* might have a similar mechanism to those of *E. coli* and *S. enterica* Typhimurium (4).

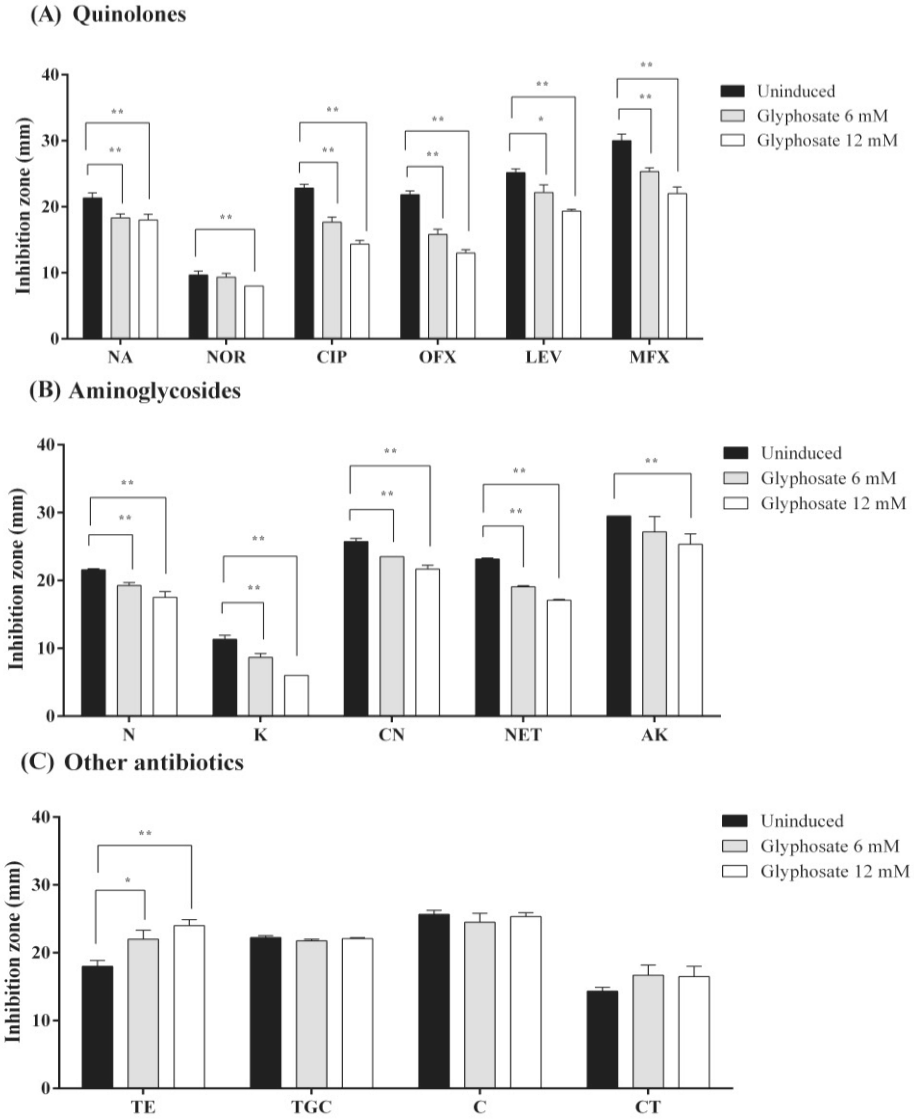

Figure 1 Antibiotic susceptibility in *S. maltophilia* induced by glyphosate (Roundup) in quinolones (A); Nalidixic acid (NA), Norfloxacin (NOR), Ciprofloxacin (CIP), Ofloxacin (OFX), Levofloxacin (LEV), and Moxifloxacin (MFX), aminoglycosides (B); Neomycin (N), Kanamycin (K), Gentamycin (CN), Netilmicin (NET), Amikacin (AK), other antibiotics (C); Tetracycline (TE), Tigecycline (TGC), Chloramphenocal (C), Colistin sulphate (CT). Results shown are mean ± SDs from three independent experiments. The * and ** represented statistically significant difference using *t*-test with $P < 0.05$ and $P < 0.01$, respectively.

The gene expression of quinolone resistance-associated genes, *qra1*, *qra2*, and *qra3*, induced by glyphosate (Roundup)

According to the quinolones-resistant phenotype of *S. maltophilia* induced by glyphosate (Roundup), the transcriptional levels of genes associated with quinolones resistance were measured. The *qra3* has been reported as putative quinolone-resistant protein, which is regulated by Qra2 regulator. Based on gene organization (Figure 2), *qra1* is located at the downstream of *qra2* in an operonic structure (5). Hence, the *qra1*, *qra2*, and *qra3* gene expression was measured. The expression levels of *qra1*, *qra2*, and *qra3* were increased when *S. maltophilia was* exposed to glyphosate at 6 and 12 mM, compared to uninduced cells (Figure 3). Thus, glyphosate might be a potential inducer of transcriptional regulator, Qra2, was associated with the antibiotic resistance. However, the precise mechanisms need to be confirmed.

Figure 2 Gene organization of quinolone resistance-associated genes, *qra1*, *qra2*, and *qra3*, in *S. maltophilia* K279a

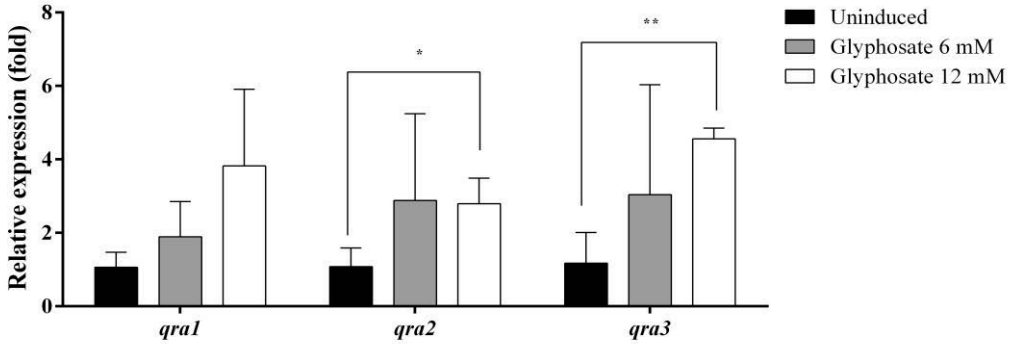

Figure 3 The gene expression of quinolone resistance-associated genes, *qra1*, *qra2*, and *qra3*, induced by glyphosate (Roundup) in *S. maltophilia*. Results shown are mean ± SDs from three independent experiments. The * and ** represented statistically significant difference using *t*-test with $P < 0.05$ and $P < 0.01$, respectively.

Conclusion:

Exposure to glyphosate (Roundup) increased the level of *qra1*, *qra2*, and *qra3* gene expression, resulting in elevated antibiotic resistance in *S. maltophilia.* It suggested that glyphosate plays an important role in antibiotic resistance. The observed linkage between antibiotic resistance and herbicide will raise the awareness of herbicide usage, resulting in a decline in the antibiotic resistance incidence.

References:

1. J. S. Brooke, *Stenotrophomonas maltophilia*: an emerging global opportunistic pathogen. *Clin Microbiol Rev* **25**, 2-41 (2012).
2. L. S.-M. Richard Schwalbe, Avery C. Goodwin. (CRC Press, 2007).
3. A. W. Bauer, W. M. Kirby, J. C. Sherris, M. Turck, Antibiotic susceptibility testing by a standardized single disk method. *Am J Clin Pathol* **45**, 493-496 (1966).
4. B. Kurenbach *et al.*, Sublethal exposure to commercial formulations of the herbicides dicamba, 2,4-dichlorophenoxyacetic acid, and glyphosate cause changes in antibiotic susceptibility in *Escherichia coli* and *Salmonella enterica* serovar Typhimurium. *mBio* **6**, (2015).
5. Y.-C. Chang, M.-J. Tsai, Y.-W. Huang, T.-C. Chung, T.-C. Yang, SmQnrR, a DeoR-type transcriptional regulator, negatively regulates the expression of *Smqnr* and *SmtcrA* in *Stenotrophomonas maltophilia*. *Journal of Antimicrobial Chemotherapy* **66**, 1024-1028 (2011).

THE IMPACT OF GLYPHOSATE ON THE TRANSCRIPTIONAL LEVELS OF GENES INVOLVED IN SHIKIMATE/CHORISMATE IN RICEBERRY RICE

Pattana Srifah[1,3], Kisana Bhinija[1], Skorn Mongkolsuk[1,3], Piyada Juntawong[4], Nuchanart Rangkadilok[2,3], Sumontha Nookabkaew[2] and Jutamaad Satayavivad[2,3]

[1]Laboratory of Biotechnology, Chulabhorn Research Institute, Bangkok 10210, Thailand
[2]Laboratory of Pharmacology, Chulabhorn Research Institute, Bangkok 10210, Thailand
[3]Center of Excellence on Environmental Health and Toxicology (EHT), OPS, MHESI, Thailand
[4]Department of Genetics, Faculty of Science, Kasetsart University, Bangkok 10900, Thailand

Abstract:

In this study, we determined to evaluate the effect of low dose root-applied glyphosate on the transcriptional levels of genes involved in shikimate biosynthesis in root, leaf, and seed of Riceberry (*Oryza sativa* L. *indica* cv. Riceberry) . The transcriptomic analysis showed that the glyphosate accumulated in Riceberry plant altered the transcriptional levels of 4 genes related to shikimate biosynthesis including *3- deoxy- D- arabino- heptulosonate 7- phosphate synthase*, *dehydroquinate synthase*, *shikimate kinase*,and *5-enolpyruvylshikimate-3-phosphate synthase*. The expression of those genes was up- regulated in seed, but the *shikimate 5- dehydrogenase* was up- regulated in leaf tissue. The results suggested that a low concentration of glyphosate absorbing through the root system and accumulation in plants enhanced the expression of genes involved in shikimate biosynthesis in seeds.

Keywords: Glyphosate, riceberry, shikimate biosynthesis, transcriptome

Introduction:

The commercial glyphosate (N-(phosphonomethyl) glycine) is one of the most common broad- spectrum herbicides used in agriculture. However, the distresses about the glyphosate accumulation in soil may affect plant growth, the environment and cause human health problems are still discussed (Kanissery et al. , 2019) . Glyphosate interrupts the shikimate metabolic pathway and also blocks the production of aromatic amino acids, which are the basis for several plant metabolites (Tzin et al., 2010). Glyphosate residues are reported in soils from various environments, but the effects on plant physiology and consequences for species interactions are basically unknown (Fuchs et. al., 2020; 2022). In this work, we aimed to study the effect of the low- dose glyphosate treatment which may affect the shikimate biosynthesis for the precursor of secondary metabolite that plays an important role in the plant interaction with the environment.

Methodology:

Plant material

One month old seedlings were cultivated in soil contained glyphosate 15. 85 µM. The leaf and root sample were harvested after 50 days and the young seeds were harvested after 105 days after glyphosate treatment. All of samples were kept immediately under - 80ºC condition prior to RNA extraction.

RNA extraction and sequencing

200 mg of fine ground sample in liquid nitrogen extracted in TRIzol reagent. The total RNA was dissolved in 30 μL of RNase-free water, and qualified the quality using Agilent RNA 6000 Nano Kit on Agilent Bioanalyzer 2100 for RNA Integrity Number (RIN) and then stored at -80 ºC. RNA sequencing was performed by BGI Transcriptome Sequencing services (BGI-Hong Kong). The transcriptome sequencings are executed with the Illumina sequencing system with BGISEQ Technology Platform.

Data analysis

The expression analysis data were subjected to Fuzzy k- means clustering with Euclidean correlation for the distance measure, a membership exponent of 1. 1, maximal number of iterations of 5000 and 30 clusters (Juntawong et al., 2013). The mean SLR value for each cluster was determined for summary visualization. Functional analysis of co- regulated genes was analyzed by gene ontology enrichment analysis using Singular enrichment analysis tool and hypergeometric test with Hochburg FDR < 0.05 in AgriGO version 2 (Tian et al., 2017).

Cluster analysis of transcript expression level was performed by Multiple Experimental Viewer software (MEV) using hierarchical clustering (HCL) based on the Pearson correlation with average linkage clustering and using a graphical user interface for bioconductor applications in microarray data analysis (Chu et al., 2008). The different tissues were compared under t test significance of $P < 0.05$. Color scale of the heatmap presented the expression level; red indicates high transcript abundance genes while green indicates low abundance genes.

Results, Discussion and Conclusion:

Effects of low dose glyphosate on shikimate biosynthesis

To determine the effect of a low dose of glyphosate root- applied treatment, the vegetative samples (leaf and root) and reproductive samples (young seed) were collected after 50-day and 105-day treatment, respectively. The transcriptomic analysis revealed that total 21,971 transcripts (7,324 in leaf; 7,394 in root; and 7,253 in seed) had significant changes in abundance (FDR 0. 05). The transcriptional levels of 4 genes involved in shikimate biosynthesis showed a high differential expression (DEGs) in seed than in leaf and root (Figure 1A). Among those 4 genes, *3-deoxy-D-arabino-heptulosonate 7-phosphate synthase* (*DAHPS*) was up-regulated at the highest expression level in seed at level 1.56, but the expression in root was as much as low at level of -1.94. The similar expression pattern was found in *shikimate kinase* (*SK*), *dehydroquinate synthase* (*DHQS*) and *5- enolpyruvylshikimate- 3- phosphate synthase* (*EPSP*). In contrary to the gene expression pattern of *shikimate 5-dehydrogenase* (*SDH*) was up- regulated in leaf at the level of 1. 32 and down- regulated in roots at the level of - 0. 10 (Figure 2A).

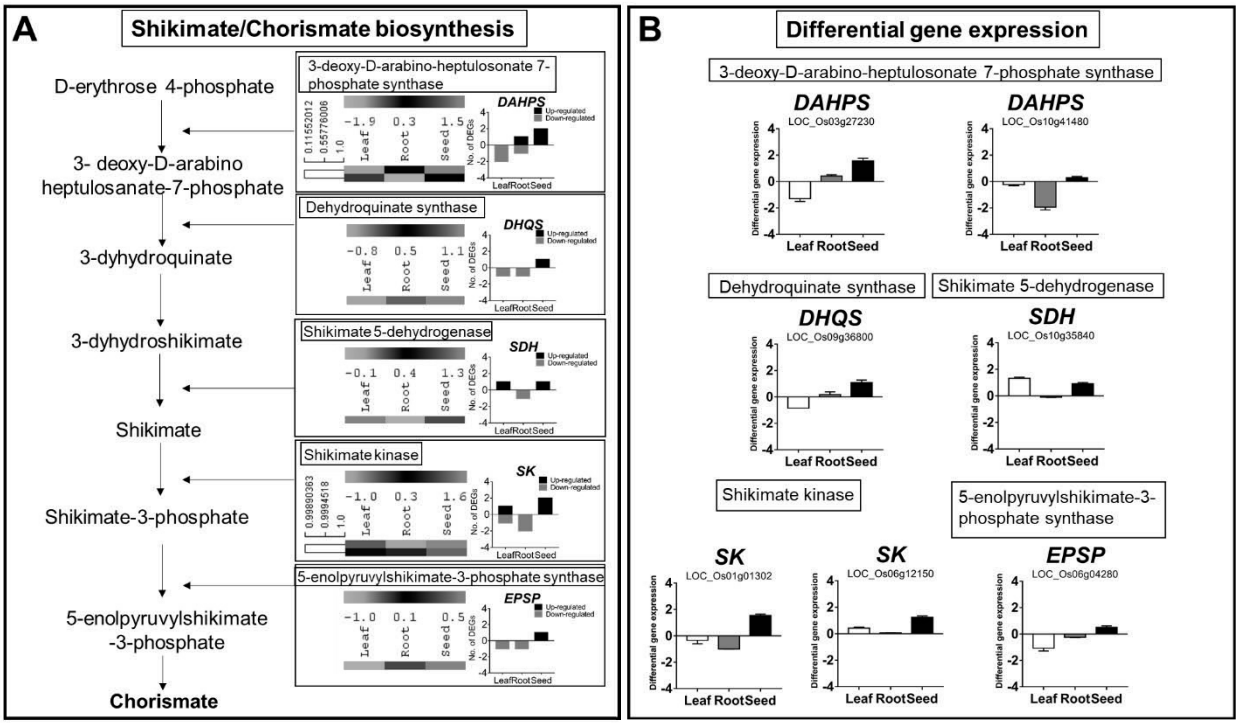

Figure 1 Schematic expression levels (A) and the differential gene expression (DEGs) values (B) of genes involved in shikimate biosynthesis in leaf, root, and seed of Riceberry rice treated with low dose of glyphosate.

Our result was inconsistent with the previous report on the foliar-applied glyphosate which has been expected to the result of inhibition of [(14)C] shikimate into all three aromatic amino acids, and shikimate accumulated in the tissue of buckwheat (Ausamrhein et.al., 1980). The results lead to the conclusion that glyphosate interferes with the shikimate pathway at or prior to the formation of chorismate. In current study, low dose of root-applied glyphosate induced increasing of the gene related to shikimate biosynthesis in seed tissue which may be translated into crop enhancement which may increase in related aromatic amino acids (phenylalanine, tryptophan, tyrosine) and may increase biomass growth lead to induce pathogen defense mechanism and other valuable agronomic effects (Belz et al., 2011).

Conclusion:

The low dose of root-applied glyphosate can alter the regulation of some genes involved in shikimate biosynthesis in seeds more than that in leaf and root tissues.

Acknowledgments:

This research was supported by Center of Excellence on Environmental Health and Toxicology and The Chulabhorn Research Institute research fund, BKK, Thailand.

References:

1. Belz RG, Cedergreen N, Duke SO. Herbicide hormesis – can it be useful in crop production? Weed Research 2011: 51: 321–332. doi:10.1111/j.1365-3180.2011.00862.x.
2. Chu VT, Gottardo R, Raftery AE, Bumgarner RE, Yeung K. MeV+R: using MeV as graphical user interface for Bioconductor applications in microarray analysis. Genome Biol. 2008:9: R118.1-11. doi: 10.1186/gb-2008-9-7-r118.
3. Fuchs, B, Saikkonen K, Helander M. Glyphosate-modulated biosynthesis driving plant defense and species interactions. Trends in Plant Sci. 2020: 26(4) : 312-323 doi:10.1016/j.tplants.2020.11.004.
4. Fuchs B, Laihonen M, Muola A, Saikkonen K, Dobrev PI, Vankova R and Helander M. A Glyphosate-based herbicide in soil differentially affects hormonal homeostasis and performance of non-target crop plants. Front. Plant Sci. 2022: 12: 787958. doi: 10.3389/fpls.2021.787958.
5. Ausamrhein N, Brigitte D, Gehrke P, Steinrücken Hans C. The site of the inhibition of the Shikimate pathway by glyphosate: II. Interference of glyphosate with chorismate formation in *vivo* and in *vitro*. Plant Physiol. 1980:66(5): 830–834. https://doi.org/10.1104/pp.66.5.830.
6. Juntawong P, Sorenson R, Bailey-Serres J. Cold shock protein 1 chaperones mRNAs during translation in *Arabidopsis thaliana*. Plant J. 2013: 74(6) : 1016-28. doi: 10.1111/tpj.12187.
7. Kanissery R, Gairhe B, Kadyampakeni D, Batuman O, Alferez F. Glyphosate: Its environmental persistence and impact on crop health and nutrition. Plants (Basel) 2019. 8(11): 499. doi: 10.3390/plants8110499.
8. Tian T, Liu Y, Yan H, You Q, Yi X, Du Z, Xu W, Su Z. AgriGO v2.0: a GO analysis toolkit for the agricultural community, 2017 update. Nucleic Acids Res. 2017:45(W1): W122-W129. doi: 10.1093/nar/gkx382.
9. Tzin V, Galili G. New insights into the shikimate and aromatic amino acids biosynthesis pathways in plants. Mol. Plant. 2010:3(6):956-72. doi: 10.1093/mp/ssq048.

WATER FOOTPRINT IN GOLF COURSES: A CASE STUDY IN NAKHON RATCHASIMA PROVINCE, THAILAND

Bhumibhat Wongmanee[1], Chate Jaikanlaya[2,3], Supawadee Polprasert[2,3], Chatchawal Singhakant[2,3], Nitchaphat Khansakorn[2] and Thanakrit Neamhom[2,3,*]

[1]Master of Science Program in Environmental Health, Faculty of Public Health, Mahidol University, Rajvithi Road, Bangkok, 10400, Thailand
[2]Department of Environmental Health Sciences, Faculty of Public Health, Mahidol University, Rajvithi Road, Bangkok, 10400, Thailand
[3]Center of Excellence on Environmental Health and Toxicology (EHT), OPS, Ministry of Higher Education, Science, Research and Innovation, Thailand

Abstract:

Golf course is a type of green space which can generate recreational, functional, aesthetic benefits, and also cause of pollutions both in quality and quantity. This study aimed to evaluate the water footprint of golf courses in Thailand. Three golf courses in Nakhon Ratchasima province were visited to acquire the relevant information. Input data of water consumption, types of trees, grass species, water bodies, drainage system, and total playing area were obtained from interviewing with managers and owners. Results show that the largest greening space of golf course is used for plantation of playing areas. Following the water footprint concept, the value of direct water footprint was in average of 2.5 million m^3/year. This value was computed from rainwater consumption (Green water footprint of 1.109 L/y) and water irrigation (Blue water footprint of 2.58 million m^3/y). While the amount of indirect footprint was evaluated to be 0.26 million m^3/y (89% from electricity use and another from fuel consumption). In the whole operation of golf course, the amount of water footprint was 5.42 million m^3/y. Moreover, results also revealed that the maintenance services of mowing, irrigation, and fertilizer play as the major parts of water consumption for turf management and rely on input resources for maximum performance and quality. From this finding, the database of water footprint is transferrable and adaptive to water sustainability management prevailing conditions at the golf course, landscape, urban planning, and design at the scale of greens and fairways.

Keywords: Water footprint, golf course, environmental performance, turfgrass, Thailand

Introduction:

Urbanization is a complex socio-economic process that transforms the built environment, converting formerly rural into urban settlements, while also shifting the spatial distribution of a population from rural to urban areas. It shaped by spatial and urban planning as well as by public and private investments in buildings and infrastructure. The future growth of cities and concomitant appropriation of land and natural resources will determine success towards an environmentally sustainable future. In some cities, unplanned or inadequately managed urban expansion leads to rapid sprawl, pollution, and environmental degradation, together with unsustainable production and consumption pattern. Environmental sustainability is additionally challenged by the consumption patterns that prevail in urban settings. Environmental sustainability is additionally challenged by the consumption patterns that prevail in urban settings [1]. Recreation area is supposed to promote mental health, serving physical activities, reducing mortality, and also promote interaction between each people in the city [2]. Golf is one of the most popular sports for a hundred years and there're over

32,000 golf courses around the world including Thailand. Golf course is one type of green space which can generate recreational, functional, and aesthetic benefits [3]. The increasing of golf course has been changing of land use and land development, most of them located in the fringe of urban area. Since the golf course business is a very popular tourism sector today. As a result, the number of golf courses increased as it grew in line with its popularity causing the demand for water usage in golf courses to increase as well. The water consumption rate of a golf course is usually 3,500 m3 / rai / year and the water reserves required for golf courses each year are approximately 800,000 - 1,200,000 m^3 [4]. When comparing the proportion of water use in golf courses, it was found that one golf course has the same proportion of water use as the water used in one district for maintenance about grass and all other field-related activities [5]. For some type of a recreation area the water footprint is not widely in case study such as semi-public area and private area like golf course. The important of water footprint assessment is to know the amount of water consumed to produce goods and operate the services, also measure the human appropriation of global water resources which measured by volume of water consumption and pollution [6].

To address the problems mentioned above, aim of this study is to determine the water footprint in golf course to establish the alternative sustainable management practices. This will help the golf course manager and owner to save cost of water and achieve the SDGs goals in sustainable cities and communities.

Materials and Methods:

Sample size determination

In field survey and data collection will be conducted to gather the information about the golf course profile and water footprint. The sample size was computed following non-probability sampling from accessible population which convenient or volunteer to provide the information of golf course business in Nakhon Ratchasima. From the non-probability sampling technique found that there was only three from golf course business capable of providing information for this research.

Field survey and data collection

The data collection of water usage in water management practices are 1) Direct water footprint, and 2) Indirect water footprint. The selected golf course in Nakhon Ratchasima will be visited to gather the relevant information. The information will be gathered from face-to-face interviewing with golf course managers and/or owners. The details of water consumption were collected using an in-depth interviewing.

Water footprint model

The data of water consumption will be interpreted in terms of water footprint. Using an approach of water footprint [6] based on water management practice in playing areas, the association of water footprint can be classified into two differences types which are blue water footprint, and green water footprint. The concept of water footprint is the indicator of using fresh water which is directly used by a person in the whole volume of the supply chain of products. Hence, water footprint refers to the consumption of water of freshwater both from direct and indirect water consumption. The calculation method of water footprint of single step is the sum of the direct and indirect water footprints.

Regarding of the mentioned total water footprints including blue, green, and grey water footprints (WF). In terms of blue WF comes from the natural resources in the golf course such as lake and pond inside the area. It is calculated using equation (1). Green WF indicates

the water used to maintain the golf course which comes from stormwater captured from January to June 2021. In this calculation does not include grey water footprint due to each golf course does not release the water after maintenance the playing area to the public canal which calculated using equation (2).

For indirect WF, it could be calculated from gather the resources consumption following equation (3). Where EF_{fuel} = 0.0023 m^3/kW-hr, $EF_{electricity}$ = 0.0376 m^3/y, and Q = Quantity of resources. The resources in this study are fuel and electricity which are operated daily in each golf course.

Blue WF = Blue Water Evaporation + Blue Water Incorporation (1)

Green WF = Green Water Evaporation + Green Water Incorporation (2)

Indirect WF = $\sum_{i=1}^{n}(Q_i * EF_i)$ (3)

Results and Discussion:

The Characteristics of selected golf courses

The three different golf courses have similar management practices and grass types as shown in table 1. The data shown the rage of information between January – May 2021. The selected golf courses in this study have comparable in management procedures. Whereas they are operating the water, the quantity of water lost after watering the playing areas to sub drains accounts for 85% of total water loss. However, this varies according on the weather and seasons. Additionally, the golf course measures rainfall to replace watering the playing areas as shown in figure 1.

Table 1 Summary data on three different golf courses

Items	Golf course I	Golf course II	Golf course III
Playing area (m^2)	430,515	880,000	393,765
Basin (m^2)	40,000	78,400	167,357
Water resources	Surface water	Surface water	Surface and Ground water
Turf	Bermudagrass	Bermudagrass, Manila grass	Bermudagrass, Manila grass
Staff (person)	36	56	30
Visitor/month	180	300	750

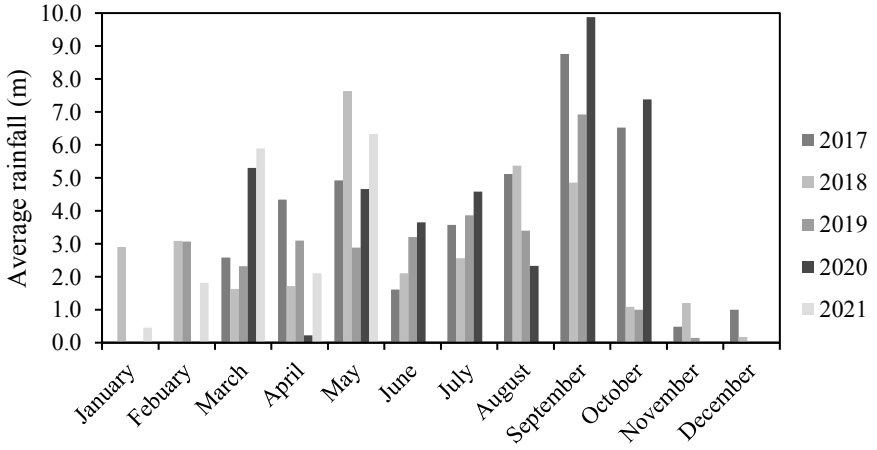

Figure 1 Average rainfall in Nakhon Ratchasima Province during the year 2017 to 2021

Water footprint

The water footprint assessment in each of the three golf courses was calculated by adding the blue and green water footprints. Table 2 shows the presence of water consumption on three different golf courses. The indirect water footprint considered the amount of power and gasoline utilized on each golf course. The indirect water footprint was computed by multiplying the amount of energy and fuel used by the water consumption. Blue WF is determined from the storage of water basins in each golf course which are 40,000 m^3, 78,400 m^3, and 167,357 m^3 in order of each golf course following table 1. Green WF is determined by the amount of stormwater that the operator in each golf course captured from the rain gauge per day, which is shown in figure 1. Regarding figure 1, the year 2017 has the highest average annual rainfall of the others which is 3.24 mm./year. Grey WF is the description of water management practice after the maintenance of turf in playing areas, the water run to the basin 15% which mean the total of water usage for maintenance in the golf course is 85% of all.

Due to some data being strictly confidential, the results were shown in table 3. This result missed the result of the fuel consumed from the golf course I. The whole operation of water footprint in three different golf courses was 5,427,975.02 m^3/year by the results of direct water footprint in 2,583,909.11 m^3/year which computed from blue water footprint 2,583,799.15 m^3/year (99.99%), and green water footprint 1.109 L/y (0.001%). While the amount of indirect water footprint was 260,156.79 m^3/year which computed from electricity consumption 38,187.92 m^3/year or 11.02 m^3/cap-y and from fuel consumption equals 1,968.87 m^3/year or 0.32 m^3/cap-y.

Table 2 Water consumption in three different golf courses

Site	Playing area (m^2)	Water consumption	
		(m^3/year)	(Million m^3/m^2-year)
Golf course I	430,515	600,000	0.72
Golf course II	880,000	1,687,687.15	0.52
Golf course III	393,765	305,112	1.29
Average ± SD.			**0.84 ± 0.40**

Table 3 Average annual resource usage of three selected golf course

Site	Water Footprint	Resource	Unit	Annual Consumption
Golf course I	Direct	Surface water	m^3	821,250
		Wastewater	m^3	123,187.50
	Indirect	Electricity	kwh	432,080
		Fuel	Lire	-
Golf course II	Direct	Surface water	m^3	1,678,687.15
		Wastewater	m^3	251,803.07
	Indirect	Electricity	kwh	1,296,235
		Fuel	L	16,363.64
Golf course III	Direct	Surface water	m^3	305,112
		Wastewater	m^3	45,766.80
	Indirect	Electricity	kwh	347,115
		Fuel	L	36,000

The maintenance practice in the golf courses including mowing means the maintenance of the grass in the playing area by using the machine which uses fuel to run the engine, irrigation means circular water management which uses the water after watering the greens and runs to the manhole which will run to the basin in its areas. Fertilizer in this process there is only one left using fertilization sometimes to keep the greens always green. All these management practices play significant parts in water consumption for turf management and rely on input resources for maximum performance and quality.

Conclusion:

The investigation of this study showed the background data and water footprint in golf courses located in Nakhon Ratchasima from January to June 2022 using field survey data. The overall water footprint in three different golf courses can be described as blue water footprint is 2,583,799.15 m^3/year and green water footprint is 1.109 L/y, on the other hand, the amount of indirect water footprint was 260,156.79 m^3/year, so, the whole golf courses business operation is 5,427,975.02 m^3/year. This study found that the process of golf courses consumed high water consumption in Pakchong district, Nakhon Ratchasima which is the factor that golf course in each area needs to maintain playing areas even it out of season.

Moreover, results also revealed that the maintenance services of mowing which is the trimming of grass in playing areas which each golf courses have its own practice, each golf course trims the grass if the grass has grown in an average of 2.8 millimeters, irrigation this part is the management of water as circular water because its reuse the water from maintenance which runs from the playing area into their the basin, and fertilizer most of the golf course didn't put the fertilization into the playing area, which it would destroy the grass and environmental while it has been dissolved and run to their basin except the golf course III which using the fertilization sometimes, but this golf course has its own treatment system. The management practice of these golf courses plays a major part in water consumption for turf management and relies on input resources for maximum performance and quality.

References:

1. United Nations, D.o.E.a.S.A., Population Division, *World Urbanization Prospects: The 2018 Revision,*. 2018.
2. Schipperijn, J., et al., *Influences on the use of urban green space – A case study in Odense, Denmark.* Urban Forestry & Urban Greening, 2010. **9**(1): p. 25-32.
3. Wenjie, W., Y. Chen, and L. Ye, *Perceived spillover effects of club-based green space: Evidence from Beijing golf courses, China.* Urban Forestry & Urban Greening, 2020. **48**: p. 126518.
4. Carlos Peña-Guzmán, G.B., Lina Restrepo, Melissa Pimiento, *Evaluation of Water Consumption at a Golf Club in Colombia for the Formulation of a Program of Savings and Efficient Use of Water by Indexes.* International Journal of Applied Environmental Sciences, 2018.
5. Throssell, C., et al., *Golf Course Environmental Profile Measures Water Use, Source, Cost, Quality, and Management and Conservation Strategies.* Applied Turfgrass Science, 2008. **6**.
6. Arjen Y. Hoekstra, A.K.C., Maite M. Aldaya and Mesfin M. Mekonnen,, *The Water Footprint Assessment Manual,*. 2011.

Development of biologically active compounds for control, prevention and treatment of environmental health problems /diseases

EVALUATION OF ANTI-INFLAMMATORY AND ANTI-CANCER ACTIVITIES OF SPIKE MOSS *Selaginella plana* EXTRACTS

Ugyen Lhamo[1], Jaruwan Chatwichien[1], Nopporn Thasana[1,2,3*]

[1]*Chemical Sciences Program, Chulabhorn Graduate Institute;*
[2]*Laboratory of Medicinal Chemistry, Chulabhorn Research institute;*
[3]*Center of Excellence on Environmental Health and Toxicology (EHT), OPS, MHESI, Thailand*
**Corresponding author* E-mail: nopporn@cri.or.th

Abstract:

Selaginella plana belongs to family of *Selaginellaceae*. Aim of this study is to investigate the inhibitory activities of methanol extract from *S. plana* and its partitions on A549 and HepG2 cells proliferation and migration and lipopolysaccharide (LPS)-induced nitric oxide (NO) production in RAW 264.7 macrophages. The safety against L929 mouse fibroblast cells was also determined. The results showed that the crude methanol extract could inhibit the cancer cells proliferation and migration, and the NO production presumably due to presence of various compounds such as biflavonoids, flavonoids, phenolic compounds, lignans, triterpenoids and fatty acids. Among its subfractions, the hexane partition was the most bioactive fraction for anti-cancer and anti-inflammatory activities.

Keywords: *Selaginella plana*, anti-cancer, anti-inflammatory, cell migration, bioactivity.

Introduction:

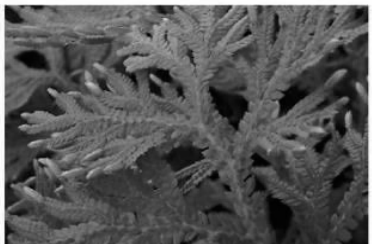

Figure1. *Selaginella plana*

Selaginella plana (Desv.) Hieron., known as Asian spike moss, belongs to the family of *Selaginellaceae*. It is seedless vascular herbaceous shrub that mostly grows in tropical climatic conditions. *Selaginella* species has been used in traditional medicine for treatment of diseases such as cancers, cardiovascular diseases, diabetes, hepatitis, skin diseases and urinary tract infections.[1] These biological activities are attributed to the presence of flavonoids, biflavonoids (such as amentoflavone, robustaflavone, isocryptomerin), phenolics, alkaloids and lignans.[2] *S. plana* has been used as traditional medicine, vegetable and ornamental plants. The extracts from *S. plana* are bioflavonoids-rich and possess anti-cancer, anti-oxidant, anti-viral, anti-inflammatory, anti-malarial, anti-fungal and anti-bacterial properties.[3] Recently in our group, we reported two new *nor*-lignans, siamensionols A and B and three new bioflavonoids, siamenflavones A-C from *Selaginella siamensis* Hieron. and *Selaginella bryopteris* (L.) Baker. These new compounds were potent anti-cancer compounds and particularly, siamenflavone B, for the first time, was found to be potent inhibitory activities against wild-type EGFR.[4,5] Previously, the anti-inflammatory activity against skin erythema, anti-bacterial activity and anti-cancer activity against MCF-7 and T47D cells of *S. plana* have been studied.[6-9] To further explore its biological activity, herein we report anticancer activities of methanol extract of *S. plana* against A549 and HepG2 cancer cells. In addition, its potential to inhibit the LPS-induced NO production in RAW264.7 was also evaluated.

Methodology:

Plant material and extraction

Fresh *Selaginella plana* (cultivar) were collected from BaanFa-PaFern, Bangkok on 6th January 2022. Whole plant was washed, air dried and finely chopped. The plant (1120 g) was extracted three times in 6 L of methanol at room temperature, 3 days each. The extracts were combined and dried under vacuum to yield the crude methanol extract (47.9 g) which then redissolved in water and sequentially partitioned with hexane, dichloromethane, ethyl acetate and butanol, respectively, to yield corresponding subfractions. For bioactivity evaluation, these extracts were prepared as stock solutions in dimethylsulfoxide (DMSO) and stored at –20ºC until used.

Cell lines and cell culture

A549, HepG2, L929 and RAW 264.7 cells were cultured in minimum essential medium (MEM) supplemented with 10% FBS and 100mL of 1% penicillin-streptomycin, under 5% CO_2, at 37 ºC.

MTT assay

Cells at the density of 10^4 cells/well were seeded in 96-well plates and incubated for 16 hours before being exposed to extracts, cisplatin and afatinib (reference compounds) or DMSO (vehicle control). After 48 hours of incubation, the culture medium was replaced with 100 µL of 0.5mg/mL (3-[4,5-dimethylthiazol-2-yl]-2,5 diphenyl tetrazolium bromide), MTT solution and incubated for 3 hours. The MTT solution was replaced with 100 µL DMSO. Absorbance at 570 nm was measured. All experiments were done in triplicate and IC_{50} values was calculated using the GraphPad Prism 7 software.

Nitric oxide (NO) assay

RAW 264.7 cells at the density of 10^5 cells/well were seeded into 24-well plates and incubated for 18 hours before being pre-treated with extracts at the non-toxic concentrations (more than 80% viability), bay11-7082 (reference compound) or DMSO (vehicle control) for 1 hour. The cells were then stimulated with 0.1 µg/mL LPS for 24 hours. Griess reagent was used to measure the NO production. All experiments were done in triplicate and NO levels were calculated by using a standard curve of sodium nitrite.

Scratch (Wound healing) assay

Cells were seeded in 24-well plates and incubated for 24 hours to form monolayer which then scraped off in a straight line using a sterile 200µL pipette tip. The detached cells were washed away using PBS and then the cells were treated with extracts, cisplatin (reference compound) or DMSO (vehicle control) in 5% FBS culture medium. The scratched areas were photographed under microscope at three time points (0, 24 and 48 hours). The experiments were done in triplicate. Wound width was measured as distance between the edges of the scratches. The %wound closer was calculated according to the following equation:

$$Wound\ closure\ \% = \left(\frac{width_{t=0\ h} - width_{t=24\ or\ 48\ h}}{width_{t=0\ h}}\right) \times 100\%$$

Results:

Anti-cancer properties of Selaginella plana extracts

Table 1 Antiproliferative activities of *S. plana*

Samples	IC_{50} value (µg/mL) ± SEM, n=3		
	A549	HepG2	L929
Methanol	132.9 ± 23.7	NI	NI
Hexane	64.0 ± 8.3	61.8 ± 7.5	72.3 ± 7.0
Dichloromethane	80.6 ± 5.7	78.8 ± 9.5	54.2 ± 4.5
Ethyl acetate	104.0 ± 9.6	79.9 ± 25.0	102.4 ± 4.4
Butanol	118.1 ± 3.2	109.4 ± 2.9	140.1±9.5
Water	NI	NI	NI
Cisplatin	2.9± 0.1	7.2± 0.9	NI
Afatinib	93.1± 2.0	58.6± 21.0	NI

NI: IC_{50} > 150 µg/mL

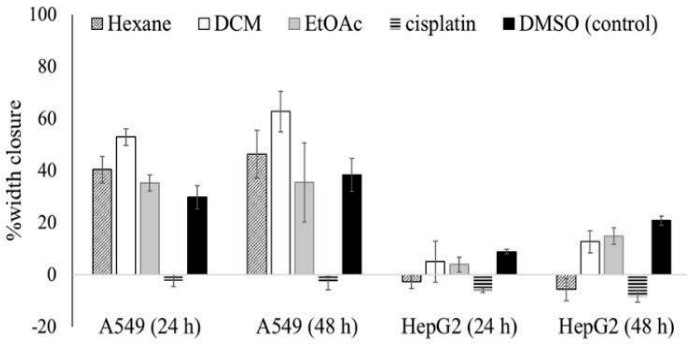

Figure 2 Inhibitory activities of *S. plana* extracts (50µg/mL) and cisplatin (5µM), as compared to vehicle, on A549 and HepG2 cell migration.

From MTT assay (Table 1), the crude methanol extract showed promising antiproliferative activity against A549 but weak activity to HepG2 and L929 cells, indicating the high selectivity of the methanol extract to A549. Among its partitions, hexane subfraction showed the most potent antiproliferative activities against the cancer cells with IC_{50} values of 64.0±8.3µg/mL (A549) and 61.8±7.5µg/mL (HepG2). However, the selectivity was not observed since the hexane extract was also toxic to the L929 normal cells at the similar potency (IC_{50} = 67.0±21.3µg/mL). The water subfraction did not exhibit significant cytotoxic effect against all tested cell lines. Meanwhile, the dichloromethane subfraction, showed more than 1.5-folds more cytotoxicity against L929 normal cells than A549 or HepG2 cancer cells. From the scratch assay (Figure 2), the hexane, dichloromethane (DCM) and ethyl acetate (EtOAc) subfractions at 50 µg/mL could slightly inhibit the migration of HepG2 cells but not A549 cells, as compared to the vehicle control (DMSO).

Anti-inflammatory activity of Selaginella plana extracts

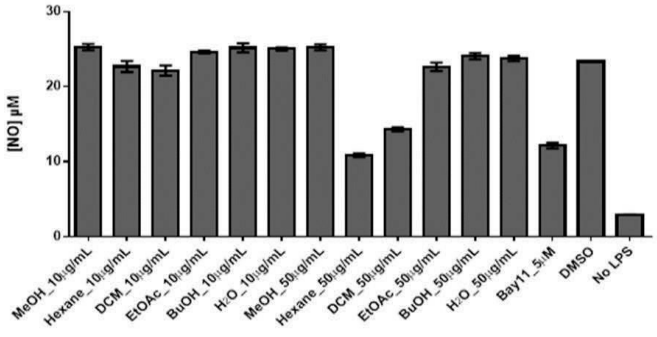

Figure 3 Inhibitory activity of S. plana extracts on LPS-induced NO production in RAW264.7 cells.

In the NO assay, the extracts at the non-toxic concentrations (50µg/mL and 10µg/mL) were tested. As shown in Figure 3, although the activity of the crude methanol was not observed, its hexane and dichloromethane subfractions at the concentration of 50 µg/mL exhibited significant inhibitory activity on NO production in LPS-stimulated RAW 264.7 cells, as compared to the DMSO vehicle control, in the same manner as a known anti-inflammatory agent, bay11-7082.

Discussion:

S. plana extracts have been known to exhibit promising anti-cancer and anti-inflammatory activities (2, 8, 9). This work showed that the methanol extract of *S. plana* exerted selective anticancer activity to A549 cells over HepG2 and L929 cells. Its hexane, dichloromethane and ethyl acetate partitions showed higher cytotoxicity to all tested cell lines, as compared to the crude extract and the butanol and water partitions. The results from scratch assay suggested that the active fractions exhibited antiproliferative effects with no significant inhibitory activity of the cancer cell migration. In addition, the hexane and dichloromethane subfractions showed significant anti-inflammatory activity. Our ^{1}H NMR study revealed the presence of various fatty acids in the hexane and DCM fractions and biflavonoids in the ethyl acetate fraction. These compounds are known as bioactive compounds and possibly attributed to the observed anti-cancer and anti-inflammatory activities.

Conclusion:

The methanol extract of *S. plana* and its hexane, dichloromethane and ethyl acetate subfractions possessed promising anti-cancer and anti-inflammatory activities. Phytochemical study and the chemical components responsible for the bioactivities are under investigation in our laboratory.

Acknowledgment:

This work is supported by Chulabhorn Graduate Institute, Thailand Science Research and Innovation (TSRI) for Chulabhorn Royal Academy and Center of excellence on Environmental Health and Toxicology (EHT).

References:

1. Mishra A. Screening and characterization of potential bioactive compounds from Selaginella wightii. 2020.
2. Setyawan AD. Natural products from genus Selaginella (Selaginellaceae). Nusantara Bioscience. 2011;3(1).
3. Hassan G, Zahra Q, Ali I, Engel N, Ali K, Bahreen G, et al. Tropical Journal of Natural Product Research. 2020.
4. Thamnarak W, Eurtivong C, Pollawatn R, Ruchirawat S, Thasana N. Two new nor-lignans, siamensinols A and B, from Selaginella siamensis Hieron. and their biological activities. Natural Product Research. 2021:1-9.
5. Demehin AA, Thamnarak W, Lamtha T, Chatwichien J, Eurtivong C, Choowongkomon K, et al. Siamenflavones AC, three undescribed biflavonoids from Selaginella siamensis Hieron. and biflavonoids from spike mosses as EGFR inhibitor. Phytochemistry. 2022:113374.
6. Wulandari F, Djajadisastra J, Elya B. Efficacy of lotion containing fractions of Selaginella Plana leaves and Lagenaria Siceraria (molina) standl. Fruit for relief of skin erythema. International Journal of Applied Pharmaceutics. 2018;10(Special Issue 1):182-4.

7. Novita H, Novitaningrum A, Madusari B, Nugraha M, Rajamuddin M, Yunita R, et al., editors. Antibacterial activity of Anadendrum microstachyum and Selaginella plana against two pathogenic bacteria (Edwardsiella ictaluri and Streptococcus agalactiae) causing freshwater fish diseases. IOP Conference Series: Earth and Environmental Science; 2020: IOP Publishing.
8. Risdian C, Handayani S, Udin Z, Andriyani R, Angelina M. Anticancer Activity Of Ethanolic Extract Of Selaginella Plana Hieron. On T47d Cell Line In Vitro. Jurnal kimia terapan Indonesia. 2011;13(2).
9. Handayani S, Risdian C, Meiyanto E, Udin Z, Andriyani R, Angelina M. Selaginella Active Fractions Induce Apoptosis on T47D Breast Cancer Cell. Indonesian Journal of Pharmacy. 2012;23(1):48-53.

FIVE NEW COMPOUNDS FROM THE WHOLE PLANTS OF *Kaempferia saraburiensis* AND THEIR BIOACTIVITY STUDIES

Pornpuk Booranaseensuntorn[a], Jutatip Boonsombat[b,c], Paratchata Batsomboon[b], Sanit Thongnest[b,c], Prasat Kittakoop[a,c,d] and Somsak Ruchirawat [a,c,d]

[a]Chemical Biology Program, Chulabhorn Graduate Institute, Chulabhorn Royal Academy, Kamphaeng Phet 6 Road, Bangkok, Thailand.
[b]Laboratory of Natural Products, Chulabhorn Research Institute, Kamphaeng Phet 6 Road, Bangkok, Thailand.
[c]Center of Excellence on Environmental Health and Toxicology (EHT), OPS, MHESI, Thailand.
[d]Program in Chemical Science, Chulabhorn Graduate Institute, Chulabhorn Royal Academy, Kamphaeng Phet 6 Road, Bangkok, Thailand

Abstract:

The study of *Kaempferia saraburiensis* for its secondary metabolites led to the isolation of five new compounds, saraburol (**1**), saraburane A and B (**2–3**), *E*/*Z*-saraburinic esters (**14–15)**, along with ten known compounds oxygenated isopimarane diterpenoids. The structures were established by spectroscopic studies including 1D & 2D NMR, IR, $[\alpha]_D$, CD, and HRESIMS, and comparison with literature values. Their absolute configuration were determined by comparing with computed ECD and observed ECD spectra as well as hydrolysis reactions. The cytotoxicity results showed that *E*-saraburinic ester had the most activity against MOLT-3 cells, with an IC_{50} value of 12.0 μM and a selectivity index of 12.5.

Keywords: Antimicrobial activity, cytotoxic activity, DP4+, diterpenoids, *Kaempferia saraburiensis*, saraburanes, saraburol, zingiberaceae

Introduction:

Kaempferia produce inflorescense directly from pseudostems such as *K.galanga*, *K.saraburiensis*, *K.elegans*. Subgenus *Protanthium* will create inflorescence from rhizome above the surface of the soil. When the flowers are gone, it will develop leaves and artificial stems for example *K.takensis, K.albiflora*, *K.lopburiensis*. In this work, we interested in *Kaempferia saraburiensis*, a new specie from Saraburi Province, Thailand. Nowadays, This plant no report about the chemical structure and biological activity. It is a perennial herb, the flower has white, purple colors and contain several roots.

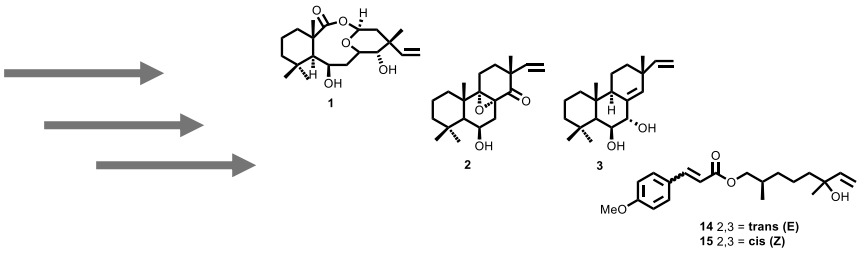

Methodology:

Plant material:

The rhizome of *K. Saraburiensis* were collected from Wat phra phuttabat, Saraburi Province, Thailand.

Extraction and Isolation:

The rhizome of *K.saraburiensis* were extracted with EtOH AR grade (2x30 L) to afford the crude EtOH extract. After that, it was extracted with MeOH-CH_2Cl_2 to afford the crude MeOH-CH_2Cl_2 extract. A part of EtOH and MeOH-CH2Cl2 was subjected to sephadex LH-20 eluted with isocratic solvent systems 80%MeOH/DCM to afford 5 fractions (fraction 1-5). One of fraction got compound 4 (23.3 mg). Fraction 4 (883.7 mg) was purified by silica gel column chromatography with a gradient solvent of Hexane:CH_2Cl_2 (70:30) to CH_2Cl_2: MeOH (95:5) to give compound 5 (47.8 mg), $[\alpha]_D^{25}$ = -26.3 (c 0.49, MeOH). Fraction 5 was separate by silica gel CC with isocratic solvent system Hexane:CH_2Cl_2 (60:40) and 5% MeOH:CH_2Cl_2 to afford compound 6 (226.8 mg), $[\alpha]_D^{25}$ = +3.57 (c 0.53, MeOH). Fraction 6 was subjected to C_{18} reverse phase CC eluted with a gradient solvent ACN: H_2O (75:25) to (100:0) to give compound 6 (40.3 mg). Fraction 8 was further purified by silica gel CC elutes with a gradient Hexane:CH2Cl2 (30:70 to 0:100) to afford 10 fractions. Subfraction 8/2 (52.2 mg) was separated by HPLC using ACN: H_2O (20:80 to 90:10) to give compound 1 (3.6 mg) and (2.7 mg). Subfraction 8/4 (86.9 mg) was purify by HPLC using ACN: H_2O (60:40 to 100:0) to give compound 7 (5.8 mg), $[\alpha]_D^{25}$ = -11.25 (c 0.67, MeOH), compound 15 (4.0 mg). Subfraction 8/5 was further purify by HPLC using ACN: H_2O (80:20 to 100:0) to give compound 3(11.4 mg), 7(4.1 mg), 12(11.5 mg), 15(8.1 mg). Subfraction 8/6 was subjected to sephadex LH-20 using isocratic solvent system CH_2Cl_2: MeOH (80:20) and further purify by C_{18} reverse phase CC using isocratic solvent system ACN: H_2O (70:30) to give compound 7 (8.8 mg), 14 (21 mg). Subfraction 8/7 (1.9 mg) was separated by sephadex LH-20 using isocratic solvent system CH_2Cl_2: MeOH (20:80) and further purify by HPLC using ACN: H_2O (80:20 to 100:0) to give compound 10 (22.8 mg), $[\alpha]_D^{25}$ = -19.5 (c 0.98, MeOH), 12 (7.1 mg), 13 (5.5 mg), $[\alpha]_D^{25}$ = -15.8 (c 0.25, MeOH). Subfraction 8/9 (1.2 g) was separated by sephadex LH-20 using isocratic system CH_2Cl_2: MeOH (20:80) and further purify by HPLC using ACN: H_2O (80:20 to 100:0) to give compound 11 (495.4 mg), $[\alpha]_D^{25}$ = +87.05 (c 0,2, MeOH).

Cytotoxicity assay:

The cytotoxicity assay was estimated against several human cell lines consist of MOLT-3, A-549, HepG2, T-47D, H69AR, HeLa, MRC-5, MDA-MB-231, HuCCA-1 and S102. All of compound test with incubated cells for 48h. The alive cell was measured by MTT and XTT assays.

Results and Discussions:

Table 1 Results of cytotoxicity of compounds 2-15 on different human cancer cell lines.

Compounds	Anti-cancer Activity (μM)				
	S-102	MDA-MB-231	HepG2	MOLT-3	MRC-5
2	13	16	0	0	20
3	92.8 [1.1]	90.3 [1.1]	97.1 [1.0]	52.1 [1.9]	97.9
4	0	2	11	4	0
5	106.4	87.8	97.9	71.9 [1.1]	81.5
6	15	135.9	126.5 [1.1]	38	136.9
7	13	35	0	7	23

Compounds	Anti-cancer Activity (μM)				
	S-102	MDA-MB-231	HepG2	MOLT-3	MRC-5
8	7	8	0	11	22
9	5	30	8	40	20
10	129.6[1.1]	128.0 [1.1]	157.9	63.4 [2.2]	138.9
11	93.2	92.9	82.8 [1.1]	43.7 [2.1]	92.6
12	89.3	82.5	92.1	56.7 [1.5]	82.6
13	5	6	10	127.0	11
14	29.7	35.7	33.3	12.0 [12.5]	25
15	21	28	40	62.9 [2.4]	47
Doxorubicin Hydrochloride (MW=579.98)	2.45	3.12	51.2	0.04	3.17
Etoposide (MW=588.56)	ND	ND	0.62	0.016	ND

Compounds **2**-**15** were evaluated for their cytotoxic activities in a panel of four human cancer cell lines, S-102, MDA-MB-231, HepG2, MOLT-3 and a normal human lung cell line, MRC-5 (Table 1). The *E*-conformer **14** showed the most potent activity in MOLT-3 cells (IC_{50} = 12.0 μM, SI = 12.5). As compounds with SI value ≥ 3 have been considered to possess cancer-selective cytotoxicity [1]. Compound **14** had highly selective cytotoxicity activity toward MOLT-3 cell line.

Table 2 NMR calculation results of four plausible epimers (5S,6S,10S,11R,13R,14R-**1a**, 5S,6S,10S,11R,13R,14S-**1b**, 5S,6S,10S,11S,13R,14R-**1c**, 5S,6S,10S,11S,13R,14S-**1d**) at the mPW1PW91/6-31+G(d,p) level

	Isomer 1	Isomer 2	Isomer 3	Isomer 4
sDP4+ (H data)	0.00%	0.00%	0.12%	99.88%
sDP4+ (H data)	0.18%	0.00%	5.31%	94.52%
sDP4+ (H data)	0.00%	0.00%	0.01%	99.99%
uDP4+ (H data)	0.39%	0.32%	0.20%	99.08%
uDP4+ (H data)	0.00%	0.00%	88.96%	11.04%
uDP4+ (H data)	0.00%	0.00%	1.59%	98.41%
DP4+ (H data)	0.00%	0.00%	0.00%	100.00%
DP4+ (H data)	0.00%	0.00%	31.14%	68.86%
DP4+ (H data)	0.00%	0.00%	0.00%	100.00%

The relative stereochemistry at C-5, C-6 and C-14 of compound **1** was elucidated by NOESY between H-5 and H_3-19; H-6 and H_3-19; H-14 and H_3-17. The relative stereocenter at C-11, C-6 and C-14 could not be determined owing to the lack of proton correlations, resulting in the four possible structure (**1**a-**1**d). The DP4+ probability analysis, based on the gauge-independent atomic orbital (GIAO) method at the PCM/mPW1PW91/6-311++G(d,p) level, was used to indicate the relative configurations. Based on DP4+ protocol, both proton and carbon data of four possible isomers (5S*, 6S*, 10S*, 11R*, 13R*, 14R*-**1**a, 5S*, 6S*, 10S*, 11R*, 13R*, 14S*-**1**b, 5S*, 6S*, 10S*, 11S*, 13R*, 14R*-**1**c and 5S*, 6S*, 10S*, 11S*, 13R*, 14S*-**1**d) were calculated, and the results were analyzed with the experiment values.[2] The statistical comparison showed that the isomer **1**d was the equivalent structure with a probability of 100% confidence (Table 2). The relative configuration 1 was determined as 5S*, 6S*, 10S*, 11S*, 13R*, 14S*.

Conclusions:

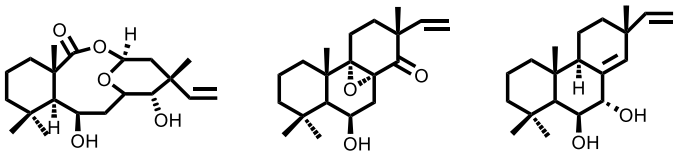

saraburol (1) saraburane A (2) saraburane B (3)

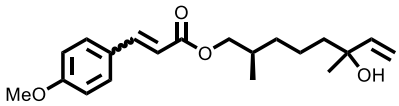

14 2,3 = **trans (E)-saraburinic ester**
15 2,3 = **cis (Z)-saraburinic ester**

Five new compounds were extracted from *K. saraburiensis*. The five new compounds are compound **1** (saraburol), compound **2** (saraburane A), compound **3** (saraburane B), compound **14** (*E*-saraburinic ester), compound **15** (*Z*-saraburinic ester).

The cytotoxicity results showed that *E*-saraburinic ester had the most activity against MOLT-3 cells, with an IC_{50} value of 12.0 μM and a selectivity index of 12.5.

Reference:

1. Prayong P, Barusrux S, Weerapreeyakul N. Cytotoxic activity screening of some indigenous Thai plants. Fitoterapia. 2008; 79:598-601.
2. Grimblat N, Zanardi M.M, Sarotti A.M. Beyond DP4: an improved probability for the stereochemical assignment of isomeric compounds using quantum chemical calculations of NMR shifts. J. Org. Chem. 2015;80: 12526-12534.
3. Booranaseensuntorn P, Boonsombat J, Mahidol C, Reuk-Ngam N, Khlaychan P, Batsomboon P, Techasakul S, Thongnest S. Diterpenoids and *p*-methoxycinnamic acid diol esters from *Kaempferia saraburiensis* Picheans. (Zingiberaceae): Structural assignment of saraburol and their biological activities. Phytochem. Lett. 2022;199: 113181.
4. Tungcharoen P, Wattanapiromsakul C, Tansakul P, Nakamura S, Matsuda H, Tewtrakul S. Anti-inflammatory effect of isopimarane diterpenoids from Kaempferia galangal. Phytotherapy Research. 2019;1–12.
5. Jenjittikul T, Ruchisansakun S, Kew. 2020; 75(13): 1-5.

INFLUENCE OF PROBIOTIC BACTERIA ON MOSQUITO SIZE AND FLIGHT ABILITY OF RADIO-STERILIZED *Wolbachia* TRANSINFECTED *Aedes aegypti*

Konkamon Sujijun[1,2,3], Parinda Thayanukul[1,2,3], Pattamaporn Kittayapong[1,2]

[1]*Department of Biology, Faculty of Science, Mahidol University, Bangkok, Thailand*
[2]*Center of excellence for Vectors and Vector-Borne Diseases, Nakhon Pathom, Thailand*
[3]*Center of Excellence on Environmental Health and Toxicology, OPS, MHESI, Bangkok, Thailand*

Abstract:

Aedes aegypti mosquitoes are the main vectors for dengue fever, Chikungunya fever, yellow fever, and Zika virus causing public health problems around the world. One of the biological control methods for the *Ae. aegypti* is the sterile insect technique (SIT) in which the radio- induced sterile males will be released to mate with fertile native females. Unfortunately, the radiation lowered the mosquito survival rate, longevity. The irradiation has been used in combination with *Wolbachia* bacteria that can induce cytoplasmic incompatibility causing nonviable egg production in mosquitoes (SIT/IIT). Besides, many studies on fruit flies demonstrated that feeding larvae with probiotic bacteria-containing diets could enhance insect growth and survival This study aims to investigate the effects of selected probiotic bacteria on mosquito ecological fitness parameters including mosquito size and flight ability. The potential probiotic bacteria were isolated from pools of 50 Gy irradiated mosquito guts. From 49 bacterial isolates, 3 potential probiotic bacteria were selected based on colony morphological difference, Random Amplified Polymorphic DNA (RAPD) pattern, DNA sequencing results, and literature search of insect probiotic research. Three potential probiotic bacteria included *Enterobacter mori*, *Aeromonas dhakensis* and *Elizabethkingia anopheles*. The bacteria will be mixed with larval diet and supplied to the mosquitoes before exposure to irradiation The mosquito fitness tests including longevity, wing size, and flight ability will be determined. This study will contribute to improve the survival of sterile male mosquitoes after irradiation, which will further promote the implementation of SIT or SIT/IIT projects on reducing the mosquito vector population and vector borne diseases.

Keywords: Sterile insect technique, probiotic, gut microbial community, *Aedes aegypti*, *Wolbachia* bacteria.

Introduction:

Aedes aegypti is a major mosquito vector for dengue, chikungunya, yellow fever and Zika viruses which are important diseases causing death worldwide. The controls of mosquito populations that carry these diseases are of particular importance. One of the effective ways to control mosquito populations is the ionizing radiation induced Sterile Insect Techniques (SIT). SIT is a sterilization method of insects being applied in fruit flies and mosquitoes using Gamma ray or X-ray irradiation typically around 50-70 Gy. Irradiation will damage chromosome and somatic cells of the insects causing sterility. When sterile male mosquitoes are released into natural environment, mating between sterile male and natural fertile female mosquitoes will result in no viable eggs, i.e., female mosquitoes will lay eggs that cannot hatch into larvae. On the other hand, irradiation has a negative impact on mosquito fitness and reduce longevity of mosquitoes. The structure of bacterial communities in insect was also changed after being exposed to radiation.

Previous studies showed that the introduction of radio-resistant probiotic bacteria from the insect gut could extend longevity or increase fitness of irradiated fruit flies. Probiotic microorganisms promote the production of important compounds including vitamins, amino acids, carbohydrates, and steroids, which are necessary for mosquito development and survival. *Enterobecter* sp. exhibited the up-regulated expression of the immune gene attacin and PGPR-LC in irradiated *Ceratitis capitata* males (Msaad Guerfali et al., 2021). Therefore, the probiotic microbes might help restoring or preventing the negative effect of radiation on *Ae. aegypti*, and enhancing success of the SIT project.

Materials and Methods:

Mosquito rearing

The mosquito colonies of *wAlbB*-TH (*Wolbachia* trans-infected *Aedes aegypti*) and JJ (wild-type *Wolbachia* non-infected *Aedes aegypti*) were used in this study. Larvae were reared in 32×42 cm plastic trays. Adult mosquitoes were reared in aluminum mesh cages sized 30 cm x 30 cm x 30 cm. The larvae were ad libitum fed with a combined diet of fish meal, chicken liver powder, and yeast powder at 3.3 g, 0.1 g, 0.56 g, respectively. Adult mosquitoes were fed with 10% sucrose solution. All the mosquito rearing containers were kept in an insectary room controlled with 75 ± 2 % humidity, 27 ± 2 °C and photoperiod of 12/12 h day/night.

Irradiation

Male pupae aged 20-30 hours were transferred into clear plastic cups. Each cup contained 100 pupae. All mosquitoes were irradiated at the dosage of 50 gy (around 2 minutes) using RS 2400•Q Irradiator (Rad Source Technologies Inc, USA) at the Thailand Institute of Nuclear Technology (TINT). The irradiated male pupae were placed in the mosquito cages, along with a 10% sucrose solution.

Gut extraction and isolation

Ten whole guts were dissected from 5 days emerging adults (Gusmão et al., 2010) from both *wAlbB*-TH and JJ colonies. The mosquito dissection was performed in sterile 1x PBS (81 mM Na2HPO4, 19 mM NaH2PO4, 150 mM NaCl, pH 7.) under the stereomicroscope. The pools of ten guts of *Ae. aegypti* were homogenized using sterile pestle homogenizers. Serial dilution (10^1-10^6) of homogenized gut extracts was performed using 1× PBS and then spreaded on trypticase soy agar (TSA) and Macconkey agar. The morphological different colonies were selected and purified with streaked plate method on fresh TSA agar.

Random Amplified Polymorphic DNA (RAPD)

DNA was extracted using lysis buffer and freeze/thaw 5 cycles by -80°C freezer and 95°C water bath. The rapid screening of bacterial diversity was performed randomly amplified polymorphic DNA (RAPD) method using primers 640 (5'-CGTGGGGCCT-3') and OPAR8 (5'-TGGGGCTGTC-3) following;initial denaturation at 94°C for 2 min, denaturation at 94°C for 30 seconds, annealing at 42°C for 1 min, extension at 72°C for 2 min, Go to step 2 for 35 cycles, and final extension at 72°C for 10 min (Abbas et al., 2017).

Bacterial identification

The bacterial colonies were chosen based on morphological difference and RAPD profile. DNA amplification of the 16S rRNA gene was performed by using the primer 27F (5'-AGAGTTTGATCMTGGCTCAG-3') and 1492R (5'-TACGGYTACCTTGTTACGACTT-3'). Bacteria DNA was amplified in 100 µl PCR master mix (Vivantis, Malaysia). The program was set as follows: initial denaturation at 94°C for 2 min, denaturation at 94°C for 30 seconds, annealing at 55°C for 1 min, extension at 72°C for 2 min, Go to step 2 for 35 cycles, and final extension at 72 °C for 10 min. The amplified 16S rRNA fragments were sequenced and compared with sequences available at the NCBI database using the blast algorithm.

Probiotic diet preparation and fitness tests

Three chosen potential probiotic bacteria were cultured in sterile trypticase soy broth (TSB) and adjusted final concentration to be 10^8 CFU/ml using 1× PBS. The individual bacterial suspension volume 2 ml was added to 100 g of larval diet (Augustinos et al., 2015). For longevity test, 50 sterile male mosquitoes for each bacterial isolate were maintained in a cage. The numbers of dead mosquitoes were recorded every day. For wing size determination, the right wings of 20 probiotic-fed and 20 non-probiotic-fed male mosquitoes. The distance between the axillary incision (alula) and the apical border was measured as the wing length. For flight ability, a cup of 100 pupae was placed in a flight ability cylinder for each selected condition. The numbers of passed mosquitoes were recorded in 1 hour.

Results and Discussion:

Selection potential probiotic bacteria from *Ae.aegypti* gut

In the study, total 49 bacterial colonies were obtained from the agar plates applying mosquito gut extracts based on morphological difference. To select different types of bacteria, RAPD method with short random primers of 650 and OPAR8 was used as a pre-screening step. Bacterial isolates showing different band patterns were likely be different species. With the RAPD results along with the colony morphology, therefore, 10 isolates were selected. They were the sample numbers 2, 9, 11, 15, 16, 27, 30, 34, 44 and 46 (Figure 1), which were further conducted the DNA sequencing of 16s rRNA gene.

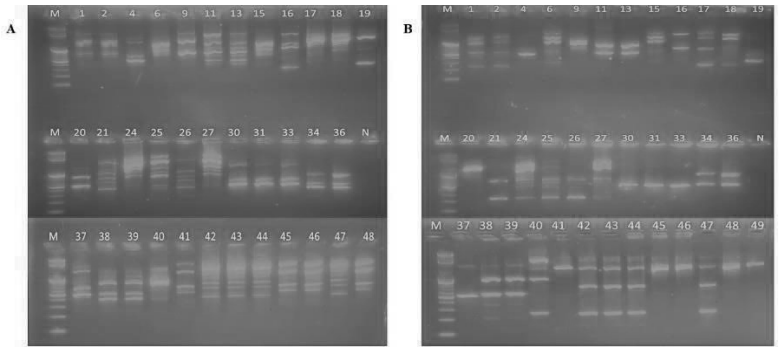

Figure 1. DNA bands by RAPD method. A; 640 primer, B; OPAR8 primer.

BLAST algorithm was used to preliminary identify the bacterial species of the chosen isolates. Because isolate C2, C9, C11, C15, C16, C27, C30 (Table 1) were characterized as the pathogenic risk group 2 which were not able to distribute in the market, we could not use them in further study. In addition, based on literature search results of the potential probiotic bacteria in insect host, *Enterobacter mori* (C44), *Aeromonas dhakensis* (C46) and *Elizabethkingia anopheles* (C31) were chosen for study of the impact of probiotic bacteria on the mosquito fitness.

Table 1 Identification of bacterial isolates from *Aedes aegypti* gut based on 16s rRNA gene.

Isolate	Closest matched strain (Accession number)	Max Score	E-value	%identity
C2	*Klebsiella variicola* (MK894865.1)	2041	0	100
C9	Enterobacteriaceae bacterium (DQ837052.1)	1916	0	100
C11	*Enterobacter hormaechei* (MN911370.1)	1720	0	100
C15	*Klebsiella pneumonia* (CP052181.1)	1916	0	99.81
C16	*Acinetobacter pittii* (MT378403.1)	1818	0	99.7
C27	*Enterobacter cloacae* (MT613381.1)	1777	0	100
C30	*Elizabethkingia anopheles* (CP034594.1)	1720	0	100
C34	*Enterobacter hormaechei* (CP041733.1)	1923	0	100
C44	*Enterobacter tabaci* (MN733344.1)	1629	0	99.23
C46	*Aeromonas dhakensis* (MT474858.1)	1801	0	99.9

Conclusion:

Almost 50 bacterial isolates were obtained from the guts of irradiated *Aedes aegypti* mosquitoes. RAPD and colony morphology were used to pre-screened the bacterial cultures and 10 isolates were selected. Based on the literature search and Thailand Ministry of Health pathogenic risk group, only three bacterial strains were chosen, i.e., *Enterobacter mori*, *Aeromonas dhakensis* and *Elizabethkingia anopheles*, as the potential probiotic bacteria. The three strains will be added to the mosquito diet for studying the effects on the mosquito size and flight ability in further step.

Acknowledgements:

This study was supported by International Atomic Energy Agency on the project managing and controlling *Aedes* vector populations using the sterile insect technique (RAS5082) and Mahidol University on the project diversity of bacteria and virus associated with ectoparasites of bats for monitoring of emerging infectious diseases in Thailand.

References:

1. Abbas, Y. A., & Radhi, G. F. (2017). Genetic Variation of Enterobacter cloacae Using Random Amplified Polymorphic DNA (RAPD-PCR).
2. Augustinos, A. A., Kyritsis, G. A., Papadopoulos, N. T., Abd-Alla, A. M., Cáceres, C., & Bourtzis, K. (2015). Exploitation of the medfly gut microbiota for the enhancement of sterile insect technique: Use of Enterobacter sp. in larval diet-based probiotic applications. PLOS ONE, 10(9). https://doi.org/10.1371/journal.pone.0136459
3. Gusmão, D. S., Santos, A. V., Marini, D. C., Bacci, M., Berbert-Molina, M. A., & Lemos, F. J. (2010). Culture-dependent and culture-independent characterization of microorganisms associated with Aedes aegypti (Diptera: Culicidae) (L.) and dynamics of bacterial colonization in the Midgut. Acta Tropica, 115(3), 275–281. https://doi.org/10.1016/j.actatropica.2010.04.011
4. Msaad Guerfali, M., Charaabi, K., Hamden, H., Djobbi, W., Fadhl, S., Mosbah, A., & Cherif, A. (2021). Probiotic based-diet effect on the immune response and induced stress in irradiated mass reared Ceratitis capitata males (Diptera: Tephritidae) destined for the release in the sterile insect technique programs. PLoS ONE, 16(9). https://doi.org/10.1371/journal.pone.0257097

MOSQUITO AGE IMPACT ON STERILITY OF RADIO-STERILIZED *Wolbachia* TRANS-INFECTED *Aedes aegypti*

Preeyapron Ruaysawat[1,2,3], Parinda Thayanukul[1,2,3] and Pattamaporn Kittayapong[1,2]

[1]*Department of Biology, Faculty of Science, Mahidol University, Bangkok, Thailand*
[2]*Center of Excellence for Vector and Vector-Borne Diseases, Nakorn Pathom, Thailand*
[3]*Center of Excellence on Environmental Health and Toxicology, OPS, MHESI, Bangkok, Thailand*

Abstract:

Aedes aegypti mosquito is the main vector of the dengue virus causing dengue fever and dengue hemorrhagic fever. Because the number of dengue patients have been increasing annually especially in Thailand, the elimination of *Ae. aegypti* population is crucial. *Wolbachia pipientis* is an intracellular symbiont of *Ae. aegypti* that can be used as a biological control agent. *Wolbachia* can induce the cytoplasmic incompatibility during the fertilization process in mosquitoes leading to non-viable egg production in turn reducing the vector population. Recently, *Wolbachia* control has been applied in combination with ionizing radiation to induce mosquito sterility as the radiation technique also can damage mosquito germ cells causing sterility. However, the irradiation can reduce the mosquito longevity and the *Wolbachia* titers were changing with age. This study investigated the effect of aging on the sterility of *Wolbachia* trans-infected female *Ae. aegypti* mosquitoes. Native *Ae. aegypti* without *Wolbachia* infection was included as a control. Our results showed that aging had no impact on the female mosquito sterility rates. Surprisingly, *Wolbachia* infection reduced the egg hatch rate and increased the egg sterile rate especially in the blood-fed aged population (d15). *Wolbachia* trans-infected female *Aedes aegypti* rather have lower ecological fitness compared to the native non-infected wild-type. This implied the advantage of combining the ionizing radiation technique with *Wolbachia* bacteria for mosquito control.

Keywords: *Aedes aegypti*, *Wolbachia,* radio-sterilization, sterility, mosquito age

Introduction:

Aedes aegypti is a mosquito species in Culicidae family. It is characterized by a dark body with white bands at the bases of leg segments and a lyre-shaped structure on the mesonotum. *Ae. aegypti* has four stages of its life cycle including (1) egg, (2) larva, (3) pupa, and (4) adult. Only female mosquitoes bite for blood feeding to mature their eggs. *Ae. aegypti* is a major vector transmitting several harmful viruses such as dengue, chikungunya, yellow fever, and Zika into humans. In 1906, Thomas Bancroft demonstrated that *Ae. aegypti* can transmit the dengue virus [1]. After a female mosquito is fed infectious blood from a patient containing the viruses in the bloodstream, the viruses can replicate in the midgut and disseminate to salivary glands and legs within 6-15 days [2, 3]. Moreover, if a female mosquito can survive longer than the extrinsic incubation period (EIP) of the virus, the mosquito can transmit the virus to the new host [4]. For the treatment of patients, there is no specific treatment. Elimination or reduction of *Ae. aegypti* population is more effective. Biological control of *Ae. aegypti* mosquito using *Wolbachia pipientis* which is an intracellular bacterial symbiont in insect species, was found to be effective. *Wolbachia* bacteria can affect invertebrate hosts including male killing, feminization, parthenogenesis, and cytoplasmic incompatibility causing vector elimination. Moreover, the radiation can also induce vector sterility. It has been used in combination to control the population of *Ae. aegypti.* However, the radiation impacted not only sterility but also the reduction of longevity [5].

It can affect the somatic cells impairing body function, aging, and longevity, which is a drawback of the irradiation technique. It is important to investigate the effectiveness of sterility after the *Wolbachia* trans-infected mosquito being irradiated. This study investigates the effect of aging on the sterility of female *Wolbachia* trans-infected *Ae. aegypti* mosquitoes.

Materials and Methods:

Mosquito rearing

Wild-type *Ae. aegypti* (Aeg-JJ) and the *Wolbachia* *w*AlbB trans-infected *Ae. Aegypti* (*w*AlbB-TH) were used in this study. The rearing condition was controlled at 27 ± 2˚C and 70 ± 5% humidity. The mosquito eggs were hatched in 1000 mL of warm water. Larvae were raised in 30 × 60 × 2 cm plastic trays containing 2 L of water. Larvae were fed daily with a mixture of fish feed, chicken liver powder, and baking yeast at a ratio of 3.3: 0.1: 0.56 g. Then, the female pupae were transferred to clear plastic cups for radiation. The cups of irradiated pupae were placed into cages. After adult emergence, they were fed with a sugar solution (10% sucrose). After mating, female mosquitoes were transferred into hatching tubes for egg laying.

Radiation

Five hundred female pupae placed in each clear plastic cup containing 500 mL RO water. The X-ray irradiation was performed using RS 2400V Irradiator (Rad Source Technologies Inc, USA) at the 30 Gy dosage at the National Institute of Nuclear Technology, Nakhon Nayok, Thailand.

Mosquito mating and sterility test

After adult emergence, the irradiated females and non-irradiated males were mixed for mating. The radio-sterilized females of *w*AlbB (ir-*w*AlbB) were mating with the *w*AlbB males and compared with the mating of non-irradiated *w*AlbB females. On another hand, the radio-sterilized females of Aeg-JJ (ir-Aeg-JJ) were mating with the Aeg-JJ males and compared with the mating of non-irradiated Aeg-JJ females. The test conditions were divided into young blood feeding (day 5) and old blood feeding (day 15). After blood feeding, the female mosquitoes were separated individually into hatching tubes laid with wet cotton. A 10% sucrose syrup-soaked cotton was provided on the top of the meshed cap and replaced daily. The number of eggs on filter paper was counted using a stereomicroscope. After 3 days, the eggs were transferred to a plastic container for hatching observation. The numbers of larvae were counted. A comparison of two conditions were assessed using t-test.

Results and Discussion:

All irradiated mosquito conditions completely sterilized the egg production. The egg hatch rate of the Aeg-JJ groups on day 5 and 15 were not statistically difference ($P = 0.41$); although the rates for *w*AlbB-TH on day 5 and day 15 were significantly difference ($P = 0.006$). *Wolbachia* infection reduced the egg hatch rate and increased the egg sterile rate in the aged blood-fed population (d15). Long sperm storage period impacted on lowering egg hatching ability in *Wolbachia* infected mosquitoes.

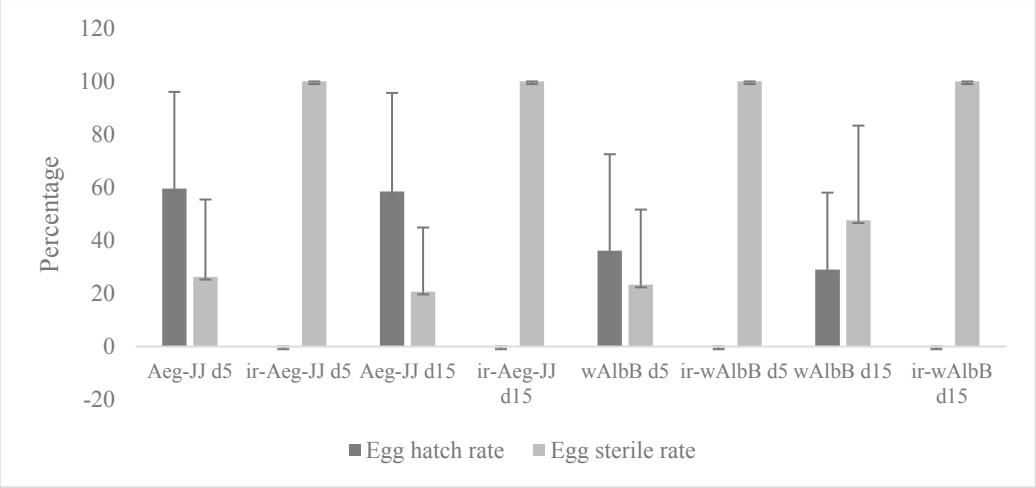

Figure 1 Comparison of sterility on radio-sterilized *Wolbachia* trans-infected *Aedes aegypti* mosquitoes of different ages.

Conclusion:

In this study, we compared the sterility of *Wolbachia* trans- infected *Ae. aegypti* mosquitoes of different blood- feeding ages. Irradiation of all female mosquito colonies suppressed the fertility rate. *Wolbachia* infection reduced the egg hatch rate especially in the aged population. *Wolbachia* trans- infected female *Aedes aegypti* rather have lower ecological fitness compared to the native non-infected wild-type.

Acknowledgments:

This study was supported by International Atomic Energy Agency on the project managing and controlling *Aedes* vector populations using the sterile insect technique (RAS5082) and Mahidol University on the project diversity of bacteria and virus associated with ectoparasites of bats for monitoring of emerging infectious diseases in Thailand.

References:

1. Bancroft, T.L., On the aetiology of dengue fever. Austral. Med. Gaz., 1906. 25: p. 17-18.
2. Mulatier, M., et al., DEET Efficacy Increases with Age in the Vector Mosquitoes Anopheles gambiae s.s. and Aedes albopictus (Diptera: Culicidae). J Med Entomol, 2018. 55(6): p. 1542-1548.
3. Salazar, M.I., et al., Dengue virus type 2: replication and tropisms in orally infected Aedes aegypti mosquitoes. BMC microbiology, 2007. 7: p. 9-9.
4. McMeniman, C.J., et al., Stable Introduction of a Life-Shortening Wolbachia Infection into the Mosquito Aedes aegypti. Science, 2009. 323(5910): p. 141-144.
5. Kittayapong, P., et al., Combined sterile insect technique and incompatible insect technique: sex separation and quality of sterile Aedes aegypti male mosquitoes released in a pilot population suppression trial in Thailand. Parasites & Vectors, 2018. 11(2): p. 657.
6. Sinkins, S.P., H.R. Braig, and S.L. O'Neill, Wolbachia superinfections and the expression of cytoplasmic incompatibility. Proc Biol Sci, 1995. 261(1362): p. 325-30.
7. Werren, J.H., L. Baldo, and M.E. Clark, Wolbachia: master manipulators of invertebrate biology. Nature Reviews Microbiology, 2008. 6(10): p. 741-751.

THE FIRST BIOLOGICAL ACTIVITY STUDY OF SPIKE MOSS *Selaginella padangensis* EXTRACTS

Yudis Ananda Putra[1], Jaruwan Chatwichien[1], Nopporn Thasana[1,2,3*]

[1]Chemical Sciences Program, Chulabhorn Graduate Institute, Chulabhorn Royal Academy, Bangkok, 10210, Thailand
[2]Laboratory of Medicinal Chemistry, Chulabhorn Research Institute, Bangkok, 10210, Thailand
[3]Center of Excellence on Environmental Health and Toxicology (EHT), OPS, Ministry of Higher Education, Science, Research and Innovation, Bangkok, 10400, Thailand
** Corresponding author email: nopporn@cri.or.th*

Abstract:

The crude methanol extract of *Selaginella padangensis* and its partitions were evaluated for antiproliferative activities against A549 and HepG2 cancer cells. The results showed that the crude methanol extract exhibited moderate inhibitory activities against both cell lines with IC_{50} greater than 100µg/mL. Interestingly, the hexane, dichloromethane, and ethyl acetate extracts showed better activities as compared to the crude extract with IC_{50} values in the range 40-80 µg/mL. Moreover, the hexane and dichloromethane subfractions were found to exert the ability to inhibit the cancer cell migration, according the scratch assay.

Keywords: Selaginellaceae, *Selaginella padangensis* Hieron., biological activity, anti-cancer, MTT assay

Introduction:

Selaginella, known as spike moss, is the sole existing genus of the Selaginellaceae family. *Selaginella* has more than 700 distinct species. Another name for *Selaginella* is "*Tanaman Ceker Ayam*" in Bahasa. These plants have been used as decorative plant and in traditional medicine[1] to cure various diseases including wounds, bloody stools, and uterine disorders[2]. *Selaginella* genus is a source of medicinal plants[3]. Recently, our group reported a mild inhibitory effect on cancer cells (HepG2, A549 and HuCCA-1) of lignans isolated from *S. siamensis* Hieron[4]. Biflavonoids, isolated from *S. siamensis* and *S. bryopteris*, also showed effective antiproliferative against A549, H1975, T47D and HepG2 cancer cells[5]. Since no report on the bioactivity of *Selaginella padangensis* Hieron., a spike moss native to Malaysia and Indonesia. In this work, we reported the first potential anticancer property of the partitioned extracts of this plant.

Figure 1 *S. padangensis* Hieron.

Methodology:

Plant Material and Extraction

S. padangensis Hieron. (3.2 kg) was collected from Baan Fa-Pa Fern, Bangkok, Thailand. MeOH (12 L) was applied to the *S. padangensis* for 9 days, changing it out every 3 days. The MeOH was then evaporated using a rotatory evaporator to produce the MeOH crude extract. The MeOH crude extract was redissolved in DI water and sequentially partitioned with hexane, dichloromethane, ethyl acetate and butanol, respectively, to yield the corresponding extracts.

MTT Assay

A549, HepG2 or L929 cells at the density of 10^4 cells/well in a 96-well plate were cultured in modified eagle medium (MEM) supplemented with 10% FBS and 1% penicillin-streptomycin under 5% CO_2, at 37 $^{\circ}$C for 16 h. The cells were then treated with the extracts, cisplatin, afatinib (reference compounds) or DMSO (vehicle control) in the culture medium for 48 h. The cell viability was then determined by using (3-[4,5-dimethylthiazol-2-yl]-2,5 diphenyl tetrazolium bromide), MTT. IC_{50} values were calculated by using GraphPad Prism7 software.

Scratch Assay

HepG2 cells were seeded in 24-well plates and incubated for 24 hours. The cell monolayer was scratched off in a straight line using a sterile 200 µL pipette tip. The detached cells were washed using PBS and then the cells were treated with extracts, cisplatin (reference compound) or DMSO (vehicle control) in 5% FBS culture medium. The scratched areas were photographed under microscope at three time points (0, 24, and 48 hours). The experiments were done in triplicate. Wound width was measured as distance between the edges of the scratches. The %width change was calculated according to the following equation:

%Width change = [width (t=0h) – width (t=24 or 48 h)/ width (t=0 h)] x 100%

Results and Discussion:

From the extraction, 3.2 kg of the fresh *S. padangensis* yielded 157.2 g of the crude methanol extract. The sequential partition afforded 13.9 g, 9.4 g, 4.2 g, 13.2 g and 66.6 g of the hexane, dichloromethane (DCM), ethyl acetate (EtOAc), butanol (BuOH) and water (H_2O) extracts, respectively.

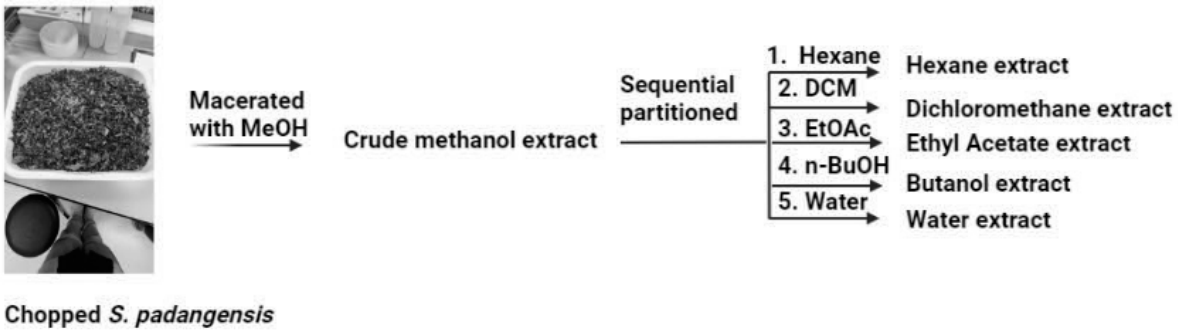

Figure 2 Preparation of *S. padangensis* extracts

Antiproliferative activity of *S. padangensis* extracts using MTT assay was evaluated as shown in Table 1. The crude methanol showed very weak antiproliferative activity with IC_{50} > 100 µg/mL to all the tested cell lines. However, hexane, dichloromethane and ethyl acetate extracts exhibited higher potency to A549 and HepG2 cancer cells (IC_{50} ranging from 40-80 µg/mL), with good selectivity over the L929 normal fibroblast cells. The butanol extract exhibited selective antiproliferation to HepG2 cells and the water extract did not show the inhibition for all cell lines.

Table 1 Antiproliferative activity of *S. padangensis* extracts against A549 (lung) and HepG2 (liver) cancer cells and L929 normal fibroblast cells

	IC_{50} (µg/mL) ±SD, n=3		
Extracts	A549	HepG2	L929
MeOH	> 100	> 100	> 100
Hexane	70.1 ± 9.0	69.5 ± 24.2	> 100
DCM	73.1 ± 22.1	44.2 ± 14.5	> 100
EtOAc	74.7 ± 4.0	77.7 ± 2.0	> 100
BuOH	> 100	65.9 ± 18.4	> 100
Water	> 100	> 100	> 100
Cisplatin	0.5 ± 0.6	19.3 ± 5.7	> 100
Afatinib	0.02 ± 0.0	58 ± 29	> 100

The active fractions from the MTT assay were then tested for the inhibition of cancer cell migration by using scratch assay. The result, shown in Figure 3, indicated that the hexane and dichloromethane extracts could significantly inhibit the migration of HepG2 cells, as compared to the vehicle control (DMSO).

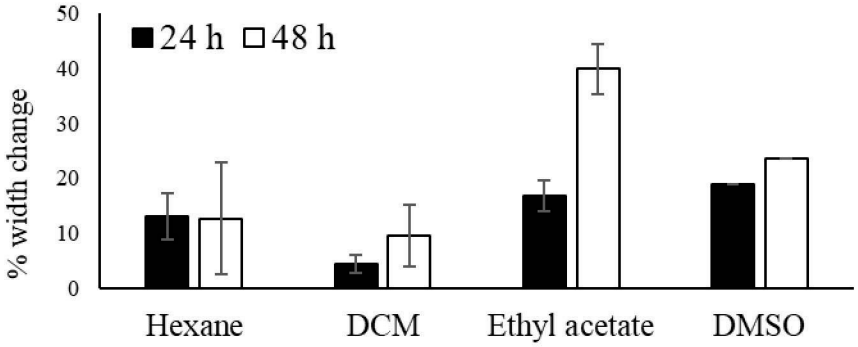

Figure 3 Inhibitory activity of *S. padangensis* extracts at 50 µg/mL on HepG2 cell migration.

Conclusion:

In conclusion, the crude methanol extract of *Selaginella padangensis* possessed weak cytotoxicity to both cancer cells, A549 and HepG2, and normal cells, L929. Interestingly, its hexane, dichloromethane, and ethyl acetate extracts exhibited promising antiproliferative activities with high selectivity to the cancer cells. Moreover, the hexane and dichloromethane extracts could inhibit the HepG2 cancer cell migration. The results suggested the potential uses of this plant for anticancer agents. Further study on the phytochemicals presented in this plant is under investigation in our laboratory.

References:

1. Almeida JR, Sá P, Macedo L, Siqueira Filho J, Oliveira V, Barbosa Filho J. Phytochemistry of the genus Selaginella (Selaginellaceae). Journal of Medicinal Plant Research. 2013;7: 1858.
2. Dwi A. Traditionally utilization of Selaginella; field research and literature review. Nusantara Bioscience. 2009;1.
3. Weng J-K, Noel J. Chemodiversity in Selaginella: a reference system for parallel and convergent metabolic evolution in terrestrial plants. Frontiers in Plant Science. 2013;4(119).
4. Thamnarak W, Eurtivong C, Pollawatn R, Ruchirawat S, Thasana N. Two new nor-lignans, siamensinols A and B, from *Selaginella siamensis* Hieron. and their biological activities. Natural Product Research. 2021:1-9.
5. Demehin AA, Thamnarak W, Lamtha T, Chatwichien J, Eurtivong C, Choowongkomon K, Ruchirawat S, Thasana N. Siamenflavones A-C, three undescribed biflavonoids from *Selaginella siamensis* Hieron. and biflavonoids from spike mosses as EGFR inhibitor. Phytochemistry. 2022;203: 113374.

Innovative technology for production, detection, treatment, detoxification, remediation, reduction, reuse and recycling of chemicals

BIO-FERTILIZER PRODUCTION FROM THE SPENT MUSHROOM SUBSTRATE WITH WASTE-ACTIVATED SLUDGE

Manasawan Worralakkulwong[a,b], Tawach Prechthai [a,b], Withida Patthanaissaranukool[a,b] and Chaowalit Warodomrungsimun[a,b*]

[a]Department of Environmental Health Sciences, Faculty of Public Health, Mahidol University, Bangkok 10400, Thailand
[b]Center of Excellence on Environmental Health and Toxicology (EHT), OPS, MHESI, Thailand

Abstract:

This study aim to investigate the optimum condition for bio-fertilizer productions of the spent mushroom substrate (SMS) with waste-activated sludge (WAS) and to observe the change in physical and chemical parameters and the quality of final products from the compost of SMS with WAS under different SMS: WAS ratios-a control group (SMS only), 50:50, 60:40, 80:20, and 40:60. The results of this study showed that the composting time affects the decline of EC and OM values. On the contrary, it was found that the plant nutrients had N, P, K values increased from the initial. In addition, the effecting of ratio in SMS:WAS revealed that a high SMS ratio affected to high EC value and OM percentage. On the other hand, a high SMS ratio affected the lower macronutrient percentage. When considering the standard of organic fertilizer in Thailand B.E. 2548, all treatments of EC, OM and N in T1, T2, T4 were optimal for plants and comply with the standard whereas P and K were below standard. In summary, in this experiment the SMS: WAS at 40:60 ratios is the optimum ratio for use as compost or soil amendment in plants. In addition, it is recommended that adding phosphorus and potassium in appropriate proportions is essential for plant growth.

Keywords: Spent mushroom substrate (SMS), waste activated sludge (WAS), composting, plant nutrient

Introduction:

Pleurotus spp. (oyster mushroom) are produced around the world in about 25 countries in Asia, Europe, and America. China was the main country that contributes the oyster mushroom to 90 percentage of the total world production. The other major producing countries are South Korea, Japan, Italy, Taiwan, Thailand, and the Philippines [1].

After the period of harvesting, the agricultural residues from this process are called spent mushroom substrate (SMS). The spent mushroom substrate contains a large amount of fungal mycelium and extra-cellular lignocellulosic enzymes along with various organic substances (carbohydrates, proteins, and fats), as well as a considerable quantity of inorganic nutrients such as ammonium nitrate, superphosphate, and potassium salts [2]. Approximately, 5 kg of the spent mushroom substrate is produced for each kilogram of fresh mushroom [3].

SMS residue is frequently discarded as waste after harvesting mushrooms in many countries, most SMS is spread on farmland as fertilizer or disposed by incinerating. Therefore, SMS in the mushroom farm is the largest challenge for disposal management. The major applications of SMS consist of five categories as follows: animal feedstock, fertilizer, energy, wastewater treatment, and other applications.

Waste-activated sludge (WAS), or biosolid, is a by-product of wastewater treatment plants that had to be eliminated from the system to prevent the excessive solids in the aeration tank of the activated sludge process. Waste-activated sludge is abundant in organic matter and nutrient elements, for example, nitrogen, phosphorus, and potassium.

The three main directions to dispose of the waste-activated sludge consist of a landfill, agricultural use, and incineration. In agricultural use composting is a simple and low-cost method for converting waste-activated sludge into a safe and stable product [4].

Natural fertilizers such as garden wastes, cow manure, and agricultural wastes are another option to reduce the use of synthetic fertilizers and prevent soil degradation. Composting is a biological process employing decomposers through which the recycling of nutrients and energy takes place. SMS can be merged using new formulas and methods with the added advantage of reducing production, reducing costs, and reducing environmental impact [3].

Nowadays, there are many small-scale mushroom organic farms in Thailand. In organic farming systems, the use of factors of production such as pesticides and fertilizers is restricted naturally [5] so using spent mushroom substrate in the production of bio-fertilizer is an attractive alternative for organic farming systems. Therefore, this research is focused on investigating the optimum condition for bio-fertilizer productions of the spent mushroom substrate with waste-activated sludge.

This research aims to investigate the optimum condition for bio-fertilizer productions of the spent mushroom substrate with waste-activated sludge. Additionally, this study observed the change in physical and chemical parameters and the quality of final products from the compost of spent mushroom substrate with waste-activated sludge under different SMS:WAS ratios.

Materials and methods:

Sample preparation and the characteristics of raw materials

SMS: After the period of harvesting Pleurotus spp. (oyster mushroom), the agricultural residues from this process are called spent mushroom substrate (SMS). The SMS was obtained from a “happy life farm”, which is a local farm in Kamphaengsan district Nakhon Pathom province as shown in figure 1.

WAS: The waste-activated sludge was obtained from the Nhongkham wastewater treatment plant in Bangkok as shown in figure 1.

Initial characteristics of raw materials were analyzed with the parameters pH, EC, moisture, C/N ratio, N, P, K OM.

Figure 1 The spent mushroom substrate and waste-activated sludge.

The ratio between the spent mushroom substrate and waste-activated sludge for producing bio-fertilizer

In this experiment, there were four SMS:WAS ratios studied as 50:50, 60:40, 80:20, and 40:60 (T0, T1, T2, T3, T4).

The experiment was performed at the laboratory of the Department of Environmental Health Sciences, Faculty of Public Health, Mahidol University.

Sampling and analytical method

The experiment was conducted for 40 days. The temperature and moisture of each treatment were monitored every day. The sample was collected on days 0, 5, 10, 15, 20, 25, 30, 35, and 40. The sample size was 50 grams for each treatment and the sample was taken at 3 replications. Collect sampling from the top to the bottom.

Each composite sample was divided into two parts. The first part was for moisture content analysis, and the second was oven-dried at 65 °C. All dried samples used for analysis of EC, N, P, K, and OM.

The EC, the content of nitrogen (N), phosphorus (P), potassium (K), and OM, of each treatment were conducted following the guideline method of the land development department, the procedure for analyzing crops, fertilizers, and soil improvements OSD-07 [6]. Moreover, interpretation of the results with the standard of organic fertilizer in Thailand B.E. 2548. [7].

Results and discussion:

The Characteristics of the spent mushroom substrate and waste-activated sludge

The physical and chemical properties of SMS and WAS were shown in table 1. The pH and EC values of SMS and WAS were closely. The moisture content was higher in WAS (67.33%) than SMS (57.78%). The C/N ratio and OC were different, SMS (C/N ratio 50.32, OC 20.63%) was higher than WAS (C/N ratio 2.31, OC 7.18%). The concentration of plant nutrients N and P was richer in WAS whereas K of SMS was higher.

Table 1 The Characteristics of spent mushroom substrate and waste-activated sludge.

Parameters	SMS	WAS
pH	6.75	6.32
EC (decisiemens/m)	0.15	0.16
Moisture %	57.78	67.33
C/N ratio	50.32	2.31
OC %	20.63	7.18
N (%)	0.41	3.11
P (%)	0.22	1.77
K (% K as K2O)	0.20	0.12

The effecting of composting time

EC - During the composting process EC of each treatment was a similar trend, slightly decreased. EC of T0 was the highest and T4 was the lowest. The final value of all treatments was lower than the initial except T0 was slightly increased from the initial. The final EC of T0, T1, T2, T3 and T4 were 0.22, 0.14, 0.15, 0.17, 0.13 decisiemens/m, respectively, as shown in Figure 2.

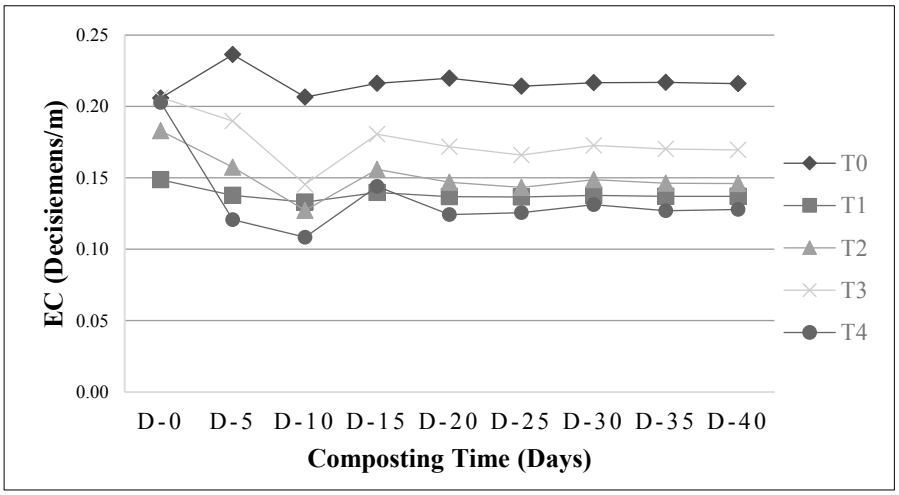

Figure 2 EC during the composting process in five treatments.

N, P, K - The results showed that the composting time affected to increasing macronutrients (N, P, K) as shown in Figure 3. The comparison between composting time showed that all macronutrients were the highest in T4. The final concentration of nitrogen at T0, T1, T2, T3 and T4 were 0.32%, 1.83% 1.62%, 0.89% and 1.67%, respectively. The concentration of phosphorus (P) was increased from the initial. The final value of all treatments was higher than the initial except T1. The concentration of phosphorus at T0, T1, T2, T3 and T4 were 0.04%, 0.10%, 0.15%, 0.09%, 0.17%, respectively. While the trends of potassium (K) were similar, there was fluctuating value and increased from the initial. The final potassium percentage of all treatments was in the range of 0.23-0.26%.

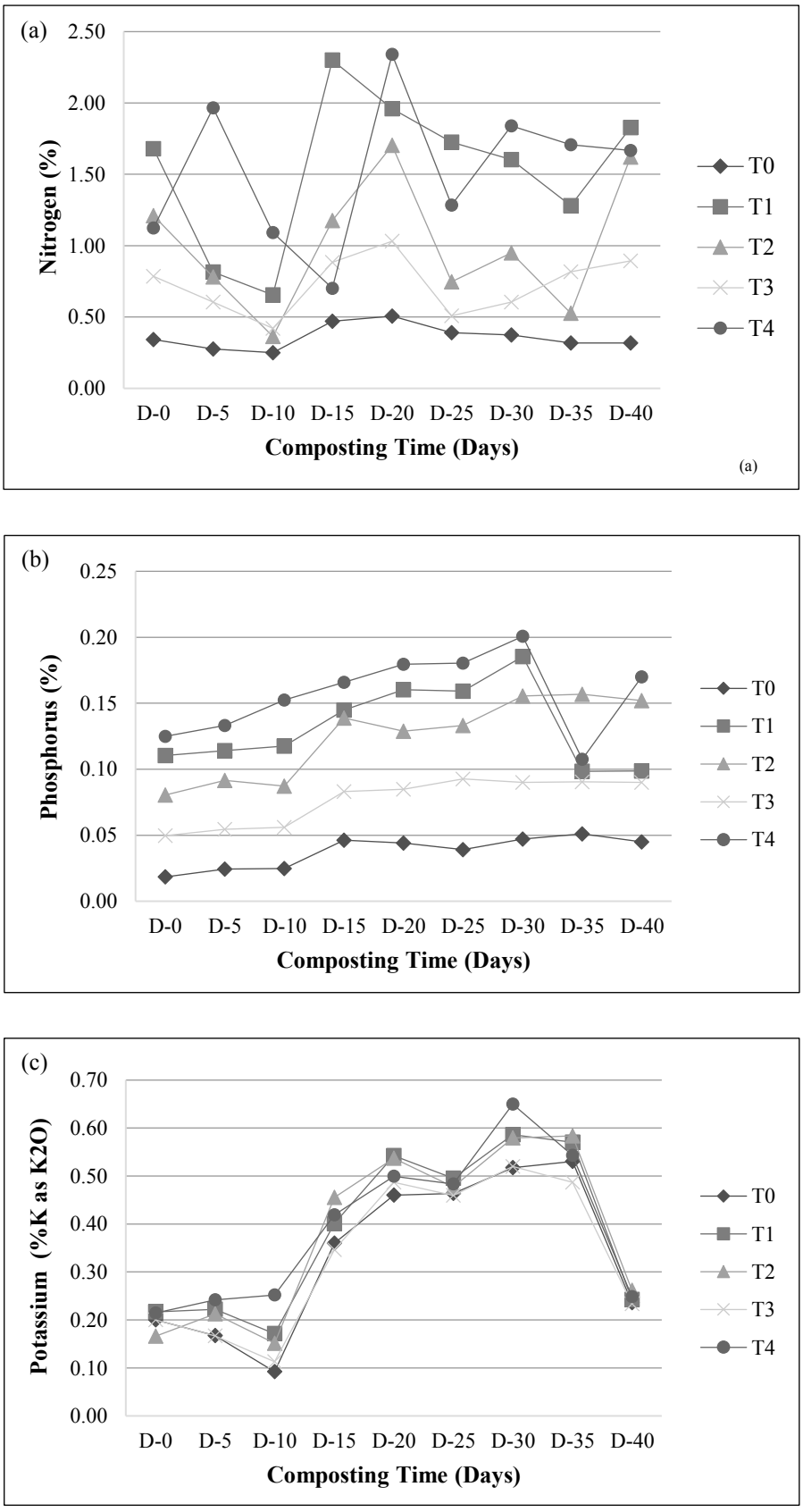

Figure 3 Concentration of Nitrogen (a), Phosphorus (b), Potassium (c) during the composting process in five treatments.

OM - The trend of organic matter (OM) of all treatments was similar, until the end of the composting process. When considered, T0 conditions were the highest percentage, while T4 was the lowest. The final OM percentage had both increased in T0, T2, and T3 (81.25%, 55.80%, 70.64%) and decreased in T1 and T4 (47.89%, 31.56%) from the initial as shown in Figure 4.

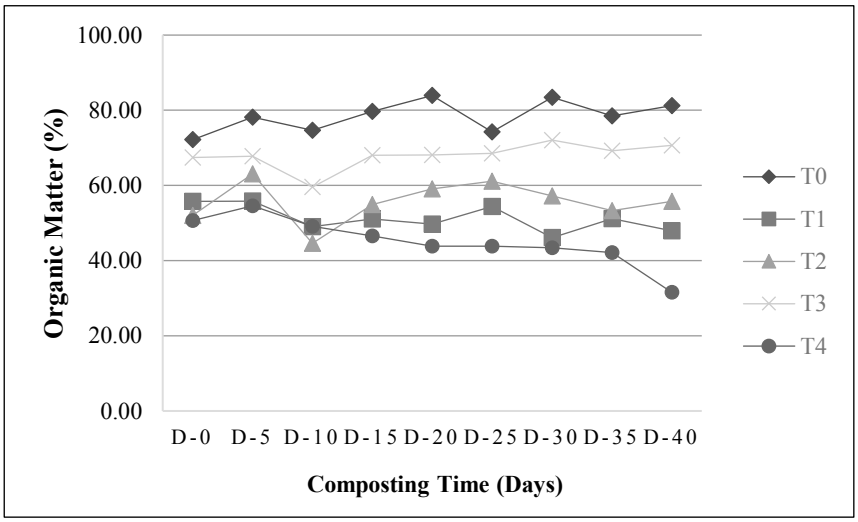

Figure 4 OM during the composting process in five treatments.

The effecting of SMS: WAS ratio

EC - The results revealed that a high SMS ratio effect to high EC value which means T0 had the highest EC value followed by T3, T2, T1, and T4 respectively.

N, P, K - The results presented a high SMS ratio effecting the lower macronutrient percentage which means T4 had the highest followed by T1, T2, T3, and T0 respectively.

OM - The results revealed that a high SMS ratio effect to high EC value which means T0 had the highest EC value followed by T3, T2, T1, and T4 respectively.

Conclusion:

The experimental results of this study showed that the composting time affects the decline of EC and OM values. On the contrary, it was found that the plant nutrients had N, P, and K values increased from the initial. In addition, the effecting of SMS:WAS revealed that a high SMS ratio effecting to high EC value and OM percentage. On the other hand, a high SMS ratio effect the lower macronutrients percentage

When considering the standard of organic fertilizer in Thailand B.E. 2548 all treatments of EC, OM and N in T1, T2, T4 were optimal for plants and comply with the standard whereas P and K were below standard.

To conclude, in this experment the SMS: WAS at 40 : 60 ratios is the optimum ratio for use as compost or soil amendment in plants. In addition, it is recommended that adding phosphorus and potassium in appropriate proportions is essential for plant growth.

Acknowledgement:

This research work was fully supported by the grant from the Center of Excellence on Environmental Health and Toxicology. Also, the authors would like to thank for all supports and assistances during the experimental study from the staff at the Environmental Health Sciences Laboratory, Mahidol University.

References:

1. Upadhyay, R.C. and M. Singh, *Production of Edible Mushrooms*, in *Industrial Applications*, M. Hofrichter, Editor. 2011, Springer Berlin Heidelberg: Berlin, Heidelberg. p. 79-97.
2. Gong, X., et al., *Spent mushroom substrate and cattle manure amendments enhance the transformation of garden waste into vermicomposts using the earthworm Eisenia fetida.* Journal of environmental management, 2019. 248: p. 109263.
3. Mohd Hanafi, F.H., et al., *Environmentally sustainable applications of agro-based spent mushroom substrate (SMS): an overview.* Journal of Material Cycles and Waste Management, 2018. 20(3): p. 1383-1396.
4. Nafez, A.H., et al., *Sewage sludge composting: quality assessment for agricultural application.* Environmental monitoring and assessment, 2015. 187(11): p. 1-9.
5. Flores-Félix, J.D., et al., *Future perspective in organic farming fertilization: Management and product*, in *Organic farming*. 2019, Elsevier. p. 269-315.
6. Development, D.o.L., *The process of analyzing crops, fertilizers and soil improvements manual.* B.E. 2553.
7. Cooperatives, N.B.o.A.C.a.F.S.M.o.A.a., *The standard of organic fertilizer in Thailand* B.E. 2548

CO-SEQUENTIAL PRODUCTION OF ESSENTIAL OIL AND BIOETHANOL FROM LEMONGRASS BIOMASS AFTER PHYTOREMEDIATION OF PETROLEUM HYDROCARBONS: THE WASTE TO WEALTH CONCEPT

Kwang Mo Yang[1,2], Toemthip Poolpak[1,2*], Prayad Pokethitiyook[1,2], Maleeya Kruatrachue[1,2], and Patompong Saengwilai[1,2]

[1]Department of Biology, Faculty of Science, Mahidol University, Bangkok, Thailand
[2]Center of Excellence on Environmental Health and Toxicology, OPS, MHESI, Bangkok, Thailand

Abstract:

Biotechnology for zero waste is an emerging waste management technique in demand due to growing concerns about the global waste crisis. The present study aimed to develop an effective biotechnological process to make beneficial use of lemongrass biomass after performing phytoremediation of petroleum hydrocarbons contaminated soil. The lemongrass was grown in crude oil contaminated soil for 60 days and the essential oil of the plants was extracted by hydrodistillation. Then, the lemongrass distillation waste (LDW) was collected and converted to bioethanol. The results showed that lemongrass removed 48.69% of total petroleum hydrocarbons in the soil after 60 days of phytoremediation treatment. The GC/MS results showed that the lemongrass essential oil was rich in citral isomers (neral and geranial) which accounted for 71.18 of all chemical constituents detected. Furthermore, the yield efficiency of bioethanol production was 69.47% which was comparable to other studies. Thus, this study suggests a novel approach that provides a compatible and consolidated bioprocessing system of lemongrass biomass in the phytoremediation of petroleum-contaminated soil.

Keywords: Essential oil, bioethanol, zero-waste, phytoremediation, lemongrass

Introduction:

Soil contamination with petroleum hydrocarbons (PHCs) is a serious environmental problem across the globe. Large quantities of petrochemicals are released to the environment by anthropogenic activities such as transportation, refining and processing, accidental spills, and pipeline breakage [1]. Phytoremediation is a promising green technology that uses the ability of the plant to promote rhizosphere microorganisms to degrade organic pollutants in the soil [1]. Plants remediate organic pollutants by recruiting beneficial microorganisms in the rhizosphere through the secretion of various phytochemicals.

Lemongrass (*Cymbopogon flexuosus*) is an economical plant that contains a high value in its essential oil [2]. In general, the essential oil of lemongrass is extracted by the hydro-distillation process which produces large quantities of lemongrass distillation waste (LDW) with high levels of sugars and plant metabolites. Recycling distillation waste could save water resources and provide an innovative way to recover energy from waste [3]. The waste to wealth concept is the transformation of waste to valuable products as a mechanism for effective solid waste management. Therefore, the present study attempted to develop an innovative technology to recover economical revenue and bioenergy from biomass after the phytoremediation of PHCs.

Materials and Methods:

Phytoremediation study

The lemongrass was cultivated in crude oil-contaminated soil holding the initial concentration of 9200.87 mg kg^{-1}. The phytoremediation experiment was conducted in round plastic pots (22 cm diameter × 19 cm height). Each pot was filled with approximately 4 kg of petroleum-contaminated soil and the pot was kept outside under the prevailing natural environment. Contaminated soil without lemongrass was served as a control treatment. Plants were watered with 150 ml of tap water every alternative day. The experiment was performed in triplicate for 60 days. The soil samples were collected periodically on day 0, 10, 20, 30, and 60 for TPH analysis. The residual TPH was extracted and analyzed by GC-FID equipped with a DB5-MS column as described previously [1].

Essential oil extraction and analysis

The harvested plants were oven-dried at 60°C for 48h, and the dry biomass was grounded into a powder. The lemongrass essential oil was extracted by hydrodistillation for 4 h. In brief, 20 g lemongrass shoots (DW) were soaked in distilled water at a ratio of 1:20. The chemical composition of the lemongrass essential oils was analyzed by GC/MS (GC 7890A equipped with MSD 5975C, Agilent Technology, USA). The compounds were identified based on the NIST08 Mass Spectral Library and NIST Chemistry WebBook, SRD 69 database.

Sugar contents in distillation waste

The reducing sugar contents in lemongrass distillation waste (LDW) were determined colorimetrically by a standard 3,5-dinitrosalicylic acid (DNS) method using d-glucose as standard [1].

Fermentation and bioethanol production

The fermentation was carried out in 250 ml Erlenmeyer flasks with a working fluid of 50 ml (autoclaved LDW, pH 5.5). One milliliter of log-phase cells of commercial yeast (*S. cerevisiae*, OD_{600nm} =1) pre-cultivated in YPD medium was inoculated to each fermentation broth. Fermentation was performed in semi-anaerobic conditions by sealing the flasks with parafilm. The fermentation was performed for 3 days at 37°C in the dark. Then, the samples were collected on the last day by centrifugation at 8000 rpm for 5 min. Ethanol concentration was determined by using dichromate oxidation [4]. The fermentation yield efficiency was calculated according to Bautista et al. [5].

Data and Statistical analysis

The kinetic rates of TPH biodegradation were calculated. The data on oil biodegradation were analyzed by one-way ANOVA using SPSS version 18.0. The analysis was done at a 95% confidence level ($p \leq 0.05$) by Tukey's range test.

Results and Discussion:

Total petroleum hydrocarbon (TPH) degradation

The results showed that the overall degradation efficiency of TPHs reached 48.69% after 60 days of phytoremediation treatment (Figure 1). The TPH degradation occurred most rapidly during days 10-20 with average removal of 176.79 mg kg^{-1} day^{-1}. This indicates that lemongrass could actively promote the biodegradation of petroleum hydrocarbons by recruiting soil indigenous microbes. The degradation of TPH slowed down after day 30 with average removal of 18.88 mg kg^{-1} day^{-1}. In general, high molecular weight TPHs are considered

persistent organic pollutants as they are biologically unavailable to surrounding microbes. Furthermore, complex forms of petroleum hydrocarbons such as polycyclic aromatic hydrocarbons (PAHs) require key biodegrader (s) that can cleave the complex aromatic compounds [1]. Studies have demonstrated that inoculation of PAHs biodegrading PGPR can significantly accelerate the biodegradation of petroleum hydrocarbons in soil [1]. Therefore, further investigation on plant-bacterial partnership could further improve the remediation ability of lemongrass.

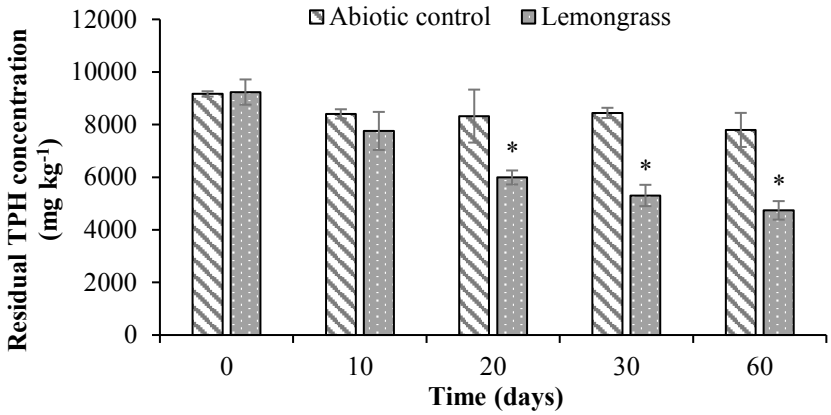

Figure 1 Residual TPH concentration during 60 days of phytoremediation treatment. Each value is the mean of triplicates. * indicate the statistical significance ($p < 0.05$) by one-way ANOVA.

Lemongrass essential oil composition

The major constituents of lemongrass essential oil were found to be citral isomers (neral and geranial which accounted for 71.18% of all chemical constituents detected by GC/MS (Figure 2). This result is consistent with earlier studies which indicate the suitability of growing lemongrass in petroleum-contaminated soil [2, 6]. The concentration of citral isomers in lemongrass essential oil generally determines its quality [2, 6]. Given the economic importance of citral isomers in the fragrance industry, growing lemongrass in petroleum-contaminated soil is a safe option that can generate reasonable economical revenue.

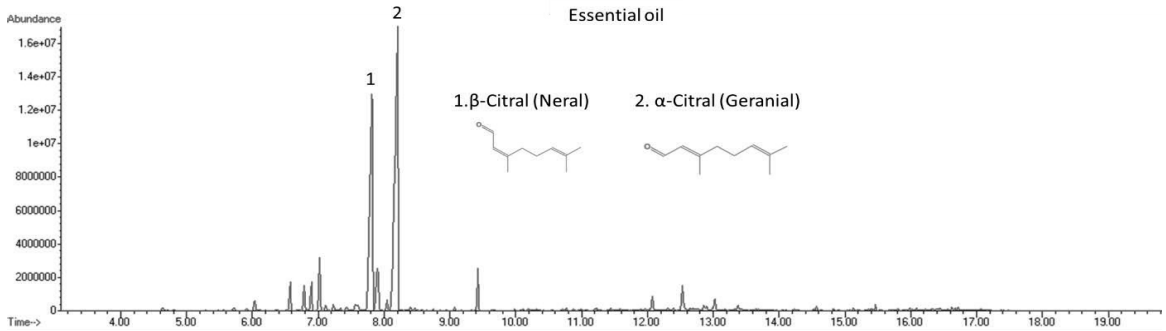

Figure 2 GC/MS chromatogram of lemongrass essential oil

Bioethanol production

The LDW contained the initial reducing sugar concentration of 78.76 g l^{-1} which yielded 33.49 g l^{-1} bioethanol after 3 days of fermentation (Table 1). The results showed high ethanol productivity which is comparable to bioethanol yield from corn stalk juice [5]. Considering that bioethanol from plant biomass generally undergoes acid or alkaline pretreatment followed by enzymatic hydrolysis to maximize the level of reducing sugar to improve the yield of bioethanol [4, 5], the yield of bioethanol production from lemongrass essential oil waste can be further improved.

Table 1 Total sugar, bioethanol concentration, and yield efficiency of different crops

Treatments	Total sugar (g l^{-1})	Bioethanol (g l^{-1})	Yield efficiency (%)	Reference
LDW	78.76	33.49	69.47	This study
Corn stalk juice	130.62	47.39	74.85	Bautista *et al.* [5]
Sugar Beet juice	190.00	80.00	82.56	Tan et al. [7]

Conclusion:

In this study, co-sequential production of essential oil and bioethanol using lemongrass biomass after phytoremediation of petroleum hydrocarbon has been verified. The results showed that lemongrass was an effective phytostimulator for petroleum degradation removing 48.69 % of total petroleum hydrocarbons in the soil after 60 days of treatment. The cultivation of lemongrass in petroleum-contaminated soil for essential oil has been proven to be safe with high citral contents. Furthermore, the yield efficiency for bioethanol using lemongrass hydrodistillation waste was 69.47%. A three-in-one waste to wealth technology has been developed in this study which requires further field trials for application in the acctual field sites.

Acknowledgements:

This work was supported by grants from the Center of Excellence on Environmental Health and Toxicology (EHT), OPS, MHESI, and Mahidol University, Bangkok, Thailand

References:

1. Yang KM, Poolpak T, Pokethitiyook P, Kruatrachue M (2022) Assessment of dynamic microbial community structure and rhizosphere interactions during bioaugmented phytoremediation of petroleum contaminated soil by a newly designed rhizobox system. International Journal of Phytoremediation, *In press*, 1-13
2. Rajeswara Rao BR, Adinarayana G, Kumar AN, Rajput DK, Syamasundar KV (2016) Chemical-profile variations in essential oils isolated from lemongrass (Cymbopogon flexuosus) biomass and condensate wastewater by re-distillation and solvent extraction techniques. Journal of Essential Oil Research 28, 557-64
3. Su W, Yu M, Ma H, Gao M, Wang Q (2015) Research on the recycling of distillation waste in ethanol fermentation from food waste and its influence. International Journal of Green Energy 12, 737-42

4. Seo H-B, Kim H-J, Lee O-K, Ha J-H, Lee H-Y, Jung K-H (2009) Measurement of ethanol concentration using solvent extraction and dichromate oxidation and its application to bioethanol production process. Journal of Industrial Microbiology and Biotechnology 36, 285-92

5. Bautista K, Unpaprom Y, Ramaraj R (2019) Bioethanol production from corn stalk juice using Saccharomyces cerevisiae TISTR 5020. Energy Sources, Part A: Recovery, Utilization, and Environmental Effects 41, 1615-21

6. Gautam M, Pandey D, Agrawal M (2017) Phytoremediation of metals using lemongrass (Cymbopogon citratus (D.C.) Stapf.) grown under different levels of red mud in soil amended with biowastes. International Journal of Phytoremediation 19, 555-62

7. Tan L, Sun Z-Y, Okamoto S, Takaki M, Tang Y-Q, Morimura S, Kida K (2015) Production of ethanol from raw juice and thick juice of sugar beet by continuous ethanol fermentation with flocculating yeast strain KF-7. Biomass and Bioenergy 81, 265-72

EFFECT OF SOLIDS RETENTION TIME (SRT) ON THE NUTRIENT RELEASE EFFICIENCY IN THE TREATMENT OF WASTE ACTIVATED SLUDGE USING ASD PROCESSES

S. Buayoungyuen[a,c*], B. Panyapinyopol[a,c], P. Fongsatitkul[a,c], W. Patthanaissaranukool[b,c], and C. Warodomrungsimun[b,c]

[a]Department of Sanitary Engineering, Faculty of Public Health, Mahidol University
[b]Department of Environmental Health Sciences, Faculty of Public Health, Mahidol University, Bangkok 10400, Thailand
[c]Center of Excellence on Environmental Health and Toxicology (EHT), OPS, MHESI, Thailand
**Corresponding Author: surusnut@gmail.com*

Abstract:

The study evaluated the effects of solid retention time (SRT) on the efficiency of nutrient (nitrogen and phosphorus) release in the treatment of waste activated sludge using an anaerobic sludge digestion (ASD) process. Experimental results under the difference of SRT (10, 20, and 30 d) at a cycle time of 24 h showed that each SRT waste sludge was highly digested during the anaerobic condition. As a result, both the concentration of organic matter in the sludge solids and amount of solid in the system decreased. In addition, the results also found that large amounts of nutrient concentrations were released from the waste sludge into the liquid fraction of the digestates, which showed a good opportunity for the removal and recovery of these compounds through this process. With increasing SRT, the releasing of nutrients decreased while the rate of decay was improved due to the metabolic activity of bacteria decreased. Consequently, the optimal conditions for releasing nutrients in the ASD process were obtained at SRT 10 d, with average release efficiencies of nitrogen and phosphorus of 43.77% and 37.66%, respectively.

Keywords: Waste activated sludge (WAS), anaerobic sludge digestion (ASD), solid retention times (SRTs), nutrient release

Introduction:

Waste activated sludge (WAS) is a by-product in the wastewater treatment plants (WWTPs), which has to be removed from the system to prevent the accumulation of excessive solids in the aeration tank of activated sludge process. It contains principally water, fixed solids (inorganic) and volatile solids (organic). Moreover, these solids also contain pollutants, such as heavy metals, synthetic organic compounds, and pathogenic organisms. Consequently, both the disposal of untreated sludge and direct agricultural application of waste sludge may cause several environmental problems affecting surface and groundwater pollution, leading to the risk of human health [1-2]. In order to prevent these potential effects, this excess sludge should be stabilized and detoxified before the final disposal or use for land application [3-4].

Anaerobic sludge digestion (ASD) is the most popular system for sludge stabilization technology since it is a very simple technique and low operating costs. It is a biological process that breaks down organic materials in the absence of oxygen and transforms organic matter into a mixture of methane (CH_4) and carbon dioxide (CO_2). As a result, not only reduction of sludge volume requiring ultimate disposal and production of biogas as alternative energy, but it also releases a high concentration of nutrients from sludge into the digested effluent which offers a good opportunity for the removal and recovery of these compounds [5-6]. Therefore, the treatment of waste sludge using anaerobic digestion may result in the production of effluent that can be reused in agriculture. With a rich in the recoverable nutrients, it is a benefit for plant growth and suitable substitute for commercial fertilizers [7-9].

The anaerobic degradability of the sludge generated in ASD process is directly linked to solid retention time (SRT). Since it relates to the retention time for substrate degradation and microbial growth [10]. Generally, the high SRT (15-30 d under mesophilic conditions) is used in digestion for better performance of organic removal and CH_4 generation due to methanogens are the slowest growing populations in the ASD process. Hence, it may be washed out when the SRT is too low (below 6 d) [5,11-12]. However, some studies have suggested that shortening SRT is an effective strategy for limiting methanogenesis within the process while maintaining hydrolysis and fermentation, resulting in the accumulation of volatile fatty acids (VFAs) and the inhibition of methanogenesis [5], [13-15]. In addition, it is likely to release the accumulated nutrients (nitrogen and phosphorus) in sludge into the digested effluent [14], [16].

Moreover, several studies have gone into the effect of SRT on the anaerobic digestion process. But still not available to clarify the effect of SRT on nutrient release. Therefore, the objective of this study is to investigate the effect of SRT on the nutrient release efficiency in the treatment of waste activated sludge using ASD process.

Materials and methods:

Waste sludge sample

The waste sludge samples were obtained from the thickened sludge in the drum thickener of the slaughterhouse wastewater treatment plant using AnA^2/O^2 SBR. It was stored in a refrigerator at 4˚C to keep the characteristics of waste sludge received. Before being used, it was taken out and stored at room temperature for about 1-2 h and then diluted with tap water until an initial controlled of MLSS concentration is of about 6,000-7,000 mg/L and feeding into the reactor.

Anaerobic digestion reactor set-up and operational process

A bio-reactor of ASD process was set up and carried out at the laboratory of Sanitary Engineering Department, Faculty of Public Health, Mahidol University. Three identical ASBR reactors were constructed of a 5 L acrylic cylinder. Each reactor was performed by electric stirrers as linking with a slowly revolving motor (50 rpm) and controlled by microprocessor time controllers (timers).

During the acclimatization period, the waste sludge was gradually fed every two days until the full capacity of the working volume (4.5 L) with different volumes as designated by SRT. After that the digester was operated using the semi-continuously and the feeding and discharge operation is performed once a day until reached a steady state, which was defined through the volatile solid (VS) removal varied less than 10%, and the total VFA concentration unchanged [17-18].

The reactor was operated in the sequencing batch mode with four phases under the cycle time of 24 h, consisted of a 0.5 h filling, a 18 h reacting followed by 3 h of solid settling, and finally a 2.5 h on the decanting and idling time [19]. By continuous mechanical mixing and intermittent mechanical mixing was proceeded by 2 h per time every 2.5 h during the reaction period. After that, the solid and liquid fractions were separated during the settling period. A liquid fraction was then withdrawn from the reactor with an equal amount of waste sludge fed into the reactor.

Analytical methods

The concentrations of COD, TKN, NH_3-N, TP, VFA, SS, and VSS in influent and effluent, including phosphorus (P) and nitrogen (N) content in the sludge of each reactor were measured according to the Standard Methods for the Examination of Water and Wastewater [20] to determine their release efficiencies under different conditions of SRTs (10, 20, and 30 d). In addition, all data were analyzed to test for statistically significant differences among the levels of dependent variables, which considered by using the analytical software SPSS 18.0.

Results and discussion:

Treatment of waste activated sludge using ASD process

Experimental results found that large amounts of organic concentrations in the sludge solids decreased as well as the amount of solid in the system. It showed that the disintegration of activated sludge occurs greatly during the anaerobic condition of the digestion process, which indicated that this process not only enhanced the degradation of organic matter from the sludge solids, but it also reduced the volume of waste sludge requiring disposal.

In addition, the results also found large amounts of nutrients were accumulated in the liquid fraction of the digestates, as shown in Figure 1. It showed that the nutrients in both nitrogen and phosphorus were released from the waste sludge into the liquid phase during anaerobic digestion, which indicated that this process could lead to the possibility of recovering nutrients.

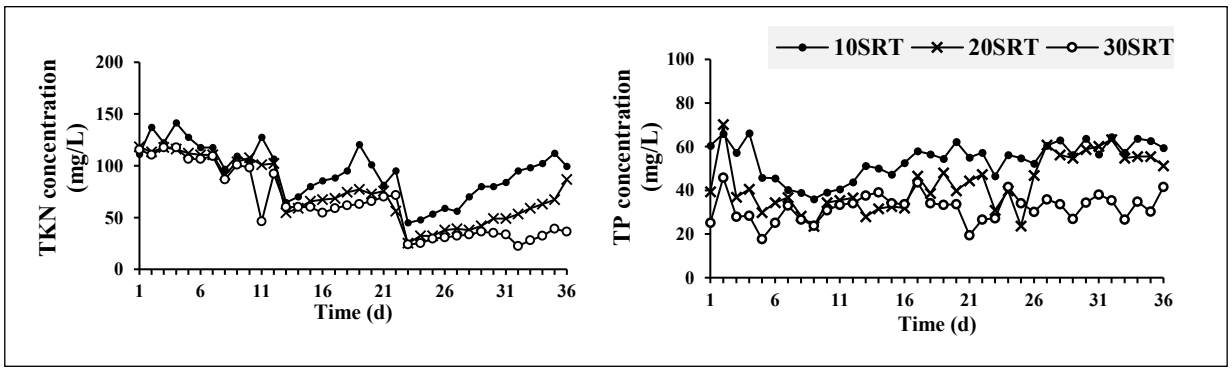

Figure 1 Nutrient (N and P) concentration in the digested effluent of ASD process

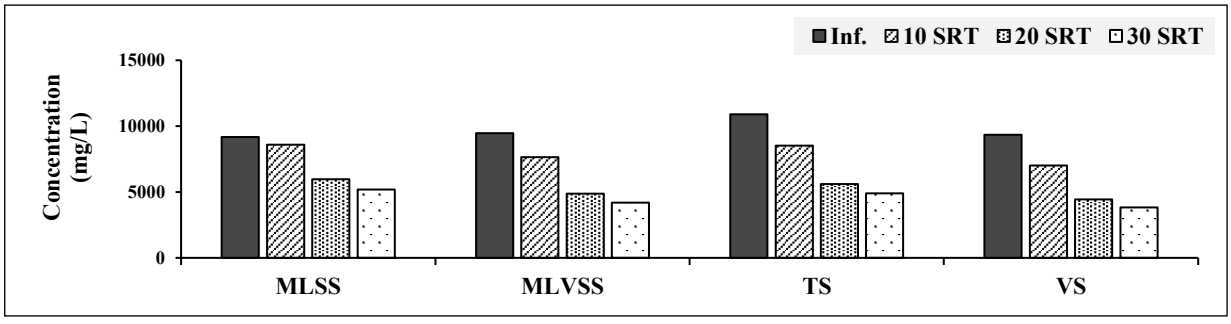

Figure 2 MLSS, MLVSS, TS and VS concentrations in ASD process

Effect of SRT on nutrient release efficiency using ASD process

The experimental results under different SRT conditions are shown in Figure 2. It showed that a MLSS and MLVSS concentration was decreased as well as the amount of TS and VS in the system when increasing of SRT, indicating that the breakdown of sludge solids increased. Due to the anaerobic bacteria had enough time to degrade in the digestion, this resulted in better hydrolytic degradation [21-23].

Moreover, the characteristics of the sludge and supernatant before and after the ASD process are shown in Table 1. It found that the increasing of SRT had the following affects; (1) decrease in SS and VSS concentrations, and (2) decrease in both organic matter and nutrient concentrations in the effluent at the end of ASD process. These results demonstrated that a higher SRT was very effective for sludge stabilization than a shorten SRT. Hence, the increasing of SRT in ASD process led a reduction in the volume of solids requiring disposal. However, increasing of SRT in ASD process caused a reduction in the releasing of nutrients from the waste sludges. This because the metabolic activity of bacteria decreased while the rate of decay improved with increasing of SRT [22], [24].

In accordance with the statistical results, it was found that the organic matter and nutrient concentration in the final effluent of the treatment process at SRT 10 d was significantly higher than that of SRT 20 and 30 d. Therefore, the optimal operating conditions for WAS treatment using ASD process in this study were obtained at SRT 10 d, with the average release efficiencies of nitrogen and phosphorus were 43.77% and 37.66%, respectively.

Table 1 Characteristics of the sludge and supernatant before and after the ASD process

Parameter	Unit	Non-digested sludge		Digested sludge					
				10 SRT		20 SRT		30 SRT	
Supernatant:									
SS	mg/L	146.74	± 39.2	232.15	± 75.7	210.76	± 66.7	153.00	± 84.1
VSS	mg/L	132.08	± 31.0	171.67	± 40.5	140.00	± 37.8	85.63	± 49.2
VFA	mg/L	37.81	± 23.9	36.11	± 9.86	31.14	± 8.18	28.19	± 11.1
COD	mg/L	253.01	± 66.8	249.23	± 72.9	161.15	± 29.5	124.62	± 34.4
TKN	mg/L	52.79	± 16.7	93.87	± 25.2	73.55	± 28.9	63.10	± 32.0
NH_3-N	mg/L	40.42	± 16.8	79.61	± 24.4	64.63	± 28.3	57.24	± 28.8
TP	mg/L	33.63	± 6.57	53.95	± 8.47	43.00	± 12.2	34.64	± 5.31
Waste sludge:									
N content	mg/g	95.40	± 14.8	93.64	± 9.72	81.00	± 13.9	77.14	± 18.1
P content	mg/g	35.22	± 4.19	33.03	± 4.62	33.10	± 3.31	34.04	± 3.53

Conclusion:

The experimental results of this study confirmed that the disintegration of activated sludge occurred greatly during the anaerobic condition of the digestion process. Simultaneously, a large amount of nutrients (nitrogen and phosphorus) was released from the waste sludge into the liquid fraction of the digestates, which could be used for recovering nutrients. By the result of different SRT on the nutrient release efficiency indicated that the increasing of SRT in ASD process led to a reduction in the release of nutrients from the waste sludges while it enhanced the effective for sludge stabilization. Therefore, the optimal conditions for releasing nutrients in the ASD process were obtained at SRT 10 d, with average release efficiencies of nitrogen and phosphorus were 43.77% and 37.66%, respectively.

Acknowledgement:

This research work was fully supported by the grant from the Center of Excellence on Environmental Health and Toxicology. Also, the authors would like to thank for all supports and assistances during the experimental study from the staff at the Sanitary Engineering Laboratory, Mahidol University.

References:

1. Farzadkia, M. and Bazrafshan, E. (2014). Lime stabilization of waste activated sludge. *Health Scope*, 3(1), e16035.
2. Cieślik, B. and Konieczka, P. (2017). A review of phosphorus recovery methods at various steps of wastewater treatment and sewage sludge management. The concept of "no solid waste generation" and analytical methods. *Journal of Cleaner Production*, 142, 1728-1740.
3. Chang, T.C., You, S., Damodar, R.A., Chen, Y. (2011). Ultrasound pre-treatment step for performance enhancement in an aerobic sludge digestion process. *J. Taiwan Inst. Chem. Eng.*, 42, 801-808.
4. Anjum, M., Al-Makishaha, N.H., Barakat, M.A. (2016). Wastewater sludge stabilization using pre-treatment methods. *Process Safety and Environmental Protection*, 102, 615-632.
5. Vanwonterghem, I., Jensen, P.D., Rabaey, K., Tyson, G,W. (2015). Temperature and solids retention time control microbial population dynamics and volatile fatty acid production in replicated anaerobic digesters. *Sci Rep*, 5:8496, doi: 10.1038/srep 08496.
6. Liu, X., Xu, Z., Peng, J., Song, Y., Meng, X. (2016). Phosphate recovery from anaerobic digester effluents using $CaMg(OH)_4$. *J Environ Sci (China)*, 44, 260-268.
7. US.EPA. (1999). *Biosolids Generation, Use, and Disposal in the United States*. Washington, DC.
8. Mtshali, J.S., Ababu, T.T., Amos, O.F. (2014). Characterization of Sewage Sludge Generated from Wastewater Treatment Plants in Swaziland in Relation to Agricultural Uses. *Resources and Environment*, 4(4), 190-199.
9. Gordon, M.I. (2015). *Nutrient recovery by anaerobic co-digestion of lipid-extracted Chlorella vulgaris and waste activated sludge*. B.S. Thesis in Bioresource Research with an option in Bioenergy, Oregon State University, Oregon.
10. Ge, H., Batstone, D.J., Keller, J. (2013). Operating aerobic wastewater treatment at very short sludge ages enables treatment and energy recovery through anaerobic sludge digestion. *Water Res*, 47(17), 6546-6557.
11 Lee, I.S., Parameswaran, P., Rittmann, B.E. (2011). Effects of solids retention time on methanogenesis in anaerobic digestion of thickened mixed sludge. *Bioresource Technology*, 102, 10266-10272.
12. Hu, J. (2013). *Anaerobic digestion of sludge from brackish RAS: CSTR performance, analysis of methane potential and phosphates, struvite crystallization*. M.Sc. Thesis in Civil Engineering, Delft University of Technology, Delft.
13. Amani, T., Norsati, M., Sreekrishnan, T.R. (2010). Anaerobic digestion from the viewpoint of microbiological, chemical, and operational aspects - a review. *Environ Rev*, 18, 255-278.

14. Wang, Y. (2014). *Phosphorus-recovery from waste activated sludge (WAS) in enhanced biological phosphorus removal (EBPR) processes*. M.Sc. Thesis in Environmental Engineering, Northeastern University Boston, Massachusetts.

15. Ho, D., Jensen, P.D., Batstone, D.J. (2014). Effects of temperature and hydraulic retention time on acetotrophic pathways and performance in high-rate sludge digestion. *Environ Sci Technol*, 48, 6468-6476.

16. Yu, Y., Lei, Z., Yuan, T., Jiang, Y., Chen, N., Feng, C. (2017). Simultaneous phosphorus and nitrogen recovery from anaerobically digested sludge using a hybrid system coupling hydrothermal pretreatment with MAP precipitation. *Bioresour Technol*, 243, 634-640.

17. Usack, J.G., Spirito, C.M., Angenent, L.T. (2012). Continuously-stirred anaerobic digester to convert organic wastes into biogas: system setup and basic operation. *J Vis Exp*, 65: e3978, doi:10.3791/3978.

18. Abel-Denee, M. (2015). *Recalcitrant nutrient removal using heterogeneous struvite precipitation in anaerobic digestion dewatering centrate*. B.A.Sc. Thesis in Civil Engineering, University of British Columbia, Columbia.

19. Wang, Z., Wang, W., Zhang, X., Zhang, G. (2009). Digestion of thermally hydrolyzed sewage sludge by anaerobic sequencing batch reactor. *J Hazard Mater*, 162(2-3), 799-803.

20. APHA. (2012). *Standard methods for the examination of water and wastewater*. 22nd ed. American Public Health Association, Washington, DC.

21. Roman, H.J., Burgess, J.E., Pletschke, B.I. (2006). Enzyme treatment to decrease solids and improve digestion of primary sewage sludge. *African Journal of Biotechnology,* 5(10), 963-967.

22. Nges, I.A. and Liu, J. (2010). Effects of solid retention time on anaerobic digestion of dewatered-sewage sludge in mesophilic and thermophilic conditions. *Renewable Energy*, 35, 2200-2206.

23. Moragaspitiya, C., Rajapakse, J., Millar, G.J., Ali, I. (2019). Optimization of mesophilic anaerobic digestion of a conventional activated sludge plant for sustainability. *Alexandria Engineering Journal*, 58, 977–987.

24. Xiong, H., Chen J., Wang, H., Shi, H. (2012). Influences of volatile solid concentration, temperature and solid retention time for the hydrolysis of waste activated sludge to recover volatile fatty acids. *Bioresource Technology,* 119, 285–292.

ELUCIDATING CIRCADIAN RHYTHM AND TIME-DEPENDENT CHEMOTHERAPY TREATMENT IN CHOLANGIOCARCINOMA CELL LINE: KKU-M213

Pornthep Chokratum[1], Kittipong Prajanpol[1], Thaned Kangsamaksin[2], and Pagkapol Y. Pongsawakul[1]

[1] Department of Biology, Faculty of Science, Mahidol University, Bangkok, Thailand
[2] Department of Biochemistry, Faculty of Science, Mahidol University, Bangkok, Thailand

Abstract:

The circadian clock controls many rhythmic homeostasis processes of the body that are controlled by the expression of core clock genes such as *PER2* and *BMAL1*. Chronotherapy is the concept of optimizing the timing of chemotherapeutic drug treatments based on the expression of the target gene to maximize drug efficacy. Cholangiocarcinoma is a bile duct cancer that has been reported to have a very high number of new cases in Thailand, Lao, China, and South Korea. Therefore, we are interested in investigating the expression of circadian genes in cholangiocarcinoma cell line: KKU-M213, and to test the gemcitabine, a chemotherapeutic drug, at different times based on *PER2* expression. We found that KKU-M213 lacks a functional circadian clock because *PER2* have a period of expression at 32.5 hours, outside the range of the normal circadian period. Secondly, *PER2* and *BMAL1* do not exhibit the antiphase relationship. Then, we measured the IC_{50} of gemcitabine on unsynchronized KKU-M213 and found that it is 22.61±3.17 nM. We found that *PER2* expression varies at 16, 28, and 40 hours post synchronization and shows different responses when treated with chemotherapy drug gemcitabine. Our results demonstrated that time-dependent treatment or chronotherapy can improve drug efficacies and emphasized the need to consider the 24-hr circadian time on human health and treatment.

Keywords: Circadian clock, cholangiocarcinoma, KKU-M213, *PER2* gene, chronotherapy

Introduction:

The circadian clock coordinates multiple physiological processes in the body such as cell cycle, DNA repairing, apoptosis, and regulation of metabolism that are controlled by the master pacemaker suprachiasmatic nucleus (SCN) in the hypothalamus that signals neural and humoral factors such as glucocorticoids and melatonin to the rest of the body (1). Mechanisms of the circadian clock are based on transcription/translation feedback loops (2). CLOCK and BMAL1 are transcriptional activators that regulate the expression of other core clock genes such as CRY and PER genes and many clock-controlled genes (CCGs). With time-delayed mechanisms, CRY and PER proteins inhibit the CLOCK/BMAL1 activity creating rhythmic expression of thousand of CRY, PER, and CCGs within any tissues (3).

The International Agency for Research on Cancer has reported that circadian clock disruption or night shift schedule may increase risks of many types of cancer. In addition, many cancer cells also contain functional circadian clocks. Currently, scientists are increasingly interested in the circadian rhythms in cancer cells for medical benefits, and time-dependent treatment or chronotherapy is being increasingly investigated (4). Cholangiocarcinoma is a bile duct cancer that has been reported to have a very high number of new cases in Thailand, Lao, China, and South Korea, and patients with this disease have a high rate of mortality and resistance to treatment. There are many causes of cholangiocarcinoma. Thailand, in particular, the parasitic worm infection caused by *Opisthorchis viverrini* can induce cholangiocarcinoma (5). In this study, we seek to investigate the time-dependent treatment of cholangiocarcinoma with chemotherapy drug using KKU- M213 cell line as an *in vitro* model.

Materials and Methods:

Cell Culture

KKU-M213 cells were cultured in Gibco Ham's F-12 Nutrient Mixture (HAM's F- 12) media including 10% heat-inactivated fetal bovine serum (FBS), 1% penicillin/streptomycin at 37 °C, and 5% CO2 concentration. The cells were sub-cultured at about 80% confluency using 1X Trypsin-EDTA in PBS solution.

Gemcitabine Treatment and IC_{50} Calculation

Approximately 12,500 cells of KKU-M213 were seeded with HAM's F-12 culture medium including 10% heat-inactivated FBS, 1% penicillin-streptomycin in each well of a 24 well plate and incubated in a cell culture incubator at 37°C and 5% CO2 concentration. And after 16 hours, the culture media was discarded and replaced with concentration (0.01, 0.1, 1, 10, and 100 μM) of gemcitabine in each well. Seventy-two hours after gemcitabine treatment, the old media were removed and replaced with 500 μM of 5 mg/ml MTT solution (yellow tetrazolium salt (3-(4,5- dimethylthiazol-2-yl)-2,5-diphenyltetrazolium bromide) with culture medium to each well and incubated for 3 hours. Then, MTT-solution was discarded, and dissolve the MTT crystals using 400 μL of Dimethyl sulfoxide (DMSO). After that, absorbance of the formazan crystals solution was measured at 540 nm using a microplate reader. The absorbance data will be calculated percent of cell viability and *IC50* and generated the graph by the GraphPad Prism 9 program.

Sixteen hours before the drug treatment, 12,500 cells of the KKU-M213 were seeded in 24-well plates with HAM's F-12 culture medium including 10% heat-inactivated FBS, 1% penicillin/streptomycin. 1 μM dexamethasone with culture medium was treated for 2 hours after cell seeding. Then, the old media was removed, and gemcitabine medium mixture (0.01, 0.1, 1, 10, and 100 μM) was added to the well at 16, 28, and 40 hours after synchronization for 72 hours. The time points were chosen based on increasing the expression of *PER2* gene as a core clock gene. Each sample was taken to determine the effectiveness of the drug treatment on the survival of cells by calculating the *IC50* value.

Circadian Gene Expression Analysis

RNA Extraction To extract the RNA for gene expression measurement, 500 μL of TRIzol™ Reagent (Thermo Fisher Scientific) was added to the cell pellet in each microcentrifuge tube. Then, we added 100 μL of cooling chloroform to each sample, mixed the solution using vortex briefly, and incubated at room temperature for 2 minutes. The samples were centrifuged at 4 °C, and 12,000 rpm for 15 minutes and transfer the colorless aqueous phase containing the RNA to the new sterile-microcentrifuge tube. 2 times the volume of isopropanol was added to each tube and incubated at room temperature for 10 minutes, and centrifuged at 4 °C, and 12,000 rpm for 10 minutes. after that, the supernatant in each tube was discarded with a micropipette, and the RNA pellet was washed using 500 μL of cooling 75% ethanol at 4 °C, and 12,000 rpm for 5 minutes. the supernatant was discarded with a micropipette. The RNA pellet was air-dried for about 20 minutes and resuspended in 25-30 μL of RNase-free water. Incubate the solution in the water bath at 55 °C for 15 minutes.

cDNA Synthesis Each RNA sample was determined the absorbance at 260 nm for total nucleic acid and 280 nm for sample purity measurement by NanoDrop® Spectrophotometer. The cDNA was synthesized using RevertAid RT Reverse Transcription Kit and completed by Bio-Rad T100TM Thermal Cycler.

Quantitative PCR The expression of *BMAL1* and *PER2* as representative genes for the circadian clock. The data of each sample was normalized relative to the geometric mean of *ACTB*. Real-time PCR performed by Luna® Universal One-Step RT-qPCR Kit in a Real-Time PCR Detection System. mRNA expression can be measured by using following primers set: *PER2* 5'-TGAGAAGAAAGCTGTCCCTGCCAT-3' and 5'GACGTTTGCTCCCAACTCGCATTT–3'; *BMAL1* 5'-AGGATGGCTGTTCAGCACATGA-3' and 5'-CAAAAATCCATCTGCTGCCCTG-3'; and *ACTB* (as a negative control) 5'- AGGCACCAGGGCGTGAT-3' and 5'GCCCACATAGGAATCCTTCTGAC-3' (6).

Statistical Analysis

The student's t-test will be used to compare between control and expression of *BMAL1* and *PER2*. Cosinor Analysis (https://cosinor.online/app/cosinor.php) was used for non-linear regression of the expression of *BMAL1* and *PER2*. The data from MTT assay were calculated for IC_{50}, and the IC_{50} values between each time points were compared by GraphPad Prism.

Results and Discussion:

The expression of circadian genes in cholangiocarcinoma cell line

The KKU-M213 cells were synchronized with dexamethasone for 2 hours. Then, the expression of the circadian genes *PER2* and *BMAL1* were measured. The result showed that *PER2* and *BMAL1* display rhythmic expression as shown in Figures 1 A and C. *PER2* expression in the first 16 hours has continued to decline. Then, *PER2* expression returned to increase at the 20 to 36 hours. On the other hand, *BMAL1* expression showed fluctuations increase. After the data were analyzed by Cosinor Online Application, it was found that the *PER2* oscillation expression has a period of expression of approximately 32.5 hours, as shown in Figures 1 B. The *BMAL1* data be cannot determined its expression period because the data did not fit with any periods curve.

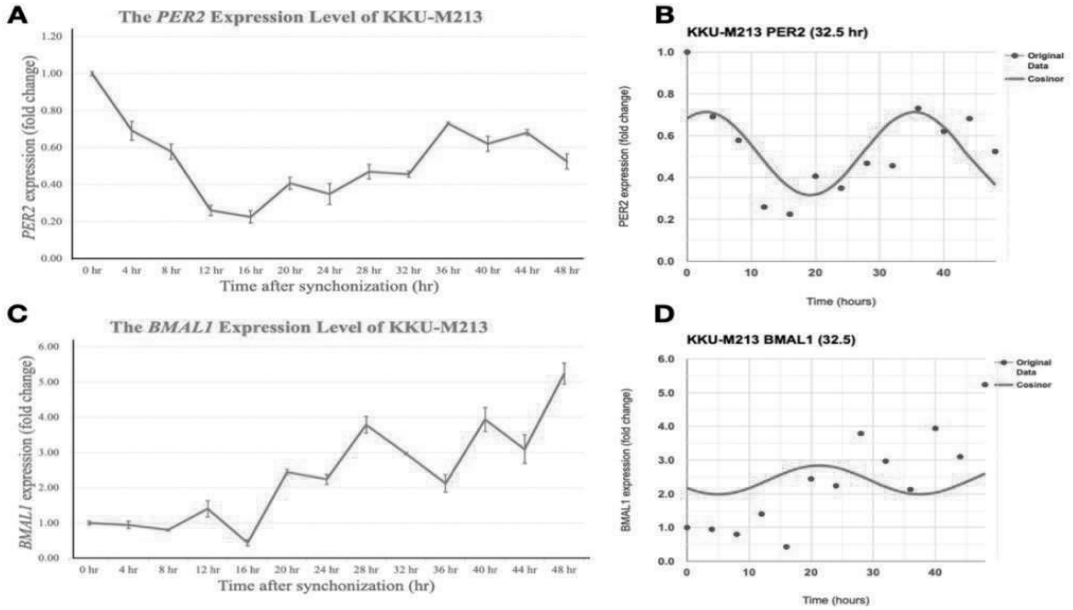

Figure 1 The circadian gene expression in KKU-M213 A and C show the expression of *PER2* and *BMAL1* gene, respectively. B and D show the analysis of respective *PER2* and *BMAL1* expression profile by the Cosinor Online Application.

Therefore, the expression of *PER2* and *BMAL1* were not in the circadian range and did not show an anti-phasic relationship. From these results, we concluded that KKU-M213 has no functional circadian clock expression but *PER2* is responsive to dexamethasone in a dosage- and time-dependent manner.

Effectiveness of gemcitabine on unsynchronized KKU-M213 cells

The effectiveness of different concentrations of gemcitabine on unsynchronized cholangiocarcinoma cells was observed using cell survival of unsynchronized KKU-M213 cells after gemcitabine treatment for 72 hours by MTT assay. The result showed that the *IC50* value of gemcitabine on unsynchronized KKU-M213 is 22.61±3.17 nM as shown in Figure 2. The absorbance data from the MTT assay was calculated the percentage of cell viability and fitted to a nonlinear regression curve using the GraphPad Prism 9 program.

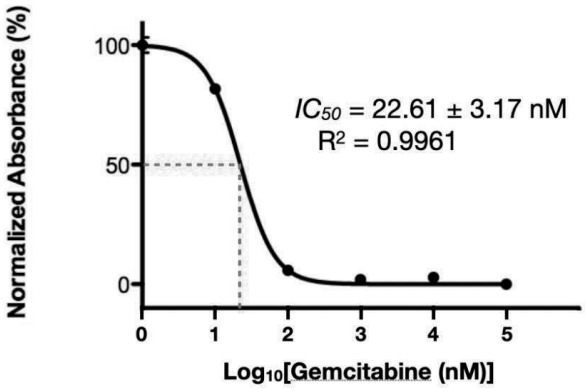

Figure 2 IC50 of gemcitabine treatment on unsynchronized KKU-M213 cholangiocarcinoma

The influence of different PER2 expression on effectiveness of the gemcitabine treatment

In a previous study, KYSE-410 cells, esophageal squamous cell carcinoma, were treated with cisplatin at 24 and 36 hours and showed different responses according to *PER2* gene expression (7). In our study, *PER2* expression of KKU-M213 was measured at 16, 28, and 40 after synchronization, and the results showed that KKU-M213 had a significantly increased the expression of the *PER2* gene.

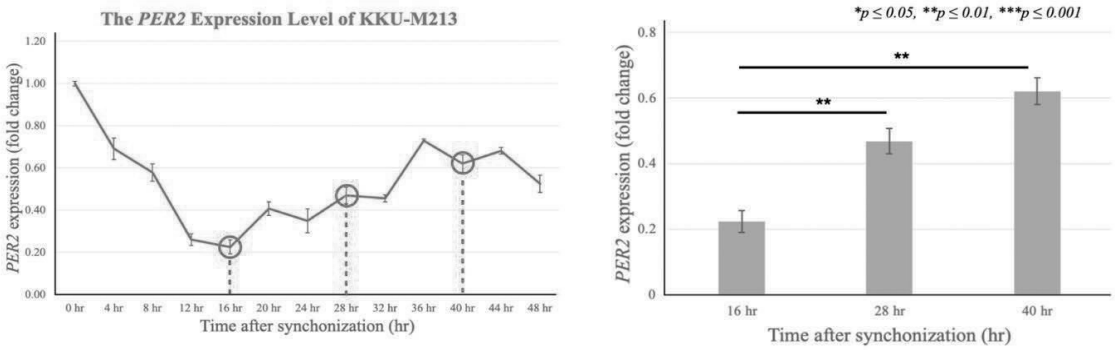

Figure 3 The expression of PER2 in KKU-M213 cholangiocarcinoma cells 16, 28, and 40 hours after synchronization by dexamethasone

The data from previous studies made us interested in studying the effectiveness of gemcitabine treated at different times based on the expression of *PER2* in KKU-M213 cells. The efficacy of the gemcitabine was measured by calculating the *IC50* value at each time point. The results showed that at specific dosage such as 0.1 and 1 μM of gemcitabine KKU-M213 cells viability differ at a time-dependent manner.

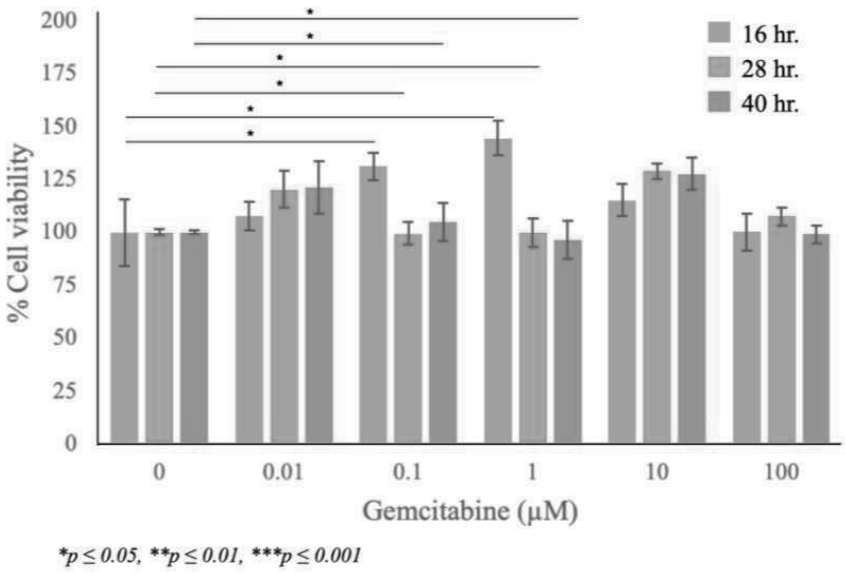

Figure 4 Percentage of cell viability of KKU-M213 cholangiocarcinoma cells after gemcitabine treatment at time 16, 28, and 40 hours post cell synchronization

Conclusion:

From our results, even though KKU-M213 cell line as our *in vitro* cholangiocarcinoma model has no functional circadian gene expression, we observed *PER2* expression that varies in a time-dependent manner after treatment with dexamethasone, a synthetic glucocorticoid. In addition, the IC_{50} of gemcitabine as a chemotherapeutic drug on unsynchronized KKU-M213 was measured as 22.61±3.17 nM. We observed the influence of *PER2* expression level on the effectiveness of gemcitabine of 16, 28, and 40 hours post synchronization at specific dosages suggesting that chronotherapy may be beneficial at specific circadian time for cancer treatment. With many clock genes function in cancer pathways (8), there is emerging evidence that chronotherapy of cancer is beneficial to patients when chemotherapy is performed at specific times of the day (9) leading to potential considerations of time-dependent treatments in patients and to investigate chronotherapy as a treatment innovation that positively impacts human health and disease treatment.

Acknowledgements:

This research project was partially supported by Faculty of Science, Mahidol University (PYP) as well as National Research Council of Thailand and Program Management Unit B (TK).

References:

1. R. Allada, J. Bass, Circadian Mechanisms in Medicine. *N Engl J Med* **384**, 550-561 (2021).
2. J. S. Takahashi, Transcriptional architecture of the mammalian circadian clock. *Nat Rev Genet* **18**, 164-179 (2017).
3. M. D. Ruben *et al.*, A database of tissue-specific rhythmically expressed human genes has potential applications in circadian medicine. *Sci Transl Med* **10** (2018).
4. A. Sancar, R. N. Van Gelder, Clocks, cancer, and chronochemotherapy. *Science* **371** (2021).
5. B. Sripa *et al.*, Liver fluke induces cholangiocarcinoma. *PLoS Med* **4**, e201 (2007).
6. E. E. Zhang *et al.*, A genome-wide RNAi screen for modifiers of the circadian clock in human cells. *Cell* **139**, 199-210 (2009).
7. J. A. Redondo *et al.*, PER2 Circadian Oscillation Sensitizes Esophageal Cancer Cells to Chemotherapy. *Biology (Basel)* **10** (2021).
8. G. Sulli, M. T. Y. Lam, S. Panda, Interplay between Circadian Clock and Cancer: New Frontiers for Cancer Treatment. *Trends Cancer* **5**, 475-494 (2019).
9. D. Adam, Core Concept: Emerging science of chronotherapy offers big opportunities to optimize drug delivery. *Proc Natl Acad Sci U S A* **116**, 21957-21959 (2019).

PREVALENCE AND ABUNDANCE OF ANTIBIOTIC RESISTANCE GENES IN WASTEWATER AND ENVIRONMENTAL WATER USING HIGH-THROUGHPUT QUANTITATIVE PCR

Thitima Srathongneam[(1)], Montakarn Sresung[(2)], Phongsawat Paisantham[(2)], Pacharaporn Ruksakul[(2)], Tharindu Pollwatta Gallage[(3)], Rojana Sukchawalit[(1),(2),(4)], Jutamaad Sattayavivad[(3),(4),(5)], Skorn Mongkolsuk[(2),(4)] and Kwanrawee Sirikanchana[(2),(4),(*)]

[(1)]Program in Applied Biological Sciences, Chulabhorn Graduate Institute, Chulabhorn Royal Academy, Bangkok 10210, Thailand;
[(2)]Research Laboratory of Biotechnology, Chulabhorn Research Institute, Bangkok 10210, Thailand;
[(3)]Program in Environmental Toxicology, Chulabhorn Graduate Institute, Chulabhorn Royal Academy, Bangkok 10210, Thailand;
[(4)]Center of Excellence on Environmental Health and Toxicology (EHT), OPS, MHESI, Thailand;
[(5)]Research Laboratory of Pharmacology, Chulabhorn Research Institute, Bangkok 10210, Thailand;
**Corresponding author: kwanrawee@cri.or.th*

Abstract:

Antibiotic resistance genes (ARGs) are emerging microbial pollutants. Their environmental contamination could contribute to antibiotic resistance dissemination to natural bacteria, thus posing a risk to human and animal health. This study aimed to investigate the presence and abundance of ARGs, integrons, and mobile genetic elements (MGEs) in water samples collected from four sites comprising influent and treated effluent of a wastewater treatment plant, freshwater, and seawater. ARG diversity and relative abundance were analyzed using a high-throughput quantitative polymerase chain reaction technique. Total ARGs comprised 289 subtypes, most diverse of which were aminoglycosides (45 subtypes; 4.03% - 9.21% relative abundance), MGEs (43 subtypes; 7.23% - 19.68%), and beta-lactam (41 subtypes; 0.40%-2.12%). Both integrons and MGEs showed the highest abundances, with *intI3* at 17.64% in seawater and *intI1* at 17.88% – 21.44% in all except seawater. The results from this study could provide insights into the environmental contamination of ARGs and facilitate the effective management and risk mitigation associated with antimicrobial resistance dissemination.

Keywords: Antibiotic resistance genes, water pollution, sewage, high-throughput Qpcr

Introduction:

Antimicrobial resistance (AMR) is one of the major concerns in many countries worldwide. AMR management and control have been emphasized through the One Health perspective by incorporating the relationship among human, animal, and environmental sectors (Booton et al., 2021; WHO, 2015). Antibiotic resistance genes (ARGs) and antibiotic-resistant bacteria (ARB) are emerging microbial pollutants due to their ability to disseminate antibiotic resistance to natural bacteria in the environment (Amarasiri et al., 2020; Verhougstraete et al., 2020). Natural bacteria can acquire AMR through free ARG uptake, gene transfer from other bacteria, and gene introduction by bacteriophages (Amarasiri et al., 2020). Community wastewaters are a reservoir for ARB and ARG transmission into the environment (Hassoun-kheir et al., 2020; Pazda et al., 2019). Contamination of ARGs in environmental water, including freshwater and seawater, has been reported but is still limitedly available, especially in tropical regions (Amarasiri et al., 2020; Makkaew et al., 2021; Zheng et al., 2021). Consequently, data regarding

contaminated levels of ARB and ARGs in the environmental sector are much needed to integrate into the more available information from the human and animal sectors as part of the One Health concept (Ministry of Public Health & Ministry of Agriculture and Cooperatives, 2020; WHO, 2015).

This study aimed to investigate the prevalence and abundance of ARGs, integrons, and mobile genetic elements (MGEs) in four water types, comprising untreated and treated wastewater, freshwater, and seawater, to provide the surveillance data supporting the effective management of ARGs contamination in the environment in Thailand.

Methodology:

One liter of untreated wastewater influent (BS-IN) and treated effluent (BS-EF) were grabbed from the Bang Sue wastewater treatment plant, at an influent sump after a bar screening and an ultrafiltration membrane unit, respectively. Two liters of the freshwater sample was collected 30-cm below the surface at mid-width of the Chao Phraya River near Wat Sai Mah Nuea (WSN), Nonthaburi Province. Two liters of seawater sample was collected 30-cm below the surface at 10-m away from the shoreline of Pattaya Beach (PTH), Chonburi Province. All samples were collected from February to March 2022. The water samples were transported on ice to the laboratory within eight h. Samples (200 – 1,500 mL) were filtered through 0.45-µm-pore size HAWP membrane filters (Merck Darmstadt, Germany), and DNA was extracted using a ZymoBIOMICS DNA Miniprep Kit (Zymo Research, Irvine, CA). DNA extracts were measured using a NanoDrop 2000 Spectrophotometer (Thermo Fisher Scientific, Waltham, MA) and stored at –80°C. A total of 384 ARGs were analyzed using the SmartChip™ Real-Time PCR system (TakaraBio, San Jose, CA) by Resistomap Oy (Helsinki, Finland). A limit of quantification is at a cycle threshold (C_q) of 27. The relative abundance of ARGs was calculated by comparing it with the 16s rRNA gene.

Results:

The total number of ARGs found in all samples was 289 subtypes, including those resistant to aminoglycosides (45 subtypes), MGEs (43 subtypes), beta-lactam (41 subtypes), macrolide- lincosamide-and-streptogramin B (MLSB) (33 subtypes), multiple-drug resistance (MDR) (29 subtypes), tetracycline (23 subtypes), phenicol (19 subtypes), trimethoprim (12 subtypes), quinolone and vancomycin (11 subtypes), sulfonamide (4 subtypes), and integrons (3 subtypes) **(Figure 1)**. The four most abundant ARGs groups were integrons (17.64% -21.63%), MGEs (7.23% - 19.68%), aminoglycosides (4.03% - 9.21%) and MLSB (2.35% - 7.21%). The *intI1* gene showed the highest relative abundance in BS-IN, WSN, and BS-EF at 21.44%, 20.63%, and 17.88%, respectively, while in PTH was *intl3* at 17.64%. The most abundant MGEs related to ARGs translocation were *IS6100* at 19.68%, 8.46%, and 7.23% in BS-IN, WSN, and BS-EF, respectively, *IS1247* at 5% in PTH. The most abundant aminoglycoside-resistant genes were *aadA7* at 9.21%, 5.67%, and 4.03% in PTH, WSN, and BS-EF, respectively, and *aadA2* at 7.48% in BS-IN. The most abundant genes resistant to MLSB were *ermX* at 7.21% and 4.28% in PTH and WSN, *ereA* at 6.93% in BS-IN, and *mphA* at 2.35% in BS-EF.

Discussion:

In this study, the highest abundance and prevalence of ARGs were present in untreated wastewater, as has been reported to be sources of ARG contamination into the environment (Pazda et al., 2019). Integrons were highly abundant in the environment, and *intI1* was considered a proxy for anthropogenic pollution (Koczura et al., 2016; Ma et al., 2017; Makkaew et al., 2021). The prevalence of integrons and MGEs raises the concern about AMR dissemination in the environment due to their capability to carry and transmit ARGs to natural bacteria through horizontal gene transfer (Ma et al., 2017). Moreover, the COVID-19 pandemic has increased the use of clinical antibiotics and disinfecting and cleansing products, which could induce resistance to antibiotics and biocides (Chen et al., 2021). Multidrug resistance genes, such as those related to efflux pumps (e.g., *acrB*), as well as biocide tolerant genes, such as triclosan-resistant gene *fabK*, were also evident in this study. Molecular mechanism studies are needed to understand multidrug resistance and environmental factors associated with AMR dissemination, such as those shown by triclosan (Lu et al., 2020; Nontaleerak et al., 2022).

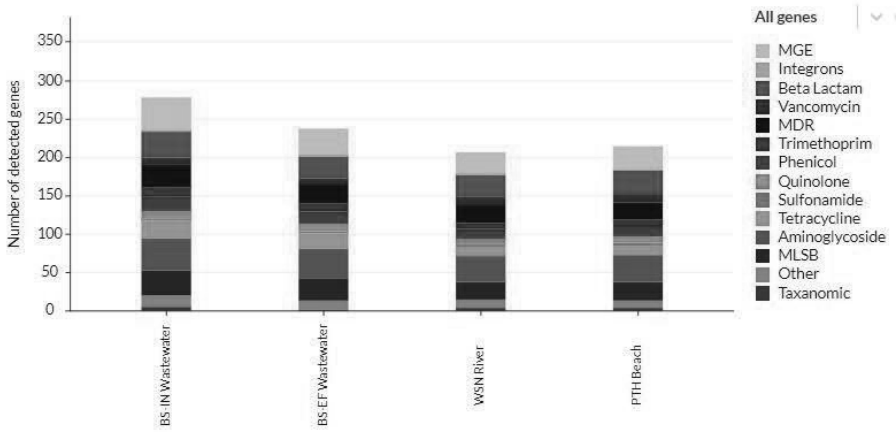

Figure 1 Numbers of detected antibiotic resistance genes (ARGs) and associated antibiotic groups in untreated and treated wastewater, freshwater, and seawater

Conclusion:

This study investigated the diversity and contamination levels of different ARG groups in Thailand's untreated and treated wastewater, freshwater, and seawater. Aminoglycoside-resistant genes were most prevalent, while integrons were found most abundant, emphasizing that horizontal gene transfer could mainly contribute to AMR dissemination in the environment. Characterizing ARGs in the environment could facilitate wastewater and water resource management to curb AMR dissemination through the environmental sector as part of the One Health perspective.

References:

1. Amarasiri, M., Sano, D., & Suzuki, S. (2020). Understanding human health risks caused by antibiotic-resistant bacteria (ARB) and antibiotic resistance genes (ARG) in water environments: Current knowledge and questions to be answered. *Critical Reviews in Environmental Science and Technology*, *50*(19), 2016–2059. https://doi.org/10.1080/10643389.2019.1692611

2. Booton, R. D., Meeyai, A., Alhusein, N., Buller, H., Feil, E., Lambert, H., Mongkolsuk, S., Pitchforth, E., Reyher, K. K., Sakcamduang, W., Satayavivad, J., Singer, A. C., Sringernyuang, L., Thamlikitkul, V., Vass, L., Avison, M. B., & Turner, K. M. E. (2021). One Health drivers of antibacterial resistance : quantifying the relative impacts of human , animal and environmental use and transmission. *One Health*, *12*, 100220.

3. Chen, B., Han, J., Dai, H., & Jia, P. (2021). Biocide-tolerance and antibiotic-resistance in community environments and risk of direct transfers to humans: Unintended consequences of community-wide surface disinfecting during COVID-19? *Environmental Pollution*, *283*, 117074. https://doi.org/10.1016/j.envpol.2021.117074

4. Hassoun-kheir, N., Stabholz, Y., Kreft, J., De, R., Romalde, J. L., Nesme, J., Sørensen, S. J., Smets, B. F., Graham, D., & Paul, M. (2020). Comparison of antibiotic-resistant bacteria and antibiotic resistance genes abundance in hospital and community wastewater : A systematic review. *Science of the Total Environment*, *743*(140804), 1–11. https://doi.org/10.1016/j.scitotenv.2020.140804

5. Koczura, R., Mokracka, J., Taraszewska, A., & Łopacinska, N. (2016). Abundance of Class 1 Integron-Integrase and Sulfonamide Resistance Genes in River Water and Sediment Is Affected by Anthropogenic Pressure and Environmental Factors. *Microbial Ecology*, *72*(4), 909–916. https://doi.org/10.1007/s00248-016-0843-4

6. Lu, J., Wang, Y., Zhang, S., Bond, P., Yuan, Z., & Guo, J. (2020). Triclosan at environmental concentrations can enhance the spread of extracellular antibiotic resistance genes through transformation. *Science of the Total Environment*, *713*. https://doi.org/10.1016/j.scitotenv.2020.136621

7. Ma, L., Li, A.-D., Yin, X.-L., & Zhang, T. (2017). The Prevalence of Integrons as the Carrier of Antibiotic Resistance Genes in Natural and Man-Made Environments. *Environmental Science & Technology*, *51*, 5721–5728. https://doi.org/10.1021/acs.est.6b05887

8. Makkaew, P., Kongprajug, A., Chyerochana, N., Sresung, M., Precha, N., Mongkolsuk, S., & Sirikanchana, K. (2021). Persisting antibiotic resistance gene pollution and its association with human sewage sources in tropical marine beach waters. *International Journal of Hygiene and Environmental Health*, *238*, 113859. https://doi.org/10.1016/j.ijheh.2021.113859

9. Ministry of Public Health, & Ministry of Agriculture and Cooperatives. (2020). *National Strategic Plan on Antimicrobial Resistance 2017-2021 Thailand: at a glance*. http://www.fda.moph.go.th/sites/drug/Shared Documents/AMR การจัดการต้านจุลชีพ/NSP-AMR_at a glan

10. Nontaleerak, B., Tasnawijitwong, N., Eurtivong, C., Sirikanchana, K., Satayavivad, J., Sukchawalit, R., & Mongkolsuk, S. (2022). Characterisation of the triclosan efflux pump TriABC and its regulator TriR in Agrobacterium tumefaciens C58. *Microbiological Research*, *263*(May), 127112. https://doi.org/10.1016/j.micres.2022.127112

11. Pazda, M., Kumirska, J., Stepnowski, P., & Mulkiewicz, E. (2019). Antibiotic resistance genes identified in wastewater treatment plant systems – A review. *Science of the Total Environment*, *697*(134023), 1–21.

12. Verhougstraete, M. P., Pogreba-Brown, K., Reynolds, K. A., Lamparelli, C. C., Zanoli Sato, M. I., Wade, T. J., & Eisenberg, J. N. S. (2020). A critical analysis of recreational water guidelines developed from temperate climate data and applied to the tropics. *Water Research*, *170*. https://doi.org/10.1016/j.watres.2019.115294

13. WHO. (2015). Global Action Plan on Antimicrobial Resistance. In *World Health Organisation*. www.wpro.who.int/entity/drug_resistance/resources/global_action_plan_eng.pdf

14. Zheng, D., Yin, G., Liu, M., Chen, C., Jiang, Y., Hou, L., & Zheng, Y. (2021). A systematic review of antibiotics and antibiotic resistance genes in estuarine and coastal environments. *Science of the Total Environment*, *777*, 146009. https://doi.org/10.1016/j.scitotenv.2021.146009

QUANTITATIVE MULTIPLEXED PROTEOMICS IDENTIFIES A PARADOXICAL ROLE PROTEIN UPREGULATION IN BREAST CANCER SPHEROID

Phanthakarn Tit-Oon[1], Klaichan Boonkanta[2], Arisa Wonglangka[2], Mayuree Fuangthong[1,3], Mathuros Ruchirawat[1,3], and Amnart Khongmanee[1,3]

[1]Translational Research Center, Chulabhorn Research Institute, Bangkok 10210, Thailand
[2]Center for Biologics Research and Development, Chulabhorn Research Institute, Bangkok 10210, Thailand
[3]Center of Excellence on Environmental Health and Toxicology (EHT), OPS, MHESI, Thailand

Abstract:

Breast cancer is the most common cancer in Thai women. The mechanisms underlying breast cancer metastasis are complicated and influenced by many factors. In this study we employed multiplexed proteomics using Tandem Mass Tag (TMT) isobaric labeling to analyze differential protein expressions between anoikis induced condition (spheroid) and monolayer culture of HER2 positive breast cancer cell—BT-474. The results provided the list of 29 upregulated proteins and 38 downregulated proteins in anoikis induced condition compared to control. Among these differential proteins, we confirmed that protein X—a protein with unclear role in breast cancer—is highly upregulated in anoikis induced condition. Further experiments are required to prove the functions of protein X in breast cancer metastasis model. However, the results provide convincing evidence that multiplexed proteomics could generate valuable information to study breast cancer metastasis mechanisms.

Keywords: Multiplex proteomics, breast cancer, metastasis, spheroid culture

Introduction:

Breast cancer is most commonly found in cancer-diagnosed women around the world with reported more than one million new cases annually (1). The mortality caused by breast cancer mainly occurs in women aged between 45 to 55 years old and the mortality rates vary depending on the different subtypes of this cancer (1, 2). Many low- and middle-income countries such as developing Asian countries showed higher breast cancer mortality rates than high-income countries, which accounted for approximately 60% of breast cancer mortality, as the access to the diagnostic and treatment of breast cancer are limited (2, 3). This leads to the patients being diagnosed with breast cancer at a late stage (2). Thailand is one of the developing countries where the incidence of breast cancer has increased over the years and it is currently the most common cancer in the female population in Thailand (3, 4). Breast cancer is like others that metastasis—cause of death in patients—are not well understood. Anoikis is the process that induced cell death under condition that the cell loss the contact to their extracellular environment. Resistant to cell death via anoikis resistant is important steps for cancer cells to invade another tissue. BT-474 has been wildly used as breast cancer model that displays the overexpression of human growth factors receptors 2 (HER-2) and estrogen receptors (ER).

In this study we use BT-474 spheroid culture—cell culture in polyHEMA coated plate—as an anoikis induced model to study breast cancer metastasis mechanisms. Multiplexed proteomics using TMT labeling is used to generate the list of differential protein expressions between anoikis induced condition and control. Prominent candidate protein that highly upregulated in anoikis induced condition were confirmed using western blot analysis. The study provided evidence that multiplex proteomics could be used to study complex biological mechanisms by providing a reliable list of differentiated protein expressions.

Methodology:

Cell culture. The 6-well plate was coated with 30 mg/mL of poly(2-hydroxyethyl methacrylate) or polyHEMA (Sigma) in 95% ethanol at room temperature and dried at 37 ℃ overnight. After that, the plate was sterile by UV light and washed with 1xPBS, pH7.2 (Gibco) before used. BT-474 cells ($0.2x10^6$ cells/mL) were seeded onto conventional or polyHEMA plate in DMEM/F-12 medium (Gibco) with 10% fetal bovine serum (FBS, Gibco). Cells were incubated in 5% CO_2 incubator at 37°C and harvested at 24, 48, and 72 hrs. Cell pellets were kept at –80 °C.

TMT-10Plex proteomic Lysis buffer was added to cell pellets, incubated on ice for 1 hr followed by 3-times sonication with a pulse on/off: 9.9/0.1 sec and 16% amplitude for 40 sec. Cell lysate was centrifuged at 14,000×g for 20 mins at 4 °C and the clear supernatant was transferred into a new tube. The protein concentration was measured using BCA protein assay (Thermo Scientific). After that, the protein was reduced and alkylated followed by trypsin digestion. Peptides were then desalted using a reverse-phase tC18 Sep-Pak vac cartridge (Waters). The eluate was taken to measure peptide concentration using Quantitative Fluorescent Peptide assay (Thermo Scientific). Afterward, the eluate was lyophilized overnight and the desired amount of peptide was calculated for TMT labeling. The peptide labeling was performed using TMT10plex Mass Tag Labeling Kits (Thermo Scientific) as described in product instruction. In brief, total amount of peptide was adjusted to 25-100 µg for labeling assay. The reaction was quenched using 5% hydroxylamine. An equal amount of each labeled sample was combined into a new tube. The pooled peptide was aliquoted and dried using speedvac. For multiplex proteomic analysis, dried peptide sample was resuspended with 0.1% FA followed by purification and concentration using ZipTip (Merck) before mass spectrometry using Orbitrap Elite™ Hybrid Ion Trap-Orbitrap Mass Spectrometer (Thermo Scientific) coupled to an ACQUITY UPLC System (Waters).

Data analysis Proteome discoverer software version 2.4 was used to analyze raw data from TMT experiment. The software was used to calculate expression ratio between the two conditions.

Western blot confirmation Protein was equally loaded (20 µg) into NuPAGE 4-12% Bis-Tris Gel (Thermo Scientific) at 100 V for 2 hrs and transferred into PVDF membrane at 100 V for 45 mins. The membrane was washed 3-times with 1xTBST for 10 mins on a rocking platform and then blocked with 5% BSA (W/V) in 1xTBST for 1 hr at room temperature. After the blocking step followed by washing, the membrane was incubated in primary antibody overnight at 4 °C. The membrane was washed and incubated in 5% skim milk for 30 mins, then secondary antibody was added and incubated for 1 hr at room temperature. Detection of bound immunocomplexes was performed after washing membrane with high amount of 1xTBST, the bound immunocomplex was visualized using Amersham ECL Prime Western blotting detection reagent (GE Healthcare) and captured the luminescent signal was analyzed using the ImageQuant™ LAS 4000 machine (GE Healthcare).

Results, Discussion and Conclusion*:*

1. Morphology of BT-474 cells in anoikis induced condition (Spheroid culture)

Morphological change of BT-474 cells were observed in non-attachment induced culture condition (polyHEMA coated plate). Cells were loosely clumped together—grape like structure—after cultured in polyHEMA coated plate for 8 hours (Figure 1). Spheroid formation of BT-474 cells were observed after cultured in polyHEMA coated plate for 24 hours while in normal plate cell were completely attached to the bottom of the plate (Figure 1). Therefore, cells from both conditions were harvested at 24-hours for multiplex proteomics analysis.

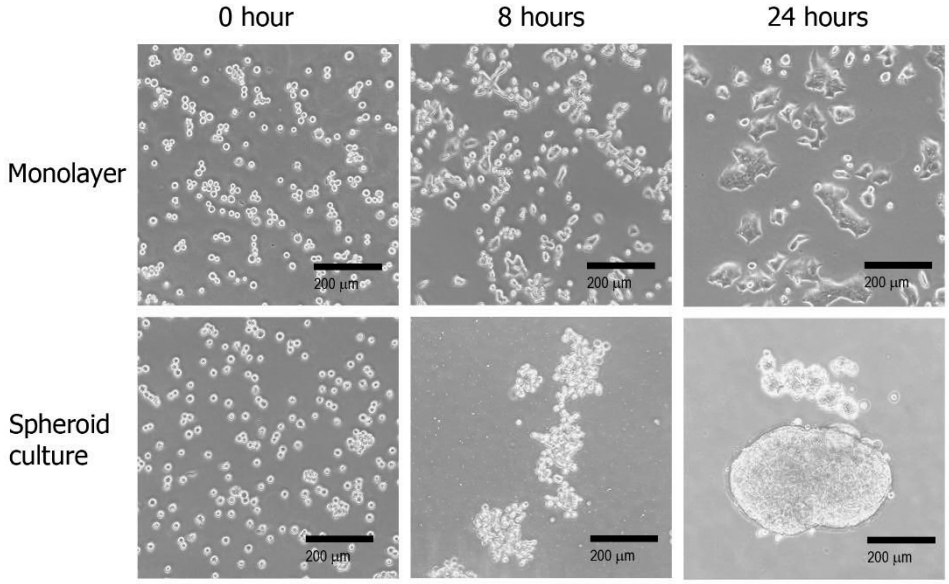

Figure 1 Morphology comparison between monolayer and spheroid culture of BT-474 cells at initial, 8 hours, and 24 hours, respectively

2. Proteomics profile comparison between attached and Spheroid culture

Multiplexed proteomics using TMT-10Plex could detect 4,176 proteins from both conditions. The volcano plot of protein expression data compares between monolayer and spheroid culture were shown in Figure 2. The data indicated that 29 proteins were upregulated in anoikis induced condition compared to monolayer culture while 38 proteins were downregulated. Among these significantly changed proteins, the selected protein (light blue dot) was chosen for confirmation using western blot analysis.

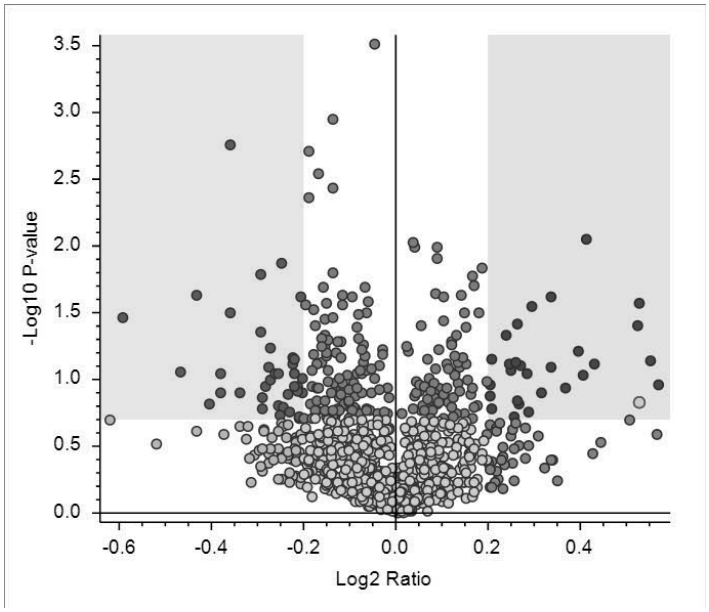

Figure 2 Volcano plot protein expression in spheroid culture compare to monolayer culture. Light blue dot is a selected protein that was chosen for confirmation

3. Confirmation of candidate protein that significantly upregulated in anoikis induced breast cancer cells.

Protein X was chosen for further confirmation using western blot analysis. The result from western blot confirmed that protein X is significantly upregulated in anoikis induced condition (Figure 3). We also included the samples from both culture conditions at 48 and 72 hours and the results were confirmed that protein X is upregulated in anoikis induced condition in all selected time points.

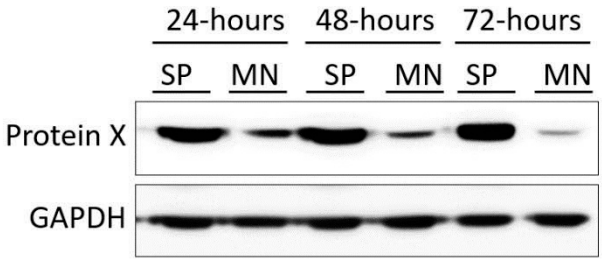

Figure 3 Western blot analysis using monoclonal antibody to protein X, GAPDH was used as a loading control. SP: Spheroid culture, MN: Monolayer culture

Protein X had been reported to be associated with breast cancer metastasis. However, some also reported that it acts as a tumor suppressor gene. We aim to knock-down this protein and observe the function of protein X in BT-474 cells. In conclusion this study demonstrated that multiplexed proteomics using TMT labeling could provide the list of differential protein expressions between two culture conditions with the results that could confirmed by western blot analysis. This powerful method enables complex proteomic analysis and could apply to several approaches for cancer biology study in the future.

References:

1. Ataollahi MR, Sharifi J, Paknahad MR, Paknahad A. Breast cancer and associated factors: a review. J Med Life. 2015;8(Spec Iss 4):6-11.
2. Harbeck N, Penault-Llorca F, Cortes J, Gnant M, Houssami N, Poortmans P, et al. Breast cancer. Nat Rev Dis Primers. 2019;5(1):66.
3. Virani S, Chindaprasirt J, Wirasorn K, Sookprasert A, Somintara O, Vachirodom D, et al. Breast Cancer Incidence Trends and Projections in Northeastern Thailand. Journal of Epidemiology. 2018;28(7):323-30.
4. Ferlay J EM, Lam F, Colombet M, Mery L, Piñeros M, Znaor A, Soerjomataram I, Bray F. Global Cancer Observatory: Cancer Today. 2020.
   [Available from: https://gco.iarc.fr/today].

Safety and toxicity of food, drugs and other chemicals including biofuels

QUANTITATIVE MICROBIAL RISK ASSESSMENT OF SPECIFIC FOOD MENU FROM RESTAURANTS IN BANGKOK, THAILAND

S. Panthong [a, b*], A. Phosri [a, b], C. Singhakant [a, b], W. Patthanaissaranukool [a, b]

[a]Department of Environmental Health Sciences, Faculty of Public Health, Mahidol University, Bangkok 10400, Thailand

[b]Center of Excellence on Environmental Health and Toxicology (EHT), OPS, Ministry of Higher Education, Research, Science and Innovation, Bangkok, Thailand

**Corresponding author: sathida.pan@outlook.com*

Abstract:

Consumption of food contaminated with pathogenic bacteria is a major factor causing high prevalence of gastrointestinal disease in Thailand. This study aims to assess the risk of illness attributed to a consumption of the Steamed Chicken with Rice (SCR), the popular food menu in Thailand, contaminated with *Escherichia coli (E. coli)* in Bangkok metropolitan area using the quantitative microbial risk assessment (QMRA) approach. The analysis was divided into three parts, including (1) exposure assessment, in which the quantity of *E. coli* contaminated in SCR from many restaurants throughout Bangkok between January and August in 2020 and 2021 was obtained from the Food Sanitation Division, Department of Health under Bangkok Metropolitan Administration. The data were then multiplied by the consumption rate obtained from a survey of 544 people who live in Bangkok to incur exposure dose, (2) dose-response assessment with the Beta-Poisson model was applied to predict the probability of illnesses of *E. coli* contaminated in the SCR, and (3) the daily and annual probability of illness was then calculated by incorporating exposure dose, consumption frequency, and Beta-Poisson model as a selected dose-response model using the Monte Carlo simulation with 10,000 iterations. The results indicated that the average risk of illness due to *E. coli* infection was 96.5% (95% CI: 40.3, 100.0), 89.4% (95% CI: 8.5, 100), 76.0% (95% CI: 1.9, 100.0) with very frequently (daily), frequently (weekly), and occasionally (monthly) consuming, respectively. Findings of this study implies that consumption of SCR contaminated with *E. coli* had high risk of *E. coli* related illness, where the specific control measures need to be implemented especially at the restaurants in Bangkok to alleviate the progression of foodborne disease related to *E. coli*.

Keywords: QMRA, *Escherichia coli*, steamed chicken with rice, food consumption

Introduction:

According to annual report of the Food Sanitation Division, Department of Health Bangkok Metropolitan Administration (BMA), the problem upon food safety situation during 2015 to 2018 in Bangkok had remained with a contamination of pathogenic microorganisms, especially *Escherichia coli (E. coli)* [1], in which *E. coli* is commonly found in the gut of human beings and warm-blooded animals. Most strains of *E. coli* are harmless, but certain strains are able to cause severe foodborne disease such as Shiga toxin-producing *E. coli* (STEC). This strain of *E. coli* is usually transmitted to human primarily through consumption of contaminated foods [2]. In 2020, the proportion of positive contamination of pathogenic microorganisms in many types of ready-to-eat-food in Bangkok was 22.57%, where the Steamed Chicken with Rice (SCR) was the most contaminated menu accounted for 67.65% [1].

The Quantitative Microbial Risk Assessment (QMRA) is one of the most valuable tools used to predict the human health risk posed by microorganisms and prevent foodborne diseases via assessing the probability of experiencing infection or illness due to contaminated pathogens [3], where many countries have used the QMRA as a tool to improve food safety surveillance system [4]. In Thailand, food quality surveillance system has been qualitatively conducted, where the data have been collected in the form of percentage and compare those data with historical data to see the trend of food safety situation. Nevertheless, predicting quantitatively the probability of risk associated with microbial contamination in foods to prioritize problem solving has not received much attention. Therefore, this study aims to assess the possibility of risk from the SCR contaminated with *E. coli* in Bangkok through QMRA approach.

Methodology:

1. Data collection

1.1 Quantity of *E. coli* in the SCR

The quantity of *E. coli* (MPN/g) in the SCR from many randomly selected restaurants across Bangkok collected between January and August, 2020 and 2021 was obtained from the Food Sanitation Division, Department of Health under the Bangkok Metropolitan Administration. The samples were analyzed using the Most Probable Number (MPN) method followed the Bacteriological Analytical Manual (BAM) (Chapter 4) recommended by the Food and Drug Administration (FDA) [5].

1.2 Consumption of the SCR

The questionnaire was used to collect the data on frequency and quantity of SCR consumption from people lived in Bangkok for at least one year throughout Bangkok via Google Form. The sample size was calculated according to the Taro Yamane's model with designated 95% acceptable error, and 544 respondents were ultimately obtained.

2. Quantitative Microbial Risk Assessment

2.1 Hazard identification

The quantity of *E. coli* was measured to estimate the exposure to bacterial contaminants that were contaminated in the SCR available in Bangkok. Data were obtained from the report of the Department of Health under the Bangkok Metropolitan Administration. In brief, sample was collected at 300 g and weighed 50 g to dilute concentration at 0.1, 0.01, and 0.001 g for detecting *E. coli*. The Most Probable Number of *E. coli* per gram of food sample (MPN/g) was then calculated from the positive number of tubes at any positive number of dilutions which can be seen from MPN table [5].

2.2 Exposure assessment

The quantity of *E. coli* that are consumed through having the SCR per day was calculated by multiplying the quantity of *E. coli* contaminated in the SCR samples with consumption rate obtained from the questionnaire using the following equation;

$$\text{Dose of exposure} = \text{Quantity} * \text{Consumption rate}, \quad (1)$$

wherein *"Dose of exposure"* indicates the amount of *E. coli* consumed per day (MPN/day); the *"Quantity"* is the quantity of *E. coli* contaminated in the SCR samples (MPN/g), and the. *"Consumption rate"* is the amount of the SCR consumed per day (g/day).

2.3 Dose-response assessment

The dose-response relationship that characterizes the association between the numbers of ingested *E. coli* (dose of exposure) and the likelihood of occurrence of an adverse consequence per day in terms of illness in this study was considered using the Beta-Poisson model using the following equation.

$$P_{ill} = 1 - [1 + \frac{dose}{\beta}]^{-\alpha}, \qquad (2)$$

wherein, the *"P_{ill}"* is the probability of illness due to ingested *E. coli* per day, and *"dose"* is the exposure dose of *E. coli* consumed per day that is obtained from the exposure assessment, whereas *"α"* is a parameter of the beta-Poisson distribution and *"β"* is a parameter computed from N_{50} (i.e., the dose at which 50% of the populations is expected to be affected), where $N_{50} = \beta*[2^{(1/\alpha)}-1]$ and $\alpha = 0.267$ and $\beta = 229.2928$ [6].

2.4 Risk characterization

The annual probability of illness due to exposure to *E. coli* contaminated in the SCR was computed using the following equation;

$$P_{ill(ann)} = 1- [1 - P_{ill}]^{n}, \qquad (3)$$

wherein the *"$P_{ill(ann)}$"* is the probability of illness due to ingested *E. coli* per year, and *"P_{ill}"* is the probability of illness due to ingested *E. coli* per day obtained from Eq. (2); *"n"* is the consumption frequency in a year.

3. Statistical analysis

The Kolmogorov-Smirnov test was used to check the appropriate distribution of each variable used to perform the QMRA, and the Monte Carlo simulation with 10,000 iterations was then used to examine the probabilistic risk of illness attributable to *E. coli* contaminated with the SCR per day and year. The annual average of illness per year and its 95% confidence interval were then reported.

Results and Discussion:

The Kolmogorov-Smirnov test showed log normal distribution ($\mu = 3.2$, $\sigma = 2.69$) for quantity of *E. coli* and consumption of SCR as uniform distribution (with minimum = 1, maximum = 3). The calculated dose of exposure was 2,237.46 MPN/day. The average probabilistic risk of illness per day was 30.8% (95% CI: 0.2, 81.2) and the annual probability of illness was shown in table 1.

Table 1 The annual probability of illness due to ingested *E. coli* contaminated in the SCR

Consumption frequency	Probability of illness per year*
Very frequently (daily consumption)	96.5% (95% CI: 40.3, 100.0)
Frequently (weekly consumption)	89.4% (95% CI: 8.5, 100.0)
Occasionally (monthly consumption)	76.0% (95% CI: 1.9, 100.0)

* Probability of illness due to the ingested *E. coli* contaminated in the SCR was indicated as percentage of risk per year in case of consuming the Steamed Chicken with Rice (SCR) every day (very frequently), once a week (frequently), and once a month (occasionally).

Finding of this study indicates that consuming the SCR contaminated with *E. coli* every day would have the average risk of illness of 96.5% (95% CI: 40.3, 100.0). Moreover, the results show that the annual average probability of illness due to ingested *E. coli* contaminated in the SCR in case of consuming the SCR once a week and once a month was 89.4% (95% CI: 8.5, 100.0) and 76.0% (95% CI: 1.9, 100.0), respectively. This study implies that high possibility of illness due to ingested *E. coli* contaminated in SCR remained even though consuming the SCR once a month. This high risk of ingested *E. coli* contaminated in the SCR might be resulted from the contamination of *E. coli* during food preparation with other meat products, as well as contaminated surfaces and utensils [7]. Specific limitation of this study should be acknowledged. In particular, the quantity of *E. coli* in this study was measured by collecting the SCR samples that combined all ingredients together, in which the amount of pathogen in individual food ingredients and sources of contamination cannot be identified. Hence, further study is required to investigate the sources of *E. coli* contamination by separately measuring the amount of *E. coli* contaminated in each ingredient.

Conclusion:

High possibility of illness due to ingested *E. coli* contaminated in the SCR is observed even though consuming the SCR once a month. Findings of this study implies that consumption of SCR contaminated with *E. coli* had high risk of *E. coli* related illness, where the specific control measures need to be implemented especially at the restaurants in Bangkok to alleviate the progression of foodborne disease related to *E. coli*.

Acknowledgement:

This research was partially supported by the Food Sanitation Division, Department of Health under the Bangkok Metropolitan Administration by providing bacterial data for the analysis in this study.

References:

1. Food Sanitation Division/Department of Health/Bangkok Metropolitan Administration. Food safety situation in Bangkok. 2020;
2. World Health Organization. *E.coli* [Internet]. 2018 [cited 2021 Oct 10]. Available from: https://www.who.int/news-room/fact-sheets/detail/e-col
3. Lee H, Kim K, Choi KH, Yoon Y. Quantitative microbial risk assessment for Staphylococcus aureus in natural and processed cheese in Korea. J Dairy Sci. 2015;98(9):5931–45.
4. Kim HJ, Griffiths MW, Fazil AM, Lammerding AM. Probabilistic risk model for Staphylococcal intoxication from pork-based food dishes prepared in food service establishments in Korea. J Food Prot. 2009;72(9):1897–908.
5. U.S. Food&Drug Administration. BAM Chapter 4: Enumeration of *Escherichia coli* and the Coliform Bacteria [Internet]. 2020. Available from: https://www.fda.gov/food/laboratory-methods-food/bam-chapter-4-enumeration-escherichia-coli-and-coliform-bacteria
6. Pang H, Lambertini E, Buchanan RL, Schaffner DW, Pradhan AK. Quantitative microbial risk assessment for *Escherichia coli* O157:H7 in fresh-cut lettuce. J Food Prot. 2017;80(2):302–11.
7. Bureau of Food and Water Sanitation. Principles of Food Sanitation. 2013.

Environment / health impact assessment and management

BIOMAGNIFICATION OF BISPHENOL A IN CULTURED GREEN MUSSEL (*Perna viridis*) FOOD CHAINS FROM MAP TA PHUT INDUSTRIAL ESTATE, RAYONG PROVINCE

Pornwipa Kunkate[a], Thanomsak Boonphakdee[a,b*,d] and Chuta Boonphakdee [c,d]

[a]Graduate Program in Environmental Science, Faculty of Science, Burapha University, Chonburi 20131, Thailand
[b]Department of Aquatic Science, Faculty of Science Burapha University, Chonburi province. 20131 Thailand
[c]Department of Biology, Faculty of Science, Burapha University, Chonburi 20131, Thailand
[d]Center of Excellence on Environmental Health and Toxicology (EHT), OPS, MHESI, Thailand
** Corresponding author: nuiosk@yahoo.com*

Abstract:

This study aimed to investigate the biomagnification of BPA in Green mussels cultured in Takuan Bay, Map Ta Phut Industrial Estate. BPA concentrations in mussels ranged of 384 - 513 ng/g and were higher than those of sediment, seawater and particulate organic matter (POM). BPA distribution in the bay is influenced from the effluent of Map Ta Phut industrial Estate. $\delta^{13}C$ and $\delta^{15}N$ values revealed BPA biomagnification in mussels. We found three trophic levels of marine organisms as producer (phytoplankton), the primary consumer (zooplankton), and predator (green mussel), consistent with BPA concemtrations in those food chain component.

Keywords: Bisphenol A, distribution, mussels, industrial, biomagnification

Introduction:

In recent decades, an increasing number of plastic products containing bisphenol A (BPA) have resulted in BPA contamination of the aquatic environment in sediment, freshwater, and seawater. [11] BPA is a chemical that can cause problems at work. Natural hormone synthesis, transport, and breakdown It is also a rare soluble substance as an endocrine disruptor, with a K_{ow} of 3.64±0.32. [2] BPA absorption was found to be greater in sediments than in water.[5] Because BPA is fat-soluble, it can accumulate in algae and primary producers, the first order of biomagnification.[4] The isotopes of stable carbon ($\delta^{13}C$) and nitrogen ($\delta^{15}N$) can be used to determine the relationship between producers and consumers within the food chain of the marine ecosystems. [3]

This study aimed to investigate BPA accumulation and transmission to mussels through the food chain in Takuan Bay, receiving wastewater from Map Ta Phut Industrial Estate. This will be extremely useful for effective BPA management and control along the coastal waters.

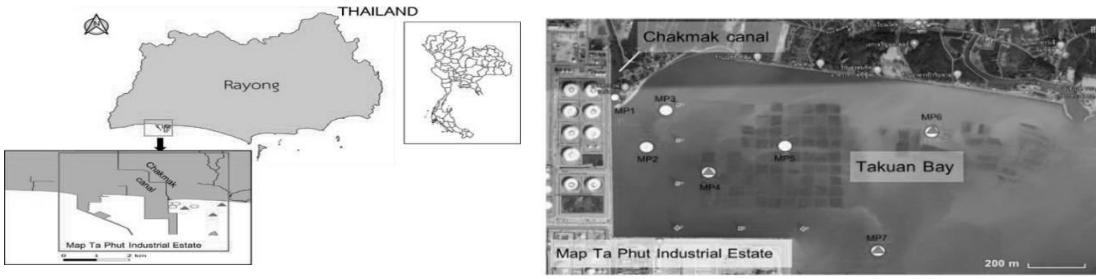

Figure 1 Map of the sampling location in Chak Mak canal and Takuan bay. Open circles (○) represent seawater and sediment sampling stations; while solid triangles (▲) represent green mussels and plankton sampling stations.

Methodology:

Seawater, sediment, phytoplankton, zooplankton, and mussel samples were collected at 7 stations (Figure 1) in Takuan Bay, during August 2019. BPA concentration was analyzed using High-Performance Liquid Chromatography (HPLC)[6] at Faculty of Science, Burapha University. Analysis of $\delta^{13}C$ and $\delta^{15}N$ values were measured by Isotope Ratio Mass Spectrometer (IRMS) were done at Cornell University according to the method of [1]. Trophic level of the food chain were calculated as described by [10].

Results and Discussion:

Contamination of BPA in seawater

BPA concentrations in seawater ranged from 50-1060 ng/L, with the highest concentrations of BPA found at the mouth of the Chak Mak canal station (MP1) 1060 ± 19 ng/L compared to other stations (Figure 2). This indicates that the wastewater from the Map Ta Phut Industrial Estate is contaminated with BPA and decreases as it enters the Bay. This is consistent with studies indicating that many BPA sources come from industrial and urban areas with high population densities[2]. However, our study found that the concentration of BPA in water from the mouth of the Chak Mak canal was higher than in the previous study [6], 50±9 ng/L. It was due to the sampling period, December 2016 to January 2017, of the previous work[6] falling in maintenance period of most petrochemical plants in the Map Ta Phut industry estate [9].

Contamination of BPA in sediment

BPA concentrations in sediment were found in St. MP1 MP2 and MP3, with the highest value at MP1 (240±8 ng/g), 97±6, and 33±4 ng/g, for MP2 and MP3 , respectively (Figure 2). We found BPA concentrations in sediment were higher than those in an industrial area along the Musa River Estuary [7]. Our results clearly show that high BPA concentration at MP1 (the mouth of the Chak Mak canal) is influenced by effluents from the Map Ta Phut Industrial Estate[5].

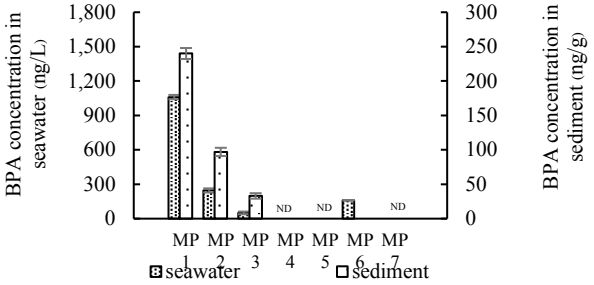

Figture 2 BPA concentrations in seawater and sediment at 7 stations in Takuan Bay. ND = Not detectable (limitation of HPLC detection is less than 1.46 ng/L)

BPA concentration in the digestive tissue of mussels

The BPA concentrations of mussels collected from the MP4; MP6 and MP7 were in the range of 384-579 ng/g (Figure 3). This is consistent with the similar study [5], which found that BPA in mussels taken nearby MP1 was higher than another seaward station. This indicates that BPA contaminated in industrial wastewater discharge may increase the concentration of nutrients and contaminants.

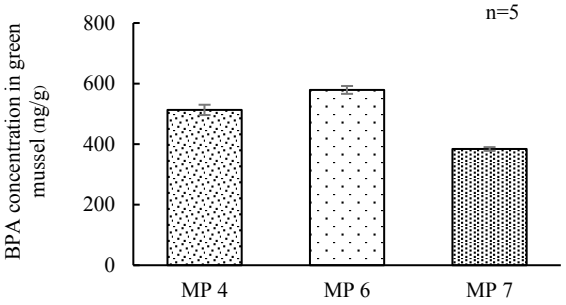

Figure 3 BPA concentration in green mussels, (*Perna viridis*) samples in Takuan Bay, Rayong.

The $\delta^{13}C$ and $\delta^{15}N$ values according to the food chain of living organisms.

Based on the trophic levels along the food chain of Green mussels, we can categorize into 3 trophic levels (Figure 4). Level 1 is the Primary Producer group, i.e., phytoplankton (diatoms), with $\delta^{15}N$ in the range 0 to 4‰, are a group of organisms that create food (Autotrophic Organism). [7]

Level 2 is the first consumer (Primary Consumer), which is zooplankton and the mussel (*Perna viridis*), which has $\delta^{15}N$ in the range 5 to 7‰ (Figure 4). Having eating characteristics, filtered food is eaten through the gills. Most of the food is microscopic unicellular algae, plant remains, bacteria and suspended particles in water. [8]

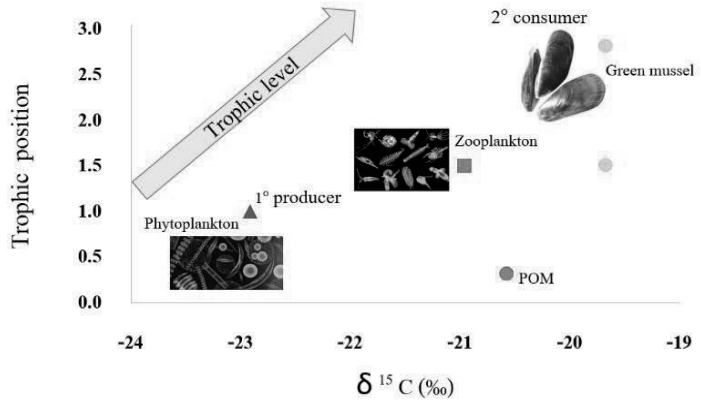

Figure 4 A dual plot trophic position (Tp) and $\delta^{13}C$ (‰) of consumer and producer in Takuan bay. The values of $\delta^{13}C$ were increased (~1-3‰) pre trophic level.

Level 3 is the second consumer or predator, green mussels, which has $\delta^{15}N$ greater than 8‰, indicating that mussels are the highest predators in the food chain (Figure 4)

Biomagnification in the food chain of living organisms.

In examining the biomagnification of BPA in the hierarchical food chain of Green mussels, zooplankton was identified as the first consumer. The previous consumer of this study, mussels (*Perna Viridis*), was the second or last consumer.

BPA concentrations in seawater, sediment, and mussels as shown in Figure 2 and Figure 3 indicate that BPA is transmitted in seawater and sediment and then magnified in the food chain. Mussels feed phytoplankton, zooplankton, and suspended particles in water. Therefore, the BPA accumulation in mussel tissue was observed.

Conclusion:

A study of BPA contamination and trophic level of food chains in the Takuan bay was revealed. Biomagnification of BPA is contaminated in seawater, sediment, and mussels at the mouth of the Chak Mak canal is the highest.

Acknowledgements:

The study was financially supported by the Center of Excellence on Environmental Health and Toxicology (EHT).

References:

1. Boonphakdee, T., Fujiwara, T. Temporal variability of nutrient budgets in a tropical river estuary the Bangpakong River Estuary, Thailand. Environment Asia. 2008;1(1): 7-21.
2. Flint, S., Markle, T., Thompson, S., Wallace, E. Bisphenol A exposure, effects, and policy: a wildlife perspective. Journal of environmental management. 2012;104:19-34.
3. Fry, B., Sherr, E. B. δ^{13} C measurements as indicators of carbon flow in marine and freshwater ecosystems. In Stable isotopes in ecological research. 1989; pp.196-229: Springer

4. Guo, R., Du, Y., Zheng, F., Wang, J., Wang, Z., Ji, R., Chen, J. Bioaccumulation, and elimination of bisphenol a (BPA) in the alga Chlorella pyrenoidosa and the potential for trophic transfer to the rotifer Brachionus calyciflorus. Environmental Pollution. 2017;227: 460-467

5. Kang, J., Kondo, F. Bisphenol A in the surface water and freshwater snail collected from rivers around a secure landfill. Bulletin of environmental contamination and toxicology. 2006;76(1): 113-118.

6. Ocharoen, Y., Boonphakdee, C., Boonphakdee, T., Shinn, A. P., & Moonmangmee, S. High levels of the endocrine disruptors bisphenol-A and 17β-estradiol detected in populations of green mussel, Perna viridis, cultured in the Gulf of Thailand. Aquaculture. 2018; 497: 348-356.

7. Persic, A., Roche, H., Ramade, F. Stable carbon and nitrogen isotope quantitative structural assessment of dominant species from the Vaccarès Lagoon trophic web (Camargue Biosphere Reserve, France). Estuarine, Coastal and Shelf Science. 2004; 60(2): 261-272.

8. Piola, R. F., Moore, S. K., Suthers, I. M. Carbon and nitrogen stable isotope analysis of three types of oyster tissue in an impacted estuary. Estuarine, Coastal and Shelf Science. 2006;66(1-2):255-266.

9. PTT Global Chemical Public Company Limited. A Sustainable Journey: Annual Report. pp. 2016. http://www.pttgcgroup.com/storage/download/cg-committeereport/ 20170315-pttgc-cg-committee-report2016-en.pdf, Accessed date: 20 May 2020.

10. Rumolo, P., Bonanno, A., Barra, M., Fanelli, E., Calabrò, M., Genovese, S., Basilone, G. Spatial variations in feeding habits and trophic levels of two small pelagic fish species in the central Mediterranean Sea. Marine Environmental Research. 2016;115: 65-77.

11. Staples, C. A., Dome, P. B., Klecka, G. M., Oblock, S. T., Harris, L. R. A review of the environmental fate, effects, and exposures of bisphenol A. Chemosphere. 1998;36(10): 2149-2173.

COMPARISON OF CYPERMETHRIN METABOLITES IN URINE SAMPLES AMONG CONVENTIONAL AND ORGANIC FARMERS

A. Tremongkoltip[a,d*], **S. Pengpumkiat**[a,d], **P. Kongtip**[a,d], **N. Nangkongnab** [a,d], **S. Siri**[b,d], **and S. Woskie**[c,d]

[a]*Department of Occupational Health and Safety, Faculty of Public Health, Mahidol University, 420/1 Rajvidhi Road, Bangkok 10400, Thailand*
[b]*Department of Epidemiology, Mahidol University, 420/1 Rajvidhi Road, Bangkok 10400, Thailand*
[c]*Department of Public Health, University of Massachusetts Lowell, One University Ave, Lowell, MA 01854-2867, USA; Susan_Woskie@uml.edu*
[d]*Center of Excellence on Environmental Health and Toxicology (EHT), OPS, MHESI, Thailand*
**Corresponding Author: atima.trm@student.mahidol.ac.th*

Abstract:

This study aimed to compare the urinary metabolites concentration of cypermethrin among conventional and organic farmers. The study recruited conventional farmers (n=209) from Nakhon Sawan and Phitsanulok provinces and organic farmers (n=224) from Yasothon province. The questionnaires were used to collect information about demographic data and history of pesticide use. First morning void urine specimens were collected from conventional and organic farmers. Urine specimens were analyzed for 3-phenoxybenzoic acid (3-PBA), cis-3-(2,2-dichlorovinyl)-2,2-dimethylcylopropane carboxylic acid (cis-DCCA), and trans-3-(2,2-dichlorovinyl)-2,2-dimethylcylopropane carboxylic acid (trans-DCCA) using GC-MS. Statistical analysis was conducted using chi-square test and independent-t test. The average urinary cypermethrin metabolites of conventional and organic were 6.01 and 5.12 for 3-PBA, 17.78 and 15.45 for cis-DCCA, 11.15 and 10.03 for trans-DCCA, 30.03 and 26.33 for cis, trans-DCCA, and 37.30 and 32.30 nmol/g creatinine for total cypermethrin. The results showed that all urinary cypermethrin metabolites of conventional farmers were higher than organic farmers, but no significant difference was observed between two groups. Female organic farmers had significantly higher cypermethrin metabolites than male organic farmers. Female organic farmers may have duty on cleaning up their house. These findings indicated that cypermethrin exposure can be non-occupationally exposed from home insecticide use and occupationally exposed from cypermethrin use in farms.

Keywords: Urinary metabolite, cypermethrin, conventional farmers, organic farmers

Introduction:

Thailand highly exports agricultural products such as fruits and rice every year. Farmers have to use pesticides (1) including organophosphates, carbamates and pyrethroids, to increase yield of agricultural products, and they are exposed to pesticides. Therefore, organic agriculture is the concept of sustainable farming that doesn't use chemicals to conserve ecosystems (2).

Cypermethrin, a pyrethroid insecticide, is commonly used as an agricultural insecticide and it is widely used in house (3) to control insects which is found in a variety of products including home insecticides and mosquito repellents. Thailand has widely used cypermethrin. In 2020, 660 tons of cypermethrin were imported (4). When exposed to cypermethrin, it is metabolized rapidly and the metabolites are 3-phenoxybenzoic acid (3-PBA), cis-3-(2,2-dichlorovinyl)-2,2-dimethylcylopropane carboxylic acid (cis-DCCA), and trans-3-(2,2-dichlorovinyl)-2,2-dimethylcylopropane carboxylic acid (trans-DCCA) (5).

These metabolites are excreted through the urine. Therefore, urinary concentrations of these metabolites are considered as biological indicators of cypermethrin exposure (6). Cypermethrin is widely used for its effectiveness against insects and have low acute toxicity in mammals. However, exposure can lead to health effects (6). Dermal exposure to cypermethrin in humans may have symptoms including skin irritation, numbness, and a burning sensation (3). Insecticides are endocrine disruptor which is substance that disrupt the endocrine system's regular operation (7). Chronic exposure of pyrethroid may cause abnormal glucose regulation (8). It also affects the male reproductive system and neurotoxicity on children (9, 10).

Based on a literature review related to cypermethrin, most studies were conducted on conventional farmers and general population. The purpose of this research was to compare the urinary cypermethrin metabolites of conventional and organic farmers.

Materials and methods:

Population and sampling

The population in this study were conventional farmers whose crops were grown using pesticides; sugar cane farmers from Nakhon Sawan and vegetable farmers from Phitsanulok provinces. Organic farmers who grew organic rice farming from Yasothon province were selected; they were certified organic farming. First morning void urine were collected from 433 conventional and organic farmers at local health promoting hospitals in their areas. Urine samples were placed into a freezer before analysis.

Chemicals

3-Phenoxybenzoic acid 98% (3-PBA), 2-Phenoxybenzoic acid 98% (2-PBA), N,N'-Diisopropylcarbodiimide 99% (DIC), and tert-Butyl-methyl ether anhydrous 99.8% were purchased from Sigma-Aldrich. Cis/trans-DCCA unlabeled 100 µg/mL in CH_3CN; chemical purity (98%) were purchased from Cambridge Isotope Laboratories. 1,1,1,3,3,3-Hexafluoro-2-propanol 99% (HFIP) were purchased from ACROS Organics. Acetonitrile (isocratic grade for liquid chromatography LiChrosolv®) and Isooctane were purchased from Supelco.

Sample preparation and analysis

Urine samples were analyzed following the method of Leng and Gries (11). The calibration curves of cis-DCCA, trans-DCCA, 3-PBA were set up at concentrations ranging from 0-100 ng/mL. The accuracy of 3-PBA, cis-DCCA, and trans-DCCA were ranged from 97.94-105.07%, 97.95-106.95%, and 95.50-104.11%, respectively at the concentrations of 10 and 60 ng/mL with relative standard deviation of less than 2 for 3-PBA and less than 5 for cis- and trans-DCCA. The detection limit of 3-PBA, cis-DCCA and trans-DCCA were 0.5 ng/mL for all metabolites. The creatinine in urine was analyzed (mg/dL) using an enzymatic method with a linear concentration range of 1-500 mg/dL and a detection limit of 0.16 mg/dL (12). All urinary metabolites were creatinine corrected to units of ng/g creatinine and converted to nmol/g creatinine for presentation. The results presented as 3-PBA, cis-DCCA, trans-DCCA, cis,trans-DCCA is cis-DCCA and trans-DCCA, and total cypermethrin is cis,trans-DCCA and 3-PBA.

Statistical analysis

Statistical analysis was performed using SPSS Statistics 18.0. Demographic data between conventional and organic farmers were compared using independent t-test and chi-square test. The geometric mean of urinary cypermethrin metabolites between conventional and organic farmers were compared using independent t-test. Comparison of urinary cypermethrin metabolites between male and female of conventional and organic farmers and comparison of urinary cypermethrin metabolites between conventional and organic farmers classified by sex (male and female) were independent t-test.

Results and discussion:

Study population

Conventional farmers had higher percentages of male (74.2%) than female (25.8%), while percentages of male and female organic farmers were almost the same. The average age of organic farmers was significantly higher than that of conventional farmers (50.10 and 53.22 years) (Table 1). The inclusion criteria required farmers to use pesticides on their own farms. Therefore, the majority of conventional farmers should be men because most of men were performed agricultural tasks such as applying pesticides (13). Organic farmers were older than conventional farmers. These findings are in line with the study of Chouichom. According to Chouichom's research, having more agricultural experience over a longer period of time as well as being older supported shifting to an organic agriculture (14, 15).

Table 1 General characteristics of conventional and organic farmers

Characteristics		Conventional farmers n(%)	Organic farmers n(%)	p-value
Sex	Male	155(74.2)	115(51.3)	<0.001*[1]
	Female	54(25.8)	109(48.7)	
Age	Mean(SD)	50.10(11.1)	53.22(10.3)	0.003*[2]

(1) Chi-square test, (2) Independent t-test

Urinary cypermethrin metabolites

The average urinary cypermethrin metabolites of conventional and organic were 6.01 and 5.12 for 3-PBA, 17.78 and 15.45 for cis-DCCA, 11.15 and 10.03 for trans-DCCA, 30.03 and 26.33 for cis,trans-DCCA, and 37.30 and 32.30 nmol/g creatinine for total cypermethrin. There was no significant difference between two groups (Table 2). The urinary 3-PBA, cis-DCCA, cis,trans-DCCA, and total cypermethrin of female organic farmers were significantly higher than those of male organic farmers. The urinary cis-DCCA of female conventional farmers were significantly higher than those of male conventional farmers (Table 3). The urinary 3-PBA, cis-DCCA, cis,trans-DCCA, and total cypermethrin of male conventional farmers were significantly higher than those of male organic farmers. However, there were no significant difference was observed between female conventional and female organic farmers (Table 4).

Table 2 Comparison of urinary cypermethrin metabolites between conventional and organic farmers.

Cypermethrin metabolites	Conventional farmers (nmol/g creatinine)		Organic farmers (nmol/g creatinine)		p-value[1]
	GM(GSD)	Median	GM(GSD)	Median	
3-PBA	6.01(3.31)	1.86	5.12(3.13)	1.55	0.159
cis-DCCA	17.78(2.46)	2.78	15.45(2.54)	2.52	0.112
trans-DCCA	11.15(2.40)	2.37	10.03(2.48)	2.1	0.219
cis,trans-DCCA	30.03(2.32)	3.28	26.33(2.45)	3.07	0.113
total cypermethrin	37.30(2.36)	3.52	32.30(2.46)	3.28	0.089

(1) Independent t-test

In this study, the urinary cis-DCCA, trans-DCCA and 3-PBA of conventional farmers were in line with the study of Panuwet (16). In Panuwet's study, the geometric mean urinary 3-PBA 5.97 nmol/g creatinine. However, the mean urinary 3-PBA in this study was considerably lower than the Kimata study of pest control operators (116.71 nmol/g creatinine). This is because they applied pyrethroid in indoor with limited ventilation (17).

Our study also reported that organic farmers used pesticides at home which is similar to Qi's study (18). Qi's study measured pyrethroid metabolites among woman in an agricultural area. The median urinary cis-DCCA, trans-DCCA and 3-PBA were 3.49, 9.13, and 7.14 nmol/g creatinine, respectively. Woman in Qi's study didn't expose to pyrethroid occupationally, but Qi's study reported that about half of them had applied indoor insecticides.

Table 3 Comparison of urinary cypermethrin metabolites between male and female of conventional and organic farmers.

Cypermethrin metabolites	GM(GSD) (nmol/g creatinine)		p-value[1]	GM(GSD) (nmol/g creatinine)		p-value[1]
	Conventional farmers			Organic farmers		
	Male	Female		Male	Female	
3-PBA	5.67(3.41)	7.08(3.02)	0.241	3.91(2.97)	6.81(3.11)	<0.001*
cis-DCCA	16.35(2.50)	22.61(2.25)	0.022*	13.13(2.38)	18.35(2.65)	0.007*
trans-DCCA	10.87(2.47)	12.00(2.22)	0.477	8.99(2.41)	11.26(2.54)	0.064
cis,trans-DCCA	28.46(2.36)	35.18(2.19)	0.112	23.02(2.30)	30.34(2.56)	0.019*
total cypermethrin	35.32(2.40)	43.63(2.20)	0.119	27.66(2.29)	38.04(2.56)	0.008*

(1) Independent t-test

Table 4 Comparison of urinary cypermethrin metabolites between conventional and organic farmers classified by sex (male and female).

Cypermethrin metabolites	GM(GSD) (nmol/g creatinine)		p-value[1]	GM(GSD) (nmol/g creatinine)		p-value[1]
	Male			Female		
	Conventional farmers	Organic farmers		Conventional farmers	Organic farmers	
3-PBA	5.67(3.41)	3.91(2.97)	0.010*	7.08(3.02)	6.81(3.11)	0.176
cis-DCCA	16.35(2.50)	13.13(2.38)	0.047*	22.61(2.25)	18.35(2.65)	0.668
trans-DCCA	10.87(2.47)	8.99(2.41)	0.085	12.00(2.22)	11.26(2.54)	0.319
cis,trans-DCCA	28.46(2.36)	23.02(2.30)	0.043*	35.18(2.19)	30.34(2.56)	0.837
total cypermethrin	35.32(2.40)	27.66(2.29)	0.021*	43.63(2.20)	38.04(2.56)	0.358

(1) Independent t-test

Male and female conventional farmers were occupationally exposed to high levels of cypermethrin use in farms (19). The reason that female conventional farmers had higher urinary cis-DCCA than male may be due to less awareness on using pesticide. The study of Chetna et al. found that female didn't read and understand pesticide labels (20). Different working activities between males and females may result in higher exposure to females as males operate machine while females tend to harvest (21). Organic farmers only exposed to cypermethrin used at home. Females may be responsible for cleaning the house and home insecticide may be used to control insects (18), resulting in higher urinary cypermethrin metabolites than males. Male conventional farmers were occupationally exposed to cypermethrin cause them to exposed to higher levels of cypermethrin than male organic farmers. However, our study found that urinary cypermethrin metabolites of female conventional farmers and female organic farmers closed to each other. These findings supported the reason that female organic farmers used home insecticide cause them exposed to high levels of cypermethrin as well as female conventional farmers that exposed to cypermethrin occupationally.

Conclusion:

This study compares the urinary cypermethrin metabolites of conventional and organic farmers. All urinary cypermethrin metabolites of conventional farmers were higher than organic farmers but didn't reach the significant difference. However, this study found that urinary cypermethrin metabolites of organic farmers were also high due to the use of home insecticides. Based on the results, the study provided suggestion that more research should be done to get a complete view of conventional and organic farmers' exposure to cypermethrin insecticide.

References:

1. Laohaudomchok W, Nankongnab N, Siriruttanapruk S, Klaimala P, Lianchamroon W, Ousap P, et al. Pesticide use in Thailand: Current situation, health risks, and gaps in research and policy. Human and Ecological Risk Assessment: An International Journal. 2020;27(5):1147-69.
2. center ITC. Farmer's Registration and Improvement Manual 2018: Department of Agriculture Extension, Ministry of Agriculture and Cooperatives; 2018 [Available from: http://farmer.doae.go.th/farmer61.pdf.
3. Singleton ST, Lein PJ, Farahat FM, Farahat T, Bonner MR, Knaak JB, et al. Characterization of α-cypermethrin exposure in Egyptian agricultural workers. Int J Hyg Environ Health. 2014;217(4-5):538-45.
4. Control BoPaAM. Top 10 Agricultural Hazardous Substances Imports in 2020 by Volume: Department of Agriculture, Ministry of Agriculture and Cooperatives; 2020 [Available from: https://www.doa.go.th.
5. Leng G, Kühn K-H, Idel H. Biological monitoring of pyrethroids in blood and pyrethroid metabolites in urine: applications and limitations. Science of The Total Environment. 1997;199(1):173-81.
6. Bao W, Liu B, Simonsen DW, Lehmler HJ. Association Between Exposure to Pyrethroid Insecticides and Risk of All-Cause and Cause-Specific Mortality in the General US Adult Population. JAMA Intern Med. 2020;180(3):367-74.
7. Diggle P HP, Liang K, Zeger S. Analysis of longitudinal data. 2nd ed. United Kingdom: Oxford University Press2002.
8. Wang J, Zhu Y, Cai X, Yu J, Yang X, Cheng J. Abnormal glucose regulation in pyrethroid pesticide factory workers. Chemosphere. 2011;82(7):1080-2.
9. Shelton JF, Geraghty EM, Tancredi DJ, Delwiche LD, Schmidt RJ, Ritz B, et al. Neurodevelopmental Disorders and Prenatal Residential Proximity to Agricultural Pesticides: The CHARGE Study. Environmental Health Perspectives. 2014;122(10):1103-9.
10. Lifeng T, Shoulin W, Junmin J, Xuezhao S, Yannan L, Qianli W, et al. Effects of fenvalerate exposure on semen quality among occupational workers. Contraception. 2006;73(1): 92-6.
11. Leng G, Gries W. Determination of Pyrethroids in Blood Plasma and Pyrethroid/Pyrethrin Metabolites in Urine by Gas Chromatography-Mass Spectrometry and High-Resolution GC-MS. 192006. p. 17-33.
12. Coulter B. Instruction for Use. Creatinine. [Available from: https://www.beckmancoulter.com/wsrportal/techdocs?docname=/cis/A69463/%%/EN.

13. Mahaboonpeeti R, Kongtip P, Nankongnab N, Tipayamongkholgul M, Bunngamchairat A, Yoosook W, et al. Evaluation of Dermal Exposure to the Herbicide Alachlor Among Vegetable Farmers in Thailand. Annals of Work Exposures and Health. 2018;62(9):1147-58.
14. Chouichom S, Yamao M, editors. Comparing opinions and attitudes of organic and non-organic farmers towards organic rice farming system in north-eastern Thailand2010.
15. Kings D, Ilbery B. Farmers Attitudes Towards Organic and Conventional Agriculture: A Behavioural Perspective. 2012.
16. Panuwet P, Prapamontol T, Chantara S, Thavornyuthikarn P, Montesano MA, Whitehead RD, et al. Concentrations of urinary pesticide metabolites in small-scale farmers in Chiang Mai Province, Thailand. Science of The Total Environment. 2008;407(1):655-68.
17. Kimata A, Kondo T, Ueyama J, Yamamoto K, Yoshitake J, Takagi K, et al. Comparison of urinary concentrations of 3-phenoxybenzoic acid among general residents in rural and suburban areas and employees of pest control firms. Int Arch Occup Environ Health. 2009;82(10):1173-8.
18. Qi X, Zheng M, Wu C, Wang G, Feng C, Zhou Z. Urinary pyrethroid metabolites among pregnant women in an agricultural area of the Province of Jiangsu, China. Int J Hyg Environ Health. 2012;215(5):487-95.
19. Hernández-Valero MA, Bondy ML, Spitz MR, Zahm SH. Evaluation of Mexican American migrant farmworker work practices and organochlorine pesticide metabolites. Am J Ind Med. 2001;40(5):554-60.
20. Chetna D, Vaibhav K, Pallavi N, Jitendra R. Gender differences in knowledge, attitude and practices regarding the pesticide use among farm workers: A questionnaire based study. Research Journal of Pharmaceutical, Biological and Chemical Sciences. 2012;3:632-9.
21. Kasner EJ, Keralis JM, Mehler L, Beckman J, Bonnar-Prado J, Lee SJ, et al. Gender differences in acute pesticide-related illnesses and injuries among farmworkers in the United States, 1998-2007. Am J Ind Med. 2012;55(7):571-83.

INFLUENCE OF ODOR HEDONIC TONE ON ANNOYANCE AND COMPLAINT INTENTION OF RESIDENTS IN BANGKOK METROPOLITAN AREA

A. Soonthornsaratoon[a, c], N. Aimyong[b, c*], W. Patthanaissaranukool[a, c] and T. Sihabut[a, c*]

[a]Department of Environmental Health Sciences, Faculty of Public Health, Mahidol University
[b]Department of Epidemiology, Faculty of Public Health, Mahidol University, Bangkok 10400 Thailand
[c]Center of Excellence on Environmental Health and Toxicology (EHT), OPS, MHESI, Thailand,
**Corresponding Author: tanasri.sih@mahidol.com*

Abstract:

This research aimed to explore the role of odor hedonic tone on annoyance and complaint intention of residents in Bangkok Metropolitan Area. To carry out the study, four scales of odor intensity (light, moderate, strong, very strong) and five scales of annoyance (not at all annoyed, slightly annoyed, moderately annoyed, very annoyed and extremely annoyed) were rated and the intentions on odor complaint were decided by 133 residents living nearby 46 businesses. To analyze data, the influences of odor intensity with three different hedonic tones, i.e., offensive, unpleasant and pleasant/ neutral concerning respondents' annoyance and complaint intentions were described by frequency and percentage. The result showed that the stronger the intensity, the higher the percentage of highly annoyed (% HA) and the percentage of complaint numbers. At low intensity, %HA and the percentage of complaint numbers from offensive and unpleasant odors were higher than those from neutral/ pleasant odors. However, at higher intensity, the respondents intended to make a complaint, no matter what the odor tone was.

Keywords: Odor, hedonic tone, odor intensity, annoyance, complaint

Introduction:

Although the Thailand 4. 0 policy has driven a great development success for the Thai economy, a lack of careful management planning has resulted in serious environmental health problems in many areas including Bangkok. As a center of economic hub and trade, approximately 6 million registered population and more than 2 million latent population have resided in this small area where more than 30,000 businesses are located [1-2]. Unavoidably, public nuisance including noise, vibration, odor, heat, smoke, dust and so on have been reported. As a result, complaints received by the Bangkok Metropolitan Administration were up to 15,154 times in 2020 making Bangkok the top-ranked area with nuisance problems in Thailand. Among these, odor was in the top three most complained problems [3].

To investigate odor complaint, the inspectors need to use their own discretion to determine whether the complaint constitutes a statutory nuisance. However, confusion concerning the decision making process often occurs because of subjective feeling of residents regarding odor hedonic tone. For example, Japanese were able to accept fishy smells but Germans did not [4]. Consequently, this research was carried out to assess the role of odor hedonic tone on annoyance and complaint intention of residents in Bangkok. This finding can be used as supportive evidence for nuisance determination.

Materials and methods:

A total of 46 businesses in Bangkok reporting complaints from January to August 2022 was selected as study sites and their odor characteristics were classified in three groups, i.e., neutral/pleasant, unpleasant and offensive as shown in Table 1. All houses located within the radius of odor plumes were included and 133 house representatives, aged between 18 and 70 years, presenting no respiratory diseases and residing in the area at least one year, were asked for their perceptions concerning exposure intensity, i.e., light- barely noticeable, moderate- easily detected but without affecting daily activities, strong- effect on health and/or daily activities and very strong-unable to stay at home. Additionally, five scales of annoyance level, i.e, not at all annoyed, slightly annoyed, moderately annoyed, very annoyed and extremely annoyed were verbally rated and complaint intention on perceived odor was decided by these subjects. To report data, the amounts of complaint intention at each odor intensity and the percentage of highly annoyed (%HA), combined from the number of respondents who felt very and extremely annoyed, were descriptively explained.

Table 1 Odor characteristics and their hedonic tone

Hedonic tone	Odor characteristic
Neutral/Pleasant	burnt charcoal, boiled herbs, garlic, perfume, stench, basil, tea leaves
Unpleasant	car exhaust, petroleum, ammonia, chlorine, thinner, paint, alcohol, rubber, glue, grease, sour, burnt metal
Offensive	putrid, burnt plastic, fermented fish, fishy

Results and discussion:

In this study, odor from 46 businesses with 23 odor characteristics were divided in three groups, i.e. neutral (15%), unpleasant (65%) and offensive (20%). In general, some people started to complain at the light level and the stronger the intensity, the greater the percentage of complaint intention. Among these, more than one half of the residents exposed to moderate and strong odors tended to complain. The result was unanimous when the odor was very strong as shown in Figure 1.

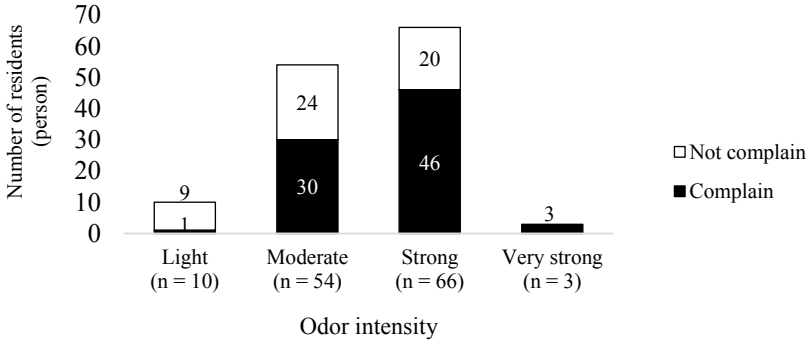

Figure 1 Complaint intentions from odor exposure at each intensity (n = 133)

To understand the role of hedonic tone, the complaint intentions from various groups of odor tone, i.e., neutral/pleasant, unpleasant and offensive were compared as shown in Figure 2(A)-(C). Although only small amounts of samples were observed during the study period, these figures obviously implied that offensive odors had the greatest impact on complaint intention, followed by unpleasant and neutral/ pleasant odors, respectively. For instance, no one intended to complain about the neutral/ pleasant odors at light level but there was a complaint about an unpleasant odor at the same level. Unfortunately, we could not collect data from residents exposed to offensive odors at this intensity. However, at moderate and strong levels, the influence of offensive odors on complaint intention was dominant.

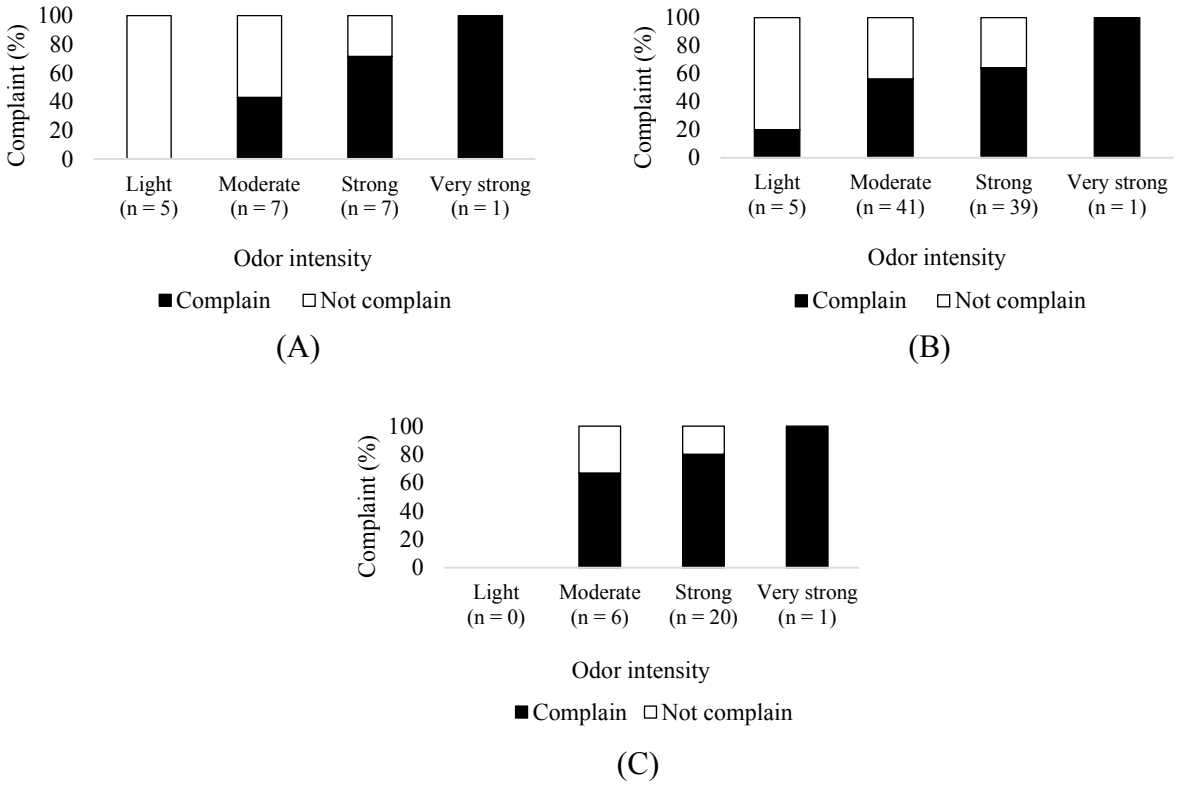

Figure 2 Complaint intentions on odor with different hedonic tones
(A) neutral/pleasant, (B) unpleasant and (C) offensive

Corresponding to complaint intention, the degree of resident's annoyance increased when the odor intensity was stronger, as shown in Figure 3. At light intensity, %HA from unpleasant odors was obviously greater than the one from neutral/ pleasant odors. However, when the intensity was stronger, % HA from all kinds of hedonic tone became closer. This result was similar to that of a study of Hirunrueng et al. (2020) reporting that offensive smells urged Thais to complain at low concentration, in contrast to fishy smells [5]. Similarly, Sucker et al. (2008) showed that neutral and unpleasant odors made residents living close to the study sites feel annoyed but pleasant odors hardly induced annoyance [6].

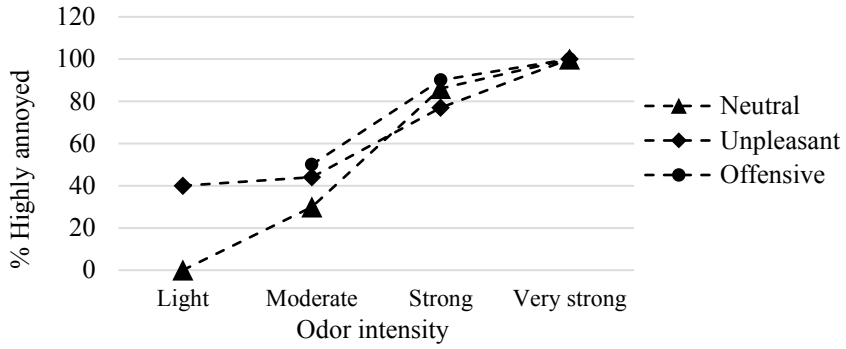

Figure 3 Percentage of highly annoyed (%HA) from odor with different hedonic tones

Conclusion:

Odor with offensive and unpleasant tones at low intensity obviously played a significant role on complaint intention. In contrast, the impact of odors with neutral/ pleasant tone at this level was negligible. At higher intensity, the residents tended to feel more annoyed and decided to complain no matter what the odor tone was.

Acknowledgement:

The authors would like to thank the staff of Environmental Sanitation Section, Health Department, Bangkok Metropolitan Administration for cooperating on data collection.

References:

1. Department of Provincial Administration, Ministry of Interior. Notification of Central Registration Bureau RE: Numbers of registered population in the kingdom according to civil registration record on December 31, 2019 [internet]. 2019 [cited 2022 Aug 24]. Available from: http://www.ratchakitcha.soc.go.th/DATA/PDF/2563/E/024/T_0017.PDF [in Thai]
2. National statistical office. Summary of latent population in Thailand in 2019 [internet]. 2019 [cited 2022 Aug 24]. Available from: http://www.nso.go.th/sites/2014/DocLib13/Social/Demographics/Latent_population./2562/Population_62.pdf [in Thai]
3. Health Department, Bangkok Metropolitan Administration. Nuisance statistics in Bangkok for fiscal year 2020 (October 2019 – September 2020) [internet]. 2020 [cited 2022 Aug 24]. Available from: https://webportal.bangkok.go.th/upload/user/00000101/image/Report/ReportDOH63/08-ReportDOH2563(P107-108).pdf [in Thai]
4. Ayabe-Kanamura S, Schicker I, Laska M, Hudson R, Distel H, Kobayakawa T, Saito S. Differences in perception of everyday odors: a Japanese-German cross-cultural study. Chem. Senses. 1998;23:31-38.
5. Hirunrueng T, Patthanaissarnukool W, Sihabut T. Odor intolerance and proposed off-site limit. J. Health Res. 2022;36:37-45
6. Sucker K, Both R, Bischoff M, Guski R, Kramer U, Winneke G. Odor frequency and odor annoyance Part II: dose-response associations and their modification by hedonic tone. Int. Arch. Occup. Environ. Health. 2008;81:683-94.

LEVELS AND RISK ASSESSMENT FOR INDOOR AIR QUALITY AMONG WORKERS IN CARD PRODUCTION DEPARTMENT: A CASE STUDY OF PRINTING INDUSTRY

Salilla Phuangchong[1], Chate Jaikanlaya[2,3], Withida Patthanaissaranukool[2,3], and Thanakrit Neamhom[2,3,*]

[1]Master of Science Program in Environmental Health, Faculty of Public Health, Mahidol University, Rajvithi Road, Bangkok, 10400, Thailand
[2]Department of Environmental Health Sciences, Faculty of Public Health, Mahidol University, Rajvithi Road, Bangkok, 10400, Thailand
[3]Center of Excellence on Environmental Health and Toxicology (EHT), OPS, Ministry of Higher Education, Science, Research and Innovation, Thailand

Abstract:

This study aimed to investigate the amount and health risk from indoor air pollutants including benzene and toluene exposure among workers in card production department of printing industry, so as to find the relationship among these pollutants using a statistical model. This study was conducted in the year 2022. The workplace pollution data were acquired from the annual environmental quality measurement reports during the year 2017 to 2021. A questionnaire was mentioned to obtain the personal information of the workers. Average concentration of benzene and toluene were found at 0.11 ± 0.10 and 4.12 ± 3.52 ppm, respectively. Health risk assessments regarding exposure among 45 workers to these pollutants were at no risk for non-carcinogenic risk (HI of 7.54E-03 and 3.17E-02 for benzene and toluene, respectively) and in the negligible level of carcinogenic risk for benzene (4.54E-06). A multiple linear regression model was used to create the predictive equation. The results verified that toluene concentration could be estimated under known benzene with the R^2 and Durbin-Watson values of 0.12 and 1.914, respectively. These findings could help provide the possibility to estimate a non-monitoring value in terms of the available data.

Keywords: Benzene, toluene, printing industry, health risk assessment, linear regression

Introduction:

Printing industry is one of a major industry in Thailand as they can lead the important message to the customer [1]. Presently, along with the printing process, they can emit pollutants from the reaction from inkjet drum burning process which may affects to workers health [2]. For card production department, they offer the printing activities on plastic cards including ID cards, credit cards, debit cards, ATM cards and merchant membership cards. Many kinds of wastes and/or by-products generated from the production process including the mixture color, thinner, ink, and organic solvents [3]. Based on the growing concern to the indoor air quality, pollutants from these processes were determined and reported the link to human health [2,4]. The degree of intoxication depends on the type and concentration of the pollutant. If taken in high concentrations, it may cause death or cause bodily changes.

Therefore, the objectives of this study were (1) to determine the concentration and index of health risk from exposure of benzene and toluene in card production department in printing industry, and (2) to investigate their relationships using the multiple logistic regression analysis. The study site was a printing industry in the Bangkok Metropolitans Administration area (BMA) in Thailand. The result could help organizations or inspectors provide possible ways to understand the current situation and estimate a non-monitoring value in terms of data available.

Materials and Methods:

Workplace pollutions data

The data of indoor air pollutants including both benzene, toluene, temperature, and humidity in this study were gathered from an annual environmental quality measurement in the year 2017 to 2021 from the selected printing industry as the source of secondary data.

Questionnaire design

To determine the degree of risk among workers in card production department (CPD), the details of personal and working behaviors were collected using a questionnaire. The study was conducted during April to July in 2022 in a printing industry in Thailand. The questionnaire was divided into two sections as follows: (1) personal characteristics including gender, age and body weight, and (2) work characteristics including department, position, work experience and hours of work each day. The inclusion criteria of the survey respondents were all employees working in card production department and have work experience of five years or more. The 45 participants were enrolled. This study was approved by the Ethics Committee for Research Involving Human Subjects (No. 2022-049) before collecting field data. Subjects provided written consent after being informed of the objectives of the study and procedures.

Health risk assessment

Human health risk assessment is the process to evaluate the probability of adverse health effects from contaminated environment exposure. It includes four basic steps including hazard identification, regarding dose-response assessment, exposure assessment, and risk characterization. The exposure was assessed by determining how much pollutants affected human health, and chronic daily intake (CDI) was evaluated using equation (1). For the last step of assessment, the hazard quotient (HQ) calculated following equation (2). To estimate the senses of control, HQ < 1 refers to the non-hazard level, 0.1 to 1.0 refers to low risk level, 1.1 to 10 refers to moderate hazard level, and HQ > 10 refers to high risk level. For carcinogenic risk, risk index was computed using equation (3). The value over than 10^{-6} refers to an acceptable level, 10^{-5} refers to moderate risk and less than 10^{-4} refers to unacceptable risk.

$$CDI = \frac{C \times IR \times ET \times EF \times ED}{BW \times AT} \quad (1)$$

$$HQ = \frac{CDI}{RfC} \quad (2)$$

$$Risk = CDI \times SF \quad (3)$$

Regression model

The statistical model was mentioned in this study to determine the relationship among benzene and toluene in terms of their quantity. Multivariate linear regression (MLR) is based on the approximate linear relationship between an independent variable and a dependent variable which is fitted to predict the linear equation [5]. MLR can be proposed according to equation (4).

$$y = b_0 + b_1 x_{1i} + b_2 x_{2i} + ... + b_k x_{ki} + \varepsilon \quad (4)$$

Where b_k is the regression coefficients, x_k is the explanatory variables, I is an constancy integer (1, 2, … k), and ε is stochastic error associated with the regression. After the regression equation is established, the model's ability to predict is determined; the testing methods needed include standard deviation and correlation coefficient (r) tests. Only when r is close to 1, can it describe the relationship between y and x using a linear regression model. The results were also further checked for first-order autocorrelation problem by Durbin-Watson statistic test. If a value of 2.0 means, there is no autocorrelation detected in the sample. Values in a range from zero to 2.0 indicate positive autocorrelation and values from 2.0 to 4.0 indicate negative autocorrelation. All statistical analysis were completed using the Statistical Product and Service Solution (SPSS, Version 18.0, SPSS Ltd., USA).

Results and discussions:

Concentration of pollutants in card production department

As shown in Figure 1, the concentration of benzene during the year 2017 to 2021 were 0.05, 0.03, 0.24, 0.21 and 0.01 ppm., respectively while for toluene were found at 3.08, 1.93, 7.06, 8.46 and 0.08 ppm., respectively. Notably, during the COVID-19 pandemic situation, the printing industry has down the product capacity, which affected to the lower emissions concentration compared to the previous years.

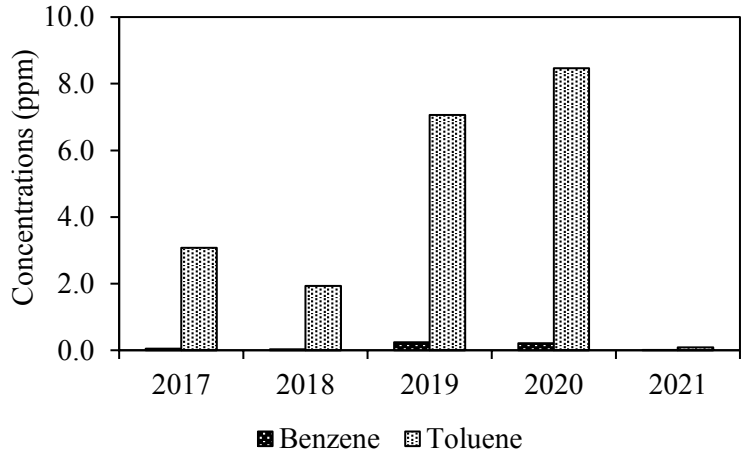

Figure 1 Concentration of pollutants in Card Production Department.

Personal Information

The personal information of the participants was collected using a self-administered questionnaire. Forty-five individuals responded to the survey. The sample included more males (73.3%) than females (26.7%). The mean age was 41.2 years (SD=6.3). Among them, most were between 40 to 50 years. Their average weight was found at 67.6 ± 14.5 kg. The frequent working hour daily and working experience were 8 hour (93.3%) and 5 -14 years, respectively. The demographic characteristics of the sample is presented in Table 1.

Table 1 Personal Information of Card Production Department

Personal Information	Detail	n	%
Sex	Male	33	73.3
	Female	12	26.7
Age	20-29 Years	3	6.7
	30-39 Years	15	33.3
	40-49 Years	24	53.3
	50-59 Years	3	6.7
	Mean ± S.D (min. – max.)	-	41.2 ± 6.3 (29.0-59.0)
Weight	Mean ± S.D (min. – max.)	-	67.6 ± 14.5 (48.0-112.0)
Working Hour	< 8	42	93.3
	≥ 8	3	6.7
	Mean ± S.D (min. – max.)	-	7.3 ± 0.3 (7.0-8.5)
Working Experience	5-14 Years	14	31.1
	15-24 Years	27	60.0
	25-34 Years	4	8.9
	35-44 Years	-	-
	Mean ± S.D (min. – max.)	-	16.6 ± 6.6 (5.0-33.0)

Health Risk Assessment

From the results of calculations with mathematical equations to find the number of pollutions workers received per day, as shown in Table 2, it was found that an average daily dose (ADD) of benzene were equal to 3.02E-04, 8.22E-15 and 2.03E-07 from the exposure route of ingestion, dermal and inhalation, respectively. Whereas that of toluene were 2.54E-03, 6.75E-14 and 3.78E-06, respectively. Table 3 shows the non-carcinogenic risk value (HQ and HI) among the workers and found that values of HQ for benzene and toluene was less than 1 (7.54E-03 and 3.17E-02 for ingestion of benzene and toluene, respectively, while 1.48E-05 and 2.57E-07 for inhalation route). In addition, HI values for both benzene and toluene were finally less than 1, it could be summarized that there is no risk to non-carcinogenic risk.

Results from carcinogenic risk (CR) calculation presents in Table 4. It was found only the risk from benzene as the carcinogenic agent of 4.53E-06 and 1.29E-08 from ingestion and inhalation routes, respectively. A valuable total risk of benzene was equal to 4.54E-06. Compare with the recommendation from US. EPA [6], it was found that CR more than 1×10^{-6} that can be implied as in a no risk to carcinogenic effect.

Table 2 Average Daily Dose (ADD) of benzene and toluene in CPD

Pollutants	ADD (mg/kg-day)		
	Ingestion	Dermal	Inhalation
Benzene (Mean ± S.D.)	3.02E-04 ± 1.35E-04	8.22E-15 ± 3.76E-15	2.03E-07 ± 4.44E-07
Toluene (Mean ± S.D.)	2.54E-03 ± 2.45E-03	6.75E-14 ± 6.50E-14	3.78E-06 ± 3.66E-06

Table 3 Non-Carcinogenic risk level of benzene and toluene in CPD

Pollutants	Non-Carcinogenic risk		HI
	HQ_{ing}	HQ_{inh}	
Benzene (Mean ± S.D.)	7.54E-03 ± 3.37E-02	1.48E-05 ± 6.76E-06	7.54E-03 ± 3.37E-02
Toluene (Mean ± S.D.)	3.17E-02 ± 3.07E-02	2.57E-07 ± 7.32E-07	3.17E-02 ± 3.07E-03

* ing means ingestion route of exposure, inh means inhalation route of exposure

Table 4 Carcinogenic risk level of benzene in Card Production Department

Pollutant	Carcinogenic risk		$Risk_{total}$
	$Risk_{ing}$	$Risk_{inh}$	
Benzene (Mean ± S.D.)	4.53E-06 ± 2.02E-06	1.29E-08 ± 5.88E-09	4.54E-06 ± 2.03E-06

Predictive equations for benzene and toluene

Multivariate linear regression (MLR) modeling was mentioned to find the relationships among the two pollutants (benzene and toluene) in the CPD. Using the environmental quality measurement data from year 2017 to 2022 (5 years recorded), the model input variables were the concentrations of benzene and toluene. Notably, other variables including relative humidity, temperature, wind speed, and speed of air exchange were not included in this study. Results of MLR analysis to predict benzene and toluene are summarized in Table 5. Both equations generated provided the R^2 value of 0.12. Thus, approximately 12% of variation in the benzene and toluene concentrations could be explained by independent variables of benzene and toluene. The coefficients of the all regressions were highly significant (P value <0.05). Moreover, the linear graphs of the contribution of toluene and benzene concentrations and benzene to toluene were plotted in Figure 2(a) and (b), respectively. The output revealed an unsatisfied distribution of values corresponding to the reported Durbin-Watson's values of 0.801 and 1.914. When the value of Durbin-Watson test statistics is close to 2, it indicates that the assumption is satisfied [7]. Between two equations generated, the toluene prediction using value of benzene provided the higher Durbin-Watson value and close to 2, hence, it could be said that the later equation can help provide the possibility to estimate a non-monitoring (toluene value) in terms of the available data (benzene value).

Table 5 Predictive results of indoor air pollutant with CARD Production department

Pollutant	Equation	R^2	Durbin-Watson
Benzene	Benzene = -0.56(Toluene)+0.646	0.12	0.801
Toluene	Toluene = -2.136(Benzene)+3.846	0.12	1.914

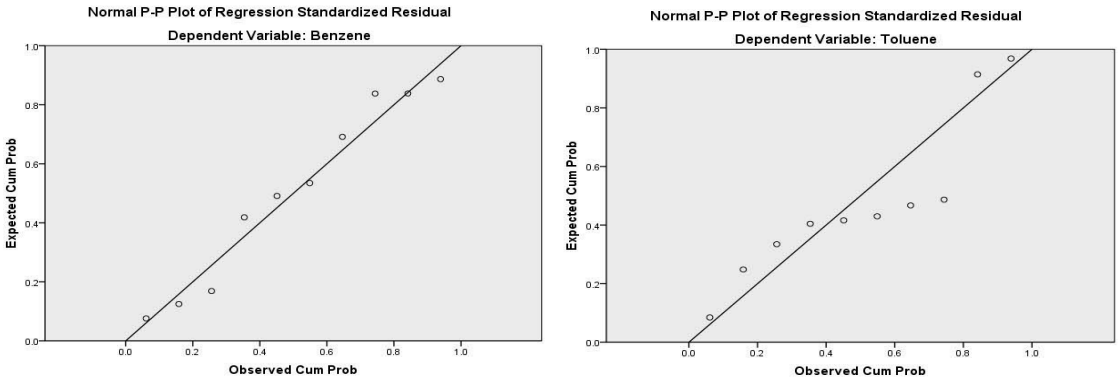

(a) (b)

Figure 2 Contribution of benzene and toluene to benzene and toluene concentration; (a) Contribution of toluene to benzene (b) Contribution of benzene to toluene

Conclusion:

Due to unsafe working environment from air pollutants (benzene and toluene) occurred in the production process, the workers in card production department (CPD) have the chance to exposure to these pollutants. From this study, it was found that workers have daily dose of benzene at 3.02E-04, 8.22E-15 and 2.03E-07 from ingestion, dermal, and inhalation, respectively. The daily dose of toluene was found at 2.54E-03, 6.75E-14 and 3.78E-06 from ingestion, dermal, and inhalation, respectively. From the results of calculations to find non-carcinogenic risk, it was found HQ of benzene was equal to 7.54E-03 and 1.48E-05 from ingestion and inhalation routes, respectively while HQ values for toluene was 3.17E-02 and 2.57E-07 from ingestion and inhalation, respectively. A HI value of benzene and toluene was 7.54E-03 and 3.17E-02, respectively. It can be implied that there is no risk to non-carcinogenic risk. Moreover, from the results of carcinogenic risk calculations, it was found that the risk of benzene was 4.53E-06 and 1.29E-08 from ingestion and inhalation, respectively, resulting in the total risk of benzene at 4.54E-06. When compared this risk value with the level based on the US. EPA recommends, the CR in this study was more than 1×10^{-6}, that there is no risk to carcinogenic effect. Further analysis was conducted to determine the relationship equations for benzene and toluene. The outcomes provided the proportion of variations in benzene and toluene concentration as explained by both levels of benzene and toluene with the R^2 value of 0.12 and Durbin-Watson's value of 0.801 and 1.914.

References:

1. Amornphon Changsuphan. (2003). Hazards from organic vapors in the working area of the printing house. *Journal of the Department of Science service,* 53(174), 14-18.
2. Kiurski, Jelena S., Marić, Branislav B., Aksentijević, Snežana M., Oros, Ivana B., Kecić, Vesna S. & Kovacˇević, Ilija M. (2013). *Indoor air quality investigation from screen printing industry*, Renewable and Sustainable Energy Reviews, Elsevier, vol. 28(C), pages 224-231.
3. Ukai H., Takada S., Inui S., Imai Y., Kawai T., Shimbo S. & Ikeda M. (1994). Occupational exposure to solvent mixtures: effects on health and metabolism. *Occupational and Environmental Medicine*, 51, 523-529. Pollution control department ministry of science technology and the environment. (2002). *Benzene (2nd edition)*. Hazardous substances information center division and convention on hazardous substances and waste management division: Idea Square Company Limited.

4. Irga, P.J., & Torpy, F.R. (2016). Indoor air pollutants in occupational buildings in a sub-tropical climate: Comparison among ventilation types. *Building and Environment*, 98, 190-199.

5. Yang, Y., Sun, L., & Guo, C. (2018). Aero-material consumption prediction based on linear regression model. *Procedia Computer Science*, 131, 825–831. https://doi.org/10.1016/j.procs.2018.04.271

6. U.S. Environmental Protection Agency. (1998) Guidelines for Ecological Risk Assessment: Environmental Research Laboratory, U.S. Environmental Protection Agency. EPA/630/R-95/002F.

7. Elbayoumi, M., Ramli, N. A., & Yusof, N. F. F. M. (2015). Development and comparison of regression models and feedforward backpropagation neural network models to predict seasonal indoor PM2.5–10 and PM2.5 concentrations in naturally ventilated schools. *Atmospheric Pollution Research*, 6(6), 1013–1023. doi:10.1016/j.apr.2015.09.001

THE CURRENT STATUS OF CONSUMPTION AND DISPOSAL OF HOUSEHOLD BEVERAGE CARTONS IN BANGKOK, THAILAND

Potchanun Leelaviroj[1,2], Suphaphat Kwonpongsagoon[1,2*], Manaporn Wongsoonthornchai[3], Nantamol Limphitakphong[4], and Kanokwan Kingphadung[5]

[1]Department of Sanitary Engineering, Faculty of Public Health, Mahidol University, Thailand
[2]Center of Excellence on Environmental Health and Toxicology (EHT), OPS, MHESI, Thailand
[3]Faculty of Public Health, Thammasat University, Pathumthani, Thailand
[4]Environmental Research Institute, Chulalongkorn University, Thailand
[5]Department of Food Technology, Faculty of Engineering and Industrial Technology, Silpakorn University, Thailand
[*]Corresponding author: suphaphat.kwo@mahidol.ac.th

Abstract:

This study aimed to investigate the characterization and composition of packaging wastes and beverage cartons in household waste in Bangkok, Thailand. The study was conducted by a questionnaire survey and waste composition sampling in 86 households between April and July 2022. The results from this study showed that among the samples, the largest proportion of household waste in Bangkok was food waste (49%), followed by general waste (38%), and packaging waste (13%). With regard to packaging wastes, 50% of households did not sort out their packaging wastes whereas 28% separated and gave them to the Bangkok waste collection system, general waste pickers (called "Saleng" in Thai), and office housekeepers for further process. The remaining 22% separated packaging wastes and intentionally sold them to Saleng and waste dealers (waste buying-selling shops). Of the samples, there were 45 households consumed and disposed of beverage cartons, accounting for 52%. The amount of beverage carton waste was estimated at 1% of the total household waste and accounted for 3.7% of the total packaging waste. It was also calculated that the average consumption and disposal of used beverage cartons is 0.12 g per household per day, and 0.04 g per person per day for household waste in Bangkok. The results can provide a current overview of the consumption and disposal of household packaging wastes, particularly beverage cartons in Bangkok, serving as baseline data to find ways to manage them in the future.

Keywords: Consumption, disposal, beverage cartons, households, Bangkok

Introduction:

Packaging is a basic necessity that comes with every product. The product cannot be stored or moved from one location to another without packaging. Packaging is generally used for fulfilling various functions including the containment, protection, storage, and transport of the product, and marketing function to provide information on product ingredients, barcodes, and even disposal notices often impacting consumers' purchasing decisions [1]. In food and beverage industries, the packaging helps prevent waste and ensures that the food retains its desired quality throughout its shelf life and product delivery to consumers. Thailand is a huge and potential packaging market due to the country's large population and the continuous growth of consumer goods industries such as ready meals, beverages, cosmetics, and daily-use products. This caused the demand for packaging product consumption to increase accordingly. The packaging industry can be categorized into 4 major types: glass, paper, plastic, and metal

packaging. According to the statistics of production and domestic sale of packaging between 2012 and 2021 reported by the Thailand Office of Industrial Economics, there is expected to be an increasing trend in the domestic distribution of all types of packaging in the future. On average over the past 10 years, paper packaging has the largest market share, accounting for 40% of all packaging types, followed by glass packaging 31%, plastic packaging 20%, and metal packaging 9% [2]. Beverage carton, both UHT and pasteurized is generally categorized as paper-based packaging.

After consumption, packaging becomes a major part of the household waste and total waste stream. Most are single-use such as food wrappers, which has created a waste problem that currently pollutes all localities, countries, and around the world [3]. With changing consumerism and market shifts, packaging industries have to innovate; a dynamic shift from heavy traditional glass bottles to lighter plastic containers and to even lighter composite beverage cartons to package liquid beverages [4]. Beverage cartons are lightweight, strong, food-safe packages that protect freshness, flavors, and nutritional qualities and are a popular packaging material to fill long-life liquid products that offer extended shelf life for ambient temperatures or under refrigerated conditions, thereby enabling extended shelf-lives for consumer beverages. Of the two types of cartons, aseptic cartons/UHT cartons contain 5% aluminum along with 75% paperboard and 20% polyethylene, whereas the chilled/pasteurized cartons contain only 20% polyethylene and 80% paper [5].

Beverage cartons are classic examples of linear consumption, used for single-use commodities. Once the product is consumed, these packaging materials are discarded and become a significant proportion of municipal solid waste. The beverage carton is a multi-layer composite packaging, made of different materials, mainly paper. It is one of the poorly characterized waste streams in Thailand and particularly challenging to recycle due to its complex makeup and a separate collection and recycling of beverage cartons are hardly in place [1]. Currently, Thailand has no available baseline data on beverage carton production, consumption, collection, and recycling throughout the supply chain, including disposal and waste management, except the waste composition report in 2002 by the Pollution Control Department [6].

The aim of this study was to examine the current state of consumption and disposal of household beverage cartons which are improperly managed and may increase risks to the environment in terms of a large amount of waste going to landfills and greenhouse gas emissions, by analyzing the characterization and composition of packaging wastes and used beverage cartons in household waste in Bangkok, Thailand. The result is expected to serve as baseline data for household beverage cartons for bringing about future collection and recycling targets and policy directions.

Methodology:

Study area: the study was carried out in Bangkok, the capital and most populous city of Thailand. The area of the city covers 156,870 ha located in central Thailand and is divided into 50 districts. In 2021, the total population of Bangkok was estimated at approximately 10.7 million, with around 5.5 million registered inhabitants, living in 3.1 million households [7, 8]. The average population density per household is about 3.4 people.

Data collection: A questionnaire survey and waste composition sampling were conducted between April 11 and July 18, 2022, investigating general related information, household waste composition, and management from residents living in 86 households in Bangkok. Three main categories of household waste involving food waste, general waste, and packaging waste e.g., plastic, metal, glass, paper, and especially beverage carton containers were all analyzed in this study.

The questionnaire consists of two main sections covering a range of questions and requests for participants. Section 1 asked about general related information including the type of accommodation, period of residence, number of household members, occupation, and household waste management methods such as disposal of all wastes in the same bin, or segregation for sales or for giving away to others for further process. In section 2, participants were asked to record the amount of food and general waste for a week using our digital scales. In addition, participants were asked to sort out their six packaging waste types in one separate bag for a week and give it to the researchers for further physical composition analysis. The six used packaging targets include 1) glass bottles for food and beverage; 2) plastics containers e.g., PET bottles, other plastic bottles (PP, HDPE), multilayer plastic bags, plastic containers/trays, plastic cups, and other plastic wastes; 3) metal e.g., aluminum and iron cans; 4) paper containers e.g., cardboard and, corrugated boxes; 5) beverage cartons for milk, flavored and fermented milk, juice, cereal milk, and coconut milk, etc.; and 6) other packaging wastes e.g., instant noodle cups, and Styrofoam containers.

Analysis of household waste composition:

Each household waste type's physical composition was calculated as a percentage using the following formula.

$$C_x = \frac{W_x}{W_t} \times 100\% \qquad \text{---------- (1)}$$

Where: C_x = Percentage of each waste type (%)
W_x = Weight of each waste type (gram or kilogram)
W_t = Total mixed waste generated (gram or kilogram)

Results, Discussion, and Conclusions:

In this study, the 86 household samples having a population of 285 people (average of 3.3 people per household) lived throughout Bangkok, distributed in 30 districts (60% of all districts). The top three accommodation types are houses with garden 34%, followed by condominiums 27%, and townhouses 21%. The period of residence ranges from less than 5 to over15 years, with the largest groups, 33%, staying in their home for less than 5 years, followed by 31% for more than 15 years. The number of household members ranges from 1 to 9 people per household, with almost 65% indicating 3 to 5 people per household, which corresponds to the average of Bangkok city at 3.4 inhabitants per household. The respondents were engaged in various kinds of employment, with the majority working as government/state enterprise officials 47%, followed by company employees 22%, merchant/personal business 9%, general employees 9%, students 7%, and others e.g., unemployed, freelance, and housewife 6%. As for the current waste management method, approximately 74% of respondents placed their mixed wastes in the same garbage bin. About 14% of the survey respondents who sorted their food waste used it mainly for composting, and pets' food and the rest did not specify details.

Concerning packaging wastes, it is found that 50% of households did not sort them out whereas 28% separated and gave them to the Bangkok waste collection system, general waste pickers (called "Saleng" in Thai), and office housekeepers for further process. The remaining 22% separated packaging wastes and intentionally sold them to Saleng and waste dealers (waste buying-selling shops). On average, the largest amount of packaging waste sold was glass bottles at 6.64 kg/household (hh)/month, followed by corrugated box 4.37 kg/hh/month, and PET bottles at 2.92 kg/hh/month. However, the highest sales revenue was PET bottles at

31.71 bath/hh/month, followed by corrugated boxes at 20.5 bath/hh/month, and aluminum cans at 7.49 bath/hh/month. For segregating packaging wastes for giving to others, the most packaging waste quantity was glass bottles at 1.33 kg/hh/month, PET bottles at 0.76 kg/hh/month, and corrugated box 0.53 kg/hh/month. In the case of beverage carton wastes, it was found that only three households separated used beverage cartons from the general waste stream, accounting for 7% of household segregating packaging waste, and 3% of all household samples. These used beverage cartons were given to the Bangkok waste collection system, and schools for further process.

Figure 1 shows the results of the physical waste composition by wet weight analyzed in this study. It was found that the largest proportion of household waste in Bangkok was food waste (49%), followed by general waste (38%), and packaging waste (13%). Based on the total quantity of solid waste generated in Bangkok recently reported in 2020 [9], the household waste analyzed in this study accounted for 34% of the total waste stream in Bangkok. The average household waste generation per household per day was 1.12 kg, and per person per day was 0.34 kg. The largest proportion of packaging waste was glass bottles at 29.51%, PET bottles at 21.21%, and corrugated boxes at 14.75%, as shown in Figure 1.

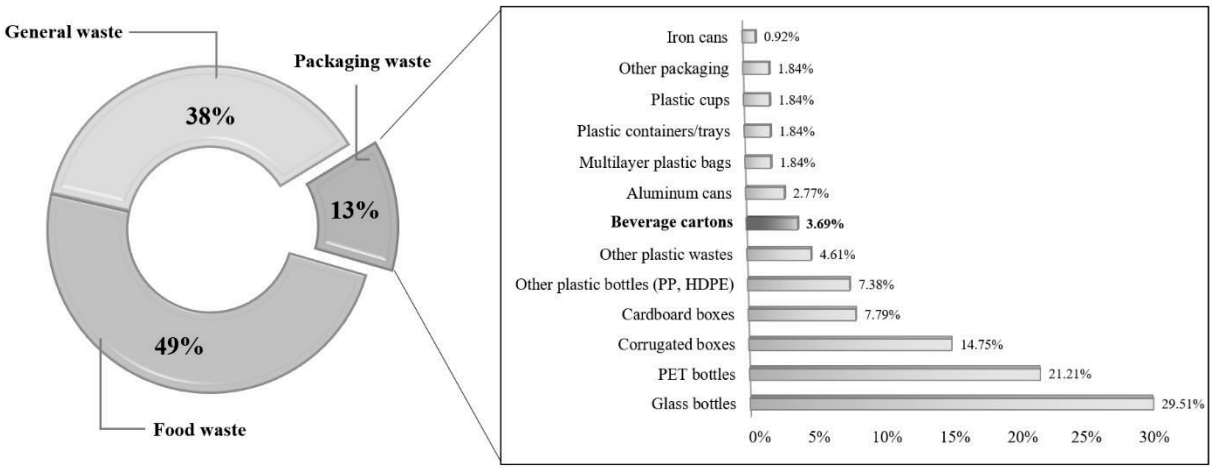

Figure 1 Composition of packaging waste and used beverage cartons by weight

In general, beverage carton is commonly categorized as paper-based packaging material. But in this study, the beverage carton was paid special attention, considered, and analyzed separately from other paper wastes. Of the 86 households, there were 45 households consumed and disposed of beverage cartons, accounting for 52%. The amount of beverage carton waste accounted for 1% of the total household waste, and around 3.7% of the total packaging wastes (see also Fig. 1). It was also calculated that the average consumption and disposal of used beverage cartons is 0.12 g per household per day, and 0.04 g per person per day for household waste in Bangkok. Therefore, the total consumption and disposal of used beverage cartons in Bangkok households can be estimated at approximately 315 to 429 kg per day. However, in 2002, a Pollution Control Department (PCD) study reported that average used beverage cartons accounted for 0.91% of total waste generation in Thailand [6]. Considering the total amount of waste generated in the same year, the beverage carton waste can be estimated to be 130,130 tons. Based on the consumption figure reported by the packaging manufacturers and this study's results, the current consumption and disposal of beverage carton wastes are markedly low compared to the 2002 PCD report. This could be due to the current smaller packaging sizes, and the steadily declining birth rate of Thai children over the past 20 years resulting in a decline in beverage cartons used for the school milk campaign in Thailand, which accounts for about 20% of the beverage carton use in Thailand.

In conclusion, the results of this study can give a current overview of household waste in Bangkok, serving as baseline data for household packaging waste, especially used beverage cartons. Ultimately, it is to find ways to manage household packaging waste and used beverage cartons by taking them back to the collection and recycling system, which can be separated at the source in the household.

Acknowledgments:

The research was funded by Program Management Unit for Competitiveness (PMUC) under the Office of National Higher Education Science Research and Innovation Policy Council, and the Thailand Institute of Packaging and Recycling Management for Sustainable Environment (TIPMSE) under the Federation of Thai Industries.

References:

1. Jacob P, Kashyap P, Suwannapan T, Visvanathan C. Status of beverage carton waste management in Thailand: Challenges and opportunities. Environmental Quality Management. 2022;31(4):249-59.
2. Office of Industrial Economics (OIE). Statistics of production and domestic sale of Packaging [Internet]. 2022 [cited 2022 Aug 29]. Available from https://packaging.oie.go.th/new/search_import_export_data.php?ACTION =SEARCH
3. Hall D. Throwaway culture has spread packaging waste worldwide: here's what to do about it [Internet]. 2017 [cited 2022 Aug 29]. Available from: https://www.theguardian.com/environment/2017/mar/13/waste-plastic-food-packaging-recycling-throwaway-culture-dave-hall
4. Agamuthu P, Visvanathan C. Extended producers' responsibility schemes for used beverage carton recycling. Sage Publications Sage UK: London, England; 2014. p. 1-3.
5. Mourad AL, Garcia EE, Vilela GB, Von Zuben F. Influence of recycling rate increase of aseptic carton for long-life milk on GWP reduction. Resources, Conservation and Recycling. 2008;52(4):678-89.
6. Pollution control department. Project to survey and analyze the composition of municipal solid waste in Thailand [Internet]. 2002 [cited 2022 Aug 30]. Available from: https://bit.ly/3wVBV8
7. Administrative Strategy Division**.** Statistical Profile of BMA 2021 [Internet]**.** 2021 [cited 2022 Aug 30]. Available from: https://bit.ly/3RhvsYX
8. National Statistical Office. The latent population survey, 2021 [Internet]. 2021 [cited 2022 Aug 31]. Available from: https://bit.ly/3wR84JS
9. The Department of Environment, Bangkok Metropolitan Administration. The Bangkok State of Environmental 2019-2020 [Internet]. 2021 [cited 2022 Sep 1]. Available from: https://bit.ly/3q9O6pK

Center of Excellence on
Environmental Health and Toxicology (EHT)

Faculty of Science, Mahidol University
K Building 5th Floor K514, Rama VI Road
Bangkok 10400, Thailand

Tel: 0-2201-5913-14
Fax: 0-2644-5428

Website - eht.sc.mahidol.ac.th